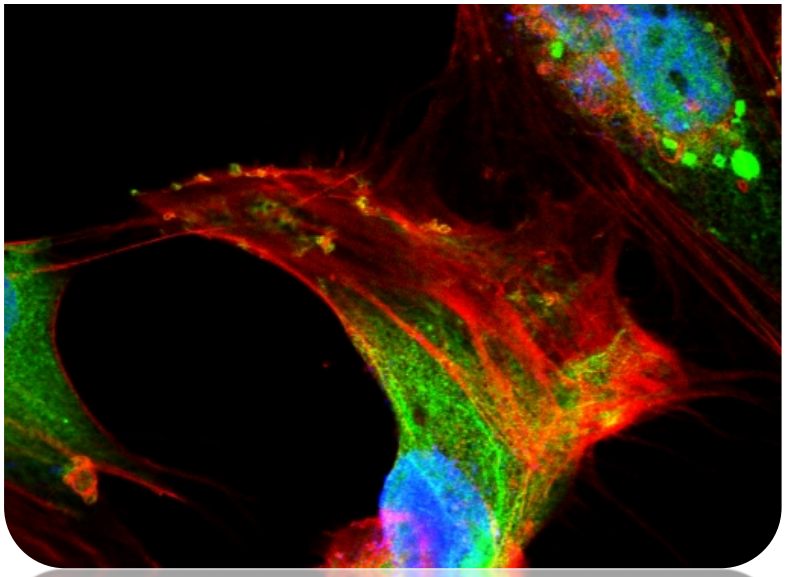

The RNA-binding protein LARP1 as potential biomarker and therapeutic target in ovarian cancer

A thesis submitted for the Degree of Doctor of Philosophy

Imperial College London
Department of Surgery and Cancer

Thomas Glass Hopkins

December 2014

DECLARATIONS

This thesis is submitted to Imperial College in support of my application for the degree of Doctor of Philosophy. It has been composed by myself and has not been submitted in any previous application for other degrees. The work presented (including data generated and analysis) represents original work carried out by the author in the laboratory of Dr Sarah Blagden in the Department of Surgery and Cancer, Imperial College London, except where clearly stated.

ACKNOWLEDGEMENTS

Firstly, I would like to take this opportunity to thank my thesis supervisor, Dr Sarah Blagden, for all her help and advice throughout this project. Her patience and enthusiasm has kept me going, and she has been extremely supportive of everything I have done. I would also like to thank my co-supervisors, Professor Martin Wilkins, Dr Richard Wooster and particularly Professor Eric Aboagye for all their helpful input throughout the last three years. This work would not have been possible without the financial support provided by the Imperial College Wellcome Trust-GSK Translational Medicine and Therapeutics PhD Fellowship, and I would like to thank Professor Martin Wilkins and Professor Paul Matthews for selecting me for this prestigious scheme.

Dr Manuela Mura in Dr Blagden's lab has been a fantastic person to work with and I have learnt a huge amount from her over my PhD. I should also like to acknowledge Dr Normala Abd-Latip, who, together with Manuela, laid much of the groundwork for my research, and Dr Katrina Sweeney, who got the lentiviral work up and running.

Everyone on the 4th floor of the Institute of Reproductive and Developmental Biology has been extremely helpful, but I would particularly like to thank Dr Jayantha Chatterjee for his support with all things ELISA-related, Haonan Lu for introducing me to 'R' and helping with data analysis, Camila Henrique De Sousa for keeping me sane, and Drs Erick Loomis, Elaina Maginn, Paula Cunnea, Rajpal Burmi and Jamie Studd for helpful discussions. Naina Patel, Jenny Steel and Nona Rama have gone above and beyond the call of duty in helping to retrieve and process patient samples.

I have abandoned my girlfriend, Lizzie Monks, on numerous weekends and evenings when the cells have demanded my attention, but she has been tireless in her support. I could not have done it without her. Finally, and most importantly, I would like to dedicate this work to my parents, Professor Robert Glass and Linda Hopkins, without whom I would, literally and figuratively, not be here today! They have been unfailing in their support and unstinting in their time, and have selflessly read pretty much everything I have ever written. I hope I've done them proud!

ABSTRACT

Ovarian cancer is the most lethal gynaecological malignancy, responsible for over 4,000 deaths each year in the UK. There is growing evidence that mRNA-binding proteins (RBPs) can be post-transcriptional drivers of cancer progression. Here, I investigated the expression of the RBP LARP1 in ovarian malignancies and role of the protein in ovarian cancer cell biology. LARP1 is highly expressed at both an mRNA and protein level in ovarian cancers compared with benign tumours and normal ovarian tissue. I show that higher levels of LARP1 in tumour tissue are predictive of poor patient survival. Consistent with this clinical finding, in xenograft studies knockdown of LARP1 expression causes a dramatic reduction in tumour growth. *In vitro*, LARP1 knockdown is associated with increased apoptosis, and is sufficient to restore platinum sensitivity in chemotherapy-resistant cell lines. Furthermore, LARP1 is required to maintain cancer stem cell marker-positive populations, and knockdown decreases tumour-initiating potential, as demonstrated by *in vivo* limiting dilution assays. Transcriptome deep-sequencing following LARP1 knockdown revealed altered expression of multiple genes linked to survival and evasion of apoptosis, including BCL2 and BIK. Transcripts of both genes are in complex with LARP1 protein, and LARP1 maintains the stability of BCL2 mRNA, whilst actively destabilising BIK transcripts. This effect is mediated at the level of the 3' untranslated region. I therefore conclude that by differentially regulating mRNA stability, LARP1 is a key post-transcriptional driver of tumourigenicity and cell survival in ovarian cancer.

PUBLICATIONS ARISING FROM THIS THESIS

Mura M, Hopkins, TG *et al.* LARP1 post-transcriptionally regulates mTOR and promotes cancer progression. 2014. Oncogene. *Accepted and in press.*

Hopkins TG, *et al.* LARP1 promotes cancer cell survival and chemoresistance in ovarian cancer. *Under submission.*

TABLE OF CONTENTS

LIST OF FIGURES

LIST OF TABLES

ABBREVIATIONS

Abbreviation	Term
5'TOP	5' terminal oligopyrimidine tract
aa	Amino acid
ADAR	adenosine deaminases acting on RNA
ARE	AU-rich element
BCL2	B-cell lymphoma 2
BIK	BCL2-interacting killer
BPS	Branch point sequence
CASK-C	Calcium/calmodulin-dependent serine protein kinase-C
CBC	Cap-binding complex
CPE	Core promoter elements
CSC	Cancer stem cell
CTD	C-terminal domain
eIF	Eukaryotic initiation factor
EMT	Epithelial-mesenchymal transition
ELISA	Enzyme-linked immunosorbent assay
ESC	Embryonic stem cells
EOC	Epithelial ovarian cancer
GEO	Gene expression omnibus
GO	Gene ontology
HGS	High-grade serous
HuR	Human antigen R
hnRNP	Heterogenous nuclear ribonucleoproteins
IRES	Internal ribosome entry site
ITAF	IRES-transacting factors
LAM	La motif
LARP	La-related protein
miRNA	MicroRNA
MDR1	Multi-drug resistance protein 1
miRISC	miRNA-induced silencing complex
mRBP	mRNA-binding protein
mRNP	Messenger ribonucleoprotein particle
MUC16	Mucin 16
ncRNA	Non-coding RNA
NELF	Negative elongation complex
NLS	Nuclear localisation signal
NPC	Nuclear pore complex

NRE	Nuclear retention element
NTD	N-terminal domain
OSE	Ovarian surface epitheium
PABP	PolyA-binding protein
PBS	Phosphate-buffered saline
PBST	Phosphate-buffered saline with TWEEN
PIC	Pre-initiation complex
Pol II/III	RNA-polymerase II/III
Pre-mRNA	Precursor mRNA
P-TEFb	Positive transcription elongation factor-b
RBD	RNA-binding domain
RBP	RNA-binding protein
RIP	RNA-immunoprecipitation
RNA-seq	RNA sequencing
RNP	Ribonucleoprotein particle
RPKM	Reads per kilobase per million mapped reads
RRM	RNA recognition motif
RT-qPCR	Reverse transcription quantitative PCR
SBM	Short basic motif
snRNA	Small nuclear RNA
snoRNA	Small nucleolar RNA
SS	Splice site
STIC	Serous tubal intraepithelial carcinoma
TBP	TATA-binding protein
TBS	Tris-buffered saline
TBST	Tris-buffered saline with TWEEN
TIC	Tumour initiating cell
U2AF	U2 auxiliary factor
UTR	Untranslated region

1 CHAPTER I – INTRODUCTION

1.1 CHAPTER ONE ABSTRACT

Ovarian cancers are twice as lethal as malignancies of the breast. Improvements in survival have been hampered by the absence of an effective screening strategy to allow early detection, and the lack of treatments with activity against platinum chemotherapy-resistant disease. Despite over two decades of clinical trials, few effective strategies have been identified to tackle chemoresistant malignancies, with response rates typically under 25%. There is therefore an urgent need for novel therapies to combat treatment-resistant disease, as well as accompanying biomarkers that can be used in diagnosis, treatment stratification and to track response.

Cancer development, progression and chemoresistance are underpinned by genomic instability and alterations in gene expression. There is a growing appreciation that a significant proportion of this variation in expression is generated at the post-transcriptional level. Following transcription initiation, mRNA is capped, spliced and polyadenlylated, before export from the nucleus. Once in the cytoplasm, mRNA may be translated, stored for later use or degraded. Transcripts exist in complex with mRNA-binding proteins (RBPs), as messenger ribonucleoprotein (mRNP) complexes. These RBPs regulate all aspects of RNA fate. Increasingly, it has been demonstrated that RBPs can act as drivers of malignant progression through the post-transcriptional regulation of gene expression.

The La-related proteins (LARPs) are a family of highly conserved RNA-binding proteins. They demonstrate diverse roles in post-transcriptional regulation, including determining RNA stability and translation. There is increasing evidence linking family members to cancer. In particular, LARP1 has been described as a marker of poor prognosis in hepatocellular cancer and acts as a promoter of cell motility and proliferation. The mechanism by which LARP1 may drive malignant progression has not yet been established.

1.2 EPITHELIAL OVARIAN CANCER

Each year, epithelial ovarian cancer (EOC) is responsible for over 140,000 deaths worldwide. It is the sixth most common cause of cancer mortality amongst women in developed countries, and the most lethal gynaecological malignancy [1]. The relative five-year survival in Europe, based on Eurocare-4 data [2], is just 37%, whilst more recent figures for England places it at 43% [3]. Although advances in surgical approaches and combination chemotherapeutics have improved survival figures steadily over the past four decades [4], ovarian cancer remains twice as deadly as breast cancer (Figure 1-1) [3]. To produce significant improvements in survival two major hurdles must be overcome [5]. Firstly, the majority of ovarian cancers are currently detected after the disease has spread beyond the pelvis, whereupon the probability of achieving a surgical cure is greatly reduced. Secondly, although nearly all patients initially respond to combination chemotherapy, women with disease recurrence will inevitably develop treatment-resistant cancers [4]. Tackling these obstacles to improving ovarian cancer survival requires a detailed understanding of the pathogenesis of this complex disease.

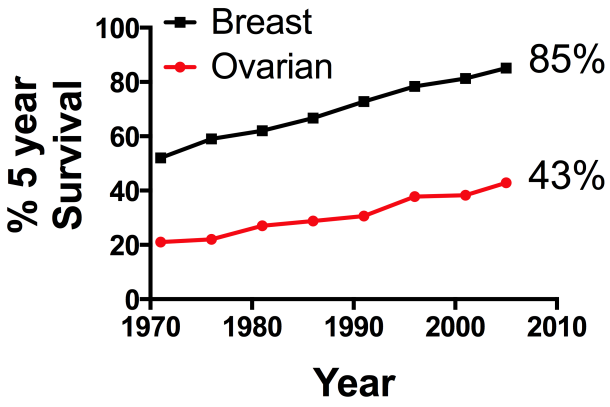

Figure 1-1. Five-year survival for breast and ovarian cancers in the UK.

Trends in five-year survival over four decades, for breast and ovarian cancer. *Data obtained from cancerresearchuk.org.*

1.2.1 OVARIAN TUMOUR CLASSIFICATION

Epithelial ovarian cancer (EOC) accounts for approximately 90% of ovarian malignancies [6]. Epithelial tumours have traditionally been sub-classified according to morphological features into serous, clear cell, mucinous, endometrioid and transitional cell ovarian carcinomas (Figure 1-2). Within each sub-classification tumours are characterised as benign, borderline or malignant. Malignant tumours are also categorised as either high-, intermediate- or low-grade, according to the degree of nuclear atypia and mitotic activity. High-grade serous (HGS) cancers are by far the most common ovarian carcinomas, representing approximately 70% of all malignancies [7], and 95% of all serous cases in the Hammersmith series (Figure 1-3). The figure below shows a breakdown of over 500 cases seen at Hammersmith Hospital.

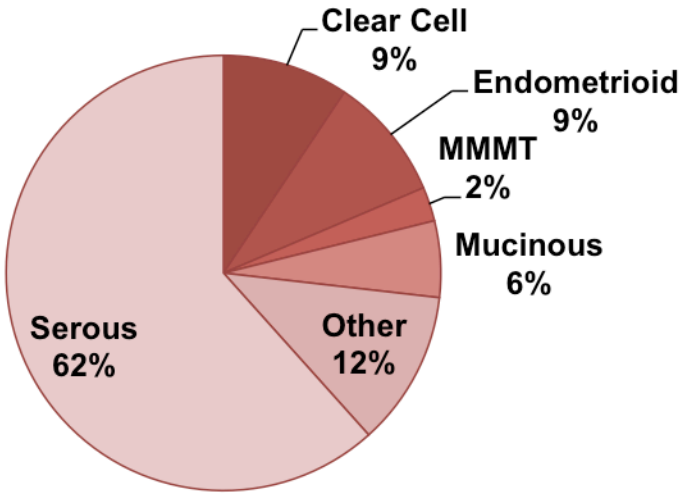

Figure 1-2 Summary of Hammersmith Hospital ovarian cancer database by histological subtype.

A breakdown of 512 cases seen at the Hammersmith Hospital over a ten year period, according to histological subtype. MMMT = Mixed müllerian mesodermal tumour. *Hammersmith Hospital clinical data analysed by TGH.*

Whilst all EOCs were once treated as a single disease, throughout the last century there has been an increasing appreciation that there are fundamental differences in the behaviours of the different histological ovarian subtypes and their responses to treatment. For example, patients with mucinous tumours, that represent 5%-10% of EOCs, have a poorer prognosis and are less likely to respond to chemotherapy treatment when compared to HGS cohorts [8, 9]. In 2004, Robert Kurman and le-Ming Shih proposed that ovarian cancers could be grouped into two broad classes, Type I and Type II tumours, based on their behaviour, histology and emerging genomic data [10], a model they continue to refine [11] (summarised in Table 1-1). Type I tumours include low-grade serous and low-grade endometrioid tumours, clear cell and mucinous carcinomas, whilst Type II tumours comprise high-grade serous and endometrioid carcinomas, carcinosarcomas and undifferentiated carcinomas.

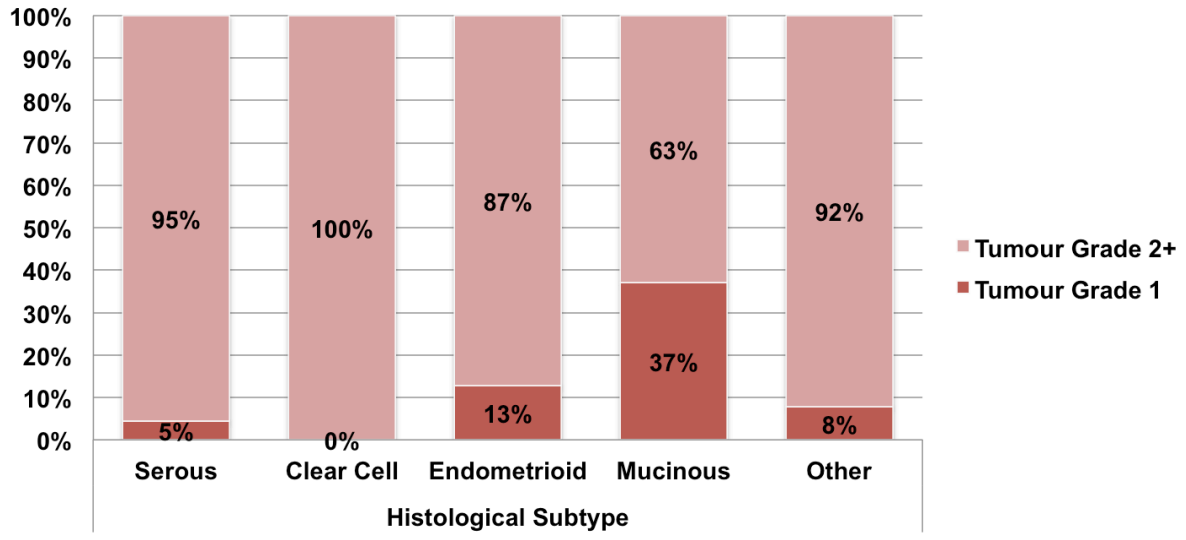

Figure 1-3. Stratification of 512 ovarian cancer cases seen at the Hammersmith Hospital according to stage.

Hammersmith Hospital clinical data analysed by TGH.

Type I tumours typically present as unilateral disease, with large cystic ovarian masses, and are characterised by slow progression. It has also been proposed that development of these tumours is due to the stepwise accumulation of mutations [11]. Type II tumours are

aggressive malignancies that usually present as disseminated disease, and show a high degree of genomic instability.

Table 1-1. Classification of malignant ovarian epithelial tumours

Adapted from Nik et al [11] with additional data from [12].

	Carcinoma	Putative precursor	Most frequent mutation(s)	Chromosomal structural alteration
Type I tumours	Low-grade serous	Serous borderline tumour	*KRAS*, *BRAF*, *ERBB2*	Low
	Low-grade endometrioid	Endometrioma	*CTNNB1*, *PIK3CA*, *PTEN*, *ARID1A*	Low
	Clear cell	Endometrioma	*PIK3CA*, *ARID1A*	Low
	Mucinous	Mucinous borderline tumour	*KRAS*	Low
Type II tumours	High-grade serous	Fallopian tube epithelium	*TP53*, *BRCA1/2, PTEN*	High
	High-grade endometrioid	Unknown	*TP53*	High
	Undifferentiated carcinoma	Unknown	Unknown	Unknown
	Carcinosarcomas	Unknown	*TP53*	Unknown

1.2.2 DIAGNOSIS

Ovarian cancers are classified by both tumour grade and stage. Tumour grade details the degree of differentiation of the tumour judged by its microscopic appearance, including the number of mitotic figures and degree of nuclear atypia. Tumours are defined as being well (grade 1), intermediate (grade 2) or poorly (grade 3) differentiated. In contrast, in ovarian cancer, tumour stage is a surgical definition of its spread around the body. There are four stages, stage I (early stage) being tumour confined to the ovary and stage IV (advanced) when it has spread outside the pelvis and is involving distant visceral organs (Table 1-2). Patients whose tumours are detected early, with low-stage, low-volume disease, have a significantly better prognosis: in one patient population, women with Stage I tumours had a five-year

survival of 92.1%, whilst for those with Stage IV tumours, only 5.6% were alive at five years [13]. Unfortunately, the majority of women present with disease that is no longer localised to the ovary. This is particularly true for serous ovarian carcinomas, the commonest EOC subtype: in the Hammersmith Cohort, 85% of patients had Stage III/IV disease at presentation (Figure 1-4), whilst figures for the Anglia Cancer Network show only 29% of all patients with EOC presented with Stage I disease [13].

Table 1-2. International federation of gynaecology and obstetrics (FIGO) staging of ovarian cancer.

The staging of ovarian cancer according to the international federation of gynaecology and obstetrics (FIGO) criteria [14].

Stage	Localisation
I	Tumour confined to one or both ovaries
II	Tumour involves one or both ovaries with pelvic extension below the pelvic brim *or* primary peritoneal cancer
III	Tumour involves one or both ovaries with peritoneal spread outside the pelvis and/or metastasis to retroperitoneal lymph nodes
IV	Distant metastasis, including pleural effusions, hepatic or splenic metastasis, or extra-abdominal organs.

There is currently no national screening program for ovarian cancer, so diagnoses are made only when patients present with symptoms, or, rarely, when it is uncovered incidentally. Clinical diagnosis is complicated by the fact that the symptoms associated with ovarian cancer, such as abdominal distension and pelvic/abdominal pain, are often vague in nature and easily attributable to other benign causes [15]. Several charities have campaigned to raise awareness of the symptoms of the disease amongst the public and general practitioners (GP). In 2011, the National Institute of Clinical Excellence (NICE) published guidelines to assist GPs in the prompt diagnosis and referral of patients with suspected EOC (CG122). Those with a history or examination findings suggestive of the disease undergo a transvaginal ultrasound scan and have a serum test for CA125. CA125 is a glycoprotein encoded by *MUC16*, plasma levels of which are elevated in 90% of patients with advanced EOC, but

only 50% of those with Stage I malignancies [16]. If the serum CA125 is elevated and/or there are worrying features on the ultrasound scan, patients are referred to specialist centres for surgery and histological assessment.

Figure 1-4 Hammersmith patient data (n=512) stratified by tumour stage at presentation

Hammersmith Hospital clinical data analysed by TGH.

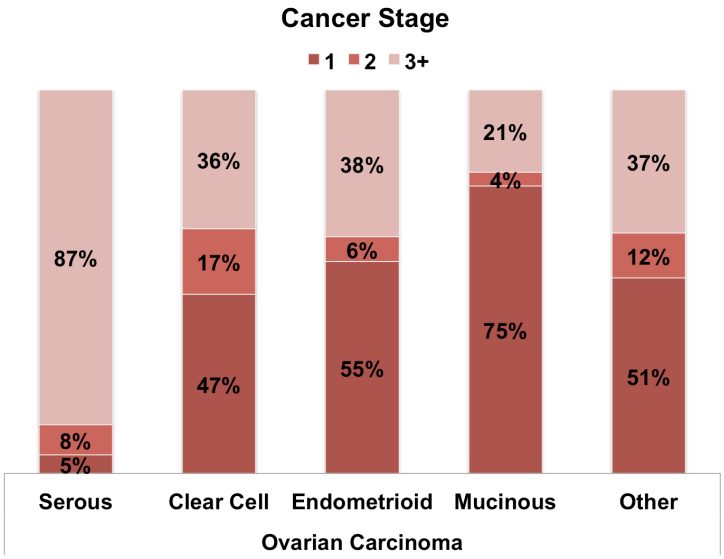

Given the poor prognosis associated with late stage disease, improving early detection is a key clinical priority [5]. National cancer screening programmes can be highly effective, with cervical cancer screening estimated to have prevented over 80% of cancer deaths since its introduction [17]. Such an approach is not yet possible for ovarian cancer, due to the lack of a high-quality screening test. Whilst a circulating tumour marker does exist for ovarian cancer in the form of the CA125 antigen, its use as a screening tool is limited by its low specificity and high false positive rate [18], with elevated levels in several benign conditions such as endometriosis [19]. In addition, a substantial proportion of patients with early stage disease do not have an elevated CA125, leading to false negatives [16]. Trials investigating multimodal screening strategies with regular transvaginal ultrasounds have shown mixed results [20, 21], and such strategies are expensive, labour-intensive and relatively invasive. Other circulating biomarkers have been investigated in ovarian cancer, though none are

currently approved for clinical use in diagnosis. In one study, 96 serum biomarkers were evaluated, with four combined together (CA125, HE4, CEA, VCAM-1) shown to detect early-stage disease with 86% sensitivity and 98% specificity [22].

In patients whose tumours express CA125, this plasma test is extremely useful in monitoring response to treatment, and in the follow-up of patients to detect disease recurrence or progression [16]. Serum human epididymis protein 4 (HE4), in combination with CA125, is also currently licensed by the US Food and Drug Administration (FDA) for use in disease monitoring [23].

1.2.3 TREATMENT

First-line therapy for all patients with advanced EOC (stage IC-IV), or early stage disease with adverse features, involves primary debulking surgery and adjuvant chemotherapy with platinum-based agents (cisplatin/carboplatin), with or without a taxane [4, 24]. Whilst 70-80% of patients initially respond to this combination therapy, the majority of patients will experience disease recurrence or progression within two years. With each recurrence, cancers become increasingly chemoresistant [25, 26] and treatment resistance is the cause of 90% of the mortality in patients with advanced cancers [24]. Clinically, the platinum status of patients is defined by the time interval between the completion of platinum-based chemotherapy treatment and disease relapse, with those with platinum-refractory disease progressing during treatment (Table 1-3). Currently, there is no way to prospectively predict the chemo-sensitivity of tumours, resulting in the potential over-treatment of some patients with sensitive disease, and under-treatment of others with highly resistant tumours. A number of agents have been trialled in platinum-resistant disease, including single agent paclitaxel or gemcitabine, but response rates are rarely higher than 10-25% [24, 27, 28].

Table 1-3. Clinical definitions of platinum status

Definitions of platinum status as set out by the Gynaecologic Oncology Group [29].

Status	Clinical features
Platinum-sensitive	Progression-free for >12 months following completion of treatment
Partially platinum-sensitive	Progression-free for 6-12 months following completion of treatment
Platinum-resistant	Progression-free for <6 months following completion of treatment
Platinum-refractory	Progression during platinum treatment

1.2.3.1 Chemotherapy action

Cytotoxic chemotherapies target rapidly dividing cells. Taxanes and platinum-based agents have different mechanisms of action, but their anti-cancer effects, and to some extent their toxicities, are based on their ability to disrupt cell division and trigger cell death. Taxanes, including paclitaxel and docetaxel, bind to the beta-actin component of microtubules and enhance polymerisation. Microtubule remodelling is essential for many cell processes, including mitosis: by blocking this taxanes induce mitotic arrest and apoptosis [30]. Cisplatin and carboplatin are hydrolysed in the cytoplasm of cells to create an active molecule that forms adducts with DNA, RNA and protein. In the nucleus, cisplatin forms inter- and intrastrand adducts with DNA that can prevent transcription and replication [24, 31]. Platinum-DNA adducts may be repaired, primarily by nucleotide excision repair, or, if the damage is too severe, may trigger cell cycle arrest and cell death [32]. Overall, cisplatin appears to accumulate to a greater extent in RNA than DNA, and cisplatin treatment is associated with a reduction in translation [33, 34]. However, the relative contribution of

platinum-RNA adducts to cellular toxicity is not well characterised. In addition, cytoplasmic cisplatin induces oxidative stress by binding to, and depleting, antioxidants such as glutathione [31]. The finding that enucleated cells still undergo apoptosis following cisplatin treatment demonstrates that DNA damage is not the only cause of toxicity [35].

1.2.3.2 Chemotherapy resistance

Despite the different mechanisms of action, resistance to both cisplatin/carboplatin and taxanes can be generated through common pathways. For example, cancer cells develop mechanisms to enhance drug removal, with overexpression of the *MDR1* gene, encoding an ATP-driven efflux pump, associated with increased resistance to both drug classes [36-39]. Similarly, enhanced pro-survival signalling can allow cells to evade apoptotic stimuli, with increased expression of the anti-apoptotic gene *BCL2* associated with increased resistance to platinum-based agents [40, 41].

Some mechanisms of resistance are also agent specific. Cisplatin-induced DNA damage can be reversed by nucleotide excision repair. One of the key proteins in this process is excision repair cross-complementation group 1 (ERCC1), and patients with high expression exhibit a poor response to cisplatin treatment, whilst knockdown of ERCC1 in cell lines enhances platinum sensitivity [42, 43]. Similarly, as aquated cisplatin binds to glutathione, cells that exhibit increased glutathione expression are more resistant to oxidative stress and minimise the amount of free cisplatin that is available to bind DNA in the nucleus, making cells more platinum resistant [37].

Paclitaxel binds to specific residues on the beta-subunit of tubulin to enhance polymerisation. Studies of taxane-resistant cell lines have shown they have acquired mutations within the beta-tubulin gene that minimise the paclitaxel-induced polymerising effect [44, 45]. There are several different tubulin isotypes that differ in their sensitivity to paclitaxel [36], and in

studies of ovarian cancer patient samples, resistant tumours show a significant shift in their isotype expression [46].

1.2.4 CELL OF ORIGIN

To understand, treat and ultimately prevent ovarian cancer it is critical to determine its point of origin. EOC is unusual when compared to other common malignancies, in that the cell of origin has remained hotly debated for some time. Recently, a combination of histological analysis and molecular biological studies has begun to address this fundamental question. It was previously thought that the ovarian surface epithelium was the source of epithelial ovarian malignancies. However, EOCs do not resemble the ovarian surface epithelium, and precursor lesions have not been found on the ovarian surface [14]. The normal epithelia that resemble the different EOC subtypes are found elsewhere in the female genital tract (Table 1-4), and these sites have a different embryological origin to the ovaries, being derived from Müllerian tissue and not mesothelium. This has led to the suggestion that ovarian malignancies may result from the neoplastic transformation of Müllerian epithelium-lined cortical invaginations and inclusion cysts [47].

Accumulating evidence now points to the fallopian tube epithelium as the site of origin, at least for HGS ovarian cancers. In patients with a genetic predisposition to ovarian cancer, dysplastic changes are seen in the fallopian tube epithelium but not the ovaries [48]. In addition, in 48-59% of HGS cases, potential precursor lesions are found in the fallopian tubes, called serous tubal intraepithelial carcinomas (STICs) [49, 50]. These STICs are also seen in over half of patients with primary peritoneal cancer, supporting a common origin [51]. Finally, it has recently been shown that the conditional knockout in fallopian tube secretory epithelial cells of genes frequently mutated in HGS cancer (*BRCA2*, *TP53* and *PTEN*), leads to the development of STICs in mice. Moreover these mice go on to develop

HGS cancers, with ovarian and peritoneal metastases, and these tumours have a genetic profile similar to human HGS malignancies [52].

Table 1-4. Morphological features of the epithelial subtypes.

Epithelial ovarian tumours have morphological features seen in extraovarian epithelial cells [10, 14].

Epithelial Ovarian Tumour	Morphological features
Serous	Fallopian tube epithelium
Endometrioid	Uterine epithelium
Mucinous	Gastrointestinal epithelium
Transitional Cell/Brenner	Bladder epithelium
Clear cell	Endocervix

1.2.5 THE MOLECULAR BASIS OF HIGH-GRADE SEROUS OVARIAN CANCER

When Hanahan and Weinberg published their seminal paper on cancer hallmarks in 2000, they identified six characteristics that normal cells needed to acquire to become neoplastic, including evasion of apoptosis and limitless replication [53]. Reviewing the subject again over a decade later, they had added four new features to the list (see Table 1-5) [54]. Multiple genes and pathways are implicated in the acquisition of these hallmark characteristics, and the molecular basis of dysregulation varies substantially between different cancers, and even within subtypes of a single cancer. With the advent of genomic analysis approaches, it has become clear that at a genetic level, as well as on a histological and clinical basis, the EOC subtypes are fundamentally different, and in particular HGS is distinct from low-grade serous ovarian cancers (summarised in Table 1-1). The most striking genetic abnormality in HGS ovarian cancer is the near universal presence of *TP53* mutations, present in >95% of cases [12, 55]. *BRCA1/2* are also mutated in 22% of tumours, with other commonly mutated genes

including *RB1* and *CDK12*, an RNA splicing factor. HGS cancers are characterised by a high degree of genetic instability, with both focal copy number changes and alterations at the chromosome-arm level [12]. It has been suggested that, based on gene expression profiles, HGS tumours can be apportioned to four classes (immunoreactive, differentiated, proliferative and mesenchymal), though these do not differ significantly in terms of prognosis. Some changes in gene expression can be explained by altered methylation status of promoters. Pathway analysis of combined genomic, epigenomic and expression data, revealed frequent alterations in the *FOXM1* transcription factor network (87%), *RB1* signalling (67%), homologous recombination pathways (50%), PI3K/RAS signalling (45%) and *NOTCH* signalling pathway (22%) [12].

Table 1-5. The hallmarks of cancer

The core abilities required by cells to become malignant. Adapted from [54].

Cancer Hallmarks
Evasion of cell death
Genome instability and mutation
Induction of angiogenesis
Activation of invasion and metastasis
Promotion of tumour-enhancing inflammation
Limitless replication
Immune evasion
Evasion of growth suppressors
Sustained proliferative signalling
Alterations in cellular metabolism

Genome-wide association studies have been conducted for EOC, and have identified susceptibility loci, but these so far account for only 4% of excess familial risk. In contrast, germline *BRCA1/2* mutations are thought to account for up to 40% of excess familial risk [56], and are seen in 8-17% of all EOC cases [12, 57]. Paradoxically, although patients with germline BRCA mutations have an increased frequency of extra-peritoneal disease, they have

a better prognosis than patients with sporadic cancers, probably due to increased sensitivity to platinum chemotherapy [57, 58].

1.2.6 OVARIAN CANCER STEM CELLS

The dominant model of cancer development is that of clonal evolution, whereby non-malignant cells acquire genetic alterations in a stochastic manner, leading to a heterogeneous tumour that is increasingly adapted for uncontrolled growth and metastasis. Recently, an alternative theory has been suggested to underpin the development of some malignancies, that of cancer stem cells (CSCs). In this model, there is a defined hierarchy of tumorigenic and non-tumorigenic cells. Non-tumorigenic cells compose the bulk of the tumour and are derived from tumourigenic CSCs (Figure 1-5).

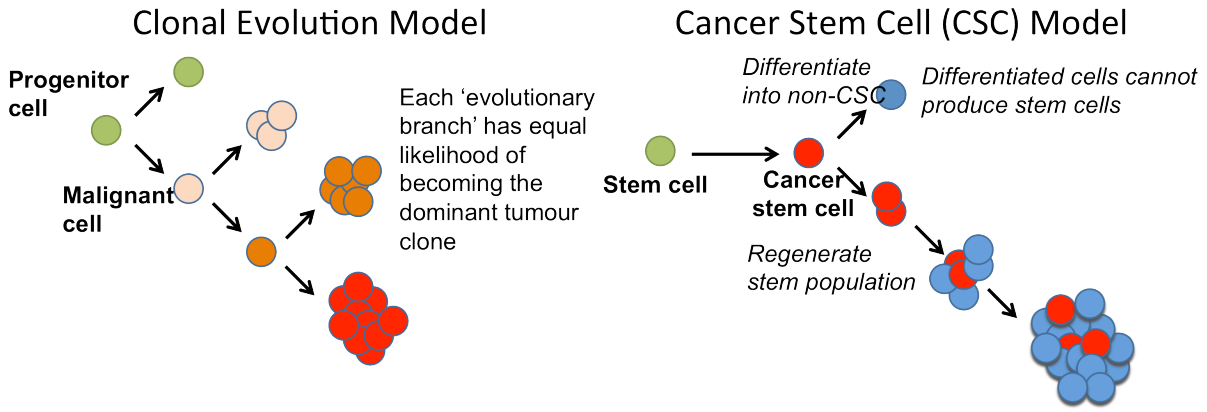

Figure 1-5. Two models of cancer evolution

Two models have been proposed for cancer evolution. In the clonal model, a precursor cell accumulates sufficient genetic aberrations to become malignant. Due to genomic instability, multiple lineages are generated in a single tumour with different mutational spectra, and one may become dominant e.g. due to enhanced chemoresistance. In the CSC model, a normal stem cell, responsible for regenerating healthy tissue becomes malignant due to mutational events. This stem cell can divide to repopulate the CSC niche, or to produce a more differentiated and highly proliferative non-CSC cell, that forms the bulk of the tumour.

These non-tumourigenic cells are not able to generate CSC populations and the tumour is therefore reliant on CSCs for tumour initiation and metastasis. CSCs tend to proliferate less

rapidly, and are therefore potentially more resistant to the majority of chemotherapeutics, whose cytotoxic effects rely on rapid cell division [59]. This has profound implications for cancer treatment; though standard therapies may lead to tumour shrinkage by killing rapidly dividing non-tumourigenic cells, if such therapies leave CSC cells alive, relapse is inevitable (Figure 1-6). Although initial work on CSCs was conducted with acute myeloid leukaemias, it was subsequently shown that CSC-like cells could be isolated in solid malignancies, including ovarian cancers [60-63].

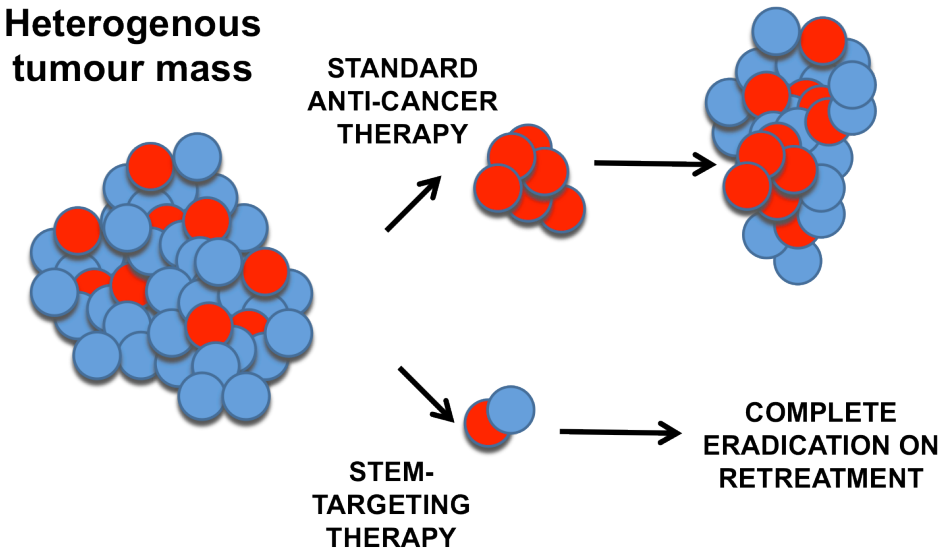

Figure 1-6. Cancer stem cell model: implications for treatment

If conventional cytotoxic chemotherapy only targets non-CSC cells, there will be tumour shrinkage but the cells capable of recapitulating the tumour will remain. This results in a rapid relapse. However, if both cell populations are targeted, for example by using a conventional cytotoxic together with a CSC-targeting agent, complete eradication of the tumour becomes a possibility.

Several flow cytometry markers have been shown to identify CSC-like ovarian populations, including aldehyde dehydrogenase activity and CD133 membrane expression [62, 64], and marker-positive cells exhibit more than 1000x the tumour-initiating potential when compared to non-CSC cells [60]. In addition, it seems that these ovarian CSCs are more chemoresistant [65]. Supporting the clinical significance of CSC-like cells in ovarian cancer, patients with a high CD133 or aldehyde dehydrogenase expression in their tumours have a significantly

worse prognosis [66, 67]. However, other studies have shown that CSC-like cells have a significant heterogeneity in marker expression, complicating their isolation and quantification [61]. Work in mice has shown that a population of stem cells clustered at the ovarian hilum give rise to the ovarian surface epithelium, and these cells have high aldehyde dehydrogenase expression. Interestingly, deletion of *TP53* and *RB1* in these cells results in tumours that resemble human EOC [68], suggesting that at least some ovarian malignancies may arise from the accumulation of mutations in a non-malignant ovarian stem cell population.

1.2.7 SUMMARY

Epithelial ovarian cancer is a far more complex and diverse disease than was previously thought. Although significant strides have been made in the last decade to improve our understanding, it remains the most lethal gynaecological malignancy, with less than half of patients surviving beyond five years. Treatment is complicated by the fact that nearly all patients present with extra-ovarian disease, and therefore a substantially reduced chance of achieving a surgical cure. Whilst the majority of patients initially respond to platinum- and taxane-based therapies, resistance becomes increasingly common with each disease relapse, and few of the second-line strategies trialled to date have produced sizeable response rates. HGS tumours demonstrate a high degree of genetic instability, and are characterised by mutations affecting *TP53* and multiple cancer-related pathways. In addition, there is significant intra-tumoural heterogeneity, with sub-populations of cells that exhibit enhanced tumour-forming ability and chemoresistance. New therapeutic targets are urgently needed if any improvements in outcomes are to be made. To be effective, it is likely that such therapies will need to target multiple signalling pathways simultaneously, and demonstrate activity against both CSC and non-CSC populations.

1.3 mRNA-BINDING PROTEINS

Ovarian cancer is a highly genetically diverse disease. With the exception of *TP53*, there are few known common mutational events [12, 55]. Although mutations in *BRCA1/2* have been shown play a significant role in the inherited predisposition to ovarian cancer, the combined efforts of several studies have so far identified loci that account for only 4% of the excess familial risk [56]. This indicates that mutations in multiple genes contribute to the risk of developing ovarian cancer, with significant heterogeneity seen between and even within patients [69]. This genetic diversity complicates both the study of ovarian cancer and the development of new therapies.

Expression profiling has demonstrated that there are substantial differences in mRNA abundance between ovarian malignancies and non-cancer tissue, and even between different EOC subtypes [70]. There is a growing appreciation that such differences in expression are not all determined at the genetic, epigenetic or transcriptional level, but can be the result of post-transcriptional regulation [71]. Interest in the role of post-transcriptional regulation in cancer was re-ignited in 1993, with the discovery of the first microRNAs (miRNAs) [72, 73]. However, miRNAs represent only one aspect of post-transcriptional regulation, a term that describes all events from the capping of nascent transcripts in the nucleus, through to their eventual translation and/or decay in the cytoplasm.

At the centre of post-transcriptional regulation, RNA binding proteins (RBPs) play a critical role in all aspects of RNA fate determination [74]. RBPs are increasingly being recognised as key drivers of cancer progression and chemoresistance in several cancers [75], including ovarian malignancies [12, 76, 77].

1.3.1 mRNA RIBONUCLEOPROTEINS (mRNPs)

Since the establishment of the central dogma of molecular biology [78], mRNA has been understood to be the intermediary molecule in the transfer of information from the DNA template to protein synthesis. Far from being a simple linear transfer of information, it has become increasingly clear that a substantial proportion of the variations in gene expression are determined at the post-transcriptional level. Indeed, work in mouse fibroblasts demonstrated that the regulation of mRNA translation was a significantly greater determinant of gene expression than transcription [71], and there may be up to twice as many factors related to processing and regulating RNA than related to transcription [79]. That so much control is exerted at the level of RNA is perhaps not surprising, as it has been suggested that RNA-based life predates the use of DNA or proteins [80]. Although initially thought of as separate processes, it now seems that all stages of the mRNA lifespan are interconnected, with events at the earliest points in transcription and transcript birth determining the eventual fate of an mRNA in the cytoplasm [81]. As well as dramatic shifts in gene expression, there is evidence that 'fine-tuning' of gene expression can also be performed post-transcriptionally, for example through miRNA-mediated processes [82].

Multiple proteins and non-coding RNAs (ncRNAs) are involved in co-ordinating post-transcriptional regulation through the formation of complex and dynamic ribonucleoprotein particles (RNP) [83]. RNA-binding proteins (RBPs) assemble on mRNAs co-transcriptionally and mRNPs are remodelled throughout the life of any given transcript to determine its fate (Figure 1-7) [84]. The complexity of this regulation is only now beginning to be understood with the use of next-generation sequencing and high sensitivity mass spectrometry.

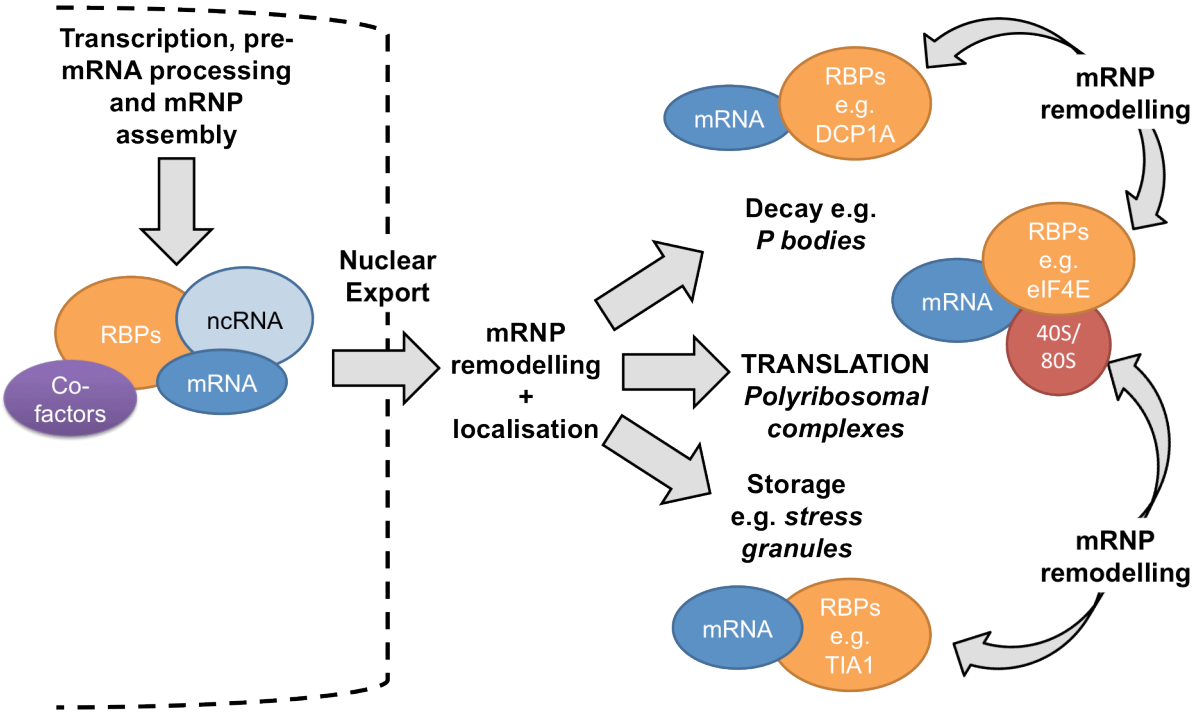

Figure 1-7. Dynamic mRNP remodelling determines mRNA fate

RNA-binding proteins assemble on nascent transcripts, and are required for capping, polyadenylation and splicing. Packaged as an mRNP, transcripts are exported from the nucleus and, once in the cytoplasm, the RBP components of the mRNP may be re-modelled to determine transcript fate. mRNAs may be stored for later use, undergo translation or be degraded. Further mRNP remodelling allows transcripts to move between silencing and active translation. ncRNA = non-coding RNA.

1.3.2 mRNA-BINDING PROTEINS

RNA-binding proteins exist at the heart of post-transcriptional regulation, being required for all aspects of RNA processing and fate determination. However, relatively few RBPs have so far been studied in significant depth. Those investigated to date reveal complex and multifunctional roles, with each RBP potentially in complex with hundreds or even thousands of different transcripts, and each transcript interacting with several different RNA-binding proteins at any given time [84]. There is accumulating evidence that RBPs can play a critical role in human pathological processes, including inflammation and cancer [74, 85].

The RNA-Binding Protein DataBase (RBPDB), published in 2012, listed 416 proteins with experimentally validated RNA-interacting properties [86]. In fact, recent work suggests that this is likely to be a significant underestimate, and many proteins with no identifiable conventional RNA-binding domain (RBD) remain to be experimentally determined [87]. In one study in mammalian cells, 860 proteins were identified as binding polyadenylated RNA, 37% of which had no predicted or experimental evidence of RNA binding properties [87]. In release 64 of Ensembl, searching for the gene ontology term 'RNA binding' (GO:0003723) returned 967 annotated human protein-coding genes [88], but in the most recent release (77) this number had increased to 1,676.

Accumulating evidence from RNA-RBP immunoprecipitation experiments supports a model whereby many RBPs interact with a large number of different transcripts, enriched for related functions [79, 89, 90]. The RBP-RNA interaction is mediated by RNA-binding domains (RBDs), such as the RNA-recognition motif (RRM), La motif (LAM) or KH domain. Diversity in RNA affinity is created by incorporating multiple RBDs in different arrangements in each RBP, either of the same class or by combining different domains [91].

1.3.3 THE mRNA JOURNEY

To understand the role of RBPs in post-transcriptional regulation, it is necessary to understand the stages in the mRNA life cycle and their potential role in the modulation of gene expression. This is an extremely complex topic, and some aspects of post-transcriptional control are only just beginning to be understood. Following the initial transcribing of DNA into pre-mRNA by RNA Polymerase II, regulation can occur at the level of pre-mRNA splicing and processing, RNA editing, nuclear export, localisation, translation and finally stability and decay.

1.3.3.1 mRNA 'birth'

1.3.3.1.1 Transcription initiation and capping

Eukaryotic transcription begins with the formation of the transcription pre-initiation complex (PIC) upstream of a gene. The ability of the PIC to form depends on the accessibility of the gene promoter and also enhancer regions that regulate promoter activity. DNA in the nucleus exists in a highly packaged form, chromatin, and by remodelling chromatin to 'open' or 'closed' states, cells can alter the transcriptional activity of a specific region [92, 93]. Assembly of the PIC is dependent on core promoter elements (CPE), such as the TATA box, recognised by CPE-binding proteins like TATA-binding protein (TBP). This interaction forms the basis for the sequential recruitment of general transcription factors and RNA polymerase II (Pol II), and the formation of the PIC. After promoter melting and escape occurs, transcript elongation precedes until the termination site is reached. Depending on the efficiency of reinitiation, multiple cycles of transcription can take place. [94-96].

The formation of the PIC does not guarantee successful transcription, as Pol II enters a paused state due to the negative regulatory effects of the DRB sensitivity-inducing factor (DSIF) and negative elongation factor (NELF) complexes. This paused state can be exited and elongation promoted by phosphorylation of both components by cyclin-dependent kinase 9 (CDK9), a protein in the positive transcription elongation factor-b (P-TEFb) complex [96, 97].

It is now clear that the processing of pre-mRNA to its mature form occurs co-transcriptionally [97]. The C-terminal domain (CTD) of Pol II is critical to this coupling, recruiting different co-factors depending on the stage of transcription. The CTD is composed of multiple copies of a six amino acid (AA) repeat motif, YSPTSPS, with 52 repeats in mammals [98]. Phosphorylation of the 2nd, 5th and 7th serine residues delineates the different

stages of transcription. The kinase activity of the cyclin dependent kinase 7 (CDK7), a component of the critical PIC general transcription factor TFIIH complex, is activated upon PIC formation; this then phosphorylates the Ser5 residues of the CTD and recruits mRNA capping enzymes (an RNA 5'-triphosphatase, a guanyltransferase and a guanine-7 methyltransferase) [98, 99]. Using a 5'-5' linkage, the 7-methylguanosine cap is attached to nascent transcripts of only 20‑30 nucleotides [100]. This cap is required for efficient splicing [101], export and later for cap-dependent translation. The cap is then bound by the cap-binding complex (CBC), composed of CBP20 and CBP80 [102].

1.3.3.1.2 Elongation and co-transcriptional splicing.

In the human genome, genes are separated into protein coding sequences, exons, interspersed with non-translated regions, introns: there is an average of just under eight introns per gene. The majority of human exons are below 200nt, and are surrounded by larger introns, which have an average length of 3,400nt, with the largest recorded being over 300kbp [103, 104]. Introns are removed prior to nuclear export by mRNA splicing. By combining exons in different combinations or including different exons, alternative splicing allows a significant amount of genetic diversity to be created at a post-transcriptional level. Indeed, it appears that up to 94% of human genes have splice variants [105], with 140,000 novel transcripts generated from less than 22,000 genes [88]. Although splicing can take place post-transcriptionally, either within chromatin or elsewhere in the nucleus [97], it was demonstrated in the late 1980's using electron microscopy in *Drosophila*, that splicing could take place co-transcriptionally [106]. As RNA elongation progresses, the P-TEFb complex, composed of CDK9 and cyclin T1, phosphorylates Ser2 residues on the CTD, whilst Ser5 residues are progressively dephosphorylated by several different phosphatases [107]. This change in the phosphorylation status of the CTD is key to the recruitment of splicing factors [108]. Exons are defined by three major sequence elements: the 5′ splice site (5'SS),

the branch point sequence (BPS), and the 3' splice site (3'SS). A polypyrimidine tract is also located between the BPS and 3'SS. The spliceosome, a large dynamic and multimeric complex composed of over 145 proteins [109] and small nuclear RNAs (snRNAs), recognises these sequence elements and assembles and remodels in a stepwise manner on the pre-mRNA [110]. The U1, U2, U4/U6 and U5 snRNPs are critical components of the major spliceosome, responsible for removing the vast majority of pre-mRNA introns. Each snRNP consists of multiple proteins associated with one or two snRNAs. Spliceosome assembly begins with U1 binding to the 5'SS, targeted by base-pairing interactions between the U1 snRNA and the 5'SS, an interaction stabilised by other proteins in the complex [111]. During assembly, the BPS is bound by the protein SF1, whilst the U2 auxiliary factor (U2AF) interacts with the polypyrimidine tract. U2AF also binds to the 3'SS to yield the spliceosome early (E) complex [112]. Binding of U2 via the *U2 snRNA* marks the formation of the A complex. By further complex remodelling, the spliceosomal B complex is formed and this catalyses the removal of introns and the rejoining of exons [110, 111].

1.3.3.1.3 mRNA editing

RNA editing is a process that modifies the primary RNA sequence of transcripts and can occur both co- and post-transcriptionally [113, 114]. The most common form of RNA editing in mammals is the deamination of adenosine to produce inosine, a reaction catalysed by the adenosine deaminases acting on RNA (ADAR) family of enzymes [115]. Because inosine pairs preferentially with cytidine, 'I' is read as 'G' during protein synthesis or during analysis in reverse transcription reactions. Supporting the importance of RNA editing, $ADAR1^{-/-}$ mice knockouts are embryonic lethal, with the gene apparently critical for promoting cell survival [114]. In high density sequencing of a single cell line, researchers in China found RNA editing to be more common than previously expected, with 16,905 edited sites in mRNA identified [116]. In a survey of 14 different human cell lines, 85% of mRNA edited variants

were A-to-G/I changes, with the vast majority located in introns and 3′ UTRs. Genes with A-to-G/I edits were enriched in functions linked to cell division, viral defence, and translation [115]. The best-studied RNA editing sites are in coding sequences that alter the amino acid sequence, as in the case of glutamate and serotonin receptors [117], but RNA edits can also occur in microRNAs, altering their targeting [118], and result in alternative splicing due to the creation or deletion of splice sites [113].

1.3.3.1.4 Termination, cleavage and polyadenylation

The progressive phosphorylation of Ser2 and dephosphorylation of Ser5 is required for transcription termination and 3'-end processing [119]. Most protein-coding eukaryotic mRNAs have, towards their 3' end, a highly conserved poly(A) signal, AAUAAA, followed by a G/U-rich sequence, with the actual polyadenylation site occurring between these two motifs [120]. The process of termination requires several protein complexes, with the CTD acting as a scaffold for their recruitment, including cleavage and polyadenylation specificity factor (CPSF), cleavage stimulatory factor (CstF) and poly(A) polymerase [121]. The process of 3'-processing is extremely complex, with 85 proteins identified as part of the processing machinery [122]. Once Pol II transcribes the poly(A) signal, it pauses downstream, resulting in endoribonucleolytic cleavage of the pre-mRNA. The upstream product is then polyadenylated, whilst the downstream sequence is degraded [96].

1.3.3.1.5 Nuclear export

At the time of export from the nucleus, mRNAs are packaged in large mRNP complexes containing a range of proteins, including the cap-binding proteins CBP20 and CBP80, polyA-binding protein (PABP) [123], heterogeneous nuclear ribonucleoproteins (hnRNPs) and splicing factors. Nuclear export of these complexes through the nuclear envelope requires specialised embedded structures called nuclear pore complexes (NPCs) [84]. During transcription, the factors responsible for coupling transcription to export become bound to

nascent transcripts. The metazoan nuclear export factor 1 (NXF1/TAP) accounts for the export of the majority of mRNAs [124, 125], with the mRNA-protein interaction facilitated by additional RBPs, RNA export factor (REF) proteins [126]. These NXF proteins have the ability to shuttle between the nucleus and cytoplasm, and, by dimerising with NTF2-related protein 1 (NXT1/p15), function as a bridge to couple mRNPs to the NPC. Interaction with phenylalanine/glycine-nucleoporin (FG-Nup) components of the NPC results in mRNP translocation [84, 127]. Once through the envelope, mRNPs are remodelled by proteins including Dbp5 (or DDX19 in humans), an RNA helicase that interacts with the N-terminal domain of NUP214, resulting in the removal of export proteins [127, 128].

1.3.3.2 Cytoplasmic mRNA localisation

It is increasingly apparent that the distribution of mRNAs within the cytoplasm is not a stochastic event. Specific examples of targeted mRNA localisation have been known for nearly three decades [129]. For example, in *Drosophila* oocytes, the asymmetric distribution of *bicoid, oskar*, and *nanos* mRNAs in the oocyte are critical to early embryonic development [130]. Similarly, in mammalian cells, it was shown in 1997 that beta-actin transcripts are concentrated at the leading edge of migrating cells [131]. Evidence is accumulating that targeted mRNA localisation is not a rare event. In a study involving high-throughput, i*n situ* hybridisations of more than 3,000 mRNAs in *Drosophila* embryos, over 70% localised to specific cellular regions [132]. In mammalian neurons, only a relatively small number of transcripts were originally thought to localise to dendrites and synapses, but high-throughput studies suggest that over 2,000 mRNAs may show dendritic enrichment [133].

Transcripts can be transported as components of motile mRNP complexes, or RNA transport granules, coupled to the cytoskeleton with motor proteins [134]. In neurones, granules containing polyadenylated mRNA, the 60S ribosomal subunit and elongation factor 1α

(EF1α), can be visualised as moving at 0.1μm/sec [135]. RNA-binding proteins are the key determinants of transcript localisation, either by actively transporting mRNAs, trapping them in a specific region, or by altering mRNA stability in a location-specific manner [134]. This effect is typically defined by sequences present in the 3'UTR of transcripts [136]. For example, in *Drosophila* embryos, localisation of *bicoid* transcripts is due the interaction of the RBP Staufen with its 3'UTR, forming a complex that is trafficked in a microtubule-dependent manner [137]. In contrast, *hsp83* mRNA is selectively degraded throughout the cytoplasm in embryos, with the exception of the posterior pole, leading to a distinct distribution; an effect mediated by the interaction of the RBP Smaug with the 3'UTR [134]. In mammalian cells, *β-actin* transcript localisation is dependent on a 54-nucleotide sequence predicted to form a stem-loop structure. This sequence is sufficient to localise transcripts, and, by treating cells with a blocking antisense oligonucleotide, *β-actin* mRNA localisation, cell polarity and movement can be disrupted [138].

1.3.3.3 mRNA translation initiation

1.3.3.3.1 Cap-dependent translation initiation

Initiation is the rate-limiting step in translation, and is followed by elongation, termination, and ribosome recycling [139]. The majority of mRNA translation in eukaryotes is cap-dependent, requiring formation of the eIF4F initiation complex on the transcript cap. eIF4F is composed of the cap-binding protein eIF4E, the RNA helicase eIF4A, and the scaffold protein eIF4G. eIF4G possesses binding domains for the eIF4F components, but also binds to mRNA [140] and interacts with PABP, via its RRM2 domain [141]. Through simultaneous binding of cap-bound eIF4E and polyA-bound PABP at the 3' end of transcripts, eIF4G can circularise the mRNA to be translated [142], forming a 'closed loop' structure (Figure 1-8). eIF4G recruits the pre-assembled 43S pre-initiation complex (translational PIC) by interacting with the eIF3 complex. The translational PIC is composed

of the eIF3 complex and the small (40S) ribosomal subunit, together with eIFs 1, 1A and 5 and met-tRNA$_i$ anchored by GTP-bound eIF2 [139]. Following recruitment by eIF4G, the translational PIC scans the 5'UTR for complementary sequences to the anti-codon of Met-tRNA$_i$. Translation initiation occurs most efficiently for start codons located within a Kozak consensus sequence (GCCGCCA/GCC***AUG***G) [143]. Once the AUG codon is located, the PIC arrests and GTP-eIF2 is hydrolysed to GDP-eIF2, leading to PIC remodelling, and the recruitment of the large (60S) ribosomal subunit by eIF5B, to form the 80S initiation complex ready for elongation [139, 144].

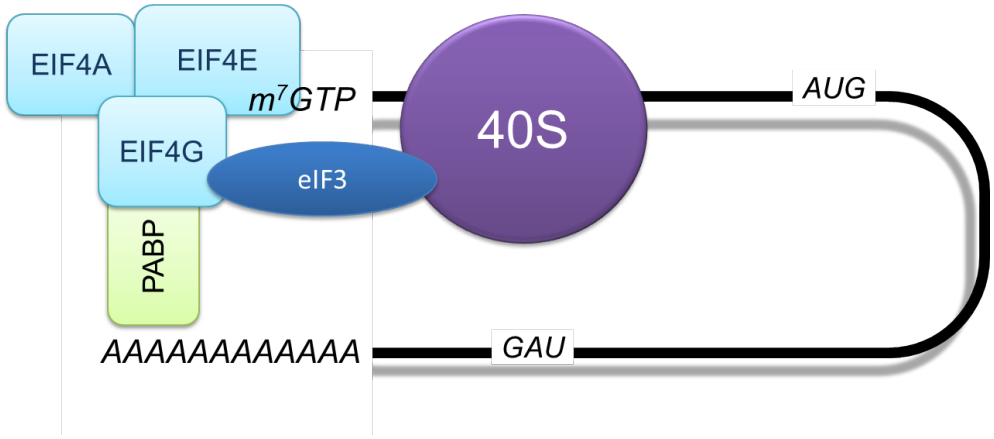

Figure 1-8. Cap-dependent translation.

Assembly of the eIF4F complex on the transcript cap results in transcript circularisation, through interactions with PABP. eIF4G also interacts with eIF3 to recruit the 40S ribosomal subunit as part of the pre-initiation complex (PIC).

1.3.3.3.2 Cap-independent translation initiation

The existence of a cap-independent mechanism of translation was discovered in 1988 from the study of uncapped poliovirus RNA, where ribosomes were found to bind a sequence within the 5'UTR to mediate translation [145]. This sequence was later termed the internal ribosome entry site (IRES). IRES-mediated translation is not restricted to viruses, and so far at least 115 eukaryotic mRNAs have been shown to have functional IRES sequences [146], with some genes translated by both cap-dependent and cap-independent mechanisms [147].

When cap-dependent translation is inhibited, for example during hypoxia [148], IRES-mediated translation provides an alternative route to allow gene expression. The sequence composition of eukaryotic IRES sites is diverse and no universal structural motif has been defined [149]. IRES-mediated translation is controlled by a number of IRES *trans*-acting factors (ITAFs), RNA-binding proteins that may be required to modulate interactions with other canonical translation components [150]. Key genes involved in cancer-related processes, such as *Myc* and *VEGFA*, have IRES sites, and IRES-mediated translation appears to be utilised by cancer cells. For example, whilst hypoxia inhibits cap-dependent translation in breast cancer cells, IRES-mediated translation of *VEGFA* is enhanced in an eIF4G- and 4EBP1-dependent manner, promoting tumour angiogenesis and growth [151]. IRES-mediated translation will be discussed again in the context of LARP3 in Section 1.4.1.

1.3.3.3.3 Translational regulation of gene expression, including 5'TOP regulation

Work in mouse fibroblasts has demonstrated that translational efficiency can vary between proteins by up to 100-fold. Indeed translational regulation appears to be more significant than transcription in determining gene expression [71]. Cap-dependent translation can be regulated globally by altering the availability of critical initiation factors to participate in translation initiation. One such rate-limiting step is the availability of eIF4E, which is targeted by the eIF4E-binding proteins (4E-BPs). When hypophosphorylated, these proteins prevent eIF4E interaction with eIF4G, thereby inhibiting cap-dependent translation. 4E-BPs are phosphorylated downstream of mTOR pathway activation, a frequent event in malignant transformation [139, 152]. Using a similar mechanistic principal, during mitosis the tumour suppressor 14-3-3σ inhibits cap-dependent translation by binding and sequestering several initiation factors, including eIF4B [153].

Efficient translation initiation requires rapid 43S scanning of the 5'UTR [139]. Therefore the structure and sequence of the 5'UTR can regulate translation. Indeed, studies have shown

that altering the GC content of the 5'UTR, or the position of hairpin structures relative to the 5' cap, can alter translational efficiency by more than 50-fold [154]. Motifs present in the UTR can be recognised by RBPs that can also block initiation. One well-characterised example of this is the iron-responsive element (IRE) in the 5'UTR of *ferritin*, involved in iron homeostasis. This conserved stem-loop structure is recognised by IRE-binding protein 1 (IRP1), which blocks the recruitment of the PIC by the cap complex [155].

Motifs present in the 5'UTR that are present in multiple different genes have the potential to activate or inhibit a program of gene expression from a single signal, regulated at the translational level. This appears to be the case for transcripts that possess a 5' UTR that starts as m7 GpppC followed by a polypyrimidine stretch, so-called 5′ terminal oligopyrimidine tract (5′ TOP) mRNAs [156, 157]. The majority of the 92 confirmed 5'TOPs so far identified encode ribosomal proteins and components of the translational machinery. During cell cycle arrest or nutrient deprivation, translation of these mRNAs is inhibited. However, following nutrient re-introduction, or the stimulation of proliferation there is a global increase in 5'TOP-mRNA translation [157]. The exact mechanism of this process is currently unknown, but occurs downstream of mTOR signalling, discovered following treatment of cells with the mTOR inhibitor rapamycin [158]. The TSC1-TSC2 proteins, tumour suppressor protein that act as upstream inhibitors of mTOR signalling, are important in the regulation of TOP translation. Deletion of either of these proteins renders cells refractory to the TOP translation-inhibiting effects of serum starvation [159]. The Meyuhas group also reported that the mTOR-mediated stimulation of TOP mRNA translation was largely independent of Raptor and Rictor expression, indicating that neither the mTORC1 nor mTORC2 complexes were involved in TOP regulation, and a new mechanism of mTOR action remained to be identified [159]. The Sabatini lab have suggested that TOP repression is mediated by the 4E-binding proteins (4EBP1 and 2) [160]; double knockout of the 4EBPs rendered TOP

translation resistant to mTOR/PI3K inhibition with Torin 1. However, the Meyuhas group found reported that 4EBP-deficient cells are not resistant to the translational repression of TOPs during oxygen or serum starvation [159], calling into question the significance of this finding. Other suggested regulators of TOPs downstream of mTOR include S6K phosphor-activity, several LARP proteins, CNBP and TIA1 [161]. 5'TOP mRNA regulation will be discussed further in Section 1.4 in the context of LARP proteins.

An additional mechanism of translational regulation is the presence of upstream open reading frames (uORFs) in the 5'UTR. Almost half of all human mRNAs possess uORFs, which are particularly common in oncogenes [162]. The presence of a uORF can regulate both mRNA translation and stability. In a global study of the effects of uORFs on translation, it was found that they can impair protein expression by up to 80% [163]. When ribosomes encounter a uORF there are three potential outcomes: they may translate the uORF and dissociate, translate the uORF and reinitiate further downstream or at a subsequent start codon, or stall on the uORF. Stalling either triggers nonsense-mediated decay [164] or creates a blockage for further ribosome progression [162]. Surprisingly, uORFs can also promote translation in the context of cellular stress [165]. ATF4 is a stress response gene with two uORFs. The second uORF overlaps the start codon of the ATF4 coding sequence. Normally, both uORFs are translated, preventing access to the ATF4 'AUG'. However, during cell stress the increased time necessary for ribosomal reinitiation reduces the probability of reinitiation at the second uORF, increasing the likelihood that the true ATF4 start codon is recognised [166].

1.3.3.4 mRNA stability and decay

1.3.3.4.1 mRNA decay

There are two major pathways for mRNA decay; deadenylation-dependent, and deadenylation-independent. Deadenylation-dependent decay (summarised in Figure 1-9), where digestion of the 5' poly(A) residues marks the first step, is responsible for the majority of mRNA degradation, [167]. Several deadenylases have been characterised, including poly(A)-specific ribonuclease (PARN) and the CCR4-NOT/Caf complex, composed of nine subunits, and representing the major deadenylase in eukaryotes [168]. Following deadenylation, transcripts are either decapped by the DCP1-DCP2 complex, allowing 5'→3' degradation by the exoribonuclease XRN1, or the exosome, a 10-12 subunit complex, digests transcripts in a 3'→5' direction [167]. This is then followed by decapping by DCPS [169]. For 5'→3' degradation, several accessory proteins are required, including the Lsm1-7 complex [168].

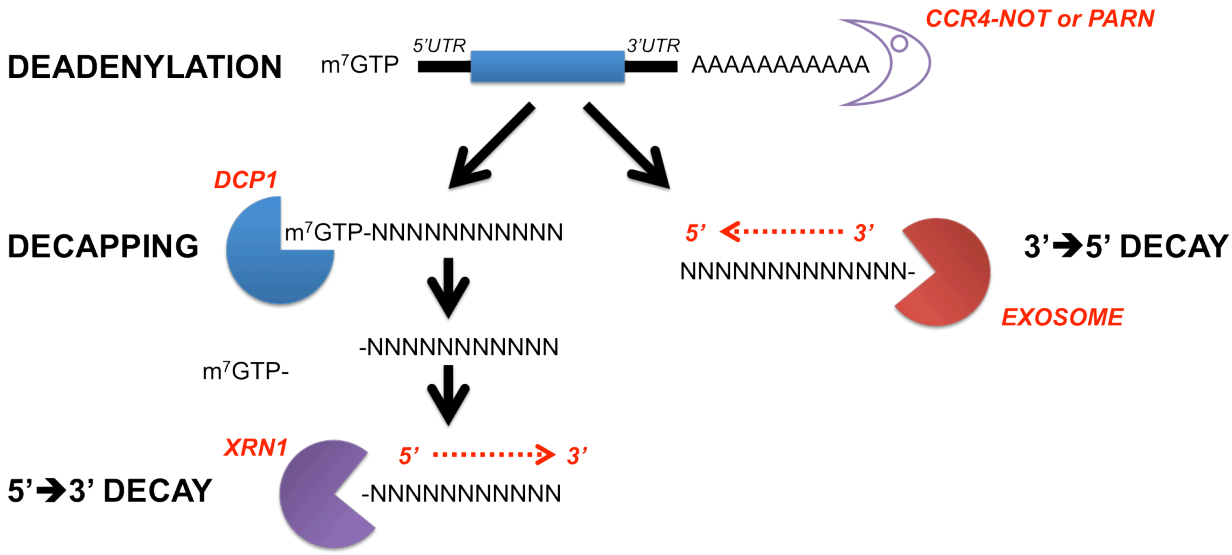

Figure 1-9. Deadenylation-dependent mRNA decay.

Following deadenylation, decay can proceed with decapping, following by 5'→3' degradation, or directly through exosome-mediated 3'→5' decay.

Many of the factors involved in mRNA degradation can be found in cytoplasmic mRNP granules called P-bodies, including Xrn1 and the CCR4-NOT complex. Transcripts that enter P-bodies can exit and re-enter translation, indication that these foci are sites of mRNA fate determination, where transcripts can be sorted for translational repression and/or degradation [170]. In contrast, stress granules are foci that lack mRNA degradation components, but contain proteins necessary for translation initiation, and are thought to represent sites of storage for translationally-stalled transcripts [167]. It has been suggested that transcripts may continuously shuttle between polysomes, P-bodies and stress granules as part of the regulation of gene expression [170] (Figure 1-7).

1.3.3.4.2 Regulating expression through mRNA stability

Modulating messenger RNA stability is a powerful tool for cells to control gene expression, determining if a transcript can be translated, and whether repeated rounds of translation are possible. Evidence suggests that there can be a huge dynamic range in mRNA half-lives. In a study investigating global mRNA stability in *Karenia brevis*, estimated mRNA half-life ranged from 42 minutes to 6 days, with a median $t_{1/2}$ of 33 hours [171]. In contrast, a study in murine embryonic stem cells found much shorter half-lives, with a median $t_{1/2}$ of 7 hours. In this study, transcripts with short half-lives were enriched for functions linked to cell cycle progression and evasion of apoptosis. Conversely, the most stable transcripts were cytoskeletal and metabolic pathway components [172], indicating that genes whose unregulated expression could have the most deleterious consequences for a cell are more likely to be heavily regulated at the level of mRNA stability. Similar results have been found in work with mouse fibroblasts [71].

This substantial variation in mRNA stability requires *cis*-acting sequence motifs and *trans*-acting RNA-binding proteins. Stability-determining motifs seem most commonly to be found in the 3'UTR, though motifs in the 5'UTR and coding sequence can also regulate mRNA

stability [173]. Underlining the importance of the 3'UTR in the regulation of gene expression, it appears that proto-oncogenes can be activated through alternative splicing of their 3'UTR, generating shorter 3'UTRs lacking regulatory motifs [174].

One of the best-characterised class of stability-regulating motifs are AU-rich elements (AREs), and they provide a useful case study to investigate the core concepts of mRNA stability regulation. AREs are composed of pentamer units of AUUUA, with or without additional A/U bases at either end, and are thought to be present in the 3'UTRs of up to 8% of human mRNAs [175]. Initially discovered in the 3'UTR of pro-inflammatory cytokines [176], stability-determining AREs have been identified in several oncogenic genes, including BCL2 and EGFR [177-179]. Underlying their importance, the deletion of the AU-rich region in TNF leads to the development of inflammatory disorders [180]. The effect of AREs on transcript stability is dependent on their recognition by specific RNA-binding proteins. Two of the best characterised are HuR and ZFP36/TTP. ZFP36, which possesses two zinc-finger domains that are critical to its mRNA-binding, acts to promote degradation of ARE-containing transcripts [181]. Work in cell-free systems demonstrated that this is due to recruitment of the exosome, mediating 3'→5' decay [182]. In contrast, HuR/ELAVL1 promotes ARE transcript stability, and may compete with ZFP36 for binding to ARE sites [183].

It is important to note that the possession of an ARE does not guarantee transcript instability. In a study of mRNA stability in a hepatocellular cancer cell line, less that 15% of transcripts with AREs had rapid decay rates [184]. It is likely that a combination of recognition motifs for RBPs and miRNAs, both in the 3'UTR and elsewhere, combine to determine the stability of a transcript. Although several stability-regulating sequences have been identified, it is likely that many more remain to be discovered. Indeed, a recent global assessment of mRNA

stability by Saeed Tavazoie's group identified eight novel RNA motifs regulating stability [173].

1.3.3.4.3 Transcriptional coupling of stability regulation

There is increasing evidence to suggest that mRNA stability can be determined co-transcriptionally. A well-studied example of this is found in the Rpb4/7 proteins. The Rpb4 and Rpb7 subunits of RNA polymerase II form a heterodimer that can bind RNA [185]. Rbp7 is indispensible to Poll II function, whilst Rpb4 is only essential during certain stresses, such as starvation. In human cells, Rpb4 and 7 are found in both the nucleus and cytoplasm [186], and during stress Rpb4 is essential for efficient mRNA transport [187]. As well as roles in transcription, Rbp4/7 appear to regulate RNA decay, with Rbp4 in particular promoting decay of translation factors, such as *RPL25* [188, 189]. Rpb4/7 therefore appears to play a role throughout the entirety of the mRNA lifecycle [190].

Stability of mRNA can also be determined at the level of the DNA promoter sequence. Researchers working with budding yeast identified *SW15* and *CLB2* as mRNAs whose stability decreased markedly during mitosis. They discovered that this decay was not due to sequences present in the 5' and 3' UTRs, but determined at the level of the promoter. They identified Ddf2 protein as being recruited co-transcriptionally to these transcripts and regulating cytoplasmic stability, potentially via a promoter-interacting transcription factor [191]. Similar findings were reported by a different group studying the stability of *RPL30* transcripts [192]. This suggests that promoter sequences may be able to determine the RBP components that assemble on nascent transcripts, and reinforces the model whereby transcripts exist in multi-protein mRNP complexes that can remain stable in the passage from nucleus to cytoplasm, where the various components determine mRNA fate.

1.3.3.5 miRNA-mediated post-transcriptional regulation

First discovered in *C. elegans* in 1993 [72, 73], microRNAs (miRNAs) are an important mechanism of post-transcriptional regulation in mammalian cells. The advent of small RNA sequencing has dramatically increased the rate of miRNA discovery [193]. The miRNA database *miRbase* had just 218 entries when it was created in 2002: the most recent release now records over 28,000 miRNA genes [194]. miRNAs themselves are ~22 nucleotide RNA molecules that act as repressors of gene expression by partial base-pairing to sequences in target transcripts, usually located within the target 3'UTR [195]. They function as part of miRNA-induced silencing complexes (miRISCs) containing argonaute protein (Ago1-4) and GW182/TNRC6A [196].

miRNAs are initially transcribed by Pol II as longer primary miRNAs (pri-miRNAs), and are capped and polyadenylated [197]. Pri-miRNAs are composed of a stem-loop structure, with terminal single-stranded RNA at the 5' and 3' ends. The microprocessor complex, comprising the RNAses Dicer and Drosha/DGCR8, cleave this to release a ~65bp hairpin structure, a pre-miRNA. Following nuclear export, the pre-mRNA loop structure is excised by Dicer to leave a ~22bp double-stranded RNA with two nucleotide 3' protrusions. One of these two strands is recruited to the miRISC [198, 199].

A 6- to 8-nucleotide sequence at the 5' end of miRNAs is most critical to determining their interaction with target transcripts, and represents a seed sequence, with each miRNA having the potential target multiple transcripts [200]. The miRISC associates with the target transcript on the basis of sequence complementarity and can induce both RNA degradation and translational repression. The timing and relative contribution of each process has been an area of intense scientific interest. Accumulating evidence now points to translational repression as the primary event, with miRISC association also capable of inducing target mRNA decapping and deadenylation [201]. The exact mechanism of translation repression remains controversial, but is thought to involve the activity of EIF4A2 [196, 202]. GW182

acts as a scaffold protein, interacting with Argonaute proteins and PABP, and recruiting the CCR4–NOT and PAN2–PAN3 complexes, which trigger deadenylation and 5'->3' decay, with CCR4-NOT appearing to play the dominant role in mRNA deadenylationa and destabilisation [201]. CNOT1, a component of the CCR4-NOT complex, has recently been shown to interact with DDX6, a translational repressor and decapping activator, implicating the complex in both translation repression and destabilisation [203, 204].

It is predicted that more than 60% of human protein-coding genes are targeted by currently known microRNAs [205], with the true figure potentially much higher. It is therefore not surprising that miRNAs have been implicated in human disease, and particularly in cancer development and progression, where they have been shown to behave as both tumour suppressors and oncogenes [206].

1.3.4 RNA-BINDING PROTEINS IN CANCER

Given the propensity of tumours to hijack normal cellular processes, it is perhaps not surprising that this protein class, with a diverse range of functions, have been increasingly implicated in cancer [207-209]. Indeed, their central role in the regulation of expression is making RBPs attractive targets for a new generation of anti-cancer drug development [210].

In all normal tissues studied, expression of RBPs is greater than that of non-RBPs, with the highest levels found in the ovaries, testis and lymph nodes [75]. Interestingly, these are tissues with high rates of cell division. In a global analysis of nine cancers, RBPs as a protein class were found to be more highly expressed compared to other genes, such as miRNAs and transcription factors. Investigating expression in cancer and normal tissue, thirty RBPs were found to have significantly dysregulated expression across multiple cancer types, with all more highly expressed in malignancy. These included RBM3 and FLNA, both previously implicated in cancer. This suggests a net oncogenic role for RBPs [75].

The first RBP to be implicated in cancer was eIF4E. As discussed above (Section 1.3.3.3), eIF4E is an mRNA cap-binding protein that, as part of the eIF4F complex, plays a central role in cap-dependent translation [139]. In the early 1990s, expression of eIF4E was shown to be upregulated in transformed cells [211], whilst forced overexpression of was eIF4E was found to be capable of transforming non-malignant cells [212, 213]. The protein has subsequently been shown to be overexpressed in a range of malignancies, including prostate, breast and colon cancers [214]. eIF4E-overexpressing transgenic mice display increased rates of tumour development, including lung adenocarcinomas and angiosarcomas [215].

Since the discovery of the oncogenic role of eIF4E, RBPs with functions throughout the RNA lifecycle have been identified as potential oncogenes. Alternative splicing is an important mechanism of generating genetic diversity, and is tightly controlled during normal development. Over 15,000 splice variants have been associated with cancer [216], and the novel isoforms generated can act as drivers of malignant progression. One example of this is CD44, where expression of a variant isoform promotes tumour metastasis [217]. The RBP Sam68 binds to the splice regulatory sequence in CD44 variant exon 5 and regulates its inclusion in response to phosphorylation by ERK. Knockdown of Sam68 abolishes expression of the variant isoform [218]. Sam68 expression is upregulated in a number of cancers, including prostate cancer, where it has been shown to promote proliferation and chemoresistance [219]. Several other Sam68 splice targets have been identified, including cyclin D1 [220].

The stability of individual mRNAs is tightly controlled, with transcripts with potentially oncogenic roles within the cell tending to have dramatically shorter half-lives [71, 172]. Altering mRNA stability provides cancer cells with the ability to silence tumour suppressors or activate proto-oncogenes at the post-transcriptional level. One well-characterised example is HuR/ELAV1, a stability-regulating RBP that is highly expressed in many malignancies,

including ovarian, prostate and colon cancers [74]. HuR binds AU-rich elements, and can have a dual role on RNA stability, stabilising oncogenic transcripts such as VEGF [221] whilst promoting decay of transcripts encoding the tumour suppressor p16INK4 [222].

RBPs can also activate specific translational programs, via recognition of 5'UTR motifs such as IRES sites or 5'TOP motifs, with significant implications for malignant potential. This will be discussed in greater depth in the context of the LARP proteins in Section 1.4.

1.3.5 SUMMARY

Cancer is a disease characterised by altered gene expression. For the past four decades, the focus in cancer research has been on studying this altered expression at the level of transcription and genomic/epigenomic changes. However, the significance of the substantial contribution of post-transcriptional regulation is now beginning to be appreciated in the context of this disease.

Although conventionally represented as distinct processes, there is accumulating evidence that transcription and mRNA fate determination are tightly linked, to the extent that non-transcribed DNA sequences appear to be able to determine the stability of the transcribed product. Transcripts are assembled co-trancriptionally with RNA-binding proteins into messenger ribonucleoprotein complexes, and the RBP components determine the localisation and fate of the complexed mRNA.

RBPs are involved at all stages of post-transcriptional regulation, sometimes acting as components of multiprotein complexes, such as the spliceosome. Although over eight hundred experimentally validated RBPs have been identified, relatively few have been studied in significant depth. However, the high expression of RBPs in both normal tissue and cancers underlines their functional significance. The RBPs that have been intensively studied

to date have shown critical roles in malignant progression. It is likely that further study of individual RBPs will lead to significant advances in our understanding of cancer development and present novel avenues to target malignant disease.

1.4 THE LARP FAMILY

The La-Related Protein (LARP) family are a highly conserved group of RNA-binding proteins [223, 224]. The first family member to be identified was SSB/La, now known as LARP3. All family members share a unique N-terminal or central RNA-binding domain, named the La motif (LAM), separated from an RNA recognition motif (RRM) by a short linker. Human LARP3 and LARP7 also possess an additional RRM [225, 226]. In a key paper published in 2009, Jean-Marc Deragon and Cécile Bousquet-Antonelli analysed genomes from 83 eukaryotic species to arrive at a proposed evolutionary structure of the protein family [223], with seven distinct LARP genes in humans; LARPs 1/1a/3/4/4b/6/7 (Figure 1-10). LAM-containing proteins are present in nearly all eukaryotes, but absent from Archaea, suggesting they originated shortly after the eukaryotic evolutionary radiation [223], 1-2,000 million years ago [227]. In high-throughput experiments to derive the mRNA-bound proteome, all LARPs, with the exception of LARP6, have been identified [87, 228].

Only in the last five years has the diversity and functional significance of this protein family begun to be uncovered. It now appears clear that, despite sharing similar RNA-binding domains, these proteins have markedly different roles within the cell, participating in multiple aspects of post-transcriptional regulation. There is accumulating evidence linking this protein family to human disease and, in particular, to cancer.

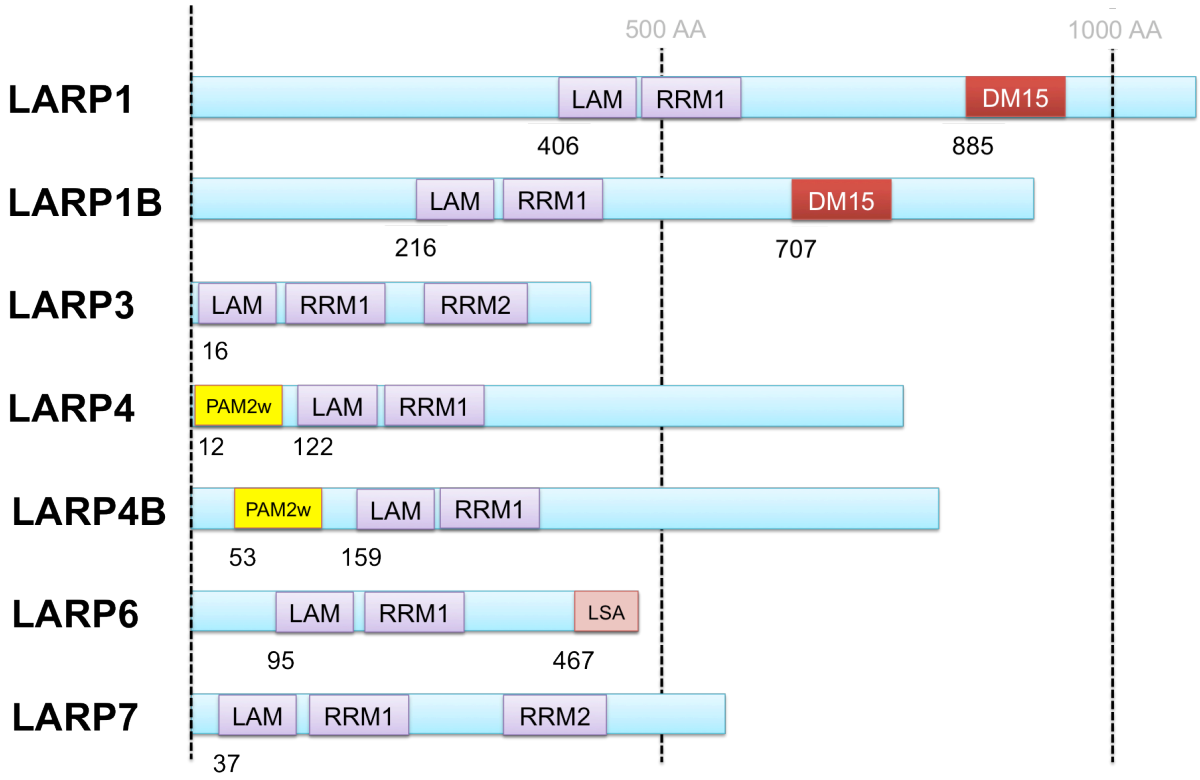

Figure 1-10. The human LARP family of proteins.

A scaled diagram of human LARP proteins, indicating the key domains. Numbers underneath indicate the first residue of the domain.

1.4.1 LARP3/LA/SSB

1.4.1.1 LARP3 functional roles

Originally identified as a serological marker of autoimmune disease, particularly Sjögren's syndrome [229, 230], LARP3/La/SSB has been studied in much greater depth than other members of the LARP family. This small, highly abundant protein [231] plays a role in an expanding number of post-transcriptional processes. Reinforcing its critical role in cell biology, LARP3 is essential in mice at a very early stage in development, where it is required for the formation of the inner cell mass [232]. The same is true in *Drosophila,* with LARP3 knockouts surviving only to the late larval stage [233]. Whilst LARP3 can be deleted from yeast cells without inducing death, a feature that facilitates studies of its function in this system, it becomes lethal when combined with mutations disrupting the secondary structure

of essential tRNAs [234]. Conditional deletion of LARP3 in mice haematopoietic B cells results in a blockage in B cell development beyond an early pro-B stage, and the absence of mature B cells and serum IgG. A similar approach with forebrain neurones showed mice developed normally up to 5 weeks, but then showed a progressive neuronal loss suggestive of impaired cell survival [235].

1.4.1.1.1 tRNA processing

Early on, it was discovered that RNPs identified by anti-LARP3 antibodies contained RNA polymerase III products. LARP3 was subsequently shown to bind with high affinity to 3' uridylate residues, characteristic of the majority of nascent Pol III transcripts [236, 237]. These UUU-3'OH tails are removed during processing and maturation, abolishing LARP3 binding [226, 238]. LARP3 plays a role both in stabilising pre-tRNA transcripts by 3' end protection (excellently reviewed by [238] and [226]), as well as having tRNA chaperone activity [239-241]. RNA chaperones are proteins that promote the correct folding of RNA, requiring the ability to dissociate and refold aberrantly folded RNA structures. Interestingly, this chaperone activity appears to be conserved in LARPs 4, 6 and 7 [241]. As well as a role in tRNA maturation, LARP3 also binds other Pol III transcripts, such as pre-5S rRNA, which share 3'-oligo(U) sequences [242], and stabilises small RNAs including the U3 snoRNA in yeast [243].

1.4.1.1.2 IRES-mediated translation

Shortly after the discovery of poliovirus as the first IRES-containing RNA [145], a protein bound to the 5'UTR sequence was identified as LARP3. LARP3 was subsequently found to promote poliovirus RNA translation [244, 245], marking it as the very first IRES *trans*-acting factor (ITAF). Poliovirus infection was also found to cause a relocalisation of LARP3 from the nucleus to the cytoplasm [244]. This is associated with C-terminal cleavage of LARP3 at

Gln358/Gly359, with the truncated N-terminal product promoting translation of viral RNA in the cytoplasm [246].

Following the discovery of the poliovirus IRES, LARP3 was subsequently found to bind the 5'UTR of Hepatitis C RNA and promote its translation in an IRES-dependent manner [247, 248]. Several other viral targets have been subsequently identified [238, 249]. The translation of several cellular IRES-containing mRNAs, such as *XIAP* and *BiP*, were also found to be promoted by LARP3 [250-252].

1.4.1.1.3 5'TOP mRNA translation

The role of LARP3 in the promotion of translation is not restricted to IRES-containing mRNAs. In 1996, it was found that two proteins bound to the 5'TOP sequence of ribosomal mRNAs in *Xenopus* embryos represented LARP3, and a cleavage product of the full length protein [253]. The same group subsequently showed that the effect of binding was to promote translation [254]. Cytoplasmic LARP3 has also been shown to bind 5'TOP mRNAs in human cells, though the role in translation has not been characterised [255]. LARP3 may not always act to promote translation. In an *in vitro* system, LARP3 was capable of repressing the translation of the 5'TOP EF1A, an effect abolished when the TOP sequence was mutated [256].

1.4.1.1.4 Additional LARP3 functional roles

Several additional roles for LARP3 in human cells have been suggested. Human LARP3 has been shown to interact with telomerase RNA, with LARP3 overexpression associated with telomere shortening [257]. LARP3 has also been suggested to play a global role in microRNA maturation, by binding to the stem-loop structure of pre-mRNAs and stabilising them, a process requiring all RNA-binding domains [258]. LARP3 has been demonstrated to regulate gene expression in a novel manner through mRNA localisation. The protein was

shown to bind the 3'UTR of peptidylglycine α-amidating monooxygenase (PAM) mRNAs, at the sequence UUAAAAUCACUAACA. In a process dependent on the NRE, increased LARP3 expression led to sequestration of *PAM* mRNAs in the nucleus, and reduced PAM expression [259].

As well as following poliovirus infection, translocation of LARP3 from the nucleus to the cytoplasm occurs during apoptosis, induced by either chemotherapy or UV irradiation [260, 261]. Cleavage occurs at Asp374, potentially by activated caspase-3, with the N-terminal region lacking the nuclear localisation signal (NLS) found in the cytoplasm [261]. Following the induction of apoptosis in keratinocytes, LARP3 is also found in 'apoptotic blebs', structures at the surface of apoptosing cells [262], suggesting that following translocation from the nucleus to the cytoplasm, LARP3 may then be transported to the cell membrane. The functional significance of these movements has so far not been explained.

1.4.1.2 LARP3 Structure

LARP3 is currently the only LARP family member for which three-dimensional structural data is available. The RRM1 motif of LARP3 has a classical structure, with a four-strand β-sheet backed by two α-helices, though the arrangement of the terminal α-helix is atypical. The La motif itself possesses a variant winged-helix structure, with three helical insertions. These two domains, separated by a short linker, appear to function together to bind RNA [225, 263-265], with just two terminal uridylates sufficient for strong binding [265]. Unusually, no contact is seen between the RRM1 β-sheet surface and RNA in crystal structures [264, 265], and this appears to represent a separate RNA-binding region, important for tRNA maturation and the RNA-chaperone function of LARP3 [239, 240].

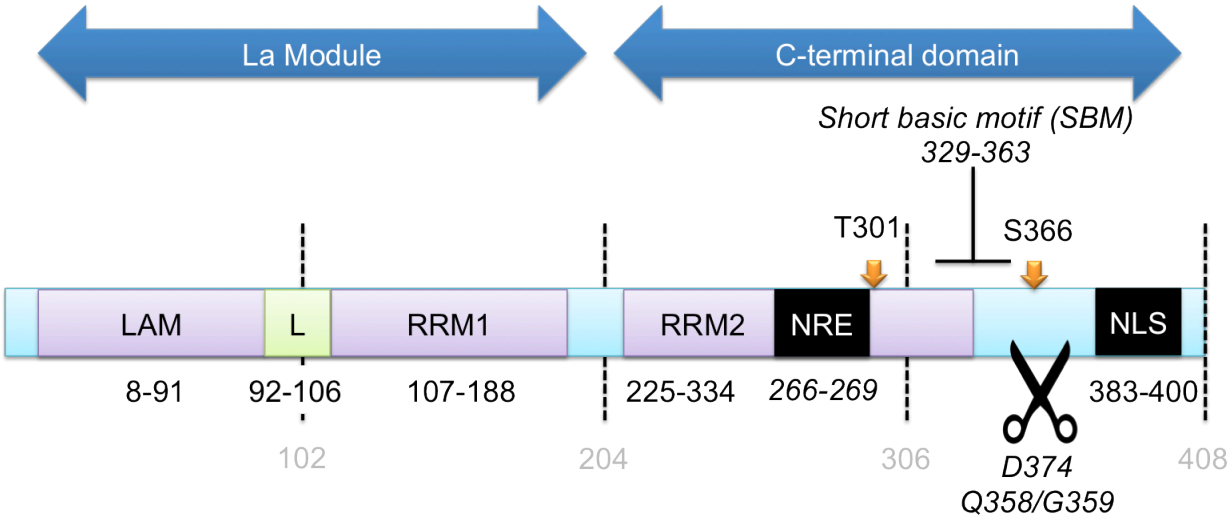

Figure 1-11. LARP3 protein architecture.

Schematic detailing the LARP3 protein structure. Residue positions are marked in grey. Key phosphorylation sites are marked with orange arrows. Approximate amino acid positions for each protein region are given below the domain. The NRE critical residues are given, though a region from residues 165 to 337 may be required [266]. A region of potential cleavage is marked by scissors (D374 = apoptosis [261], Q358/G359 = poliovirus [246]) . LAM = La Motif, L = linker region, NRE = nuclear retention element, NLS = nuclear localisation signal.

The C-terminus of the protein (residues 225-408) contains an atypical RRM, that does not regulate polyU binding, followed by a lengthy unstructured region [267]. This second RRM has been suggested to be important for other RNA interactions, such as that with HBV RNA [268]. The C-terminal region of LARP3 was found to exist as a monomer in solution [267], though previous groups have suggested it contains a dimerisation domain [269]. Other functions have also been localised to this C-terminal region. Radiolabelled LARP3 injected into *Xenopus* oocytes translocates into the nucleus, and a nuclear localisation signal (NLS) at residues 383 to 400 was shown to be responsible. In addition, retention of LARP3 within the nucleus requires a nuclear retention signal or element (NRE), located within residues 165 to 337, with amino acids 266-269 shown to be essential [266]. This nuclear retention element also appears to be critical for LARP3-mediated tRNA processing. Mutant LARP3 lacking the element enters the nucleus to stabilise nascent tRNA, but these tRNA are no longer 5'- and 3'-processed and exported, and accumulate in the nucleus in complex with the mutant

protein [270]. The effects of the NRE are opposed by the RRM1, which appears to promote nuclear export [271].

Phosphorylation of LARP3 also appears to be associated with localisation and function. Within the C-terminal domain is a short basic motif (SBM), which is important for RNA Pol III transcriptional activity [272, 273]. LARP3 protein phosphorylated just after this region, at serine 366, is found in the nucleoplasm bound to nascent tRNAs, whilst non-phosphorylated LARP3 is cytoplasmic and associated with 5'TOP mRNAs [255, 274]. This phosphorylation is accomplished in yeast by the protein kinase CK2, thereby inhibiting 5'TOP mRNA translation [274, 275].

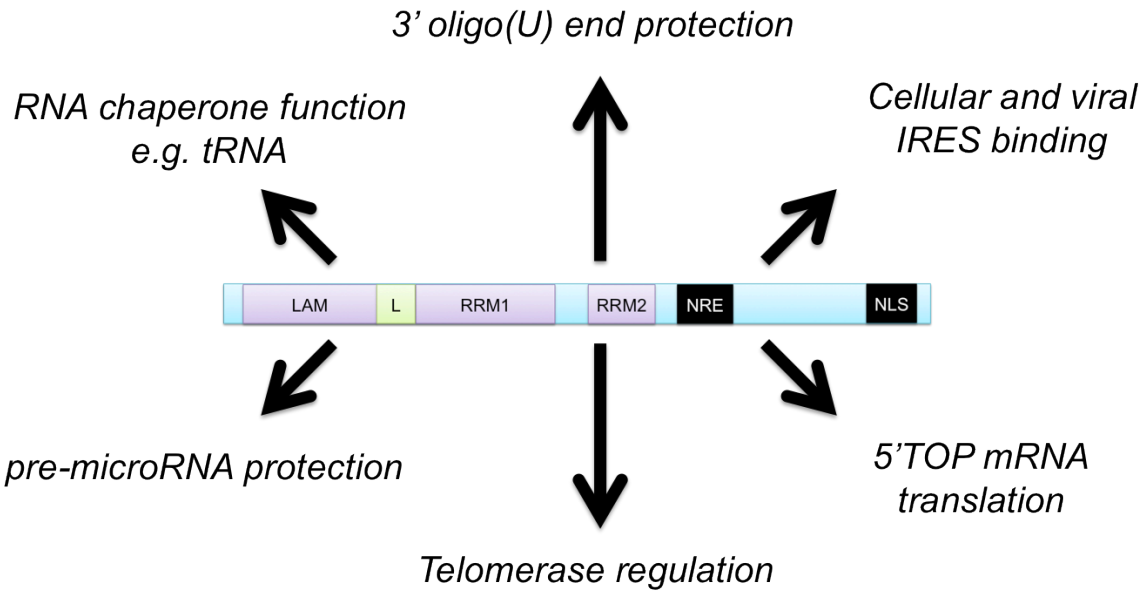

Figure 1-12. Summary of LARP3 reported cellular functions.

1.4.1.3 A role for LARP3 in cancer

Accumulating evidence supports a role for LARP3 in cancer development and progression. Expression is upregulated in cervical cancer tissue and in oral squamous cell carcinomas compared to normal controls [252, 276], as well as in multiple cancer cell lines [277].

LARP3 knockdown reduces cell proliferation in HeLa cells, without inducing apoptosis [252], although the authors did not find a cell cycle shift that could explain this change in proliferation. This effect is mediated by the binding of LARP3 to *Cyclin D1* (CCND1) transcripts, where it promotes their translation in an IRES-dependent manner [252]. Knockdown of LARP3 is also associated with reduced migration and invasion, an effect that may be mediated via the regulation of metalloproteinase expression [276]. LARP3 has also been linked to the epithelial-mesenchymal transition (EMT) in hepatocellular cancer, as the protein promotes translation of the IRES-containing transcripts of *laminin B1*, identified as a potential EMT driver [278].

Akt pathway activation is a common event in cancer [279], and work in mouse glial cells has demonstrated that LARP3 is phosphorylated by Akt at T301 [280]. This phosphorylation stimulates translocation of LARP3 protein from the nucleus to the cytoplasm. Investigating LARP3-bound transcripts, and cross-referencing this with shifts in polysomal association, LARP3 was found to preferentially regulate the translation of over 200 transcripts, including key cancer-related genes such as *VEGF*, *PDGFA*, and *BCL2L11* [280].

As discussed above, following the induction of apoptosis with UV irradiation or chemotherapy treatment, LARP3 undergoes proteolytic cleavage. The N-terminal fragment localises to the cytoplasm where it binds mRNA [261], and can act to promote IRES-mediated translation. LARP3 promotes the IRES-mediated translation of X-linked inhibitor of apoptosis protein (XIAP), a regulator of programmed cell death that inhibits apoptosis in response to DNA damage [250]. This suggests LARP3 may play a role as a cytoplasmic apoptosis inhibitor, in response to pro-apoptotic stimuli. LARP3 also enhances translation of *Nrf2* [281], a transcription factor implicated in the evasion of apoptosis via BCL2 upregulation [282]. An anti-LARP3 monoclonal antibody has been suggested as a potential mechanism for monitoring cell death in response to chemotherapy [283].

LARP3 protein has also been implicated in haematological malignancy. The characteristic genetic abnormality in chronic myeloid leukaemia (CML) is a t(9:22) translocation, creating the BCR/ABL fusion oncogene [284]. This fusion protein upregulates LARP3 expression and, in turn, promotes the translation of MDM2. MDM2, like BCR/ABL, is present at high levels in patients with CML, where it acts as a negative regulator of p53. In this scenario therefore, it appears that LARP3 acts as the effector of a key oncogene [209]. Work in myeloproliferative neoplasms (MPN) has identified a similar role for LARP3. A gain of function mutation in JAK2 (V617F), which is extremely common in MPN, was found to result in increased p53 stabilisation, mediated by enhanced translation of MDM2 by LARP3 [285]. Potential inhibitors of the LARP3-RNA interaction have recently been identified, and found to have biological activity in the inhibition of hepatitis B viral antigen production [286]. This suggests that it may be possible to generate anti-cancer therapies based around the disruption of the function of LARP3 in neoplastic cells.

1.4.2 LARP7

1.4.2.1 Structure and function

LARP7 is the only LARP family member to contain a canonical RRM1 as found in LARP3 protein, whilst the other LARP members contain RRM1-like domains [223]. LARP7 is also the only human LARP, apart from LARP3, to possess a second C-terminal RRM domain [226]. To date, only one RNA target has been confirmed for LARP7 in any given species, though the fact that it has been detected in mRNA pulldown experiments suggests other targets may exist in mammalian cells (Table 1-6) [87, 228]. Also known as PIP7S, human LARP7 binds the 7SK RNA. In *Tetrahymena* and *Euplotes*, both protist species that lack a 7SK RNA, the LARP7 homologues p65 and p43 bind and stabilise telomerase RNA [287-290].

Human 7SK RNA is an abundant small nuclear RNA (snRNA) synthesised by RNA pol III [291, 292]. The 7SK snRNA, as part of the 7SK snRNP (small nuclear ribonucleoprotein particle), which also includes methylphosphate capping enzyme (MePCE) and HEXIM1/2 [293], acts as an inhibitor of the pro-transcriptional effects of the P-TEFb complex. As discussed above (Section 1.3.3), P-TEFb is composed of CDK9 and cyclin T1, which promotes Pol II transcription elongation by phosphorylating DSIF, NELF and the CTD of Pol II [96, 97, 107]. The 7SK snRNP also plays a role in regulating alternative splicing [294]. Three papers published in 2008 showed that LARP7 binds the majority of 7SK RNA in a 3′-UUU-OH-dependent manner, and is a key component of the 7SK snRNP [295-297]. This binding is associated with increased 7SK RNA stability and P-TEFb sequestration, with an associated drop in Pol II-mediated transcription [295, 296]. The inhibitory effect requires both the N- and C-terminal regions of LARP7 [296]. Residues 375-589 are critical for interaction with the P-TEFb component CDK9 [297]. LARP7 is also required as part of the 7SK snRNPs role in alterative splicing [294]. Interestingly, LARP7 was shown to bind the 5'TOP motif of S16 *in vitro*, an effect abolished by changing the first six nucleotides of the TOP sequence [297]. Whether this binding can be recapitulated *in vivo*, and its functional significance, has not yet been explored.

Work in mouse embryonic stem cells (ESCs) has suggested that LARP7 knockdown may not always be associated with increased P-TEFb activity, possibly due to compensatory decreases in CDK9 protein expression. Instead, LARP7 knockdown leads to a shift from a naïve to primed ESC state, associated with decreased Lin28 expression, due to alterations in *Lin28* mRNA stability, and not P-TEFb-mediated transcriptional inhibition [298]. As well as expression in mouse ESCs, LARP7 is expressed throughout mouse embryos [299], suggesting it may play a crucial role in development. Interestingly, two independent studies of patients with an inherited disorders resulting in intellectual disabilities with microcephaly

or primordial dwarfism, identified frameshift mutations in LARP7 as the likely cause [299, 300].

1.4.2.2 A role for LARP7 in cancer

LARP7 may play a key role in suppressing malignant transformation. Knockdown of the gene in a benign mammary epithelial cell line, with an associated decreased in 7SK RNA abundance, led to the formation of three-dimensional colonies that were disorganised and showed irregular borders, comparable to those seen with malignant cells. This was associated with disruptions in cell polarity and increased proliferation, and enhanced expression of oncogenes parathyroid hormone-like hormone (PTHLH) and transglutaminase 2 (TGM-2). These transformational effects were reversed by treating cells with 5,6-dichloro-1-β-D-ribofuranosylbenzimidazole (DRB), an inhibitor of P-TEFb activity, confirming transformation is mediated in a P-TEFb-dependent manner [296]. In addition, analysis of LARP7 expression in breast cancer samples demonstrated low levels in invasive cancer samples compared to controls, with patients with the lowest expression having worse overall survival [301]. LARP7 knockdown in breast cancer cell lines promoted cell motility and enhanced invasion and cell metastasis *in vivo*. This effect is mediated, at least in part, through the reversal of P-TEFb inhibition, which leads to transcriptional activation of genes associated with epithelial-to-mesenchymal transition [301].

A screen of microsatellite loci of patients with microsatellite-unstable gastric cancer identified a fameshift mutation at residue 330 of LARP7, due to microsatellite instability, in over 40% of cases: 7% of colorectal cancers with microsatellite instability also exhibited the same mutation [302]. LARP7 expression was subsequently shown to be significantly reduced in tissue from gastric cancers, compared to control tissue. In non-malignant gastric cells, LARP7 knockdown led to increased cell proliferation and enhanced migration,

associated with decreased abundance of 7SK RNA [303]. LARP7 expression is also downregulated in tumours from patients with lymph node-metastatic cervical cancer, compared to those with localised disease [304], suggesting a potential role in metastasis.

1.4.3 LARP 4 AND 4B

The LARP4 subfamily is the least studied to date. Two LARP4 genes are present in the human genome, LARP4 and LARP4b (previously LARP5) [223], which share 37% amino acid identity and 53% sequence similarity [226]. LARP4 proteins are absent from plants and yeasts, with a single copy in most invertebrates [223]. A gene duplication event is likely to have occurred early within the vertebrate lineage, with sequence divergence to form the two variants [224]. LARP4 and 4B show less La Motif conservation with LARP3 than LARP7, particularly in the side chains needed for 3'UUU-OH binding [226], suggesting they may interact with different RNA targets. In contrast to LARP3 and 7, LARP4 and 4b are predominantly cytoplasmic proteins. Both also accumulate in stress granules following arsenite treatment [305, 306].

Both LARP4 and 4b possess a PAM2-like sequence in the N-terminal region, referred to as the PAM2w due to replacement of a conserved phenylalanine residue with tryptophan [306]. PAM2 motifs are conserved 15 amino acid sequences involved in binding to polyA binding proteins (PABPs), at the PABPC domain, and are found in other PABP-interacting proteins such as eukaryotic translation termination factor 3 (eRF3) [307]. There are three cytoplasmic PABPs in humans, which play a critical role in mRNA translation and modulating mRNA stability [308, 309], with PABPC1 also able to shuttle between the nucleus and the cytoplasm [310]. PABPN1, the nuclear variant of PABP, is involved in the synthesis of the poly(A) tails of nascent transcripts, and also appears to regulate alternative cleavage and polyadenylation of mRNA [309, 311]. Both LARP4 and 4b interact with PABP via the PAM2-like motif

[305, 306], which appears highly conserved, an interaction enhanced by poly(A) RNA [306]. The C-terminus of LARP4, in addition to the PAM2w region also appears to interact with PABP.

LARP4 and 4b also bind RACK1 [305, 306], a scaffold protein that interacts with the 40S ribosomal subunit [312]: the C-terminus of LARP4b contains the interaction domain [305]. Supporting a role in translation, LARP4 and 4b co-sediment with polyribosomes, and knockdown results in a 20-40% decrease in overall protein synthesis [305, 306]. In contrast to LARP4b, LARP4 has also been suggested to promote mRNA stability [306].

The N-terminal region of LARP4 binds RNA, with a greater affinity for poly(A) sequences than poly(U), and does not bind poly(C) or (G). The sequence length appears significant, with 15 nucleotides required for strong poly(A) binding [306], in contrast to LARP3, where a 10 nucleotide sequence with only two terminal uridylate residues was sufficient for high-affinity binding [265]. A LARP4 RNA-IP with microarray analysis (RIP-CHIP) experiment identified ~2000 mRNAs in complex with the protein, though with no apparent enrichment for particular functional (GO) terms [306].

Only one cancer-related study could be identified for the LARP4 family. Here, knockdown of LARP4 in prostate cancer-derived PC3 cells produced elongated, bipolar cells with increased cell motility [313]. The patterns of expression and significance of both proteins in cancer cells remains to be determined.

1.4.4 LARP6

Although plants possess three LARP6 genes, humans have a single copy. In addition to the LAM-RRM, the LARP6 family also possess a conserved C-terminal domain of unknown significance, named the La- and S1-associated (LSA) motif. This is similar to a motif found

in CSP1 proteins, which also possesses an S1-like nucleic acid-binding domain [223]. Unlike LARP4 proteins, LARP6 has preserved the amino acid residues critical to UUU-3′OH recognition in LARP3 [226]. LARP6 also possesses a functional nuclear export sequence (NES) and nuclear localisation signal (NLS), and is found in both the nucleus and cytoplasm [314-316]. Highest expression of LARP6 is seen in the brain, with heart, skeletal and testicular tissue also showing strong expression [314].

The first paper describing LARP6 was published in 2007, where it was identified in a screen of genes expressed in intersegmental muscles (ISM) of the moth *Manduca sexta* during programmed cell death at the end of metamorphosis [314]. LARP6 appears to play a role in myogenesis [317, 318]. Work in murine C2C12 myoblast cells, which can differentiate into either multinucleated myotubes, satellite-like cells, or undergo apoptosis, demonstrated that LARP6 promoted myotubule differentiation. The apoptosis normally seen when C2C12 are induced to differentiate was enhanced by LARP6 overexpression [317]. The mechanism by which LARP6 mediates these effects has not yet been elucidated.

Only one direct RNA target of LARP6 has so far been identified; the conserved stem-loop found in the 5'UTR of *collagen alpha 1(I), alpha 1(II)* and *alpha 1(III)* mRNAs. This structure plays a role in regulating transcript translation, and is required for the proper assembly of the collagen triple helix [319]. LARP6 binds the stem-loop of all three transcripts, with both the LAM and RRM required. Cai *et al* found that overexpression of LARP6 inhibited mRNA translation of all three transcripts, but LARP6 knockdown also produced the same effect [316]. They concluded that LARP6 at physiological levels promoted translation. The effect of LARP6 on the promotion of collagen mRNA translation appears to involve the recruitment of RNA Helicase A, through interaction with the C-terminal region of LARP6 [320]. LARP6 may also regulate mRNA stability, potentially by

mediating the interaction between vimentin filaments and collagen transcripts [321]. LARP6 binding to the 5'UTR also seems necessary for determining transcript localisation [316].

In a yeast 2-hybrid screen, LARP6 was found to interact with calcium/calmodulin-dependent serine protein kinase-C (CASK-C) [322]. This protein has been identified as a potential oncogene in gastric, colorectal and oesophageal cancer [323-325], relying on binding partners for its localisation [326]. The C-terminal region of LARP6 (residues 373-472) were sufficient to recapitulate binding [322].

1.4.4.1 A LARP6 role in cancer

A review of a small breast cancer study revealed higher LARP6 expression in basal-like tumours compared to normal mammary epithelium [315]. Overexpression of LARP6 in MDA-MB-231 cells enhanced proliferation and invasion, associated with increased expression of matrix metalloproteinase-9 (MMP-9) and vascular endothelial growth factor (VEGF). LARP6-overexpressing cells generated significantly larger tumours *in vivo,* compared to controls, with a significant increase in VEGF expression and tumour angiogenesis [315]. Work in Eahy926 cells, derived from the human umbilical vein endothelial cells (HUVECs), also supports a role for LARP6 in angiogenesis, where it has been shown to promote proliferation and apoptosis-evasion [327]. LARP6 also promotes VEGF expression in HUVECs following trauma [328], whilst it appears to undergo alternative splicing in hypoxic cells [329].

1.4.5 LARP1 AND 1B

In humans, there are two LARP1 proteins, LARP1 and LARP1b, whilst *Arabidopsis* and other plants have a third gene, LARP1c [223]. LARP1 and 1b, which share 59% sequence identity and 73% similarity, likely represent an ancient gene duplication event, as both are found in multiple lineages [226]. LARP1 proteins possess the LAM-RRM structure without

a second RRM and, in addition, the majority also have a C-terminal motif named the DM15 region [330]. This motif is composed of one to four tandem repeats, and is found only in LARP1 proteins. It is highly evolutionarily conserved, with 12 amino acids conserved in 90%–100% of the species investigated in one study [223], and has been suggested to possess RNA-binding properties [330]. All studies to date have focused on the function of LARP1, and not LARP1b, and LARP1 therefore forms the primary focus of the following section.

1.4.5.1 LARP1 mRNA binding

Both LARP1 and LARP1b have been identified in high-throughput experiments as binding to mRNA [87, 228]. The amino acids in the LAM required by LARP3 for UUU-3'OH binding are conserved in LARP1 [226]. In RNA-sepharose pulldowns, *C. elegans* LARP1 was precipitated with both poly(U) and poly(G), but not by poly(A) or poly(C). Full length LARP1 protein was required for maximal binding, but unlike LARP3, the C-terminal region, which contains the DM15, was still able to bind both polynucleotide sequences [330]. In contrast, human LARP1 has been reported to only bind poly(A) sequences [331]. Using an artificial construct containing an *in vitro* transcribed portion of the *ACTB* 3'UTR that was 5'-capped and polyadenylated, Aoki *et al* pulled down associated proteins and characterised them with tandem mass spectrometry [331]. LARP1, 1B, 3, 4 and 4B were identified in this pulldown as 3'UTR-associated factors, but not LARP6 or 7. However, only the binding of LARP1 and 1B, together with proteins such as PARN and PATL1, were abolished by the addition of an extra 35nt sequence, after the $polyA_{60}$ tail. Subsequent experiments demonstrated that binding was not dependent on the 5'cap, but was determined by polyA tail length, with a minimum of nine adenosine residues required. 3'UTR constructs ending with poly(C), (U) or (G) showed no binding, whilst swapping the last residue of the A_9 sequence for a different nucleotide almost totally abolished LARP1 binding [331]. It is worth noting that all the RNA binding experiments detailed in this paper utilised an artificial construct

containing a portion of the *ACTB* 3'UTR. However, in the same paper, the authors demonstrate that LARP1 binds ACTB mRNA. In addition, I report in this thesis that ACTB mRNA expression increases on LARP1 knockdown (see Section 3.4.1), suggesting that LARP1 may directly regulate ACTB mRNA stability and translation, potentially by binding sequences in the 3'UTR. The use of the *ACTB* 3'UTR in the experiments of Aoki *et al* could therefore have influenced the outcome of these reported experiments [331].

1.4.5.2 mRNA stability

As would be expected for a poly(A)-binding protein, Aoki *et al* reported LARP1 immunoprecipitated all mRNAs tested, with minimal binding of ribosomal and histone RNAs. LARP1 knockdown was associated with decreased abundance of 5'TOP mRNAs, such as *RPS6* and *RPL7*, but not non-TOP transcripts, such as *GAPDH*. This decrease was not associated with a change in pre-mRNA levels, and the authors concluded that this therefore represented a selective effect on 5'TOP mRNA stability [331]. The mechanism by which the 3'-associated protein was interacting with a 5' motif was not established.

Further evidence of a role in stability comes from a study of LARP1a in *Arabidopsis*. Heat stress-induced global mRNA downregulation was impaired in LARP1a$^{-/-}$ cells: over 1,000 transcripts that showed decreased abundance in heat-stressed wild-type plants did not alter in LARP1a$^{-/-}$ plants, an effect mediated at the level of RNA stability [332]. LARP1a was shown to with an N-terminal region of the 5' exonuclease XRN4 in a heat stress-dependent, but RNA-independent, manner: knockdown of either LARP1a or XRN4 reduced mRNA decay of selected transcripts on heat stress, suggesting LARP1 may regulate transcript stability via XNR4 [332]. XRN1, the human homologue of XRN4, was not detected in a LARP1 immunoprecipitation in human ovarian cancer cells [333], suggesting a different mechanism of action may have evolved for plant LARP1. Knockout of LARP1c in *Arabidopsis* had no

effect on growth and development of plants, though heat-stress was not investigated. In contrast, LARP1c overexpression was associated with premature leaf senescence, and increased expression of senescence-associated genes. LARP1b overexpression produced a similar, though less pronounced effect whilst no effect was seen on LARP1a overexpression, suggesting functional divergence of the LARP1 family members in plants.

Both human and *Drosophila* LARP1 interact with PABP [333-335], a protein that is known to promote mRNA stability [336, 337]. LARP1-PABP interaction has been reported to be resistant to RNAse A treatment [333]. However, as this enzyme only cleaves to the 3' of pyrimidines, it is likely the poly(A) tail is largely undigested, and could still be bridging the interaction in these experiments. Indeed, in the study of Aoki *et al.,* RNAse I treatment abolished PABP binding, suggesting it is RNA-dependent. This contrasts with the findings of Blagden *et al*, where *Drosophila* LARP1 interaction with PABP was maintained following digestion with RNAse A, I and V1 [334]. The C-terminal region of LARP1 appears critical for the interaction, with a deletion of the last 150 amino acids, including part of the DM15 repeat, sufficient to abolish binding [335].

Recent work by Dr Manuela Mura in the Blagden lab has demonstrated that LARP1 is in complex with several thousand different mRNAs in HeLa cells, the LARP1-mRNA interactome. LARP1-associated transcripts are enriched for cancer-related functions such as MAPK signalling, extracellular-matrix interactions, focal adhesion and regulation of the actin cytoskeleton (Mura M, Hopkins TG *et al., in press*). She has shown that LARP1 can act to promote the stability of selected transcripts, including mTOR mRNA.

Supporting a role in mRNA fate determination, LARP1 has been found in P bodies and stress granules in *Arabidopsis* cells [332]. In *C. elegans*, LARP1 also accumulates in P bodies, and

has been hypothesised to play a role in selectively promoting the mRNA decay of transcripts encoding MAPK pathway components [330] and *fem-3* mRNA [338].

1.4.5.3 LARP1 in mRNA Translation

As well as the 3'UTR, other groups have shown that LARP1 is associated with the 5' mRNA cap [333, 335]. In a 5' cap pulldown coupled with mass spectrometry in HEK293 cells, LARP1 was the only LARP family member identified [335]. LARP1 possesses multiple sites that are phosphorylated downstream of mTORC1 activation [339, 340], and LARP1 interacts with RAPTOR, a component of mTORC1, but not the mTORC2 component RICTOR [335]. This suggests it may be a direct mTORC1 phospho-target. LARP1 and PABP 5'cap-association is dependent on mTORC1 activation [335].

Ribosome profiling has shown that LARP1 cosediments with polysomes, as well as subpolysomal fractions [332, 333, 335]. This polysomal association appears dependent on mTOR pathway activation, as does that of PABP [335]. LARP1 mutants lacking the C-terminal region required for PABP interaction can no longer associate with polysomes, suggesting PABP may be required to localise LARP1 to actively translated transcripts. Supporting a role in translation, transient knockdown of LARP1 in HeLa cells resulted in a 15% decrease in total protein synthesis [333], whilst stable lentiviral knockdown in HEK293 cells produced a 50% decrease [335]. This knockdown is also associated with a decrease in polysome assembly in human cells [333, 335], but not in plants [332]. LARP1 knockdown also leads to an increase in the hypophosphorylated form of 4E-BP1, which binds eIF4E and suppresses cap-mediated translation [333]. When comparing the translational inhibitory effects of LARP1 knockdown, Tcherkezian *et al* found a more pronounced effect on 5'TOP mRNAs, than non-TOP mRNAs [335]. LARP1 protein was also found to be more strongly associated with 5'TOP mRNAs than controls [335], though only five 5'TOP mRNAs and 10

non-TOPs were assessed in both experiments. Total mRNA levels, and mRNA stability were not assessed. Of note, this study utilised GAPDH and ACTB to normalise their data, both genes that I find show significantly altered mRNA abundance following LARP1 knockdown (see Section 3.4.1).

1.4.5.4 LARP1 in development

Work in *Drosophila, C. elegans* and mice strongly suggest that LARP1, like LARP3, plays a critical role during development. LARP1 was first identified as part of a random P-element insertion screen of chromosome 3 mutants in *D. Melanogaster* [341]. It is highly expressed in the fly testis, and LARP1 mutations induce male and female sterility, and are associated with abnormalities in male meiosis [334, 342]. *C. elegans* homozygous for LARP1 truncating mutations also display defective oogenesis, an effect that can be reversed by upregulating Ras-MAPK signalling [330].

Interestingly, in *Drosophila*, where LARP1 has also be shown to interact with PABP, PABP mutants producing a similar phenotype to LARP1 mutants, suggesting both proteins fulfil a similar role in development [334]. Transcription of *Drosophila LARP1* is promoted by the development-associated transcription factor Ultrabithorax (Ubx), whilst Teashirt (Tsh) appears to suppress expression [343]. Work in mouse embryos showed LARP1 to be highly expressed in the spinal cord and dorsal root ganglia, developing limb buds, as well as in salivary glands and the developing lungs and gastrointestinal tract [343].

LARP1b may also be important in development. A study in mouse embryonic stem cells found LARP1b expression to be upregulated during forced differentiation [344]. Conversely, work in *Drosophila* embryos has identified high expression of LARP1 in neuroblasts, but not in more differentiated neuronal cells [334]. In mice, LARP1 binds mRNA in embryonic stem

cells, and expression drops during cell differentiation [345]. Both proteins may therefore be involved in regulating pluripotent states.

1.4.5.5 LARP1 Splice variants

Two isoforms of LARP1 are currently validated at a protein level in Uniprot (*Uniprot.org*), one of 1096 amino acids (aa), which is annotated as the dominant isoform, (1), and one of 1019aa, (2). The 1096aa variant is not recorded in Ensembl. These two isoforms are generated by alternative splicing of the first exon, leading to differences at the N-terminus of the protein, with isoform (1) possessing a unique 145 amino acid sequence, whilst isoform (2) has a unique 68 residue sequence (see Section 3.3.5 for diagram). In Western blots of LARP1 produced by different groups, different antibodies and even in different species, two protein bands are usually visible [331-335, 346], and both decrease on LARP1 knockdown [331, 333], suggesting these may represent the two isoforms. Indeed, in a survey of breast cancer lines, researchers designed primers specific for isoform (1) and showed it to only be expressed at an RNA level in one cell line, MCF7 [346]. Western blotting confirmed the higher protein band, corresponding to the 1096aa isoform (1), was present in MCF7 cells, and absent from two other cell lines that lack isoform (1) mRNA (ZR-7S, HS578T). Isoform (1) was more likely to be expressed in non-triple negative breast cancers than in other breast cancer subtypes [346], suggesting the different isoforms may play different functional roles.

Supporting the existence of multiple LARP1 isoforms, in *C. elegans*, three *LARP1* splice variants have been identified of 5, 6.7 and 7.5kb in length. The 5kb variant was abundant in adult females and embryos <2 hours old, whilst the 7kbp fragment was seen beyond this time point, and in adult males and females. The 6.7kbp fragment was found only in males and older embryos [343]. This tightly regulated distribution of isoform expression further reinforces the potential that different isoforms possess different functions.

1.4.5.6 Role in cancer

Only one study has so far investigated LARP1 expression in depth in human malignancy. LARP1 was highly expressed in hepatocellular cancer (HCC)-derived cell lines, at a protein and mRNA level, when compared to a benign cell line [347]. In addition, higher LARP1 protein levels were seen in HCCs compared to non-malignant adjacent liver tissue from the same patient. Analysis of an independent mRNA expression array dataset of 268 HCC tumours confirmed these findings, with significantly increased LARP1 expression, compared to normal adjacent tissue. In a study involving 272 patient samples, LARP1 was an independent predictor of reduced overall survival in multivariate models: patients with high LARP1 expression had a 25% increased risk of death at any time. This survival association was greater than that seen for tumour size or number, indicating a highly clinically significant trend. The ability of LARP1 protein levels to predict outcome outperformed the current gold-standard circulating biomarker, alpha-foetal protein (AFP) [347].

At the level of cell biology, LARP1 appears to play a role in promoting cell motility, interacting with cytoskeletal components and determining the organisation and distribution of actin. In addition, LARP1 protein is concentrated at the leading edge of migrating cells, suggesting it may play a role in localising mRNA expression [333]. In human cells, LARP1 knockdown inhibits proliferation, with variable effects on the cell cycle, and induces apoptosis in some cancer cell lines studied so far [333, 335].

LARP1 has been identified as a downstream phospho-target of the oncogenic PI3K signalling cascade [348] and is also phosphorylated in response to DNA damage [349], the mechanism of action of many commonly used anti-cancer agents, such as cisplatin. Significantly, LARP1 has also been independently identified in two separate studies as a downstream phospho-target of mTORC1 signalling [339, 340], a pathway frequently activated in cancer, and

capable of promoting cancer cell invasion and metastasis [152]. The effects of LARP1 phosphorylation have not yet been characterised but, like LARP3, may have a substantial impact on LARP1 localisation or function. As well as Raptor, LARP1 has also been show to interact at a protein level with RRP1B, associated with modulating metastatic potential in cancers [350], and the oncogenic transcription factor and RNA-binding protein YB-1 [333, 351].

1.4.6 THE LARP FAMILY IN SUMMARY

Despite their shared RNA-binding domains, it is clear that LARP proteins exhibit significant heterogeneity both in their RNA targets and their cellular functions (summarised in Table 1-6). Although the La motif is highly conserved, not all family members show conservation in the residues critical for LARP3 RNA-binding, suggesting the RNA affinity of this domain can be modified. There seem to be significant differences in the nucleotide binding-preferences of LARP proteins, and in the minimum number of nucleotides required for binding. The most striking structural differences between LARP proteins are found in the C-terminal regions, which appear critical to the function of several family members and may form the basis of many differences in their functions. All LARP proteins, apart from LARP6, have been identified in high-throughput experiments as binding mRNA [87, 228]. This is particularly surprising in the case of LARP7, as no mRNA targets have yet been identified, and indicates new functions may be uncovered. LARP3 appears to shuttle between the nucleus and cytoplasm, with key roles in each, and LARP6 is also present in both compartments. Whilst LARP7 is nuclear, LARPs 1 and 4 are predominantly cytoplasmic: although there is limited data to date, it is tempting to speculate that these three proteins may also shuttle in certain situations.

LARP1 stands out as the largest protein in the human LARP family, with a more central LAM-RRM structure than other family members (Figure 1-10). The DM15 region, unique to LARP1 proteins, is striking in its degree of conservation, and may represent a novel RNA-binding motif. This suggests that LARP1 protein may functionally differ from other family members. Like LARP3, LARP1 appears to have diverse functional roles, and is implicated in the regulation of both mRNA stability and translation. The recent discovery that LARP1 expression is upregulated in hepatocellular cancer, where it is a highly significant predictor of poor outcome, suggests a potential oncogenic function for the protein. This is reinforced by the finding that LARP1 appears to play key roles during embryological development, and potentially in the maintenance of a pluripotent state. Further work is needed to investigate the role of LARP1 within the cancer cell.

Table 1-6. A summary of the LARP family.

A summary of LARP proteins, with details of human isoforms (UniProt.org) and chromosomal locations. Predicted cellular localizations were provided by the online database COMPARTMENTS [352]. mRNA binding data in HEK293 cells was taken from the work of Baltz *et al*, and figures represent the log2 fold-change in protein levels between immunoprecipitations with and without mRNA-protein crosslinking. NS = non-significant. LARP6 was not identified in either mRNA-binding studies.

Protein	Size in amino acids (isoforms)	Genomic location	Predominant protein localisation	mRNA-bound in HeLa cells [87]	mRNA-bound in HEK293 immuo-precipitation (log2FC enrichment) [228]	Known domains [226] [223]	Nucleotide affinity
LARP1	**1096** (1019)	5q33.2	Predominantly cytoplasmic + Nuclear	Yes	4.06	LAM-RRM$_{L5}$, DM15	*C. elegans* PolyU> PolyG *H. sapiens* PolyA (>9nt)
LARP1b	**914**	4q28.2	Nuclear and cytoplasmic	Yes (NS)	4.15	LAM-RRM$_{L5}$, DM15	Unknown
LARP3	**408**	2q31.1	Predominantly Nuclear (Cytoplasmic following stress)	Yes	3.06	LAM-RRM1, RRM2	3’ oligo(U) Cellular and viral IRES 5’TOP mRNAs
LARP4	**724** (605, 723, 730, 653, 653, 445)	12q13.12	Cytoplasmic (annotated as cytoplasmic + nuclear)	Yes	4.44	vPAM2, LAM-RRM$_{L4}$	*H. sapiens* PolyA>PolyU (>15nt)
LARP4b	**738**	10p15.3	Cytoplasmic (annotated as cytoplasmic + nuclear)	Yes	4.45	vPAM2, LAM-RRM$_{L4}$	Unknown
LARP6	**491** (93)	15q23	Cytoplasmic + Nuclear	Not identified	Not identified	LAM-RRM$_{L3}$, LSA	Collagen 5’UTR stem loop
LARP7	**582** (214, 589)	4q25	Nuclear (annotated as cytoplasmic + nuclear)	Yes	2.06	LAM-RRM1, RRM2	3’ oligo(U) S16 TOP motif

1.5 STUDY HYPOTHESIS

Over the last two decades, significant progress has been made in determining the origins of ovarian cancer and in understanding the molecular basis of its development. Unfortunately, we now know ovarian cancer to be a complex and genetically highly heterogeneous disease. Although our increased knowledge of the dysregulated pathways in EOC has led to trials of targeted agents, these have so far met with limited success [353].

The central role of post-transcriptional regulation in the development of malignancy is an area of growing research interest. It has been suggested that the majority of the regulation of gene expression is determined post-transcriptionally [71], which has important implications for our understanding of cancer development and neoplastic cell plasticity. The journey from transcription of nascent mRNAs to their translation in the cytoplasm is a highly complex and tightly regulated process, some aspects of which we are only just beginning to clarify. At the heart of determining RNA fate are a large and diverse family of RNA-binding proteins (RBPs). More highly expressed that other regulatory proteins [75], there may be over 1,500 genes encoding proteins with RNA-binding properties. To date, the functional role of relatively few RBPs has been studied in significant depth.

La/LARP3 was one of the first RBPs to be characterised. Over forty years of research has revealed it to participate in an extensive array of functions, from promoting mRNA translation to ensuring correct tRNA folding. We now recognise LARP3 as a member of a family of highly conserved proteins that share similar RNA-binding motifs. LARPs play diverse roles within normal cells, but are increasingly being recognised as significant to cancer development and progression. In particular, LARP1 appears to regulate both mRNA stability and translation, and, at the level of cell biology, promotes cell motility, survival and proliferation. This suggests that LARP1 expression may be beneficial to the cancer cell.

Indeed, a recent study has revealed that high expression of LARP1 is seen in hepatocellular cancers, and that patients with the highest LARP1 levels in their tumours have a significantly worse prognosis [347], suggesting a key role in determining the aggressive nature of malignancies.

I hypothesise that the central role of LARP1 within the normal cell suggests it may play a key role in malignant progression, and may therefore function as oncogene in several cancer types, including hepatocellular and ovarian cancer. Ovarian cancer is disease in which the development of treatment resistance leads to unchecked progression and ultimately patient demise. Targeted agents inhibiting specific oncogenic pathways have so far showed limited benefit in this disease. LARP1 may potentially act at the post-transcriptional level to regulate the expression of genes implicated in multiple oncogenic pathways, controlling behaviours such as cell motility and survival. If this is the case, it may have potential as a disease biomarker and potential therapeutic target.

1.6 STUDY AIMS

To date, no study has investigated LARP1 expression in other cancers, nor explored in-depth the mechanism by which LARP1 may promote cancer progression. The aims of this PhD project were therefore to;

1. Investigate the link between LARP1 expression and cancer
2. Ascertain if LARP1 protein is present in human plasma and determine if levels are linked to underlying malignant pathology
3. Examine whether circulating or intra-tumoural LARP1 protein has potential as a biomarker in ovarian cancers
4. Validate *in vivo* the role of LARP1 in cancer progression
5. Determine the *in vitro* effects of LARP1 modulation on key neoplastic traits
6. Identify LARP1-regulated target to explain the observed phenotype.

2 CHAPTER II – MATERIALS AND METHODS

2.1 GENE EXPRESSION ARRAY DATA

For the Oncomine summary analysis (www.oncomine.org), studies that demonstrated a fold change in LARP1 expression of ≥1.5 between cancer and non-cancer samples and a p-value ≤ 0.05, were taken as statistically significant. Expression data for LARP1 were obtained from Oncomine for 3 independent ovarian datasets (TCGA [12], Hendrix *et al.* [354], Bonome *et al.* [355]). Fold change was calculated as median-centered intensity of each cancer sample divided by the mean of non-cancer samples. Other data were obtained from the GEO repository (http://www.ncbi.nlm.nih.gov/geo/) as described in figure legends. Significance was calculated using the Student *t*-test. Survival association was determined by Cox regression analysis using the survival package of R. Progression-free survival data in ovarian cancer and overall survival data in breast cancer were obtained from *kmplot.com* [356-358]. Array gene expression data for *PROM1* in the NCI60 panel was obtained from the CellMiner online tool [359].

2.2 IMMUNOHISTOCHEMISTRY

A tissue microarray (TMA; OV801) containing normal ovarian tissue and ovarian cancer cores (n=40) was obtained from US Biomax (Rockville, MA), as were two cervical cancer tissue arrays (CR601 and CR481) that included the following specimens: normal cervix (n=12), cervical intraepithelial neoplasia (CIN; n=35) and invasive squamous cervical cancer (n=36). Other TMAs were developed in Imperial College as detailed below. All

immunohistochemical staining was performed by the Imperial College Healthcare NHS Trust Pathology Core Facility. Briefly, paraffin was removed from slides, sections were rehydrated in graded alcohols and then heated in a microwave oven at 900W for 20 min. Slides were cooled at room temperature before adding the anti-LARP1 (SDIX, Newark, DE) or anti-Ki67 antibody (Leica Biosystems, Milton Keynes, UK) and incubated overnight. Secondary or biotinylated-secondary antibodies were applied and incubated for 1 hour at room temperature and processed with the Polymer-HRP Kit (BioGenex, Fremont, CA), Vectostain ACC Kit and Impact DAB (both Vector Laboratories Inc., Peterborough, UK). Tissues were counterstained with haematoxylin. Each patient sample was represented by one core. This core was visualised in its entirety in a single field of view and intensity of staining was defined for each specimen (0-3, with 0 being stain negative and 3 being the most intense) and multiplied by the percentage of cancer cells stain-positive in that tissue core (to give a total score out of 300). Scoring was performed by Consultant Histopathologists (Dr Justin Weir, Dr Francesco Mauri and Dr Mona El-Bahrawi), apart from that for OV801 which was scored by TGH. All images were captured by TGH using a Nikon Eclipse ME600. All analysis was performed by TGH. Xenograft samples were processed in the same manner as clinical TMAs.

2.3 CELL CULTURE AND DRUG TREATMENT

OVCAR8, HeLa, PEO1, PEO4, IGROV1 and OVCAR4 cells were kindly provided by the Ovarian Cancer Action Biobank, and were genotyped prior to use. SKOV3 and OVCAR3 cells were obtained from ATCC. OVCAR3 cells were cultured in RPMI (Gibco) supplemented with 20% foetal calf serum (FCS) and 0.01 mg/ml bovine insulin (Sigma-Aldrich, St. Louis, MO). All other lines were cultured in RPMI with 10% FCS, with the exception of HeLa cells, which were maintained in DMEM (Gibco). All media was

supplemented with L-glutamine (Life technologies, Paisley, UK) to a final concentration of 2mM. All lines were cultured at 37°C in 5% CO_2. For hypoxic challenge, cells were maintained in a nitrogen-supplemented atmosphere with 1% O_2. For serum-starvation, cells were cultured in media containing 0.1% FCS and for glumatine-depleted conditions, media containing 10% FCS, but without additional L-glutamine was used. For drug treatments, cells were exposed to cisplatin (Accord Healthcare, Middlesex, UK), gemcitabine (Hospira, Lemington Spa, UK) and paclitaxel (TEVA UK, Castelford, UK) at the stated concentrations. Salinomycin (Sigma-Aldrich) was resuspended in DMSO and added to culture medium.

2.4 MTT VIABILITY AND ACTIVATED CASPASE APOPTOSIS ASSAYS

For MTT labelling, 5-10 x 10^3 cells were cultured at 37°C in 96-well plates with 100µl of media and labelled with 20µl of MTT (Sigma-Aldrich) at 3 mg/ml for 1 hour. The resulting precipitate was solubilised overnight with 10% SDS in 0.01M HCl. Absorbance at 570 nm was recorded on an OPTImax microplate reader (Molecular Devices, Wokingham, UK). MTT assays were performed at the timepoints specified in Figure legends. Caspase 3/7 activity was assessed using the CaspaseGlo-3/7 Assay (Promega, Southampton, UK). Cells were cultured at 37°C in white opaque 96-well plates (Corning, Ewloe, UK). CaspaseGlo reagent was added to each well and plates left at room temperature for 1 hour before reading on a LUMIstar Optima plate reader (BMG Labtech, Cambridge, UK). Assays were performed at 24 hours, unless otherwise stated.

2.5 CANCER CELL-CONDITIONED MEDIA

Ovarian cancer cells were seeded in 10cm dishes overnight. The following day, cells were washed twice with PBS, then cultured for 24 hours in FCS-free media. Serum-free media was used to avoid enriching for serum components, and because *B. taurus* LARP1 has a 96% sequence identity to the human protein (as determined by protein BLAST) and could produce false positives. Cell-conditioned media was collected and spun at 300g for 5 minutes to remove floating cells. The supernatant was spun at 12,000rpm for 20 minutes at 4°C to remove cell debris. Protein remaining in the supernatant was concentrated by ultrafiltration using Amicon Ultra-4 10kDa Centrifugal Filter Units (Merck Millipore, Darmstadt, Germany) as per manufacturer's instructions. Following addition of protease (Roche, Welwyn Garden City, UK) and phosphatase inhibitors (Merck Millipore), concentrated media was frozen at -80°C. Media was mixed with Laemmli buffer (Biorad) and analysed by Western blotting. The non-conditioned media control was treated in exactly the same way as cell-conditioned media, with the exception of the omission of cancer cells from the initial 10cm plate incubation.

2.6 PROTEIN EXTRACTION AND WESTERN BLOTTING

Cells were washed and incubated with protein lysis buffer (1% NP-40, 10 mM Tris-HCl pH 7.5, 150 mM NaCl, with protease and phosphatase inhibitors as before) for 10 minutes on ice. Lysates were cleared by centrifugation and protein was quantified using the microBCA protein assay kit (Thermo Scientific, Loughborough, UK). Protein samples were boiled with Laemmli buffer and separated by SDS-PAGE using the BioRad Mini Trans-Blot system. Proteins were transferred to nitrocellulose membranes. Blocking and primary antibody incubation was performed according to the manufacturers' instructions (Table 2-1).

Appropriate horseradish peroxidase (HRP)-conjugated secondary antibodies were obtained from Dako. All washes were performed in Tris-buffered saline (TBS) supplemented with 1% TWEEN. Blots were developed using the Imobilion HRP substrate (Millipore) and luminescence visualised with X-ray film.

To separate total cellular protein into nuclear and cytoplasmic fractions, the NE-PER Nuclear and Cytoplasmic Extraction Kit was used according to the manufacturer's instructions (Pierce, Rockford, IL).

Table 2-1. Antibodies used in western blotting

Antibody	Species	Supplier	Dilution
LARP1	Rabbit	SDIX	1:5000
LARP1	Mouse	Abnova	1:1000
HSP60	Rabbit	Abcam	1:5000
BCL2	Mouse	Santa Cruz	1:200
BIK	Goat	Santa Cruz	1:200
Lamin A	Mouse	Abcam	1:1000

2.7 PATIENT PLASMA

Blood from healthy volunteers and patients was collected into lithium heparin vacutainers, transferred on ice and immediately spun at 2000g for 10 minutes at 4°C. Plasma was removed with pipettes and frozen at -80°C. Additional healthy volunteer samples were obtained from Sera Laboratories (Haywards Heath, UK).

2.8 LARP1 ELISA

Nunc MaxiSorp 96-well plates (Thermo Scientific) were coated overnight at 4°C with anti-LARP1 antibody (mouse; Abnova, Taipei, Taiwan) in carbonate/bicarbonate buffer (0.15 M

sodium carbonate, 0.35 M sodium bicarbonate, pH 9.6). Plates were blocked with 5% casein solution (Pierce), then incubated with patient samples diluted 1:20 in AD3 assay diluent (Neuromics, Minneapolis, MN). A standard curve was generated from serial dilutions of recombinant LARP1 protein (Abnova) in AD3 buffer. Plates were washed with PBS with 0.5% TWEEN (PBST), then incubated with anti-LARP1 antibody (rabbit, SDIX) diluted 1:1000 in PBST. Following a further wash in PBST, plates were incubated with peroxidase-conjugated goat anti-LARP1 secondary antibodies (Dako, Ely, UK) diluted in PBST. After a final wash in PBST, plates were developed using Luminata Forte ELISA HRP substrate (EMD Millipore, Sand Diego, CA) and read using a LUMIstar Optima plate reader (BMG Labtech). Spike-and-recovery experiments were conducted by introducing known quantities of recombinant protein to at least five healthy control plasma samples, with values compared to a PBS-spiked control. Sample values were interpolated from the recombinant protein standard curve using a four-parameter logistic regression model, with GraphPad Prism (GraphPad Software).

2.9 TRANSFECTION, TRANSDUCTION AND STABLE CLONE GENERATION

2.9.1 PLASMID TRANSFECTION

LARP1 overexpression constructs were generated by Dr. Normala Abd-Latip. Briefly, LARP1 cDNA was obtained from the pOTB7-LARP1 vector (Life technology). PCR primers were designed for gene amplification with the addition of *attB* sites. The PCR product *attB*-LARP1 was cloned into the Gateway Technology System expression plasmid pT-Rex-DEST30 (Life Technology), generating a new construct, pTrex-LARP1. The 'empty' vector

control carrying the LacZ gene was named pTrex-LacZ. Plasmids containing shGFP (TR30016) and shLARP1 (TF303581D) sequences were obtained from Origene. The Flag-BCL2 overexpression plasmid, together with a matched empty-vector control, were both sourced from Origene. Cells were transfected with 0.4ug of plasmid DNA per 6 well, or a comparable quantity relative to plate/flask surface area, using Effectene (Qiagen, Manchester, UK), as per manufacturer's instructions, and selected with 2μg/ml puromycin or 1000 μg/ml geneticin after 24 hours. SKOV3-shLARP1 cells were created by plasmid transfection of SKOV3 cells with Origene shRNA constructs (as detailed above) in two T75 flasks. After the addition of puromycin selection, a minimum of two hundred clones were obtained from each flask, and these clones were pooled, expanded and frozen down for future use, with protein extracted to confirm knockdown. Clones were not used for more than 8-10 passages and were maintained in selective media.

2.9.2 LENTIVIRAL TRANSDUCTION

Lentiviruses were produced using the Mission lentiviral system (Sigma-Aldrich). HEK293T cells were co-transfected with a packaging vector, envelope vector and shRNA transfer vector using lipofectamine. Mission shRNA constructs were also obtained from Sigma-Aldrich (Control [SHC0016] and shLARP1 [TRCN0000150984, TRCN0000152624, TRCN0000152891]). Replication-incompetent viral particles were collected at 24 and 48 hours by removing the culture medium, centrifuging at 300g to separate floating cells and then passing it through a 0.45μM filter, before freezing at -80°C. To create lentiviral-transduced lines, cells were incubated with virus and selected with 2μg/ml puromycin after 24 hours.

2.9.3 TRANSIENT KNOCKDOWN

For transient knockdown, sub-confluent cells were transfected using Dharmafect 1 (GE Dharmacon, Lafayette, CO) according to the manufacturer's instructions, with control non-targeting siRNA (GGUCCGGCUCCCCCAAAUG) or LARP1-targeting siRNA (GAAUGGAGAUGAGGAUUGC, AGACUCAAGCCAGACAUCA) synthesised by Eurofins (Hamburg, Germany), or *BCL2*-targeting siRNA (D-003307-02) obtained from GE Dharmacon. Transfection mixtures comprised siRNA diluted to a final concentration of 100nm in OptiMEM (GIBCO).

2.10 XENOGRAFT EXPERIMENTS

All animal experiments were performed in accordance with the United Kingdom Home Office Guidance on the Operation of the Animal (Scientific Procedures) Act 1986 and within the published guidelines for the welfare and use of animals in cancer research [360]. Female NOD-SCID, SCID-Beige or NOD-SCID IL2R-gamma^{null} (NSG) mice (aged 6–8 weeks; Charles River, Margate, UK) were used. HeLa (1×10^6) and SKOV3 cells (2×10^6, unless otherwise specified) were injected subcutaneously into the flanks of mice (at least 5 per cohort). For limiting dilution experiments, cells were diluted 1:1 in phenol-free growth factor-reduced Matrigel (BD Biosciences, San Jose, CA) prior to implantation. Tumour dimensions were measured using electronic callipers and tumour volumes calculated by the equation: volume = $(\pi/6) \times a \times b \times c$, where a, b, and c represent three orthogonal axes of the tumour. Tumours were classed as measureable when they reached ≥5mm in any axis. Experiments were terminated at 2 months, or before any mouse reached pre-set welfare limits. Tumours were collected and immediately fixed in 10% formalin for 48 hours before paraffin embedding and sectioning.

2.11 CLONOGENIC ASSAYS

Single-cell suspensions were seeded in 10cm plates, with 1 - 5x 10^3 cells per plate, and incubated for 2 weeks. Colonies formed were fixed in ice-cold methanol and stained with 0.5% crystal violet. Plates were photographed using a GE ImageQuant LAS 4000 and colonies were counted with ImageJ.

2.12 MIGRATION ASSAYS

Cells were cultured to confluence in 6-well plates and serum-starved (0.1% FCS) overnight before a scratch was applied with a 200µl pipette tip. Sequential images were captured at the same locations within the plate at stated time points, acquired with a Nikon Eclipse TE-2000U microscope. Images were imported into ImageJ and the cell free area was drawn around by hand, and the pixel area calculated. Cell-free area was calculated as a percentage of the zero timepoint. At least three areas were imaged for each condition in each experiment, with an overall mean area change calculated per timepoint for each experimental condition. Each experiment was repeated at least three times.

2.13 NON-ADHERENT GROWTH ASSAYS

Cells were seeded in ultra-low attachment 96-well plates (Corning) at a density of $2x10^2$ cells/well. Single-cell suspensions were incubated for 2.5 weeks. Spherosomes were counted and then dissociated with trypsin to a single-cell suspension that was confirmed visually. Cells were re-plated in 10cm dishes with full media and colonies formed after 2 weeks were fixed in ice-cold methanol and stained with 0.5% crystal violet. Plates were photographed using a GE ImageQuant LAS 4000 and colonies were counted using ImageJ.

2.14 INVASION ASSAYS

BD BioCoat Matrigel Invasion Chambers (BD Bioscience) with 8 μM pores were thawed and incubated with serum-free medium according to the manufacturer's instructions. Cells (10,000/well) were plated in serum-free medium in the upper insert of the trans-well system whilst the bottom well was filled with medium supplemented with 10% FCS. After 24 hours, non-invasive cells were removed from the upper surface of the membrane by scrubbing with a wet cotton swab. The invading cells in the lower surface of the membrane were fixed in ice-cold methanol. The insert was removed, mounted on a glass slide with DAPI-containing mounting medium (ProLong Gold, Life Technologies). Images were acquired with a Leica 500 confocal microscope and images processed with Leica LAS AF lite software. DAPI-stained nuclei were counted with Image-J.

2.15 FLOW CYTOMETRY

For cell cycle analysis, cells were trypsinised and fixed in ice-cold 75% ethanol overnight, before RNA digestion (RNAse A, 100μg/ml), followed by propidium iodide staining to a final concentration of 25μg/ml (both Sigma-Aldrich). Samples were analysed on a FACSCalibur (BD Biosciences). Cell cycle distribution was determined using FlowJo software (FlowJo LLC). For assessment of apoptosis, cells were resuspended in Annexin V-binding buffer (BioLegend, San Diego, CA) and incubated for 10 minutes with Annexin V-FITC antibody (IQ Products, Groningen, Netherlands). Cells were then washed twice and, following addition of propidium iodide analysed as before. Assessment of CD133 membrane positivity was performed using CD133/1-APC and IgG isotype-APC (both Miltenyi Biotech, Bisley, UK) and the Aldefluor assay was performed according to manufacturer's instructions (Stemcell Technologies, Manchester, UK).

2.16 RT-QPCR

Reverse transcription-quantitative polymerase chain reactions (RT-qPCR) were used to quantify relative RNA abundance. Total RNA was extracted with the miRNeasy kit following the manufacturer's instructions, with on-column DNAse digestion (both Qiagen). Extracted RNA was reverse-transcribed using MMLV Reverse Transcriptase (Promega) with random hexamer primers (Promega) according to the manufacturer's instructions. All RT-qPCR experiments were performed with exon-spanning TaqMan RNA expression assays (Table 2-2; Invitrogen) using Universal Master Mix II (Invitrogen) on a 7900HT analyser (Applied Biosystems, Paisley, UK). Treated samples were normalised to controls with the $\Delta\Delta C_t$ formula using 18S rRNA as an endogenous control.

Table 2-2. Primers used in RT-qPCR

Gene	Assay ID or primer sequence
BCL2	Hs00608023_m1
BIK	Hs00154189_m1
MAPK14	Hs01051152_m1
18S	Hs03003631_g1
LARP1	Hs00391726_m1
DAPK2	Hs00204888_m1
TNF	Hs00174128_m1
ERBB3	Hs00176538_m1
AKT3	Hs00987350_m1

2.17 RNA-SEQUENCING AND DATA ANALYSIS

Total RNA from three biological repeats was extracted from OVCAR8 cells as before (Section 2.16), following transient LARP1 knockdown. Polyadenylated RNA was enriched using the Dynabead mRNA-purification kit and fragmented using the Ambion fragmentation reagent (both Life Technologies). First-strand cDNA was generated with random hexamer-

primed reverse transcription, with First Strand Master Mix and the SuperScript II Reverse Transcriptase kit (Life Technologies), with dUTP used during second-strand synthesis. The resulting cDNA was purified with Agencourt AMPure XP Beads (Beckman Coulter, High Wycombe, UK), then end-repaired and 3'adenylated and adaptors were ligated. Products were separated by agarose gel electrophoresis, and fragments between 300 and 350bp were excised and eluted. Uracil-N-Glycosylase (UNG, Applied Biosystems) was used to degrade the second-strand cDNA, and products were amplified and re-purified. Library quantification and quality control was performed using the Agilent 2100 Bio-analyzer (Craven Arms, UK) and the ABI StepOnePlus Real-Time PCR System (Life Technologies).

Paired-end 100bp sequencing was performed using the Illumina Hiseq2000 platform and data was processed at the Beijing Genomics Institute, Shenzhen. Following quality control, clean reads were aligned to Hg19 reference sequences using SOAPaligner/SOAP2 [361], allowing for up to 5 mismatches. Gene expression was determined using the reads per kilobase per million reads (RPKM) method [362], and the ratio between siCONTROL and siLARP1 samples calculated. Functional enrichment analysis was conducted with Ingenuity Pathway Analysis (Qiagen), using a change in expression of ±25% and a false discovery rate threshold ≤0.05 to select transcripts.

2.18 RNA IMMUNOPRECIPITATION (RIP)

Cells were collected by trypsinisation and re-suspended in RIP lysis buffer: 20mM Hepes pH 7.4, 150mM KCl, 5mM $MgCl_2$, 0.5% NP40, 400 U/ml RNase inhibitor (Promega), 1mM DTT, 400μM vanadyl ribonucleoside complexes (VRC; NEB), 1x protein and phosphatase inhibitor. Lysates were stored at -80˚C overnight. RNA was immunoprecipitated with rabbit anti-LARP1 polyclonal antibody (SDIX) or rabbit IgG isotype control (Cell Signalling Technology, Hitchin, UK) following the method described by Keene *et al* [363]. Briefly,

Protein A-Sepharose beads were incubated with antibody overnight on a rotator at 4˚C. Beads were washed four times with NT2 buffer (50mM Tris-HCL, 150 mM NaCl, 1mM $MgCl_2$, 0.05% NP-40), before resuspension in immunoprecipitation buffer (200U/ml RNase inhibitor, 400μM VRC, 1mM DTT, 30μM, 15mM EDTA in NT2 buffer) and the addition of RNP lysates, in a total volume of 1ml. Samples were incubated for 4 hours on a rotator at 4˚C, before washing 4 times with wash buffer (50mM Tris-HCL, 300mM NaCl, 5mM $MgCl_2$, 0.5% NP-40, 1mM DTT). RNA was extracted with the miRNeasy kit (Qiagen) as before (Section 2.16). To generate cDNA, immunoprecipitated RNA was reverse transcribed using the SensiScript RT Kit (Qiagen) following the manufacturer's instructions. RT-qPCR was performed as described earlier (Section 2.16). The fold enrichment for each target was measured by comparing the Ct values of LARP1 immunoprecipitated fraction to the IgG Isotype fraction and normalised with the ΔC_t formula.

2.19 LUCIFERASE 3'UTR REPORTER ASSAYS

The 3'UTR sequences for BCL2 and BIK were obtained from the UCSC Genome Browser [364]. The 203bp BCL2-ARE region sequence was as described by Ishimaru *et al* [178]. These DNA sequences were cloned into 3'UTR *renilla* luciferase reporter constructs (SwitchGear Genomics, Menlo Park, CA), and cells were co-transfected with a *firefly* luciferase control plasmid using effectene as before (Section 2.9). *Renilla* and *firefly* luciferase activity were anlaysed using the Dual-luciferase reporter assay system (Promega) in triplicate in 96-well plates with luminescence recorded using the LUMOstar Optima plate reader (BMG Labtech). *Renilla* luminescence was normalised to *firefly* activity, and control and LARP1 knockdown samples compared. For luciferase mRNA analysis, total RNA extraction, with on-column DNAase-digestion, cDNA production and RT-qPCR were

performed as described above (Section 2.16). Custom *renilla* and *firefly* luciferase mRNA TaqMan assays were obtained from Invitrogen Life Technologies (Table 2-3).

Table 2-3. Taqman primer sequences

Gene	Primer and probe sequence
Renilla luciferase	F – GCTGAACCTCCCCAAGAAGATC
	R – TGCTCGTAGGAGTAGTGAAAAGC
	Probe - CTGGTGCCCACACTAT
Firefly luciferase	F – GCGCAGCTTGCAAGACTATAAG
	R – TTGTCGATGAGAGTGCTCTTAGC
	Probe - CAAGCGCCCCAGTCGT

2.20 IMMUNOFLUORESCENCE (IF) STAINING AND CONFOCAL IMAGING

SKOV3 cells were cultured on glass coverslips for 24 hours. Cytoplasmic mRNP granule formation was triggered by treatment with 500μM sodium arsenite (Sigma-Aldrich) for one hour. Cells were washed before being incubated with chilled PHEM fixative (4% PFA, 60mM PIPEs, 25mM HEPES, 10mM EGTA, 4mM $MgCl_2$) for 10 minutes. Fixative was removed and cells were washed and blocked in PBSTB buffer (1% BSA, 0.1% TritonX-100) for 1 hour. Primary antibody solution (Table 2-4) was applied and incubated overnight at

4˚C. After washing, Alexa Fluor-conjugated secondary antibodies (Life Technologies) were applied and incubated at room temperature for 1 hour. When staining for actin, Phalloidin-Alexa Fluor 546 was added at this stage (1:500). Cells were washed and mounted with ProLong Gold mounting medium with DAPI (Life Technologies). Immunofluorescence staining was analysed using a Leica 500 confocal microscope and images were processed with Leica LAS AF lite software.

Table 2-4. Antibodies used in immunofluorescence

Antibody	Species	Supplier	Dilution
LARP1	Rabbit	SDIX	1:100
PABP	Mouse	Abcam	1:100
DCP1A	Mouse	Abnova	1:100
Anti-rabbit Alexa Fluor 488	Goat	Life Technology	1:500
Anti-mouse Alexa Fluor 546	Goat	Life Technology	1:500

2.21 BCL2 PROMOTER ACTIVITY ASSAY

A BCL2 promoter construct containing P1 and P2 elements (ATG to −3934) upstream of *firefly* luciferase [365] was obtained from Addgene (plasmid LB332). Transient LARP1 knockdown was performed as before. Effectene was used to introduce the BCL2 promoter construct together with a *renilla* luciferase control for data normalisation. Twenty-four hours after transfection, total RNA was collected and relative levels of *firefly* and *renilla* luciferase mRNA were determined by RT-qPCR as described above (Section 2.16).

2.22 SILAC MASS SPECTROMETRY

Protein labelling was accomplished by incubating cells in SILAC medium, composed of RPMI with either unlabelled arginine and lysine (R0K0, light), ^{13}C-labelled arginine and ^{2}D-labelled lysine amino acids (R6K4, medium) or ^{13}C- and ^{15}N-labelled lysine (R10K8, heavy), supplemented with 10kDa-dialysed calf serum. Cells were cultured in labelling media for at least 5-6 divisions. Transient LARP1 knockdown was performed with two independent siRNAs and protein lysates were collected and quantified as described previously. Equal amounts of protein from each condition were combined and resuspended in loading buffer before boiling.

SILAC mass spectrometry and analysis were carried out by Dundee Cell Products. Briefly, the combined protein lysate was separated on an SDS-PAGE gel. The lane was excised and divided into slices. Each slice underwent overnight trypsin digestion. The resulting peptides were extracted, lyophilised and resuspended in 1% formic acid. Peptides were separated using an Ultimate 3000 RSLC nanoflow system (Thermo Scientific) and analysed on a linear ion trap Orbitrap hybrid mass spectrometer (LTQ-Orbitrap Velos, Thermo Scientific), with data acquired using the Xcalibur software. Analysis was performed using MaxQuant [366] and Andromeda search engine software [367].

Genes that displayed a fold-change in expression of ≥1.5 in both LARP1-targeting siRNA were taken as biologically significant.

2.23 STATISTICAL ANALYSIS

Statistical analyses were performed using GraphPad Prism software (GraphPad Software Inc.), unless otherwise stated. Cox regression analysis was carried out using the 'survival' package of R. Statistical tests appropriate to the experiment were chosen as indicated in

figure legends (Student *t* test, Chi-Squared, Log-Rank). $p \leq 0.05$ was taken to be statistically significant.

2.24 STUDY APPROVAL

Tissue samples were provided collaborators or by the Imperial College Healthcare NHS Trust Tissue Bank, supported by the National Institute for Health Research (NIHR) Biomedical Research Centre based at Imperial College Healthcare NHS Trust and Imperial College London. Informed consent from patients was obtained prior to sampling. Study approval was obtained from the local Research Ethics Committee (R06004/GYN2060).

3 CHAPTER III – RESULTS

3.1 CHAPTER THREE ABSTRACT

LARP1 has previously been identified as a prognostic biomarker in hepatocellular cancer, and is phosphorylated downstream of key cancer-related signalling pathways, and in response to DNA damage. I investigated the expression of LARP family members, and found LARP1 to be highly expressed in solid malignancies, including ovarian cancer. Detailed analysis of LARP1 expression revealed LARP1 expression to adversely correlate with outcomes in ovarian, breast and non-small cell lung cancers. LARP1 protein is released into cancer cell-conditioned media, and the protein is detectable in the human circulation. Higher levels are seen in patients with underlying ovarian malignancy.

LARP1 is required for clonogenicity *in vitro*, tumorigenicity *in vivo* and is necessary to maintain $CD133^+$ stem cell-like populations. Loss of LARP1 induces apoptosis and decreased viability, and is sufficient to restore platinum sensitivity in resistant cell lines.

Using RNA-sequencing, I identify BCL2 and BIK expression as being LARP1 dependent. LARP1 is a component of BCL2- and BIK-containing messenger ribonucleoprotein (mRNP) complexes and requires sequences within the 3'-untranslated region to stabilize BCL2 mRNA, and destabilise BIK. LARP1 promotes cancer cell survival in a BCL2-dependent manner.

3.2 LARP1 EXPRESSION IN CANCER

3.2.1 A GLOBAL EVALUATION OF THE LARP FAMILY IN CANCER

To evaluate general trends in the expression of LARP family members in cancer, summary data from 167 studies comparing expression in cancer and non-cancer tissue were obtained using the Oncomine portal of publicly available expression array studies (Figure 3-1). As expected LARP3, previously identified as an oncogene, was predominantly overexpressed in multiple cancer types. Similarly, the potential tumour suppressor LARP7 was downregulated in studies of breast and colorectal cancers. LARP1 expression was almost exclusively upregulated in solid malignancies and was overexpressed in nearly a third of studies in ovarian cancer, with no ovarian study returning the opposite trend. The opposite trend was seen for LARP1 expression in malignancies of the central nervous system (CNS), suggesting a potential inhibitory role in malignant progression. LARP6 expression was also

downregulated in CNS tumours, and has previously been shown to be highly expressed in neurones [317].

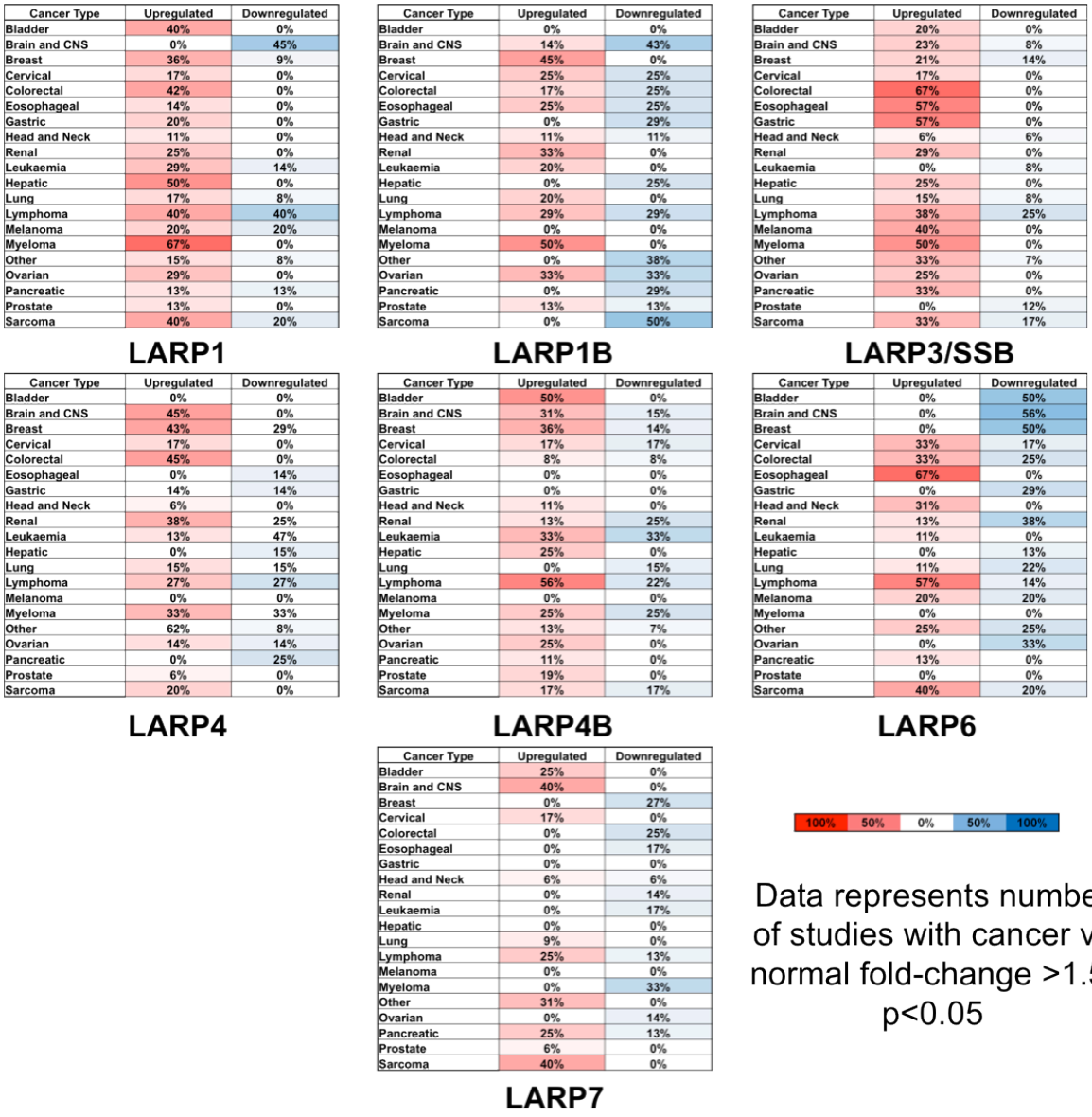

Figure 3-1. A summary of fold-change in expression of cancer compared to non-cancer samples for LARP family members

Using the Oncomine portal (www.oncomine.org), all datasets comparing gene expression in cancer and non-cancer tissue were analysed for significant differences for each LARP family member. A heat-map is presented representing the percentage of all available studies with a significant ($p<0.05$, $FC>1.5$) difference in LARP1 expression.

To evaluate LARP1 expression in more depth, I performed a systematic search for large studies investigating gene expression in cancer and non-cancer tissue, representing several different cancer types (Appendix I). Where possible, studies were restricted to those utilising the same analysis platform, and data from the same array probe were used (Figure 3-2). There was a highly significant increase in LARP1 expression in all solid malignancies surveyed, including breast, colorectal, hepatic and ovarian carcinomas, with the exception of two separate studies involving glioblastoma samples.

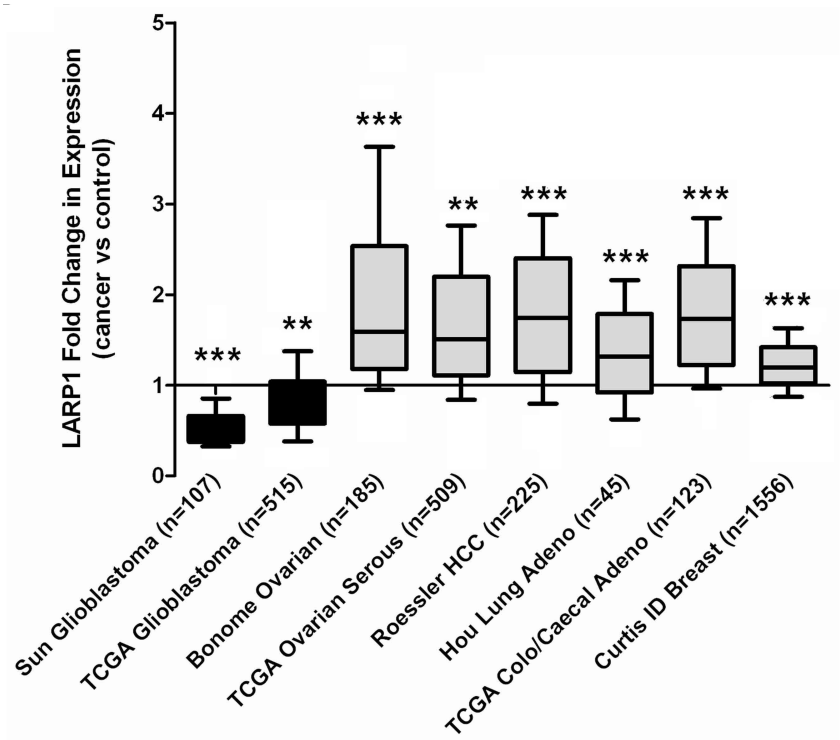

Figure 3-2. Fold change in expression of LARP1 between cancer and non-cancer tissue across multiple cancer types.

In 2013, the Oncomine database was interrogated in a systematic for studies comparing mRNA expression of LARP1 in cancer and non-cancer samples. Studies where the total number of samples were <50, or that included haematological, paediatric or connective tissue-derived malignancies were excluded. Where possible, only studies utilising the same array platform were used, in which case the same probe was taken for analysis. These studies were then analysed to find the fold-change in expression LARP1 in cancer cases, comparing to non-cancer control tissue, with significance calculated using the Student t-test. For a full breakdown of the data used for this systematic search see Appendix I. Whiskers represent 10^{th}-90^{th} percentiles. ***P < 0.001, **P < 0.01, *P < 0.05.

3.2.2 *LARP1* IS HIGHLY EXPRESSED IN OVARIAN AND CERVICAL CANCERS

To further study LARP1 expression in ovarian malignancies, I analysed mRNA expression from three independent, publically available datasets, comparing LARP1 mRNA expression in serous EOC, the most common epithelial subtype [4], to non-malignant ovarian tissue. Combined, these represent 735 patient samples [12, 354, 355]. LARP1 mRNA levels were upregulated in malignant samples in all three studies (Figure 3-3A). Similar trends were observed when LARP1 mRNA expression in serous EOC was compared to that of the normal ovarian surface [368] and fallopian tube epithelium [369] ($P = 0.0072$ and 0.022 respectively; Figure 3-3B, C), the latter having been identified as a potential site of origin for invasive disease [370]. Using the cBIO Genomics Portal [371], I found very low mutation rates for LARP1 in the TCGA ovarian dataset, with only 0.9% (3/316) of patients displaying changes. Evaluating copy number, there were gene deletions in 0.9% of cases, whilst 3.8% of patients had gene duplications.

To determine if LARP1 expression was also altered at the protein level, I performed immunohistochemical analysis (IHC) of a formalin-fixed, paraffin-embedded (FFPE) tissue microarray (TMA). Again, I found there was significantly higher expression of LARP1 protein in ovarian cancer samples compared to normal ovarian tissue ($P < 0.001$; Figure 3-3C). Similar results were obtained comparing serous ovarian cancers to benign ovarian tumours (leiomyoma, teratoma and cystadenofibroma; $P = 0.021$; Figure 3-3E), and benign and malignant mucinous ovarian tumours, rare subtypes of ovarian pathology ($P = 0.033$; Figure 3-3F).

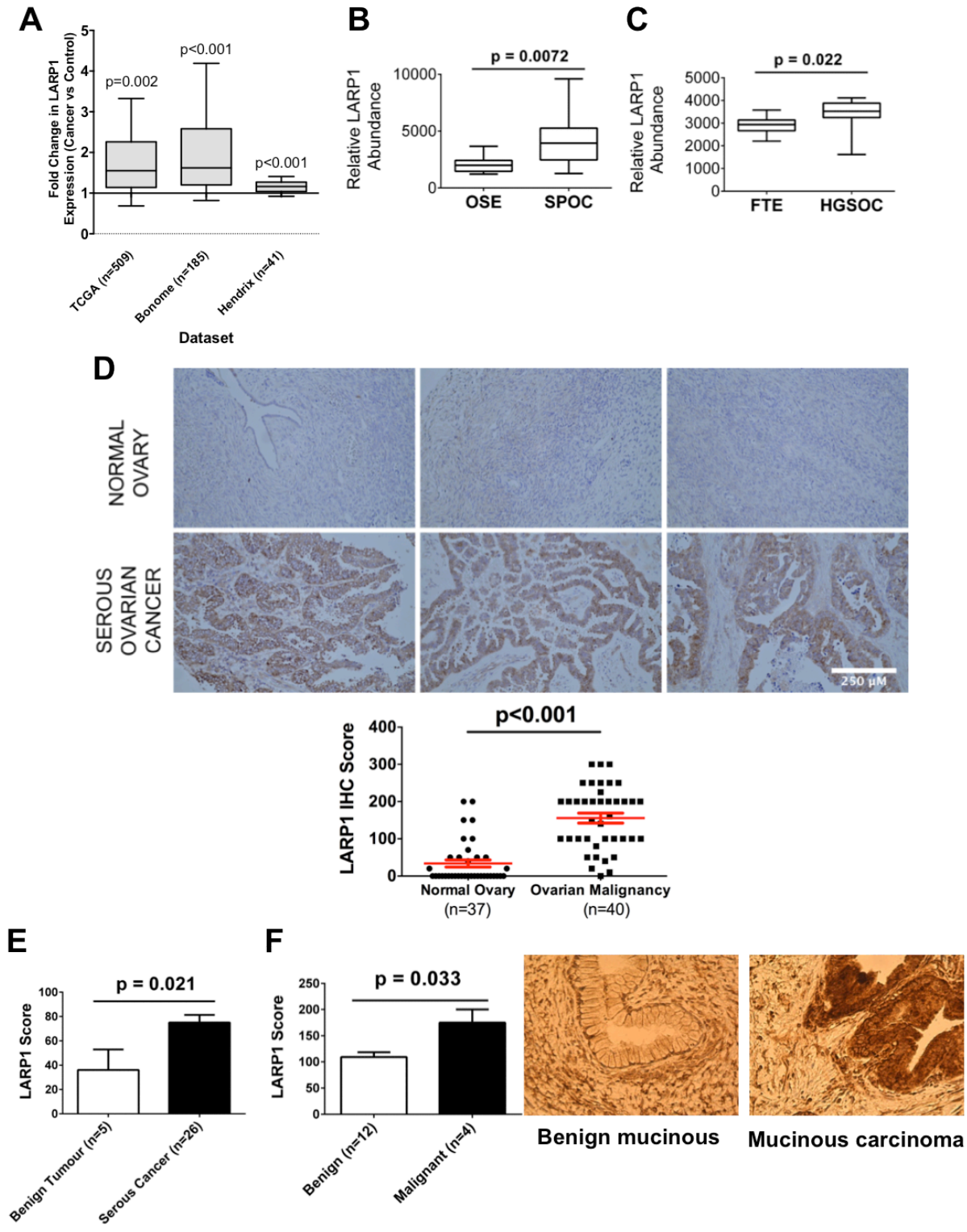

Figure 3-3. LARP1 is highly expressed in ovarian malignancies.

(A) LARP1 mRNA fold change in serous ovarian cancers compared to control tissue in 3 independent datasets (TCGA [12], Hendrix et al. [354], Bonome et al. [355]).
(B) Relative LARP1 mRNA abundance in ovarian surface epithelium (OSE, n=12) and microdissected serous papillary ovarian cancer (SPOC, n=12). Dataset GSE14407, Bowen et al. [368].

(C) Relative LARP1 mRNA abundance in fallopian tube epithelium (OSE, n=12) and high-grade serous ovarian cancer (HGOC, n=13). Dataset GSE10971, Tone et al. [369].
(D) Representative TMA cores of normal ovarian tissue and ovarian cancer samples, stained with anti-LARP1 antibody (scale bar 250μm) and immunohistochemical scoring in unmatched adjacent normal ovarian tissue and ovarian cancers. Scoring by TGH, staining by Pathology Core Facility.
(E) LARP1 score determined by IHC analysis in benign ovarian tumours and serous ovarian cancers. Analysis by TGH.
(F) LARP1 score in mucinous ovarian tumours determined by IHC analysis, together with representative images (10x magnification). Image capture and analysis TGH. Student t-test. Error bars indicate SEM.

I also evaluated LARP1 expression in cervical cancer. Searching Oncomine for expression data comparing cancer and non-cancer samples revealed a single study [304], with significantly higher LARP1 mRNA levels in squamous cell carcinoma (SCC) of the cervix compared to normal cervical tissue (Figure 3-4A). Analysis of a second dataset revealed increasing LARP1 expression with more advanced stages of invasive cancer [372] (Figure 3-4B). In support of this finding, analysing LARP1 protein levels in cervical tissue array, we found increased levels of LARP1 in CIN versus normal epithelium and SCC versus CIN (<0.0001), confirming that levels of cytoplasmic LARP1 significantly correlated with progression of cervical cancer (Figure 3-4C).

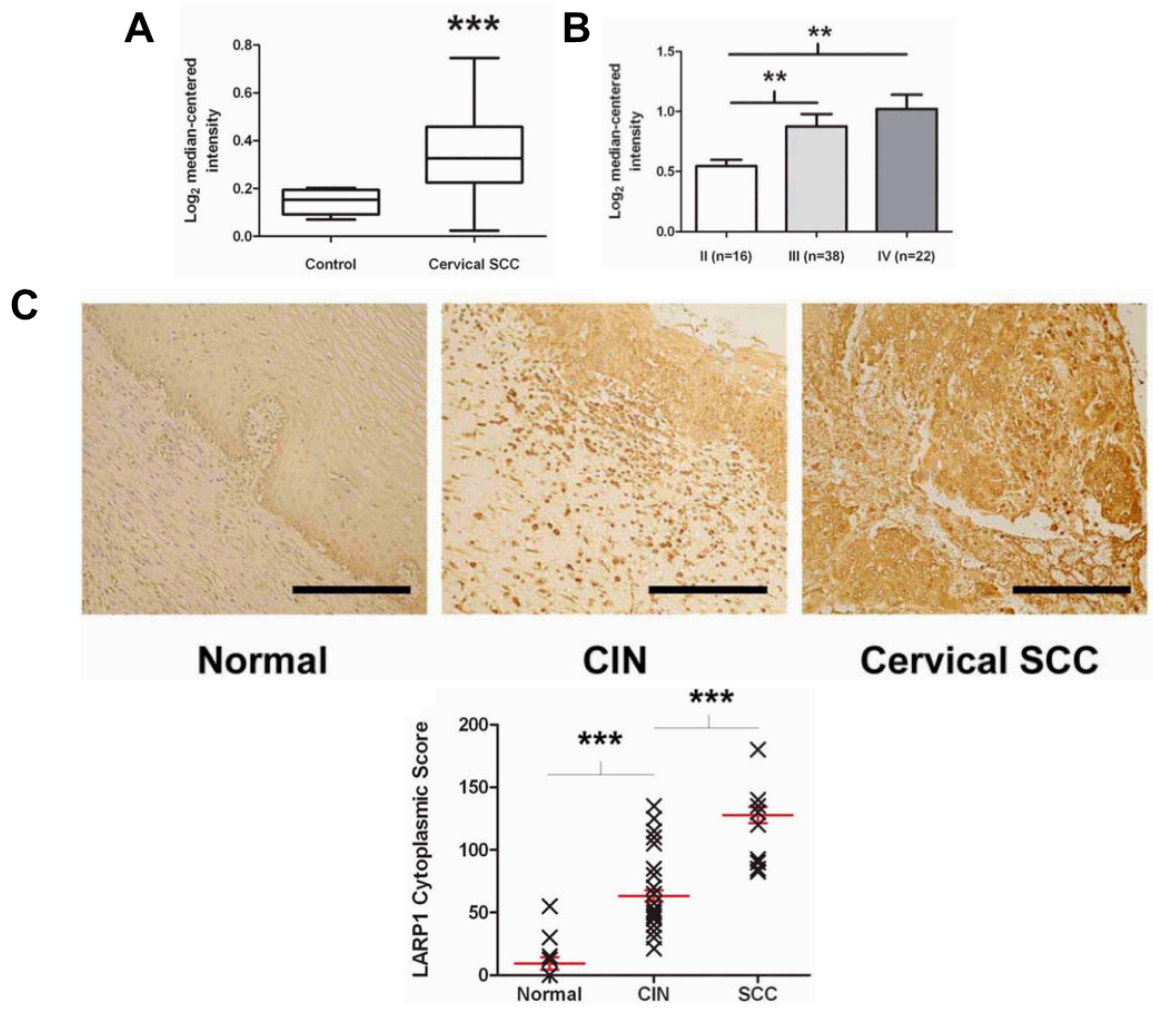

Figure 3-4. LARP1 is highly expressed in cervical malignancies.

(A) Relative LARP1 mRNA abundance in cervical cancer and normal cervical tissue (n=45). Data extracted from reference [304].
(B) Relative LARP1 mRNA abundance in cervical cancer samples (n=76) stratified according to tumour stage. Data extracted from reference [372].
(C) LARP1 cytoplasmic scores for CIN compared to normal samples and invasive SCC compared to CIN samples, together with representative LARP1 immunostaining (scale bar 200μM). Image capture and analysis TGH. ***P < 0.001, **P < 0.01, *P < 0.05. Student t-test.

3.2.3 *LARP1* IS A POTENTIAL PROGNOSTIC MARKER IN OVARIAN CANCER

Cox regression analysis of overall survival, using matched mRNA expression and patient outcome data obtained from The Cancer Genome Atlas (TCGA) project [12], revealed that

patients with the highest LARP1 expression had significantly worse outcomes, with a 29% increased risk of death at any time (Figure 3-5A, n=566, Cox regression HR 1.29, 95% CI 1.01-1.65, P = 0.042). I then assessed the effect of LARP1 expression on progression-free survival in ovarian cancer. In an analysis of 1,171 patient samples using the *kmplot* portal [357], patients with low LARP1 expression had significantly better progression-free survival than those with high LARP1 expression (HR 1.31, 95% CI 1.10-1.54, P = 0.0018; Figure 3-5B). At protein level, analysing by IHC a TMA comprising 67 cancer cases, we showed that only LARP1 expression and cancer stage were independent predictors of poor overall survival (LARP1 HR = 1.13, 95% CI 1.01-1.27, P = 0.036; Table 3-1). These data demonstrate that LARP1 is highly expressed in ovarian malignancies when compared to non-cancer tissue, and that elevated levels predict poor outcome.

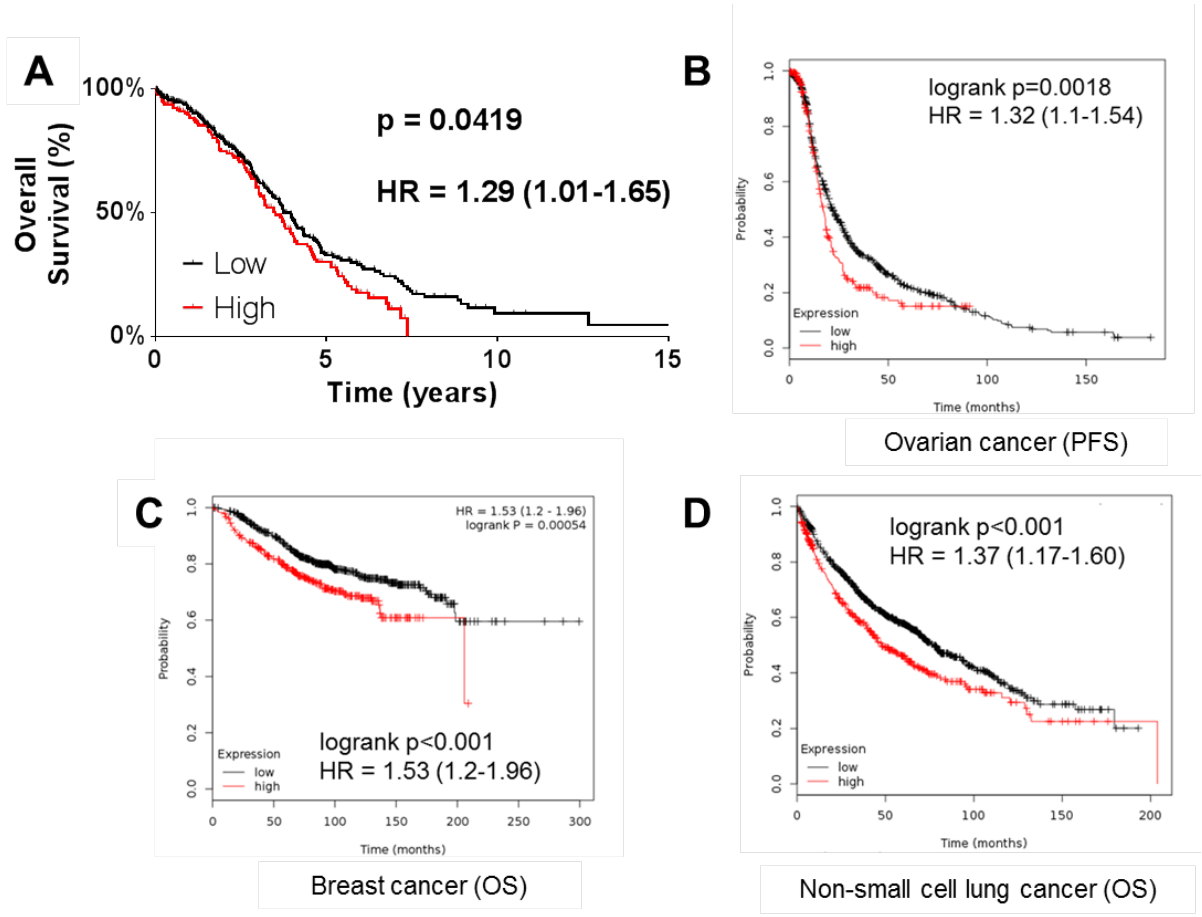

Figure 3-5. LARP1 expression predicts poor outcome in ovarian, breast and non-small cell lung cancers.

(A) Overall survival in the TCGA gene expression dataset [12], for patients stratified according to LARP1 expression (n=566).
(B) Kaplan-Meier analysis of progression-free survival in ovarian cancer patients, separated by LARP1 expression (n=1,171). Data from kmplot.com [357].
(C) Kaplan-Meier analysis of overall survival in breast cancer patients, separated by LARP1 expression (n=1,115). Data from kmplot.com [356].
(D) Kaplan-Meier analysis of overall survival in non-small cell lung cancer patients, stratified according to LARP1 expression (n=1,115). Data from kmplot.com [358].

Interestingly, this trend in outcomes was not limited to ovarian cancer; by analysing overall survival in 1,115 breast cancer patients [356], I found that high LARP1 expression was also predictive of poor outcome (HR = 1.53, p<0.001, 95% CI 1.2-1.96; Figure 3-5C). A similar result was obtained for a pooled analysis of 1,405 non-small cell lung cancer patients [358] (Figure 3-5D). These results support the trend observed for increased LARP1 expression in breast and lung cancers found in my review of Oncomine data (Figure 3-1**,** Figure 3-2), and suggest LARP1 may function as an oncogene in multiple cancer types.

Table 3-1. LARP1 protein expression in ovarian cancers is an independent predictor of poor outcome.

Uni- and multivariate Cox regression analysis of associations between clinical variables and LARP1 protein levels in tumours determined by IHC analysis, and overall survival, for 67 ovarian cancer cases. Staining and scoring performed by department of pathology. *Analysis by TGH, staining and scoring performed by collaborators*. ***P < 0.001, **P < 0.01, *P < 0.05.

Univariate

Variable	HR	HR 95% CI	*p-value*	
Histology	1.97	0.8862-4.398	0.096	
Stage	2.51	1.517-4.162	**<0.001**	***
Grade	1.73	1.124-2.653	**0.013**	*
Age	1.02	0.9911-1.043	0.201	
Residual Disease	10.88	1.405-84.210	**0.022**	*
LARP1 Score	1.15	1.006 -1.310	**0.041**	*

Multivariate

Variable	HR	HR 95% CI	*p-value*	
LARP1 Score	1.13	1.008-1.274	**0.036**	*
Age	1.02	0.9882-1.047	0.247	
Grade	1.19	0.6395-2.23	0.578	
Stage	2.70	1.4695-4.962	**0.001**	**

Histology	0.63	0.2311-1.732	0.373

3.2.4 LARP1 PROTEIN IS RELEASED BY OVARIAN CANCER CELLS IN CULTURE

Having demonstrated increased expression of LARP1 protein in ovarian malignancies, we hypothesised that patients with underlying tumours may have detectable LARP1 protein levels in their circulating plasma since RBPs such as Argonaute2 have previously been identified in human plasma [373]. To determine whether LARP1 could be detected extracellularly, I cultured ovarian cancer cells and collected the cell-conditioned media (CM) after 24 hours. Cells were maintained in serum-free conditions to avoid potential false positives from serum components. There was no difference in cell viability or levels of apoptosis at this early time point, when compared to the same cells in full media (Figure 3-6A,B). After removing floating cells and cell debris, the remaining protein was concentrated by ultrafiltration and analysed by western blotting for LARP1 protein. I obtained a single LARP1 protein band of approximately 125kDa in cell-conditioned media, which may represent a degraded or post-translationally modified form of the protein (Figure 3-6C). No LARP1 band was detected in non-conditioned media control, nor did I observe a band for the abundant cytoplasmic protein HSP60 under either condition. This suggests that LARP1 protein may be detected in conditioned media, and that its presence does not represent non-specific release of intracellular contents. Interestingly, I found that the apparent LARP1 band, whilst being detected with a polyclonal anti-LARP1 antibody raised in rabbits using an N-terminal protein fragment as an immunogen, was not detected by a polyclonal anti-LARP1 antibody raised in mice using the full length protein (data not shown). This suggested that, although raised against the full-length protein, the mouse anti-LARP1

polyclonal antibody lacked clones targeting the same N-terminal sequence used as the immunogen for the rabbit antibody. Two additional anti-LARP1 antibodies were explored, but were found to perform poorly in both the western blotting and ELISA settings.

Recent work by Dr M. Mura using media conditioned by pooled SKOV3 clones with stable knockdown of LARP1, demonstrates that this band decreases, relative to media conditioned by shControl-expressing cells. This supports my supposition that the detected band is indeed a form of LARP1 protein.

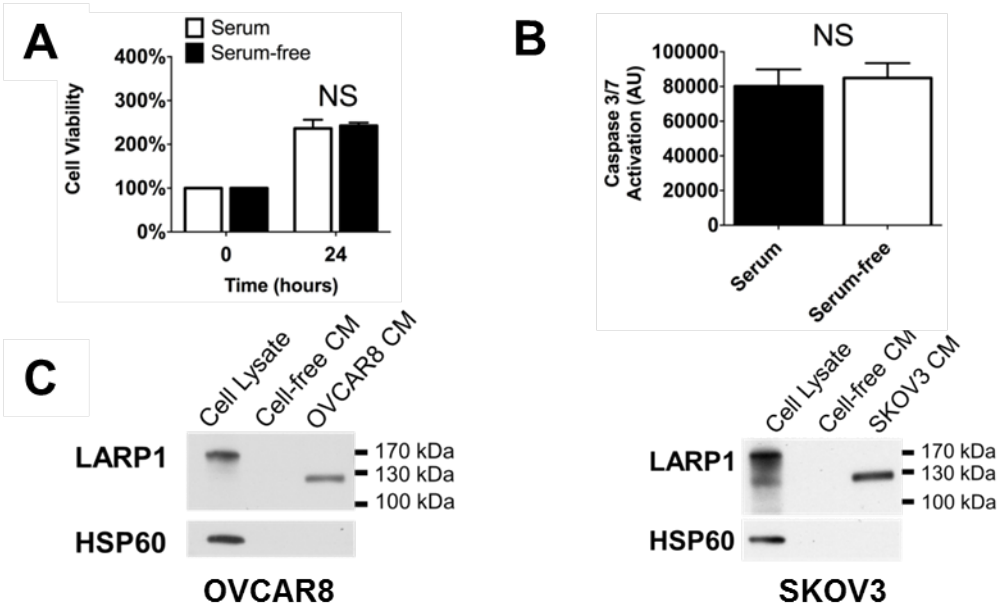

Figure 3-6. LARP1 protein is detectable in ovarian cancer cell-conditioned media.

(A) Cell viability determined by the MTT assay in OVCAR8 cells cultured in 10% FCS or serum-free conditions.
(B) Apoptosis, as determined by activated Caspase-3/7, in OVCAR8 cells cultured in 10% FCS or serum-free conditions for 24 hours.
(C) Western blot analysis of OVCAR8- or SKOV3-conditioned media concentrated by ultrafiltration and analysed using the N-terminal anti-LARP1 rabbit antibody. Representative images from three repeats. Students t-test. Error bars indicate SEM.

3.2.5 A LARP1 ELISA CAN ACCURATELY QUANTIFY PROTEIN IN HUMAN PLASMA

In order to quantify the levels of LARP1 protein in patient plasma, I developed a LARP1 sandwich enzyme-linked immunosorbent assay (ELISA). The assay utilised a sandwich format, with two antibodies against LARP1 raised in different species and against different epitopes. The optimised assay could accurately measure LARP1 protein concentration to <5pg/ml (Figure 3-7A,B). To confirm the suitability of the ELISA for use with human plasma samples, I performed spike-and-recovery experiments, demonstrating that human plasma did not interfere with the ability to detect LARP1 protein (Figure 3-7C). OVCAR8- and SKOV3-conditioned media was found to be negative for LARP1 protein when analysed on the ELISA. This result was expected, as western blotting had demonstrated that the capture antibody used in the ELISA did not detect the putative LARP1 protein band seen in conditioned media.

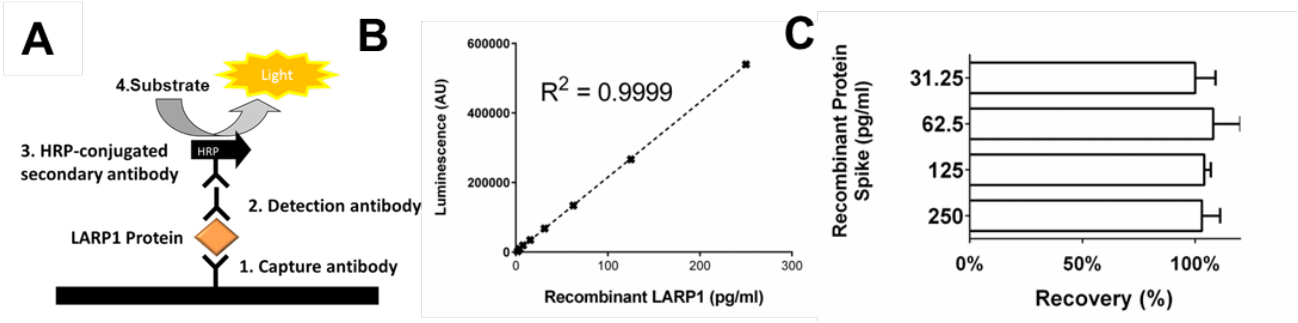

Figure 3-7. A LARP1 ELISA can accurately detect free LARP1 protein.

(A) A schematic of the LARP1 sandwich enzyme-linked immunosorbent assay (ELISA) detecting LARP1 protein in solution.
(B) The LARP1 ELISA standard curve, generated by serial dilutions of the recombinant LARP1 protein and quantified on the LARP1 ELISA.
(C) Spike and recovery experiments were performed using plasma from 5 separate healthy controls, and 4 separate spike concentrations of recombinant protein. A known quantity of recombinant protein was 'spiked' into healthy donor plasma and these samples, together with unadulterated plasma, were analysed using the LARP1 ELISA. The concentration of LARP1 detected by the ELISA in the sample spike (minus any positivity from the un-spiked plasma) was expressed as a percentage of the actual protein added, with the aim of achieving 100% recovery.

3.2.6 *PLASMA LARP1 PROTEIN LEVELS ARE HIGHER IN PATIENTS WITH UNDERLYING OVARIAN MALIGNANCY*

To evaluate LARP1 protein levels in clinical samples, I obtained plasma samples from healthy female volunteers and women with underlying ovarian malignancies, prior to surgical or chemotherapeutic intervention. I found low or undetectable levels of LARP1 protein in the majority of healthy women, but significantly higher levels in women with underlying ovarian malignancy (Figure 3-8A). Although plasma LARP1 values from both control and patient cohorts overlapped, I found, by plotting a receiver operating characteristic (ROC) curve, that the area under the curve (AUC) was significantly greater than 0.5 (AUC 0.76, 95% CI 0.65-0.87, $p<0.001$; Figure 3-8B), and for circulating plasma levels above 290.3 pg/ml, the test had a 50% sensitivity and a specificity of 90%. I obtained matched plasma from a subset of the cancer cohort after they had undergone surgery, but prior to commencing chemotherapy. For patients with detectable plasma LARP1 pre-surgery, there was a significant drop in circulating protein following removal of their primary tumour (Figure 3-8C). This indicates that levels of circulating protein may reflect underlying tumour burden.

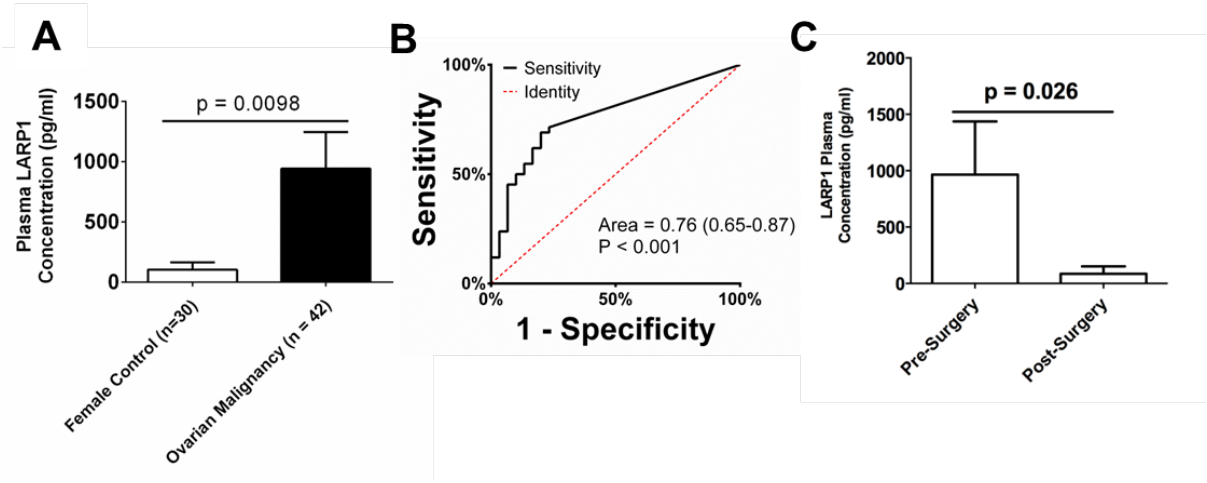

Figure 3-8. Circulating LARP1 protein levels are elevated in women with underlying ovarian malignancy.

(A) Plasma LARP1 concentration in healthy female controls and patients with primary ovarian malignancies sampled prior to surgery.
(B) The ROC-curve of data from Figure 3-8A, showing area under the curve. Analysed using GraphPad Prism.
(C) Plasma LARP1 concentration for 19 patients with underlying ovarian malignancy sampled before and after primary surgery. Students t-test. Error bars indicate SEM.

3.2.7 PLASMA LARP1 PROTEIN HAS PROGNOSTIC VALUE

Having demonstrated that intratumoural LARP1 expression correlated with prognosis, I next evaluated whether the same was true of circulating protein. Plasma obtained from a small cohort of patients attending an ovarian cancer follow-up clinic was analysed, with survival data extending over two years. I first compared the association of plasma CA-125 levels with prognosis. As expected, using a threshold of 100U/l, which has previously been reported as a predictor of prognosis following primary treatment [374], there was a significant survival association (log-rank p = 0.019; Figure 3-9A). Next, stratifying patients into those with detectable and undetectable levels of circulating LARP1 protein, the survival association was more significant (log-rank p = 0.012; Figure 3-9B). Despite similar survival trends, there was no significant correlation between CA-125 plasma levels and circulating LARP1 protein treating them either as continuous or categorical variables (Figure 3-9C,D), suggesting the two tests may identify different high-risk populations.

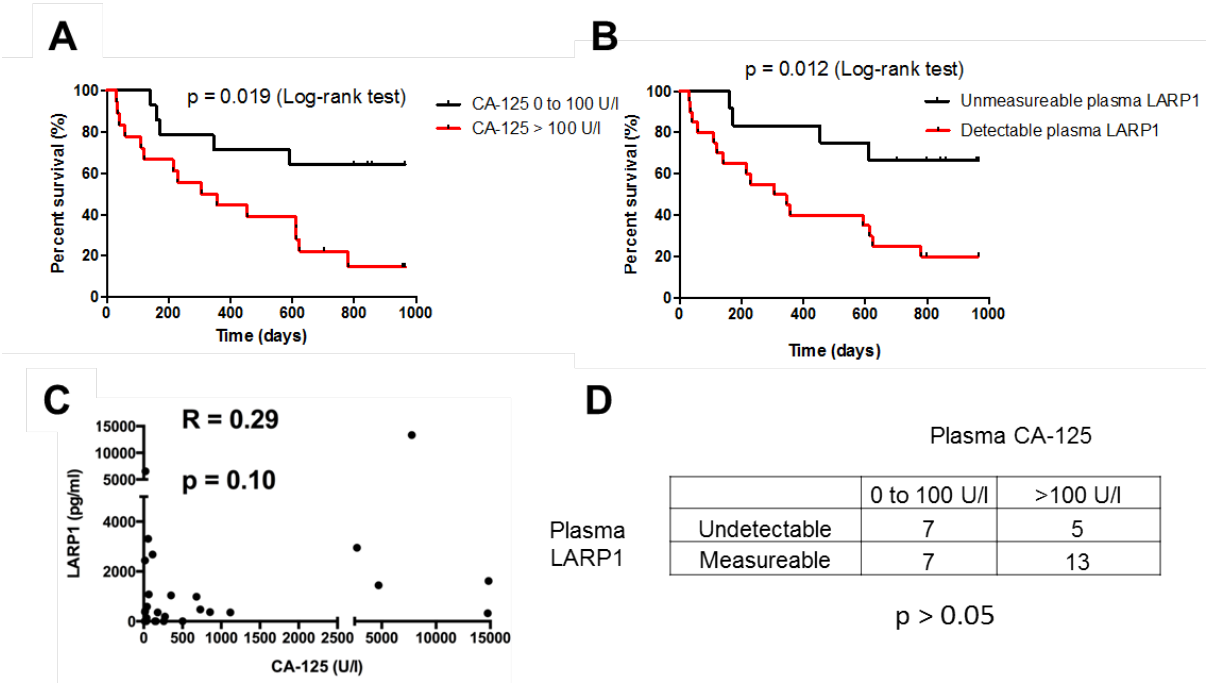

Figure 3-9. Plasma LARP1 levels predict adverse outcomes.

(A) Kaplan-Meier plot of overall survival in a post-surgical ovarian cancer cohort (n = 32) stratified according to CA-125 plasma levels.
(B) Kaplan-Meier plot of overall survival in a post-surgical ovarian cancer cohort (n = 32) stratified according to CA-125 plasma levels.
(C) Plasma LARP1 and plasma CA-125 levels for each patient (n=32) with the degree of correlation analysed with the Pearson test.
(D) A contingency table of the same data showing the association of plasma CA-125 and circulating LARP1, analysed with the Chi-squared test.

3.2.8 SUMMARY

In conclusion, in this first results section I have demonstrated that LARP1 expression is elevated in a range of solid malignancies. Specifically, at both the mRNA and protein level, LARP1 has an oncogenic pattern of expression in ovarian and cervical tumours (Section 3.2.2). LARP1 expression is a predictor of poor outcome in ovarian, breast and lung cancers, suggesting a key role in malignant progression (Section 3.2.3).

In addition, LARP1 protein is released by ovarian cancer cells in culture and is detectable in human circulating plasma (Section 3.2.5). Levels of plasma LARP1 are higher in patients with underlying malignancy than health female controls, and appear to reflect underlying tumour burden (Section 3.2.6). In a small patient cohort, plasma LARP1 correlates with outcome independently of circulating CA-125 levels (Section 3.2.7) suggesting potential as a circulating prognostic biomarker.

3.3 *LARP1* IN CANCER CELL BIOLOGY

3.3.1 LARP1 IS REQUIRED FOR TUMOUR DEVELOPMENT AND PROGRESSION

To determine whether LARP1 was required for tumour development, I induced stable knockdown of LARP1 (shLARP1) in SKOV3 cells (Figure 3-10A, *inset*) and implanted these cells into severe combined immunodeficiency (SCID)-beige mice. SKOV3 cells are an EOC-derived line that have been used extensively as an ovarian cancer model *in vivo*. Cells were transfected and selected for *en* masse, and pooled clones representing >200 individual clones were used for all experiments. Control cells (shGFP) developed measureable tumours with shorter latency (median, 22 days) compared to shLARP1 cells (median 36, $p = 0.022$, Figure 3-10B). Control xenografts also reached significantly larger tumour size (Figure 3-10A,C). To ascertain whether these differences in tumour size and latency were due to decreased proliferation in shLARP1 cells, Ki67 positivity was analysed with IHC staining of fixed tumours. Surprisingly, there was no significant difference in nuclear positivity of Ki67 between tumours from each cohort (Figure 3-10D,E), suggesting proliferation was not the dominant factor in the differential tumour growth.

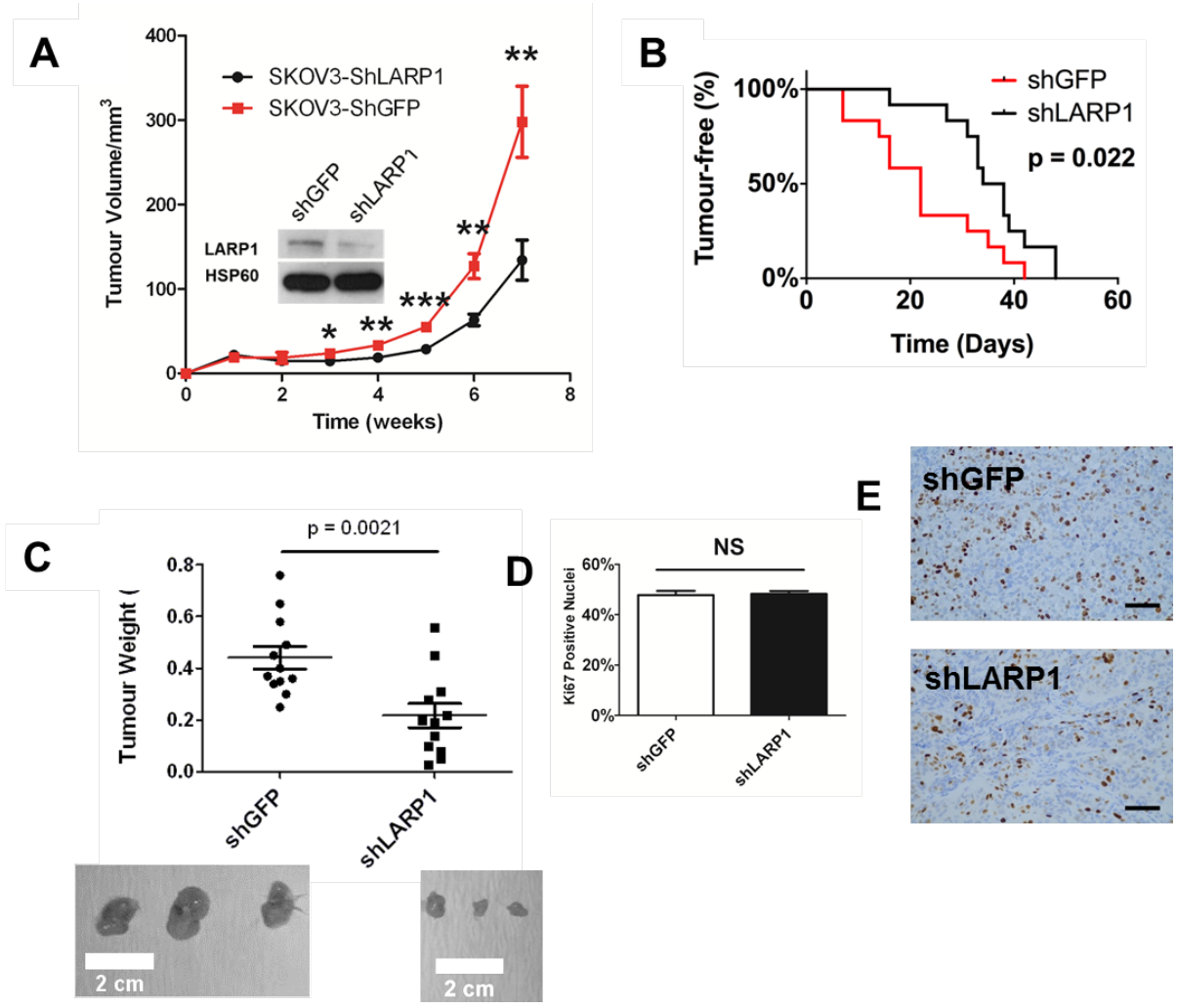

Figure 3-10. LARP1 is required for ovarian tumourigensis.

(A) SKOV3 control (shGFP) and LARP1 knockdown (shLARP1) cells were injected subcutaneously in SCID-beige mice and tumour volume monitored over time (inset, western blot of LARP1 knockdown in implanted cells. Representative images from three repeats).
(B) Kaplan-Meier curves of tumour-free survival. Log-rank test.
(C) Final tumour weights at sacrifice, with representative dissected tumours displayed below.
(D) Ki67 percentage nuclear positivity of fixed and embedded xenograft tumours analysed by immunohistochemistry. Scoring by Dr Justin Weir, analysis TGH.
(E) Representative examples of xenograft tumours stained with anti-Ki67 antibody (scale bar 100µm). Image capture and analysis TGH, staining Pathology Core Facility, scoring by Dr Justin Weir. ***$P < 0.001$, **$P < 0.01$, *$P < 0.05$. Student t-test. Minimum of three experimental repeats. Error bars indicate SEM.

I further explored the role of LARP1 in tumour formation in a different cancer model, using cervical cancer-derived HeLa cells. I created a LARP1-overexpressing line in HeLa cells (pTrex-LARP1), with an empty vector control as a comparator (pTrex-LacZ; Figure 3-11A).

Two million cells were injected subcutaneously into the flanks of non-obese diabetic–severe combined immunodeficiency (NOD-SCID) mice (n=12 tumours per cohort). The experiment was terminated when any mouse reached pre-set welfare limits. LARP1 overexpression resulted in significantly more rapid tumour growth, with a mean final tumour volume of 162.8mm^3, compared to 51.0mm^3 in the control group (Figure 3-11B,C). We subjected xenograft tumours from NOD-SCID mice to further histological examination. As before, there was no significant difference in Ki67 nuclear positivity (Figure 3-11D).

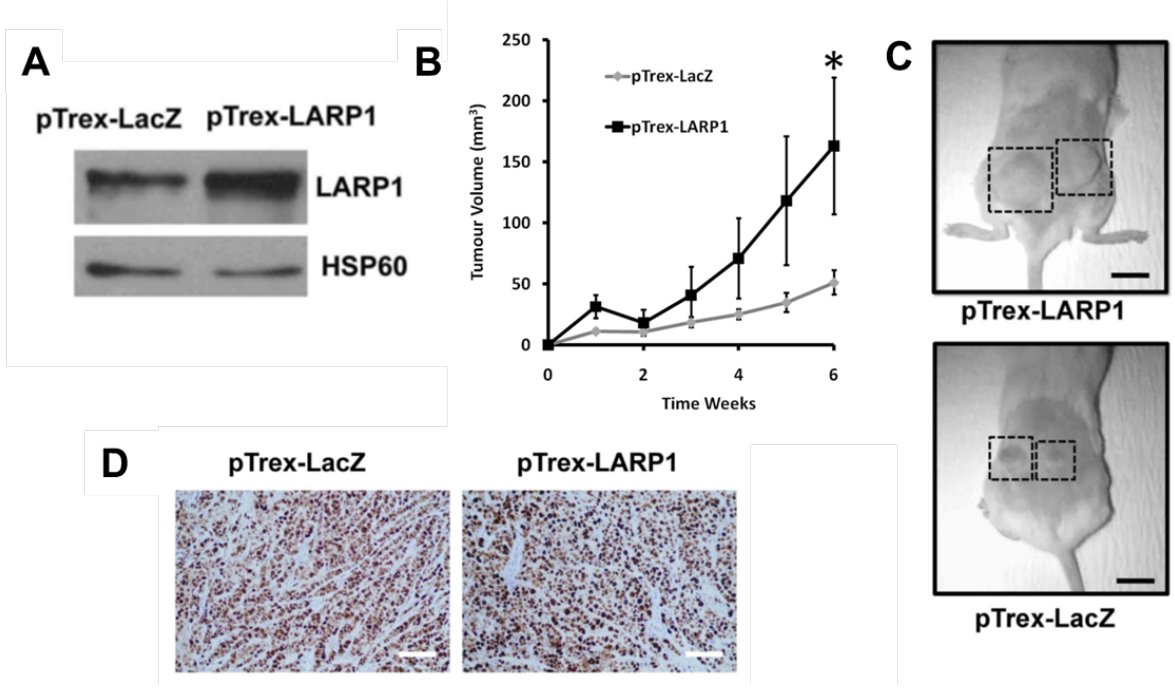

Figure 3-11. LARP1 promotes tumourigensis.

(A) Western blot of LARP1 overexpression in HeLa cells (*courtesy of Dr M Mura, representative image from three repeats)*.
(B) HeLa cells were injected subcutaneously in NOD-SCID mice and tumour volume was monitored over time.
(C) Representative xenografted mice (Scale bar 1cm).
(D) Ki67-stained xenograft tumours (Scale bar, 200µm).

3.3.1.1 LARP1 promotes clonogenicity and anchorage-independent growth

As tumour growth differences appeared to be independent of proliferation, I hypothesised that LARP1 inhibition may be affecting the tumour initiating potential of cancer cells. To model this *in vitro*, I carried out clonogenic assays following knockdown of LARP1. I found a significant decrease in colonies formed from SKOV3 and OVCAR8 ovarian cancer cells, and HeLa cells (Figure 3-12). To investigate the effect of LARP1 on cell survival in anchorage-independent conditions, I cultured LARP1 over-expressing HeLa cells in ultra-low attachment plates. Under these conditions, single cells form floating colonies termed spherosomes. LARP1 overexpression significantly increased the total number of spherosomes formed and, when spherosomes were dissociated into a single-cell suspension and re-plated under adherent conditions, the number of viable colonies (Figure 3-13A,B). Conversely, knockdown of LARP1 in OVCAR8 cells led to significantly reduced colony-formation in soft agar assays (Figure 3-13C).

These results indicate that LARP1 is required for clonogenicity and tumour development in ovarian and cervical cancer cells.

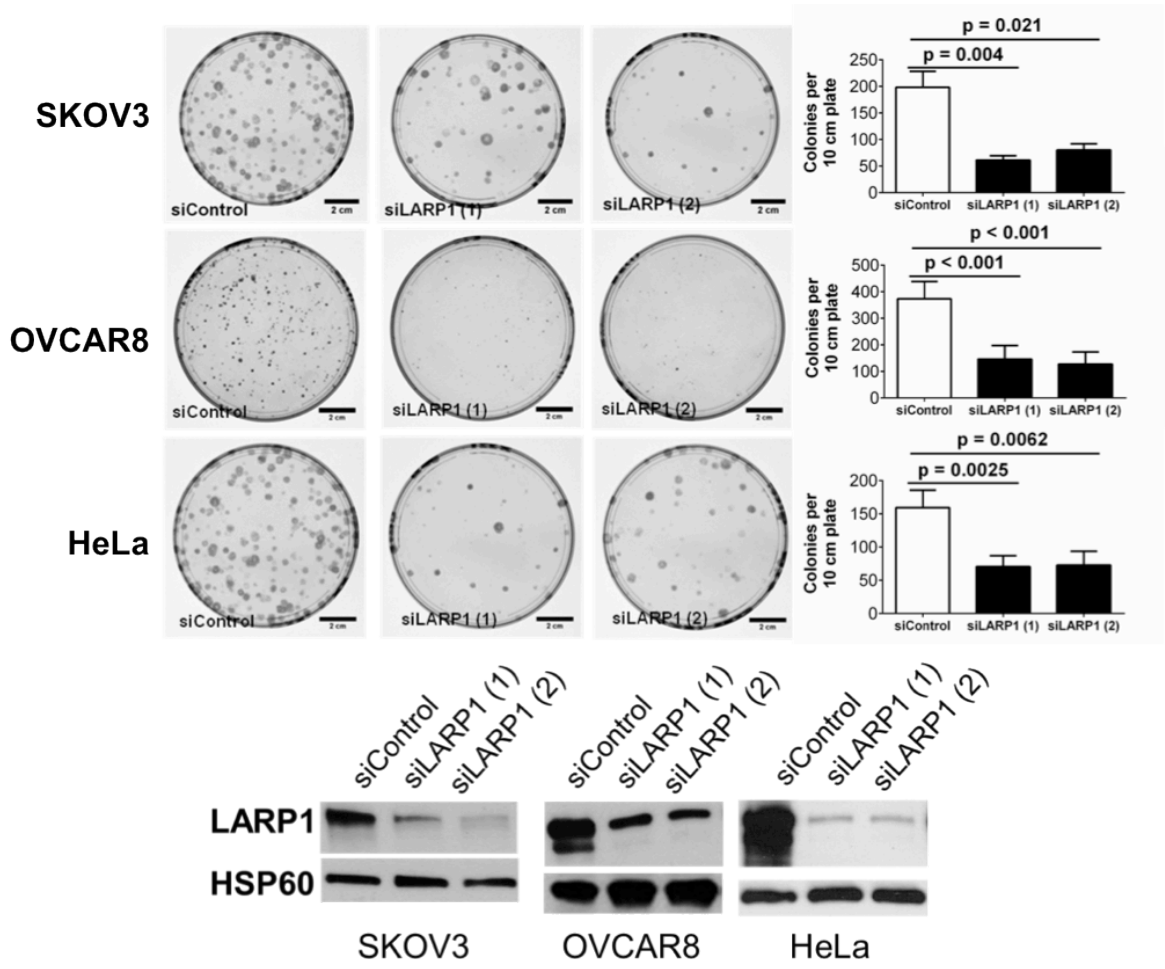

Figure 3-12. LARP1 is required for clonogenicity.

Clonogenic assays were performed in three cell lines following transient LARP1 knockdown. Briefly, transient knockdown was performed in 6-well plates. Cells were counted and re-seeded in 10cm plates and cultured for 10-14 days until visible colonies were seen, whereupon plates were stained with crystal violet. Representative 10cm plates are shown (scale bar 2cm) together with representative western blots of LARP1 knockdown in each cell line (at least three repeats performed). ***P < 0.001, **P < 0.01, *P < 0.05. Student t-test. Minimum of three experimental repeats. Error bars indicate SEM.

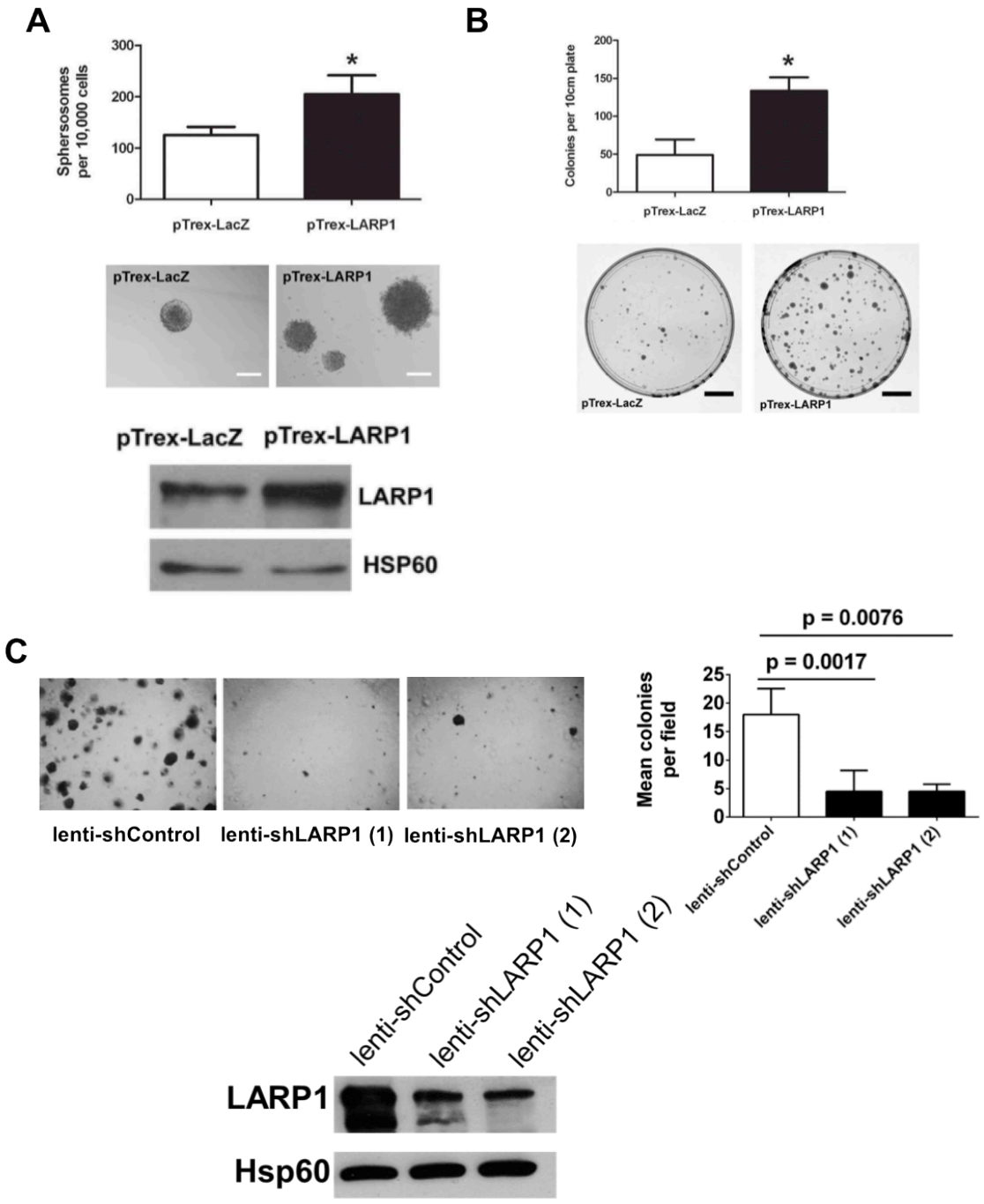

Figure 3-13. LARP1 promotes anchorage-independent growth.

(A) Number of Hela spherosomes formed 2 weeks after pTrex-LARP1 and pTrex-LacZ single cell suspensions were plated in ultra-low attachment plates. Representative images of spherosomes formed below (Scale bars, 200μM). Representative HeLa LARP1 overexpression western blot of at least three repeats shown (courtesy of Dr M. Mura)

(B) Number of HeLa colonies generated by dissociated spherosomes re-plated in adherent conditions. Scale bars 2cm.

(C) Ovarian OVCAR8 cells with stable LARP1 knockdown were plated in soft agar, and colonies formed counted. Representative images and quantification of experimental repeats. A representative western blot of LARP1 lentiviral knockdown of at least three repeats. ***P < 0.001, **P < 0.01, *P < 0.05. Student t-test. Minimum of three experimental repeats. Error bars indicate SEM.

3.3.1.2 LARP1 regulates tumour-initiating capabilities

To further investigate whether LARP1 knockdown affected the tumour initiating potential of ovarian cancer cells *in vivo*, I performed a limiting dilution assay, injecting decreasing numbers of SKOV3 cells with stable non-targeting or LARP1-targeting (shLARP1) short-hairpin expression, generated using lentiviral transduction (shControl and shLARP1 respectively). Cells were combined with Matrigel and introduced subcutaneously into NOD-SCID IL2R-gammanull (NSG) mice. To prevent bias due to host-to-host variation, control and LARP1 knockdown cells were injected into the left and right flank, respectively, of each mouse (Figure 3-14A,B). When one million cells were injected, all mice developed bilateral tumours, though the median latency was considerably greater for tumours with LARP1 knockdown compared to controls (19 vs 11 days, respectively; $P = 0.011$; Figure 3-14C). At the lower dose of 10^5 cells per injection, measureable tumours were not detected in 2/6 LARP1 knockdown injection sites. Tumour latency was more pronounced, with a median time to tumour development of 22 days in control cells, and 42 days in cells with LARP1-silencing ($P < 0.001$; Figure 3-14C). At 8 weeks following implantation of 10^4 cells, 2/6 tumours had developed in the control cohort, with no tumours found at sites of shLARP1 cell implantation. No tumours were detected when 10^3 shControl or shLARP1 cells were injected in either dose cohort (Figure 3-14B). As before (Figure 3-10), there was a striking difference in tumour volumes between control and LARP1-knockdown tumours (Figure 3-14D).

These data indicate that LARP1 silencing decreases the tumour-initiating capability of ovarian cancer cells.

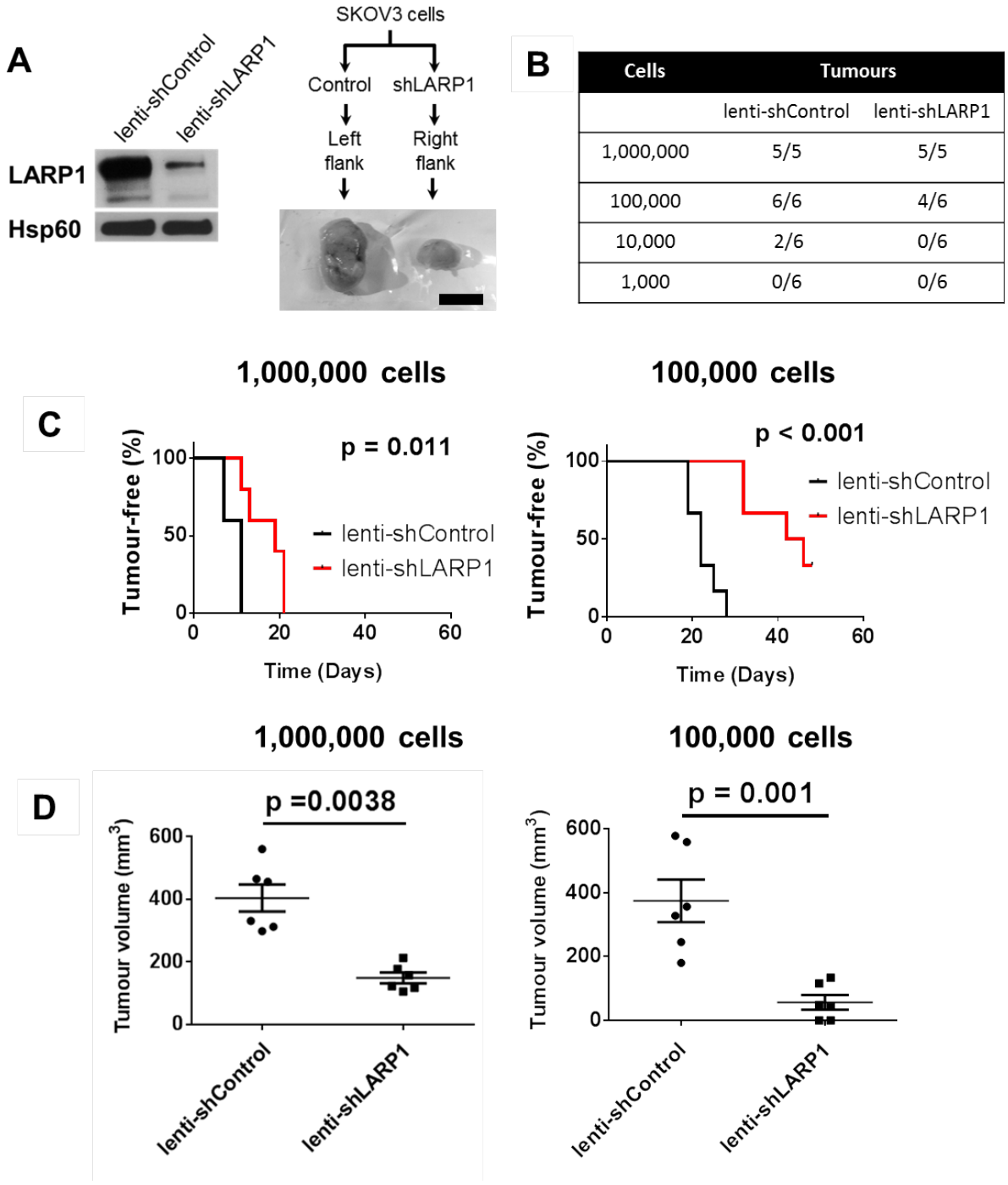

Cells	Tumours	
	lenti-shControl	lenti-shLARP1
1,000,000	5/5	5/5
100,000	6/6	4/6
10,000	2/6	0/6
1,000	0/6	0/6

Figure 3-14. LARP1 promotes tumour initiation.

(A) Western blot of LARP1 knockdown in SKOV3 stable cell lines using lentiviral transduction (representative image from at least 3 repeats), with schematic of cell injection protocol and representative tumours (scale bar 1cm).
(B) Limiting dilution assay results from SKOV3 cells injected subcutaneously into NSG mice.
(C) Kaplan-Meier curves of tumour-free survival for mice receiving $1x10^6$ cells (n=5) and $1x10^5$ cells (n=6). Log-rank test.
(D) Final tumour volumes for mice receiving $1x10^6$ cells and $1x10^5$ cells, respectively. ***P < 0.001, **P < 0.01, *P < 0.05. Student t-test. Error bars indicate SEM.

3.3.2 *LARP1* PROMOTES CANCER CELL SURVIVAL AND CHEMORESISTANCE

I hypothesised that, as differences in tumour development *in vivo* were not due to changes in cell proliferation, the observed effect on tumourigenicity of LARP1 knockdown may be due to altered cell survival. Indeed, transient LARP1 knockdown decreased cell viability (Figure 3-15A) and increased apoptosis, as indicated by increased caspase 3/7 activation, Annexin V-positivity and cleaved PARP on western blotting (Figure 3-15B-E). There was no associated change in cell cycle distribution (Figure 3-15F,G).

Laboratory culture conditions provide cells with a permissive environment for optimal growth, whilst implantation into host animals presents potential apoptotic triggers, such as decreased oxygen and nutrient availability. To model these environmental stresses, I exposed cells to 1% oxygen, serum starvation and L-glutamine depletion. In all cases, decreased LARP1 expression led to increased apoptosis in response to the stressor (Figure 3-16A-C). The fold increase in apoptosis for LARP1 knockdown cells compared to controls under hypoxia was less than that seen under optimum conditions (Figure 3-15B). This could be due to the much higher levels of apoptosis in both control and LARP1 knockdown cells under hypoxic conditions, with this powerful apoptotic trigger partially obscuring the effect of LARP1 knockdown.

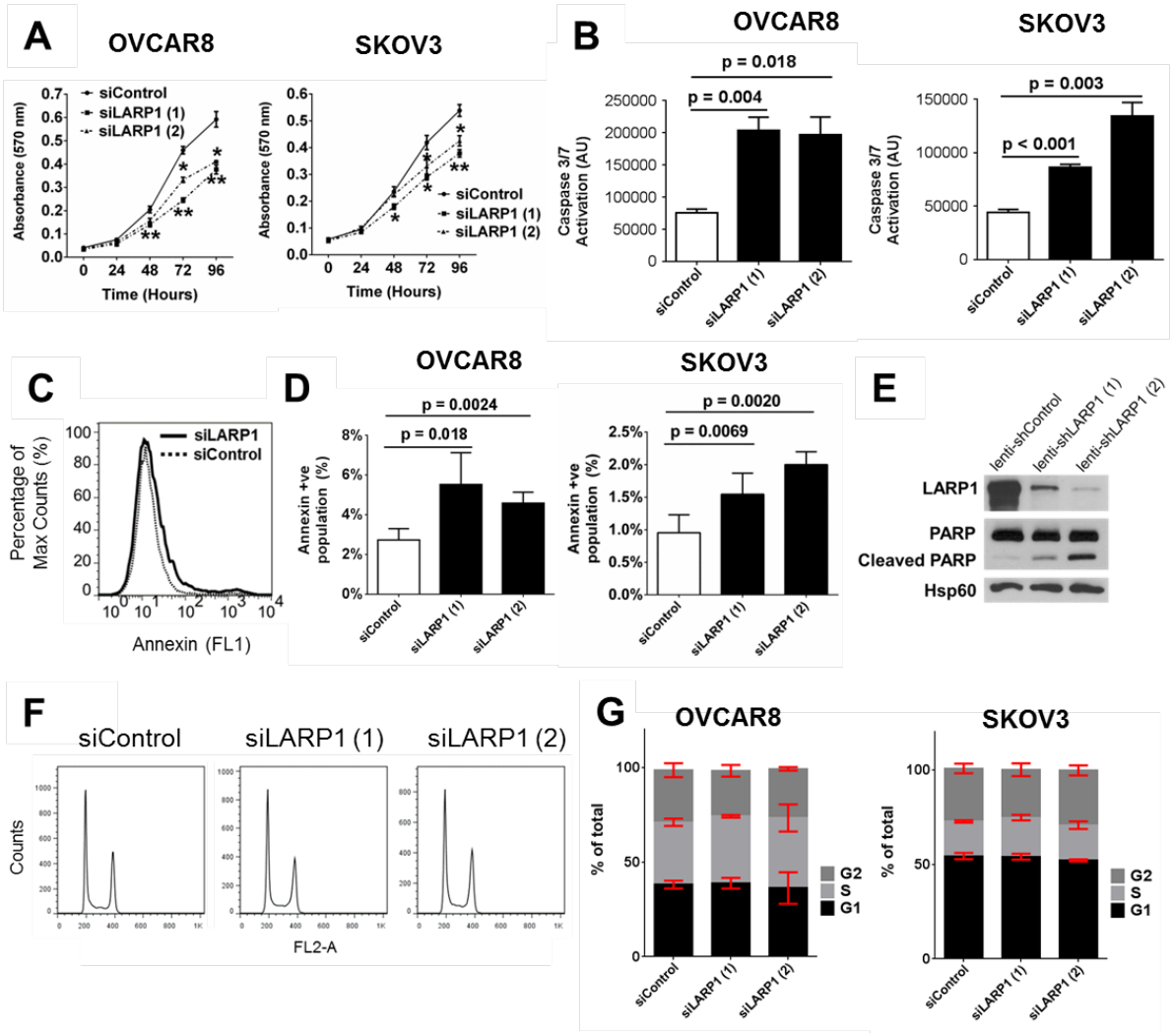

Figure 3-15. LARP1 knockdown in induces apoptosis without affecting cell cycle distribution.

(A) Cell viability following transient LARP1 knockdown determined by MTT assays.
(B) Levels of cleaved Caspase 3/7 determined by the CaspaseGlo assay in OVCAR8 and SKOV3 cells 48 hours after completion of transient LARP1 knockdown.
(C) Representative histogram plot of Annexin V-positive cells determined by flow cytometry in cells transfected with LARP1-targeting siRNA
(D) Percentage of Annexin V-positive cells at 24 hours following transient LARP1 knockdown in OVCAR8 and SKOV3 cells.
(E) Western blot analysis of cleaved PARP in OVCAR3 cells stably transduced with lentiviral shLARP1 constructs.
(F) Histogram plots of fixed and propidium iodide-stained OVCAR8 cells analysed by flow cytometry, following LARP1 knockdown.
(G) A summary of cell cycle distribution in two ovarian cancer cell lines following LARP1 knockdown. There was no statistical difference between control and LARP1 knockdown samples. Data represents at least three experimental repeats. Error bars indicate SEM. ***P < 0.001, **P < 0.01, *P < 0.05.

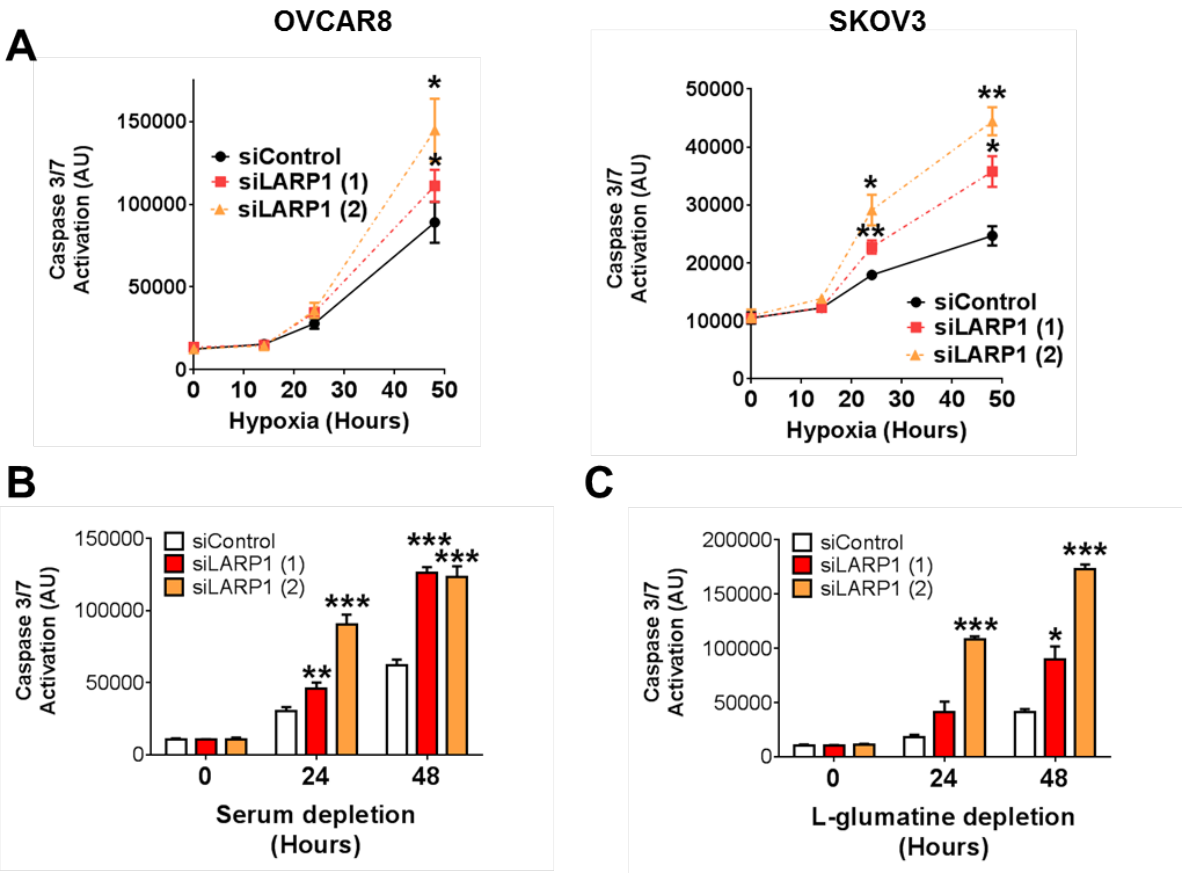

Figure 3-16. LARP1 knockdown increases apoptosis in response to environmental stressors.

(A) Apoptosis determined by the CaspaseGlo assay in response to hypoxia in OVCAR8 and SKOV3 cells following LARP1 knockdown. Cells were transferred to a hypoxic environment and transient LARP1 knockdown was performed at T=0 and T=24hrs, with apoptosis recorded at each timepoint.

(B) Apoptosis in SKOV3 cells following LARP1 knockdown and exposure to FCS-reduced (0.1%) conditions. Following LARP1 knockdown, cells were transferred to serum-reduced conditions and apoptosis was recorded at each time point (data normalised to apoptosis immediately after completion of LARP1 knockdown).

(C) Apoptosis in SKOV3 cells following LARP1 knockdown and exposure to L-glutamine-depleted conditions. Following LARP1 knockdown, cells were transferred to L-glutamine-depleted conditions and apoptosis was recorded at each time point. $P < 0.001$, $^{**}P < 0.01$, $^{*}P < 0.05$. Student t-test. Minimum of three experimental repeats. Error bars indicate SEM.

Having observed that LARP1 knockdown caused apoptosis, I hypothesised that high LARP1 levels may correlate with chemotherapy resistance, explaining its association with adverse survival in patients with ovarian cancer (Section 3.2.3). Ovarian cancer-derived SKOV3 and OVCAR8 cells are both resistant to platinum-based therapies [375]. To evaluate if LARP1 knockdown could partially restore platinum sensitivity, I transfected cells with LARP1-

targeting siRNA and then exposed cells to 25μM cis-diamine diplatinum (cisplatin/CDDP), a concentration chosen to induce significant apoptosis following 24 hours of treatment. LARP1 knockdown alone had minimal effects on cell morphology. Similarly, as expected, CDDP treatment had minimal effect on control cells at 24 hours. However, when LARP1 knockdown was combined with CDDP treatment, there was a marked change in microscopic appearance, with cells rounding and detaching (Figure 3-17A). This was associated with up to a 4-fold increase in apoptosis (Figure 3-17B, C) with a significant drop in viability (Figure 3-17D).

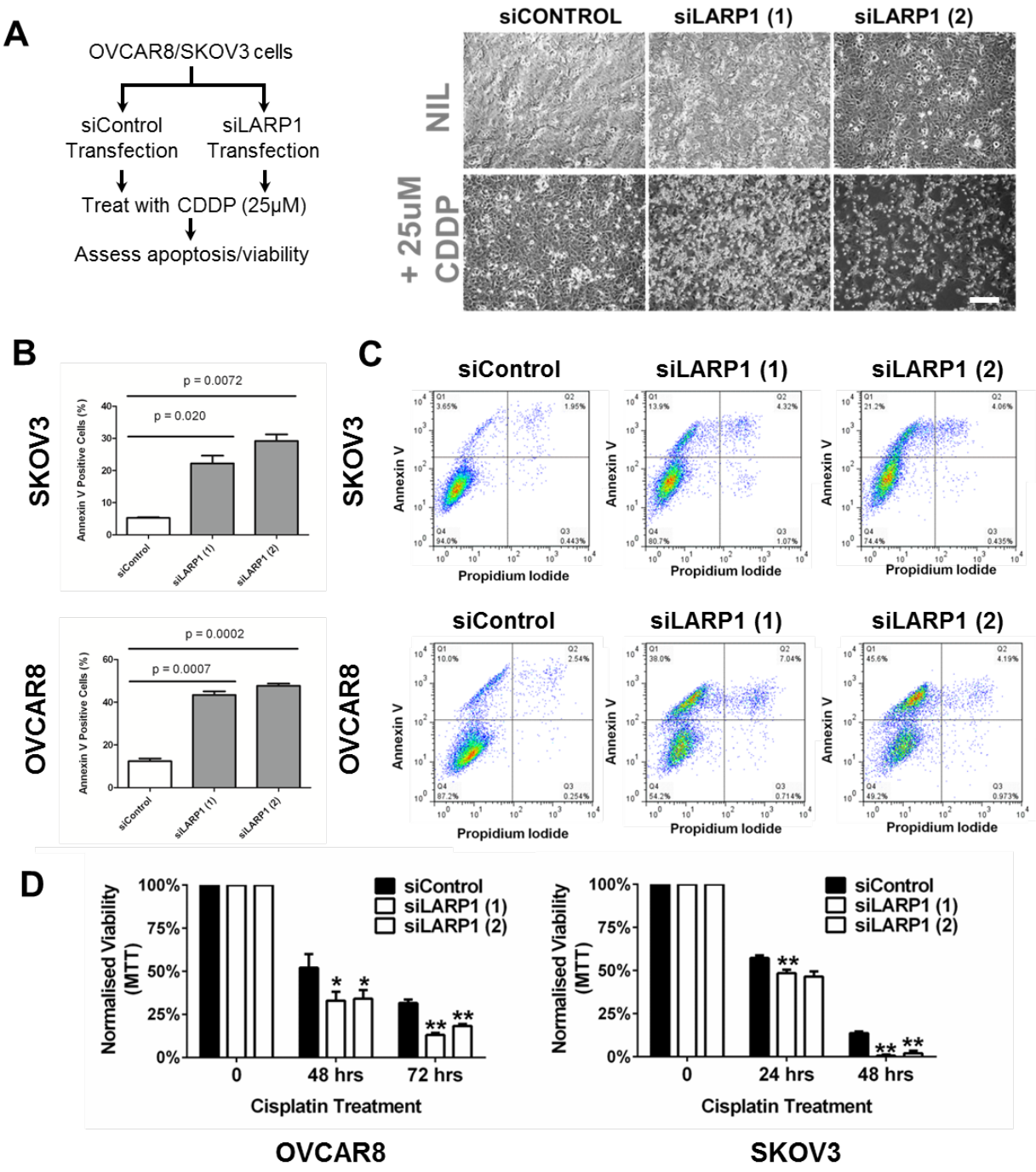

Figure 3-17. LARP1 is required for platinum resistance.

(A) Schematic of cell transfection and cisplatin (CDDP) treatment with representative OVCAR8 cell images in each condition (Scale bar 200μm)

(B) Percentage of Annexin V-positive cells following transient LARP1 knockdown and treatment for 24 hours with 25μM cisplatin in platinum-resistant SKOV3 and OVCAR8 cells.

(C) Representative dual-colour flow cytometry plots of Annexin V-FITC- and PI-stained SKOV3 and OVCAR8 cells transfected with LARP1-targeting siRNA and treated with with 25μM cisplatin.

(D) Normalised cell viability determined by MTT-based assay in SKOV3 and OVCAR8 cells following LARP1 knockdown and treatment with 25μM cisplatin. ***P < 0.001, **P < 0.01, *P < 0.05. Student t-test. Minimum of three experimental repeats. Error bars indicate SEM.

I repeated this experimental format with two other chemotherapeutics commonly used to treat EOC: paclitaxel and gemcitabine [24]. Treatment with both agents in the presence of LARP1 knockdown also led to increased apoptosis and decreased viability compared to drug treatment alone (Figure 3-18A,B). To further evaluate the platinum effect, I obtained matched cell lines from the same patient before and after the development of platinum resistance (PEO1 and PEO4, respectively). Resistant PEO4 cells have a platinum IC50 five times that of their sensitive counterpart [376]. Higher *LARP1* mRNA expression was seen in the platinum-resistant cell line (Figure 3-18C), while knockdown of LARP1 in both lines resulted in increased apoptosis on exposure to cisplatin (Figure 3-18D).

These results demonstrate that LARP1 acts as an anti-apoptotic protein, and promotes ovarian cancer cell survival in response to apoptotic triggers, including chemotherapy exposure.

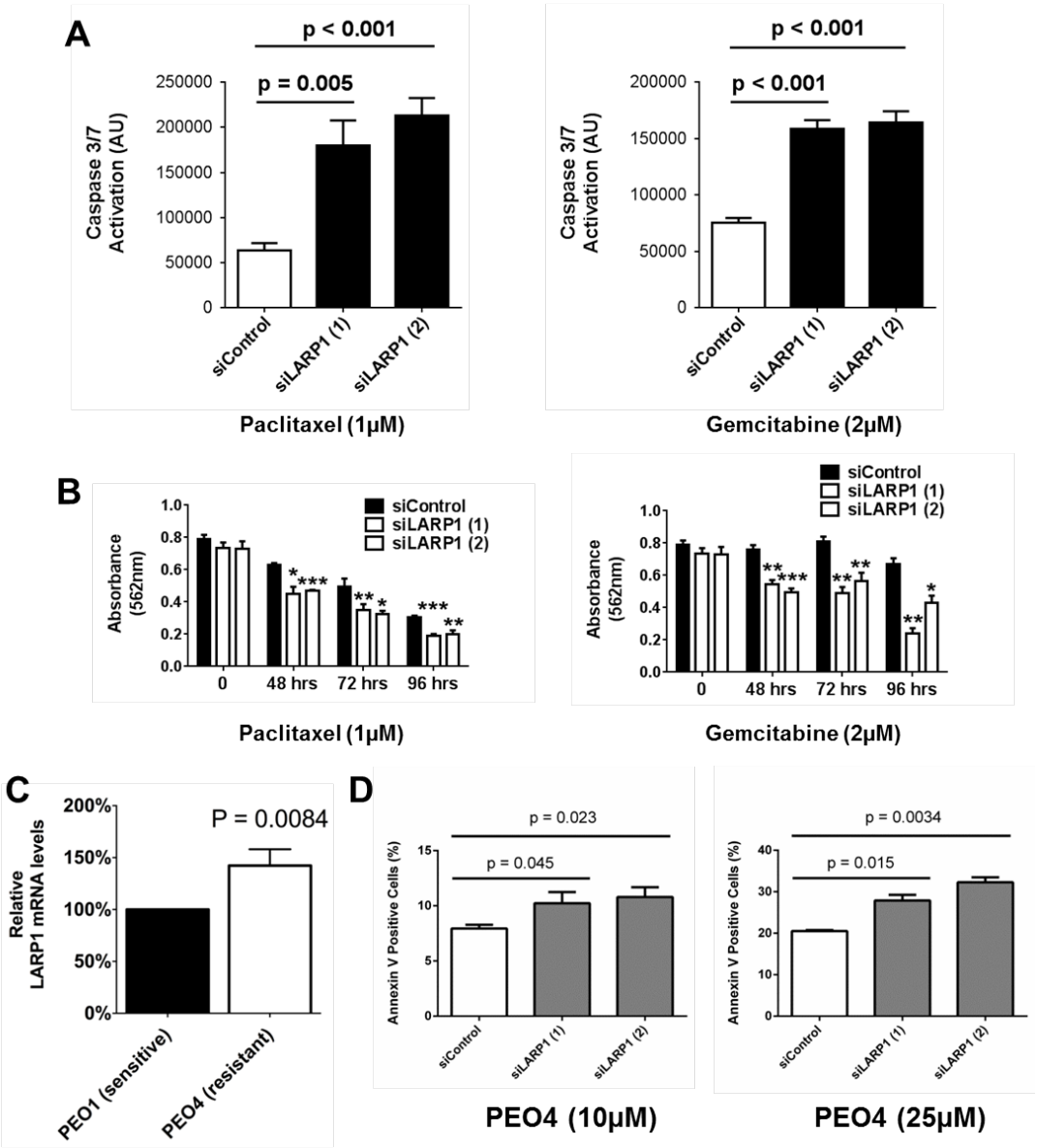

Figure 3-18. LARP1 promotes chemotherapy resistance.

(A) Apoptosis measured by cleaved caspase-3/7 in SKOV3 cells following 24 hours exposure to paclitaxel (1μM) or gemcitabine (2μM).
(B) Cell viability determined by MTT assay in SKOV3 cells following exposure to paclitaxel (1μM) or gemcitabine (2μM).
(C) Relative *LARP1* mRNA expression in PEO1 and PEO4 cells determined by RT-qPCR
(D) Percentage of Annexin V-positive platinum-sensitive PEO1 cells following transient LARP1 knockdown and treatment with 10μM cisplatin, and platinum-resistant PEO4 cells following transient LARP1 knockdown and treatment with 25μM cisplatin. ***P < 0.001, **P < 0.01, *P < 0.05. Student t-test. Minimum of three experimental repeats. Error bars represent SEM.

3.3.3 *LARP1* MAINTAINS CANCER STEM CELL-LIKE POPULATIONS

Enhanced tumourigenicity and clonogenicity are features often ascribed to cell populations with cancer stem cell (CSC)-like properties. Increased chemotherapy resistance has also been cited as a key CSC characteristic with clinical implications [55, 59, 377]. As LARP1 appears to regulate these traits, I hypothesised that it may be important in maintaining CSC-like cells. One of the best characterised markers of CSC-like populations is CD133. This is a transmembrane glycoprotein, encoded by the *PROM1* gene, originally identified as a stem marker in haematopoietic precursors [378] and proposed as a CSC marker in a range of solid malignancies, including glioblastoma and EOC [66, 379-382].

Table 3-2. CD133 membrane positivity in ovarian cancer cell lines.

Experimentally-derived CD133-positive population frequency in ovarian cancer cell lines compared with published CD133 relative mRNA abundance as determined by expression array analysis of the NCI60 cell panel [359, 383].

Cell line	Mean CD133+ population on flow cytometry	NCI60 relative expression (probe intensity – dataset minimum)
SKOV3	<0.1%	0
OVCAR8	<0.1%	0
OVCAR3	5.9%	4.56
IGROV1	4.6%	4.71

I used the NCI60 panel expression array dataset [359, 383] to identify cell lines with a PROM1/CD133 mRNA expression. There was strong correlation between published mRNA levels, and CD133 membrane positivity as measured by flow cytometry (Table 3-2).

OVCAR3 and IGROV1 cell lines had small populations of $CD133^+$ cells. Knockdown of LARP1 in these lines, and in cervical cancer-derived HeLa cells, resulted in a significant decrease in $CD133^+$ cell populations (Figure 3-19A,B).

No single marker has been shown to fully describe intra-tumoural heterogeneity. I assessed the effect of LARP1 knockdown on aldehyde dehydrogenase (ALDH) activity, another commonly used CSC marker that has been associated with stem-like properties in ovarian cancer cells [384-386], using the Aldefluor assay. Again, I saw a similar trend, with LARP1 knockdown resulting in a decrease in ALDH activity (Figure 3-19C,D). Having demonstrated that LARP1 targets CSC-like cells I wished to compare its effect with a positive control, known to selectively kill CSC-like populations. Salinomycin was identified in a high-throughput compound screen as targeting $CD44^{high}/22^{low}$ stem cell-like populations in breast cancer lines [387]. It has since been shown to have potential anti-CSC activity in other tumour types [388, 389]. As expected, salinomycin reduced $CD133^+$ populations in OVCAR3 cells, with the highest dose producing an effect equivalent to LARP1 knockdown (Figure 3-19E). High expression of several key embryonic stem cell-related transcription factors have been associated with enhanced CSC-like traits, including *SOX2*, *OCT4* and *NANOG* [390, 391]. Following LARP1 knockdown, I found reduction in expression of all three genes, with the most pronounced effect on *NANOG* (Figure 3-19F).

These results show that LARP1 promotes several characteristics associated with CSC-like cells, namely clonogenicity, tumourigencitiy, chemotherapy resistance, expression of stem cell-associated genes and maintenance of CSC marker-positive populations.

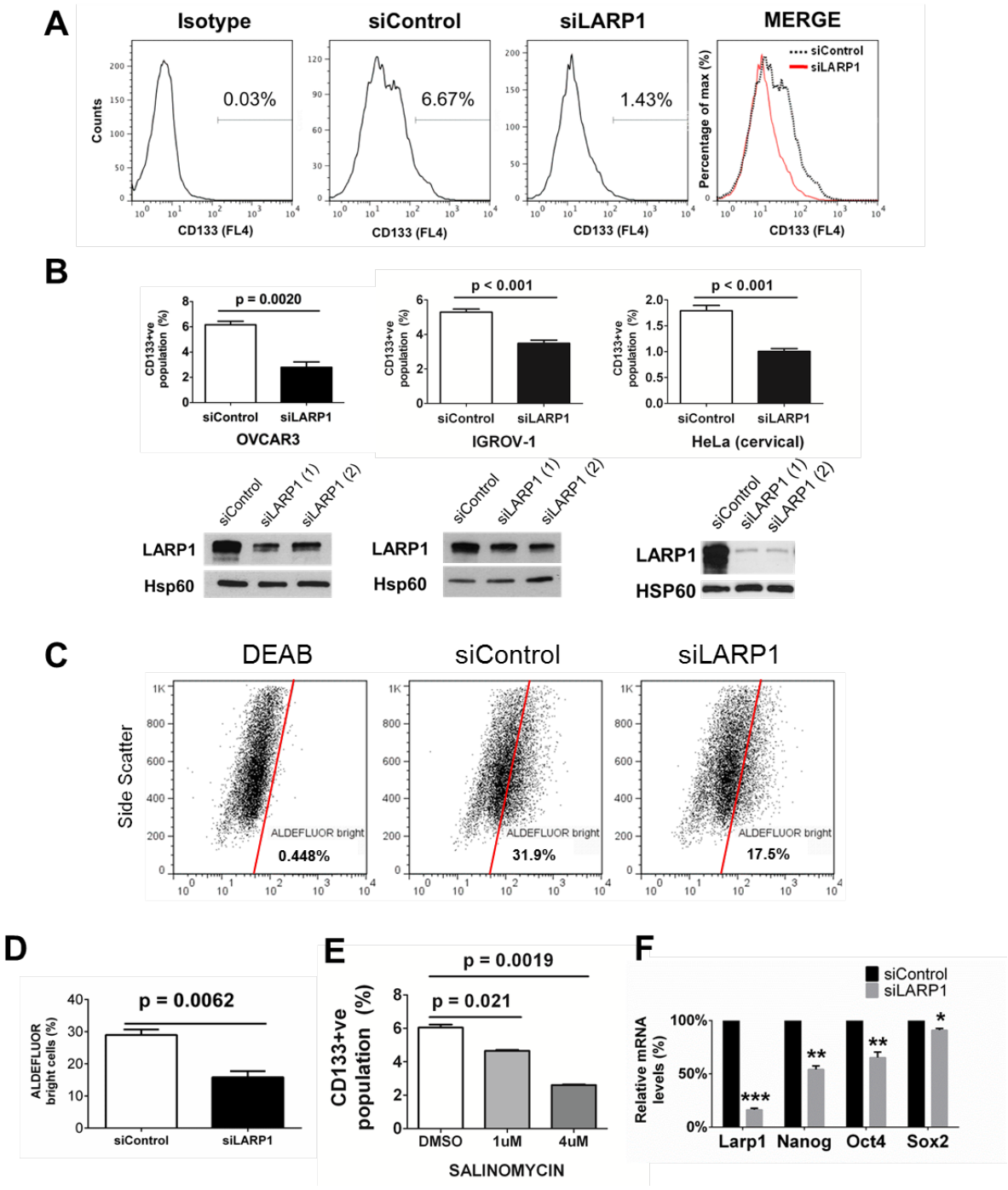

Figure 3-19. LARP1 maintains cancer stem cell (CSC)-like populations.

(A) Representative histogram plot of CD133-positive OVCAR3 cells determined by flow cytometry (a line with <10% CD133-positivity) following LARP1 knockdown.

(B) Mean CD133-positive populations determined by flow cytometry following LARP1 knockdown in OVCAR3, IGROV1 and HeLa cells, shown with western blots of LARP1 knockdown.

(C) Representative flow cytometry plots of ALDEFLUOR-positive OVCAR3 cells following LARP1 knockdown. Cells treated with diethylaminobenzaldehyde (DEAB), which inhibits aldehyde dehydrogenase activity, are used as a negative control for gating.

(D) Percentage of ALDEFLUOR-positive OVCAR3 cells following LARP1 knockdown.

(E) Percentage of CD133-positive OVCAR3 cells following treatment with the anti-CSC agent salinomycin.

(F) Relative mRNA expression of key stem cell-associated transcription factors following LARP1 knockdown (ΔΔCt, normalised to 18S RNA). ***P < 0.001, **P < 0.01, *P < 0.05. Student t-test. Minimum of three experimental repeats. Error bars indicate SEM.

3.3.4 *LARP1* PROMOTES CANCER CELL MOTILITY

A defining characteristic of malignant neoplasms is the ability to invade into surrounding tissue, requiring both cell motility and the ability to degrade the extracellular matrix. Having demonstrated a role in tumour progression, I wished to establish whether enhanced invasive abilities may be a component. Previous work in the lab had demonstrated that LARP1 knockdown in HeLa cells inhibited cell migration [333]. To further invesitgate this, I performed wound healing assays in ovarian cancer-derived SKOV3 cells following transient LARP1 knockdown. As expected, decreased LARP1 expression signifciantly inhibited cell motility (Figure 3-20A). Coversely, when LARP1 was overexpressed, cell motility was enhanced (Figure 3-20B,C). Similar results were obtained in HeLa cells overexpressing LARP1 (Figure 3-20D).

Transwell matrigel invasion assays with SKOV3 cells demonstrated that LARP1 knockdown resulted in a significant decreases in the number of invasive cells (Figure 3-20E). Using HeLa cells, LARP1 knockdown led to an 85% reduction in cell invasion (Figure 3-20F). These results indicate a fundamental role for LARP1 in cancer cell invasion.

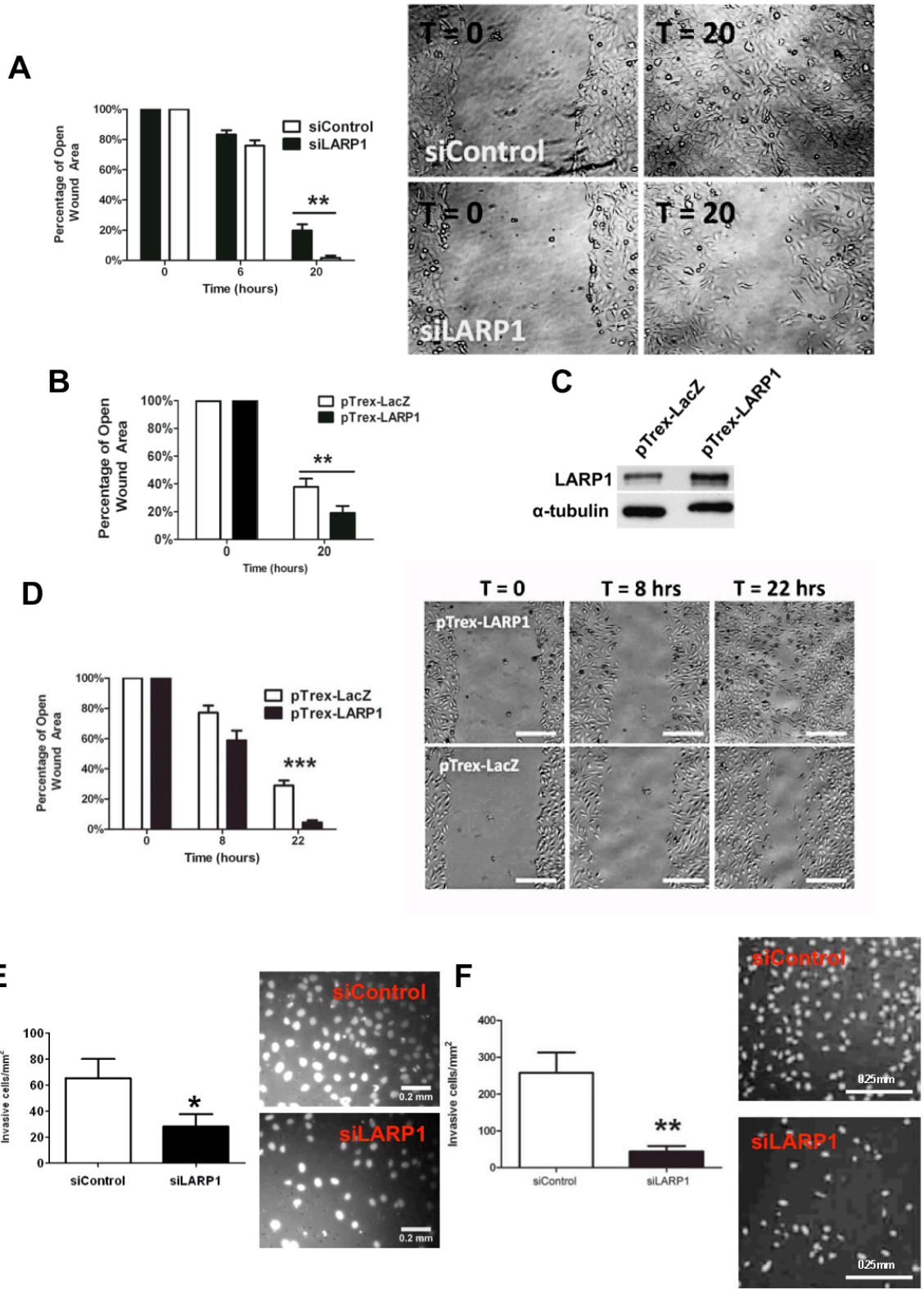

Figure 3-20. LARP1 promotes migration and invasion.

(A) Wound healing assays in SKOV3 cells following transient LARP1 knockdown. The graph shows quantification of the unhealed area at given time points. Wound array was quantified using ImageJ, by calculating the cell free area at each time point (see Materials and Methods for full details). Representative 10x images are shown to the right.

(B) Wound healing assays in SKOV3 cells stably overexpressing LARP1 (pTrex-LARP1) vs control (pTrex-LacZ).
(C) Western blot of LARP1 overexpression in SKOV3 cells (representative image of at least three repeats).
(D) Wound healing assays in HeLa cells stably overexpressing LARP1 (pTrex-LARP1) vs control (pTrex-LacZ). Representative images (200μm scale bar), and scratch area quantification.
(E) Matrigel-coated transwell invasion assays with SKOV3 cells following LARP1 knockdown. Graphs are counts of the number of invasive cells. Representative images of DAPI-stained invasive cells are shown.
(F) Matrigel-coated transwell invasion assays with HeLa cells following LARP1 knockdown. Representative images of DAPI-stained invasive cells are shown. ***P < 0.001, **P < 0.01, *P < 0.05. Student t-test. Minimum of three experimental repeats. Error bars represent SEM.

3.3.5 LARP1 LOCALISATION

LARP1 is predominantly cytoplasmic, in contrast to La/LARP3 which is mainly found in the nucleus [226]. I next investigated whether LARP1 localisation altered following drug treatment, as several RBPs have been shown to move between the nucleus and cytoplasm in response to cellular stressors [392]. To do this, I first performed immunofluorescent staining of two platinum-resistant ovarian cancer cell lines (PEO4/SKOV3), with and without CDDP treatment, and analysed the stained cells with confocal microscopy. As expected, LARP1 protein was almost completely restricted to the cytoplasm in resting cells. However, following 24 hours exposure to CDDP, a marked increase in nuclear LARP1 protein was seen in many cels (Figure 3-21A). Total levels of LARP1 protein do not alter following CDDP treatment when assessed by western blotting (data not shown). To attempt to quantify differences in nuclear LARP1 levels, I collected nuclear protein fractions from SKOV3 cells following platinum treatment. I found nuclear LARP1 protein levels increased substantially following cisplatin treatment (Figure 3-21B). There were several bands found on LARP1 immunoblotting of nuclear fractions. Whilst these may represent products of protein processing/degradation, at least two splice variants of LARP1 are known to exist (Figure 3-21C). Although no post-translational modifications are known for LARP1, LARP3 protein

undergoes C-terminal cleavage for nuclear localisation [246], and may represent a conserved feature of the protein family. Further experiments are necessary to identify what these additional band represent, and the mechanism and signficance of the nuclear enrichment of LARP1 protein.

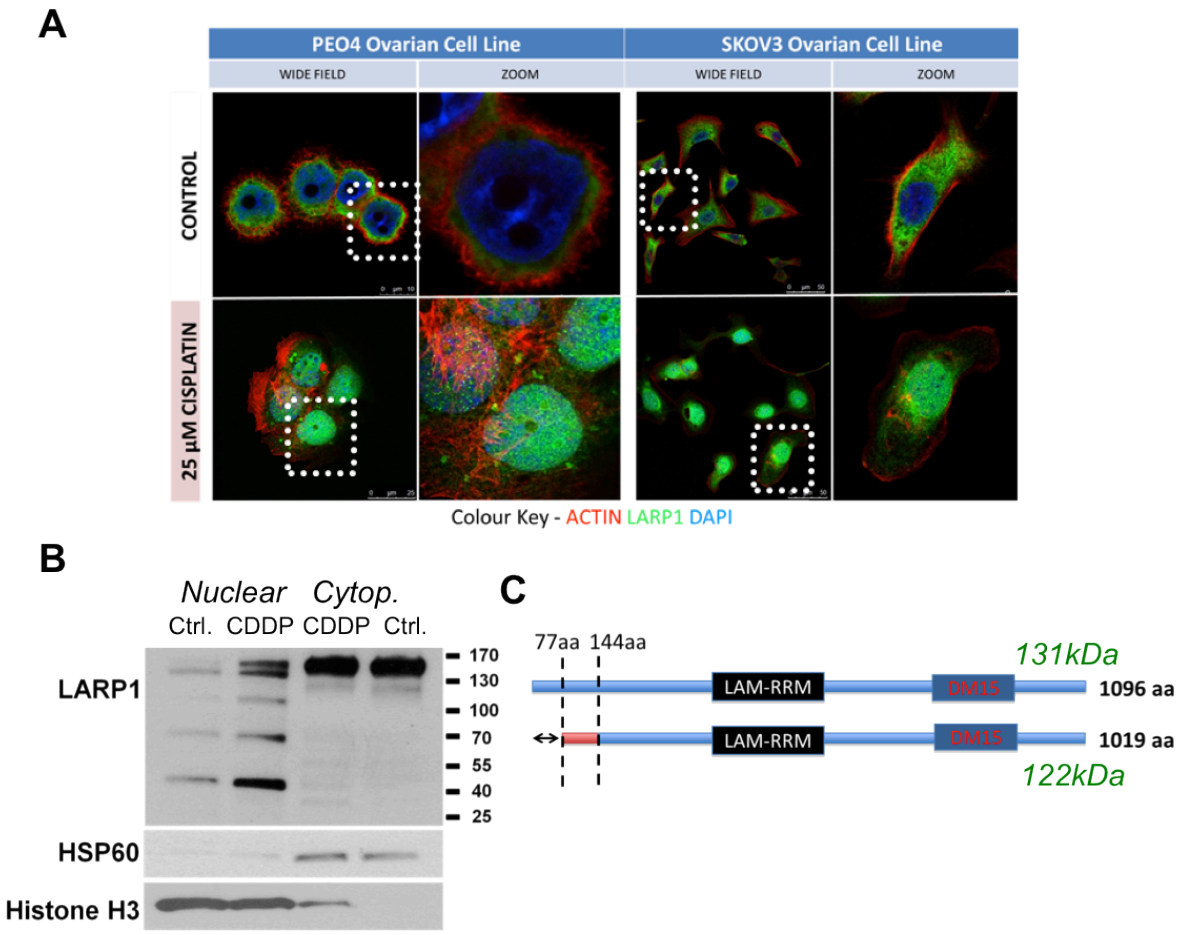

Figure 3-21. LARP1 protein levels in the nucleus increase on cisplatin exposure.

(A) Immunofluoresence confocal microscopy of LARP1 (green) and actin (red) with DAPI counterstaining (blue) in untreated PEO4 and SKOV3 cells, or following 24 hours exposure to 25µM CDDP. Images represented representative fields of view from three experimental repeats. Quantification was not done using this experimental approach, but through fractionation and western blotting (see below).

(B) Western blotting of nuclear and cytoplasmic (cytop.) protein fractions from SKOV3 cells following 24 hours exposure to CDDP. Representative image of at least three repeats. Unfortunately, cisplatin treatment appears to alter the nuclear localisation of Histone H3, giving the appearance of incomplete fractionation from CDDP-treated samples. There was not time to repeat this experiment with a more suitable nuclear loading control.

(C) A schematic of the two known splice variants of LARP1 protein, showing the alternative sequence at the N terminus. Predicted sizes are 131 and 122 kDa, for the larger and smaller isoforms, respectively.

3.3.6 SUMMARY

In this sub-chapter, I investigated, at the level of cancer cell biology how elevated levels of LARP1 protein could lead to adverse outcomes in patients. I found that knockdown of LARP1 inhibited tumour development and growth, whilst overexpression promoted tumour development (Section 3.3.1). In both cases, this difference was independent of effects on cell proliferation. I showed that LARP1 was required to maintain clonogenic and anchorage-independent growth potential *in vitro,* and that LARP1 is required for tumourigenicity *in vivo*. Tumour initiating ability is a critical feature of cancer stem cell (CSC)-like cells. I found that LARP1 knockdown also led to decreased a) abundance of CSC-marker positive cell populations, and b) expression of stem cell-related transcription factors (Section 3.3.3).

A key determinant of outcome in ovarian cancer is the response to platinum-based chemotherapy, with patients who develop resistance early having a very poor prognosis. I hypothesised that the decreased tumourigenicity seen *in vivo,* and the trend towards poor survival with high LARP1 expression in the clinical data, could be explained by a role for LARP1 in modulating cancer cell survival. Indeed, knockdown of LARP1 induced apoptosis and decreased viability, without altering proliferation. This effect was enhanced when cellular stresses such as serum-depletion and hypoxia were applied. Moreover, linking directly to the trends in the clinical data, I found that LARP1 depletion sensitised cells to chemotherapy, in line with its apparent anti-apoptotic role (Section 3.3.2). As CSC-like cells have also been shown to have enhanced chemoresistance, this suggested these phenotypic effects were linked.

3.4 IDENTIFYING LARP1 TARGETS

3.4.1 TRANSCRIPTOMIC ANALYSIS ON LARP1 KNOCKDOWN

To understand the molecular basis for the observed effects on tumourigenicity and cell survival when altering LARP1 expression, mRNA-sequencing following LARP1 knockdown was performed. Data from three biological repeats were combined. In controls cells, *LARP1* was in the top 7% most abundant mRNAs, with transcript abundance comparable to translational components such as *EIF4A3* and *RPL36A* (Figure 3-22A). Knockdown of LARP1 with siRNA achieved a 79% decrease in mRNA levels, with no significant change in other LARP family members (Figure 3-22B). Following LARP1 knockdown, there were an equal number of mRNAs that displayed increased and decreased abundance (Figure 3-22C). *Ingenuity* disease enrichment analysis revealed that transcripts with altered levels on LARP1 knockdown were significantly enriched for functions linked to cancer (Figure 3-22D). Molecular and cellular function analysis revealed a significant enrichment for genes associated with cell proliferation and cell death and survival (Figure 3-22E).

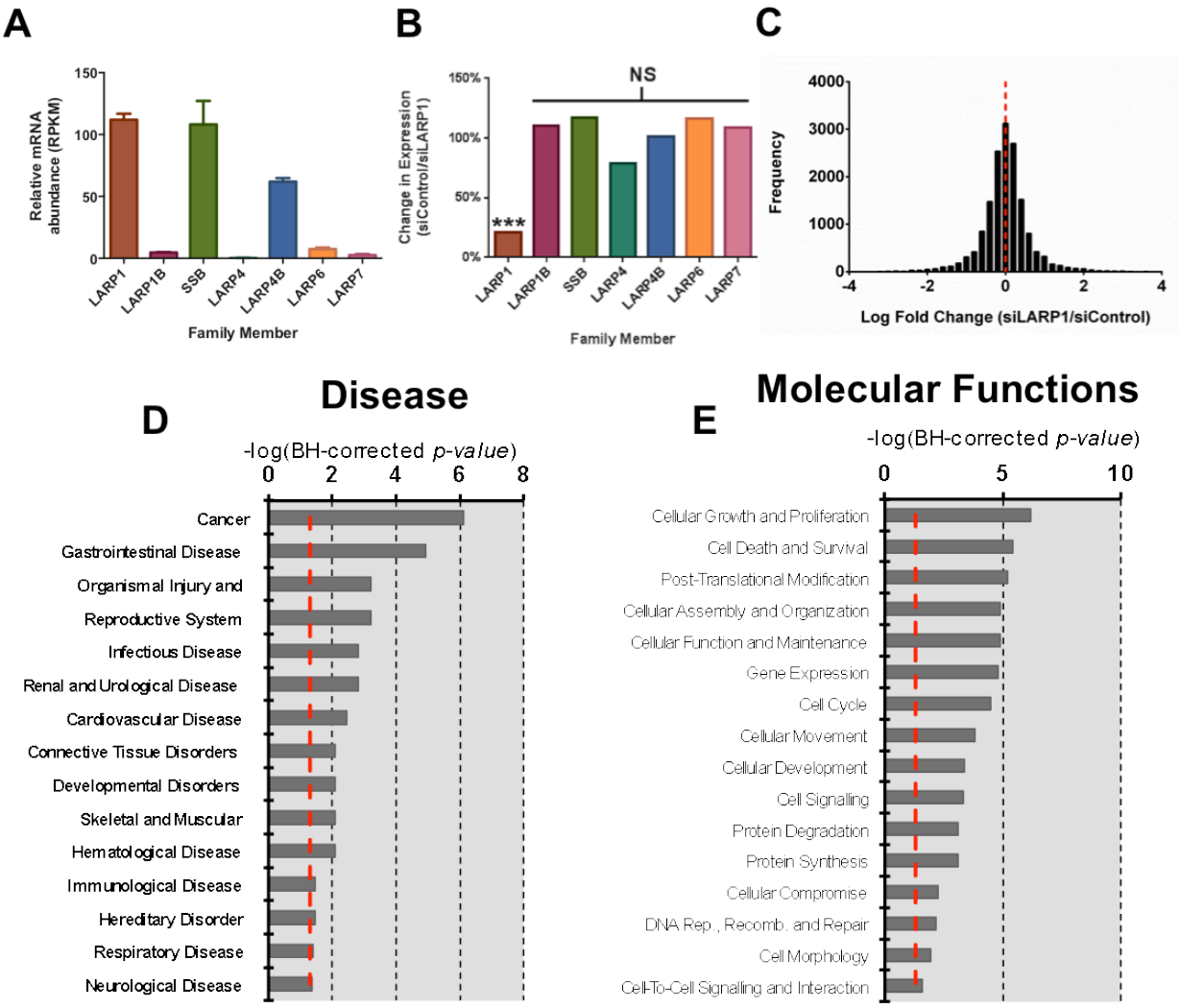

Figure 3-22. Transient knockdown of LARP1 alters the cancer cell transcriptome.

(A) Normalised transcript reads (RPKM) of LARP family members in the RNA-seq analysis of control samples.
(B) Percentage change in mRNA expression of LARP1 family members following LARP1 knockdown.
(C) Frequency distribution of Log-2 fold change in mRNA expression in OVCAR8 cells following transient LARP1 knockdown (LARP1 knockdown relative to control).
(D) Disease enrichment with Ingenuity Pathway Analysis (IPA) of genes differentially expressed following LARP1 knockdown (-log[BH-corrected p-value] shown, red dashed line indicates p = 0.05).
(E) Molecular function ontology enrichment with Ingenuity Pathway Analysis (IPA) of genes differentially expressed following LARP1 knockdown (-log[BH-corrected p-value] shown, red dashed line indicates p = 0.05).

3.4.1.1 RNA-sequencing compared to the HeLa LARP1 mRNA interactome

In order to identify transcripts potentially directly regulated by LARP1 at the level of mRNA stability, I cross-referenced my OVCAR8 RNA-seq data with data from a LARP1 RNA-immunoprecipitation and expression array analysis (RIP-Chip) experiment, performed by Dr Manuela Mura, which identified mRNAs in complex with LARP1 protein (*data in press*). I found that genes that showed altered expression following LARP1 knockdown were more likely to be represented in the LARP1 mRNA interactome (hypergeometric probability distribution, p=0.042), suggesting LARP1 interaction with mRNAs may play an important role in determining their abundance (Figure 3-23A). Of the 758 genes represented in both datasets, 49% showed decreased transcript abundance on LARP1 knockdown, whilst 51% showed increased abundance: LARP1 may therefore be capable of both stabilising and destabilising transcripts. Functional enrichment analysis of genes present in both datasets revealed that cell death and survival was the most significant biological trait (Figure 3-23A). Following LARP1 knockdown, there were reduced mRNA levels of anti-apoptotic genes such as BCL2, ERBB3 and AKT3 and increased expression of apoptosis-associated genes, including BIK, TNF and DAPK2. To validate the RNA-seq findings, we repeated LARP1 knockdown with two independent siRNAs and analysed changes in expression of these six genes with RT-qPCR (some experimental repeats performed by Dr M.Mura). Our results confirmed the RNA-seq data (Figure 3-23B). It should also be noted that LARP1 knockdown alters expression of genes frequently chosen as 'housekeepers', for normalisation in RNA and protein analysis, with significantly increased levels of *ACTB*, and decreased abundance of *TUBB* and *GAPDH*. Expression of *HSPD1*, encoding HSP60 protein used as loading controls in all westerns, did not alter on LARP1 knockdown.

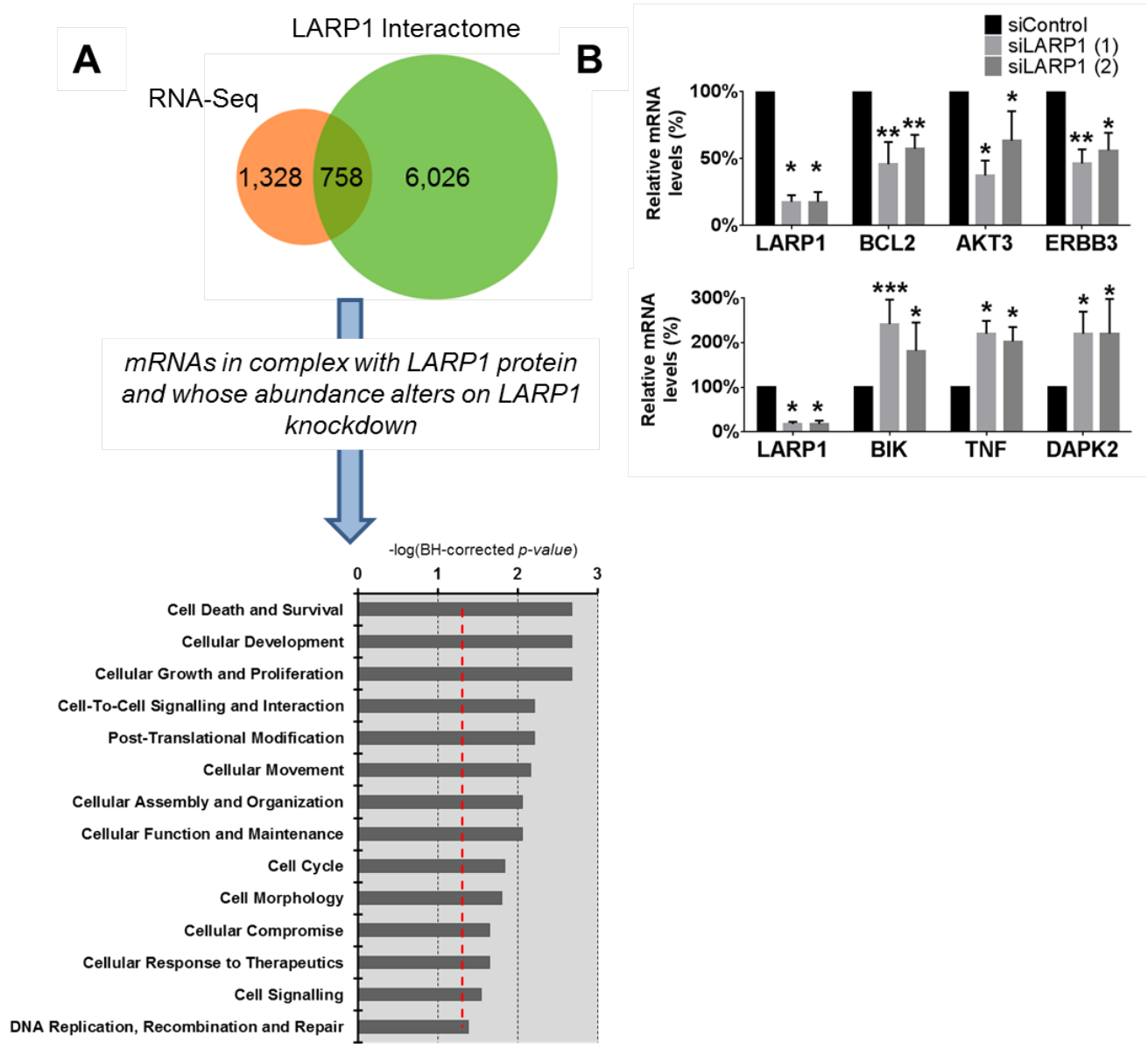

Figure 3-23. Combined analysis of RNA-seq and RIP-Chip data.

(A) Overlap between differentially expressed genes on LARP1 knockdown (RNA-seq) and mRNAs in complex with LARP1 protein in HeLa cells (LARP1 interactome) was significant (hypergeometric probability p = 0.042). Molecular function ontology analysis of genes present in both datasets revealed a highly significant enrichment of genes linked to cell death and survival.

(B) RT-qPCR analysis of percentage change in mRNA levels of putative LARP1 targets following LARP1 knockdown (ΔΔCt, normalised to 18S RNA) . ***P < 0.001, **P < 0.01, *P < 0.05. Student t-test. Minimum of three experimental repeats. Error bars represent SEM.

3.4.2 *LARP1* REGULATES THE STABILITY OF *BIK* AND *BCL2* TRANSCRIPTS

The association between LARP1 expression and *B-cell lymphoma 2* (*BCL2*) mRNA transcript abundance was of particular interest given my findings that LARP1 promotes cell survival and cancer stem cell-related traits. BCL2 is a key oncogenic anti-apoptotic protein that promotes embryonic stem cell survival [393]. Notably, BCL2 inhibition has also been shown to increase platinum sensitivity in ovarian cancer cells [394], and BCL2 inhibitors target leukaemia stem cell-like populations [395]. *BIK* transcripts, encoding a pro-apoptotic target of BCL2, exhibited the opposite trend in mRNA abundance to *BIK* following LARP1 knockdown and provided a useful comparison for further study. To confirm that LARP1 interacted with *BCL2* and *BIK* transcripts in ovarian cancer cells, we performed RNA-immunoprecipitation in two ovarian cancer cell lines (Figure 3-24A). Both *BCL2* and *BIK* transcripts were highly enriched in anti-LARP1 immunoprecipitates when compared to the *28S* control (Figure 3-24B), confirming they each associated with LARP1 in mRNP complexes.

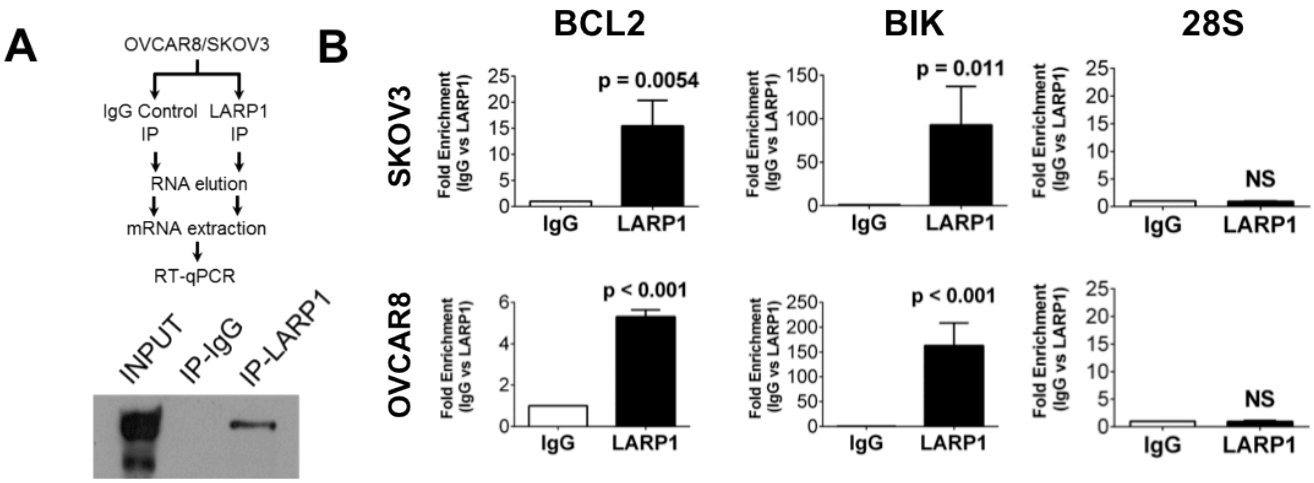

Figure 3-24. LARP1 is present in BIK- and BCL2-containing mRNP complexes

(A) Schematic of LARP1 RNA-immunoprecipitation (RIP) with representative Western blot of LARP1 protein following LARP1-immunoprecipiation in OVCAR8 cells (*IP and western performed by Dr M Mura, representative image of at least three repeats shown*).

(B) Fold enrichment of transcripts in LARP1 and isotype control RNA-immunoprecipitation analysed by RT-qPCR (ΔCt.). 28S ribosomal RNA was included as a negative control. *RIP and most RT-qPCR by Dr M.Mura, other repeats and data analysis by TGH*. Student t-test. Minimum of three experimental repeats. Error bars represent SEM

As LARP1 has been identified as an mRNA-stability regulator [331, 332], I wished to establish whether the observed changes in transcript abundance of *BIK* and *BCL2*, following LARP1 knockdown, were due to an effect on transcript stability. To assess this, I carried out transient knockdown of LARP1, then treated cells with actinomycin D to halt transcription. Subsequent changes in mRNA levels were therefore due to alterations in the stability of existing transcripts. Whilst control cells showed no change following actinomycin D treatment, cells treated with LARP1-targeting siRNA began to round and detach from 6 hours onwards (Figure 3-25A), with significantly increased levels of apoptosis when compared to control actinomycin D-treated cells (Figure 3-25B). This reinforces the importance of LARP1 in the post-transcriptional regulation of cell survival. Due to the cell death observed, I assessed transcript abundance at 6 hours. I observed a significant decrease in *BCL2* transcript levels in LARP1 knockdown cells when compared to controls, demonstrating that

LARP1 is required for *BCL2* transcript stability. The opposite trend was observed for *BIK*, with LARP1 knockdown associated with increased mRNA stability (Figure 3-25C). In contrast, there was no significant change in the transcript stability of *MAPK14* (Figure 3-25C), chosen as a negative control as it did not display altered mRNA abundance on LARP1 knockdown in our RNA-seq dataset and was not present in the HeLa LARP1-mRNA interactome. I confirmed by western blotting that LARP1 knockdown also led to altered protein expression of both BCL2 and BIK (Figure 3-25D).

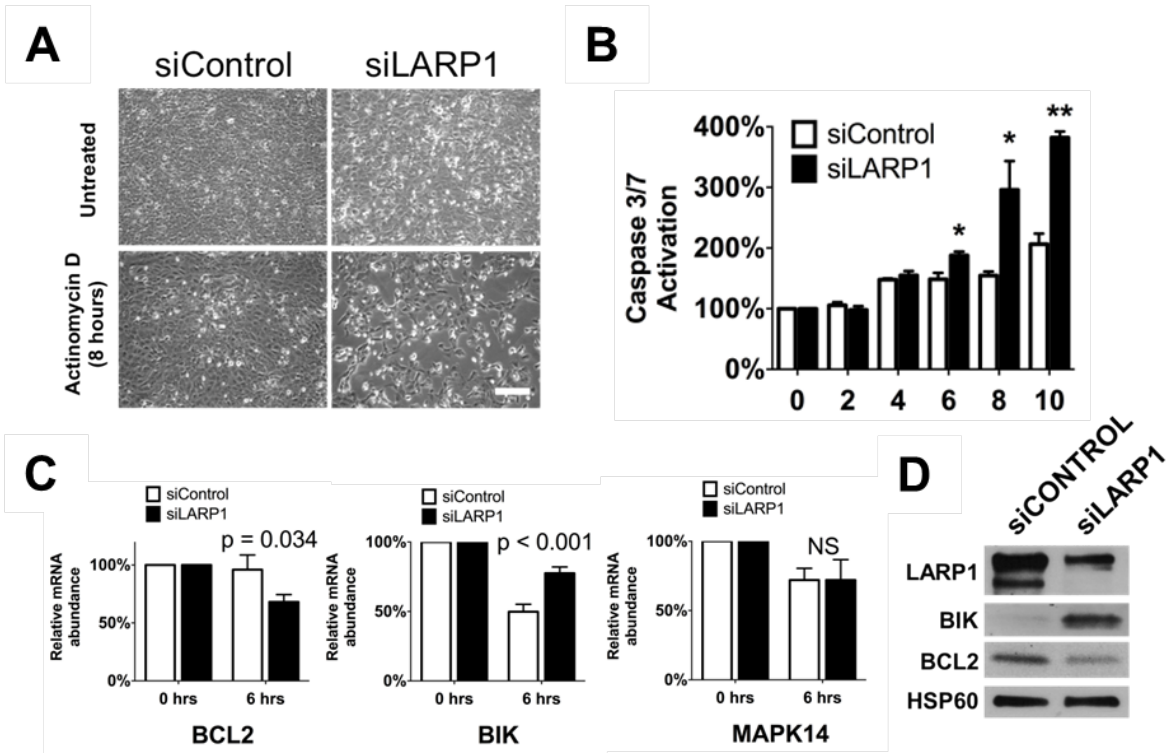

Figure 3-25. lARP1 regulates BCL2 ***and*** BIK ***mRNA stability.***

(A) (Representative cell images following LARP1 knockdown and 8 hours exposure to actinomycin D (Scale bar 200μm).
(B) Following transient knockdown of LARP1, OVCAR8 cells were treated with actinomycin D to halt transcription and apoptosis (as determined by cleaved Caspase 3/7) was monitored using the CaspaseGlo assay. $^{**}P < 0.01$, $^{*}P < 0.05$.
(C) Stability of BCL2 and BIK mRNA following treatment with actinomycin D for 6 hours. Relative abundance was determined by RT-qPCR (ΔΔCt). MAPK14 was chosen as a negative control as its mRNA abundance did not alter on LARP1 knockdown in the RAN-seq dataset. Student t-test. Minimum of three experimental repeats. Error bars indicate SEM.
(D) Western blotting of BIK and BCL2 protein levels following LARP1 knockdown. Representative image of three repeats.

3.4.3 *LARP1* REQUIRES SEQUENCES IN THE 3'UTR TO REGULATE TRANSCRIPT STABILITY

The 3'-untranslated region (3'UTR) of mRNAs are known to contain a variety of regulatory elements that can determine transcript stability [396]. I hypothesised that the effect of LARP1 on *BCL2* and *BIK* transcript stability may be dependent on sequences present in their 3'UTRs. *BIK* transcripts have a 407bp 3'UTR which has not been extensively studied. In contrast, *BCL2* has a 3'UTR that is 5.2kbp long. A number of publications have investigated the role of elements within the 3'UTR in regulating *BCL2* mRNA stability. A 203bp 3'UTR sequence proximal to the stop codon containing multiple AU-rich elements (AREs), termed the *BCL2-ARE*, has been shown to be a key regulator of BCL2 transcript stability [178]. I designed plasmids containing either fragments or the entire UTR sequences of both genes downstream of a *renilla* luciferase reporter (Figure 3-26A).

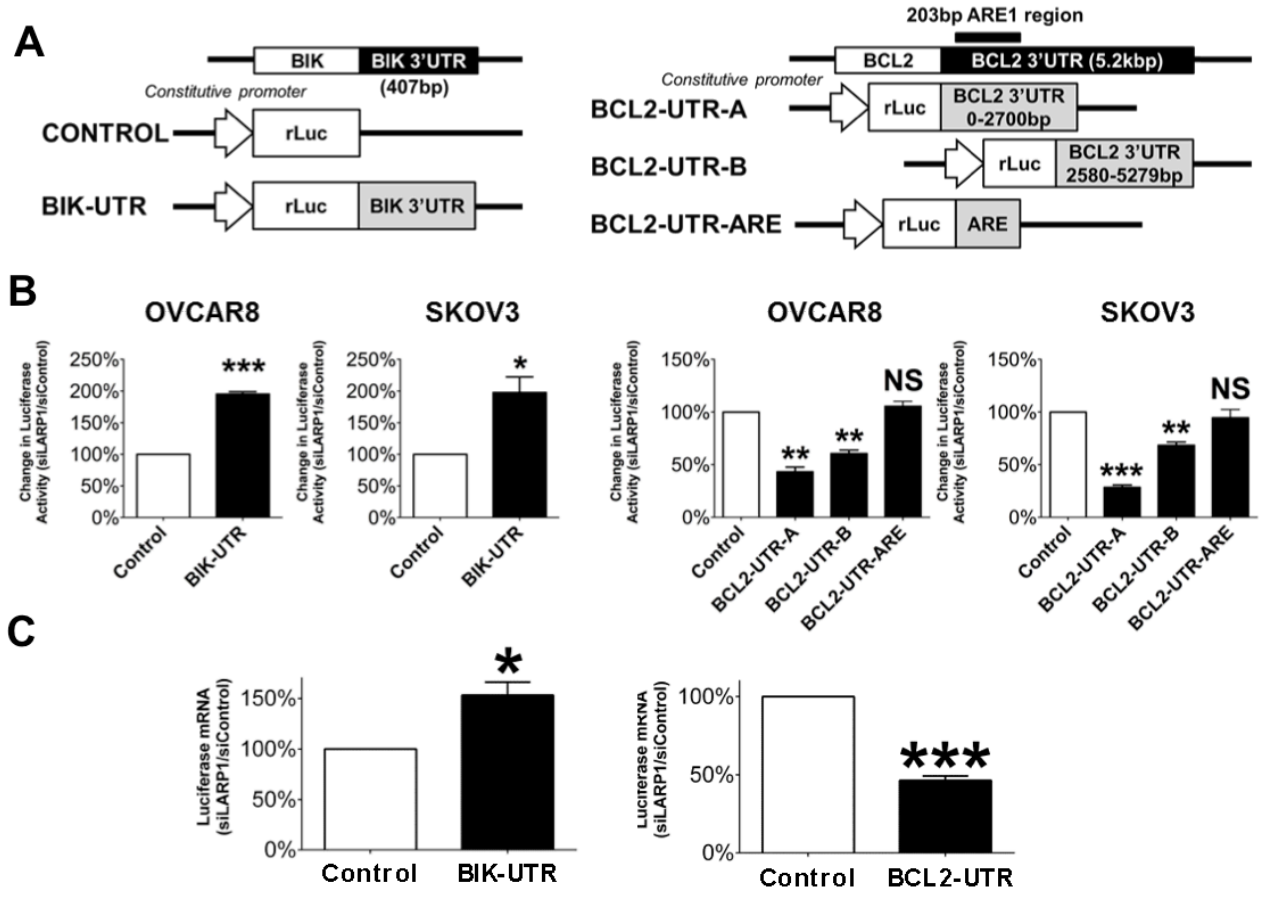

Figure 3-26. LARP1 regulates mRNA stability at the level of the 3'UTR.

(A) Schematics outlining construction of 3'-untranslated region (3'UTR) reporter constructs for BIK and BCL2, where relevant UTR sequences were cloned into a reporter vector, downstream of the *renilla* luciferase. Both were compared relative to a control vector (Control) which used the identical plasmid backbone and *renilla* luciferase sequence, but without the addition of a downstream 3'UTR sequence.

(B) OVCAR8 and SKOV3 cells were co-transfected with Renilla luciferase 3'UTR constructs and a Firefly luciferase control vector for normalisation. Renilla luciferase activity following LARP1 knockdown was determined for each 3'UTR construct cells. Data was normalised to Firefly luciferase activity. See Appendix III for raw values and examples of data processing.

(C) OVCAR8 cells were co-transfected with Renilla luciferase 3'UTR constructs and a control Firefly luciferase control vector and Renilla luciferase mRNA abundance following LARP1 knockdown was determined using RT-qPCR. Data was normalised to Firefly luciferase mRNA abundance. ***P < 0.001, **P < 0.01, *P < 0.05. Student t-test. Minimum of three experimental repeats. Error bars indicate SEM.

LARP1 knockdown resulted in a significant increase in luciferase activity in the *BIK 3'UTR* construct when compared to the empty vector control, confirming that LARP1 destabilises *BIK* mRNA, with the effect dependent on elements in the short 3'UTR (Figure 3-26B). I designed two equal-sized overlapping constructs, spanning the length of the *BCL2* 3'UTR

(constructs *BCL2-UTR-A* and *BCL2-UTR-B*). Addition of either *BCL2* 3'UTR sequences (A or B) resulted in a significant decrease in luciferase signal, with a greater effect on stability seen for the stop codon-proximal 3'UTR construct (BCL2-UTR-A). As the *BCL2* ARE lies within this region, I designed a third construct containing only this 203bp 3'UTR region (*BCL2-ARE*). Following LARP1 knockdown, there was no significant change in luciferase activity in this construct compared to the control plasmid (Figure 3-26B), indicating that the LARP1-mediated stability effect is dependent on additional sequences outside this well-characterised region. To confirm that changes in luciferase activity were due to alterations in mRNA stability, as opposed to effects on translation, I repeated the experiment and extracted total RNA. RT-qPCR was performed using *firefly* and *renilla luciferase*-specific primers following DNAse digestion. A similar trend was observed at the mRNA level, as seen from luciferase enzyme activity (Figure 3-26C), confirming the changes observed in reporter gene activity were due to effects on mRNA stability. These results indicate that the presence of LARP1 in mRNP can differentially regulate mRNA stability in a 3'UTR-dependent manner.

LARP1 has previously been reported to be present in stress granules, sites of mRNA storage, and P-bodies, foci of RNA degradation [330, 332]. As LARP1 appeared to be capable of both positively and negatively regulating transcript stability, we were interested to see if LARP1 was localised to these key sites of RNA fate determination in ovarian cancer cells. After inducing the aggregation of mRNP granules with sodium arsenite treatment , we found LARP1 to be present in both P-bodies and stress granules (Figure 9F; *experiment and images both Dr M. Mura*). Thus, LARP1 both differentially regulates transcript stability and is present at sites of mRNA fate determination.

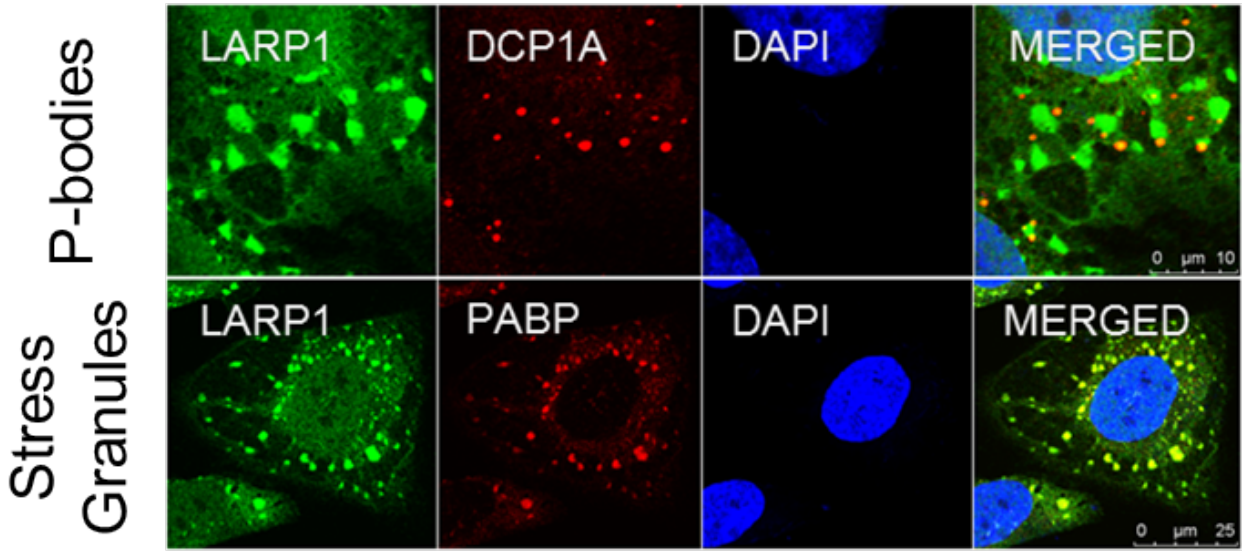

Figure 3-27. LARP1 is present in stress granules and P-bodies.

Confocal immunofluorescence microscopy of SKOV3 cells treated with sodium arsenite to trigger aggregation of mRNP bodies. Cells were stained for LARP1 protein (green) and either the P-body marker DCP1a or stress granule marker PABP (both red). Scale bar 10µm (top) and 25µm (bottom). *Experiment and images both courtesy of Dr M.Mura.*

3.4.4 LARP1 EXERTS A PRO-SURVIVAL EFFECT VIA POST-TRANSCRIPTIONAL PROMOTION OF BCL2 EXPRESSION

To determine whether LARP1 could be regulating the expression of BCL2 and BIK in ovarian cancers, we evaluated trends in LARP1, BCL2 and BIK transcript abundance in the TCGA ovarian RNA-seq dataset (tcga-data.nci.nih.gov). As expected, LARP1 and BCL2 mRNA levels showed a significant positive correlation, while LARP1 and BCL2 were negatively correlatated (Figure 3-28A,B).

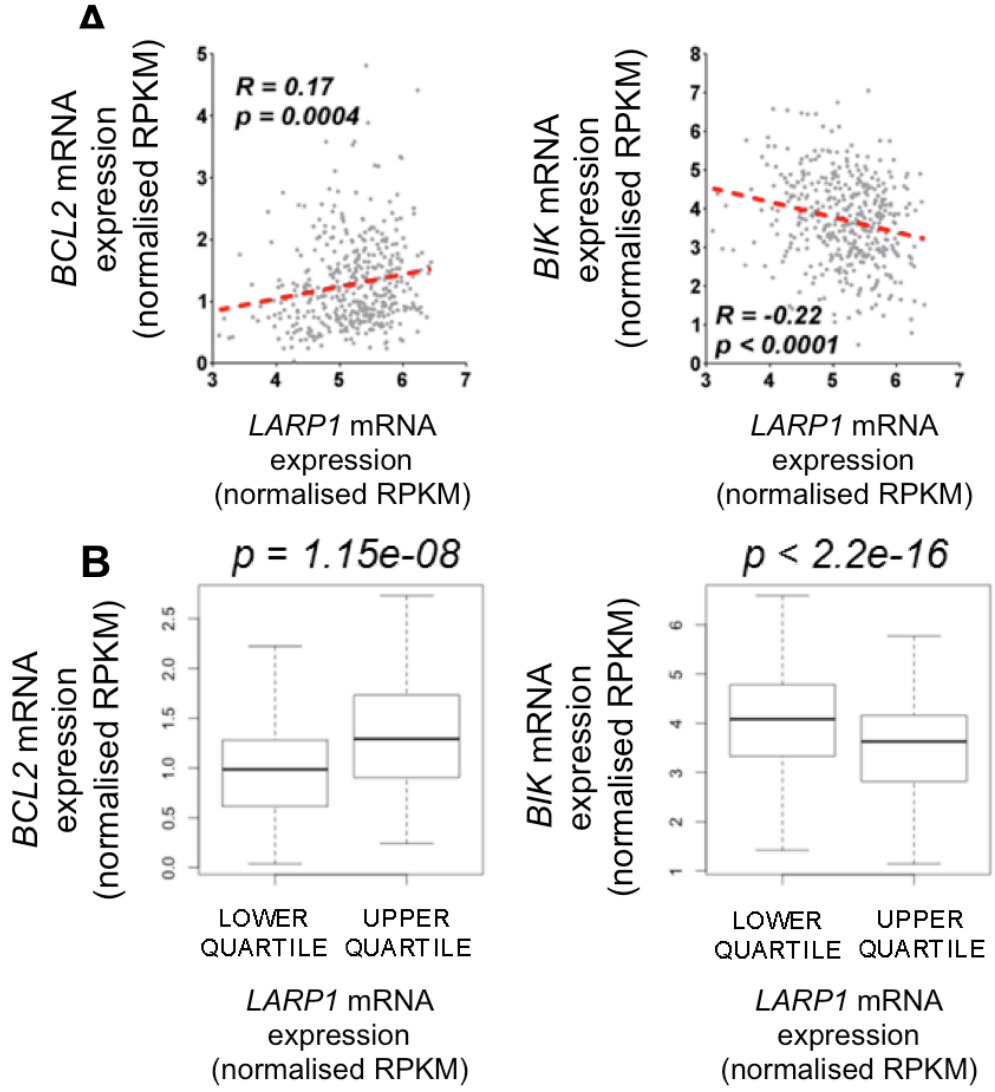

Figure 3-28. LARP1 correlates with BCL2 ***and*** BIK ***expression in ovarian cancer.***

(A) Correlation of mRNA expression (dataset normalised reads per kilobase of transcript per million mapped reads [RPKM]) in ovarian tumours (n=412) betweeen *LARP1* and *BCL2* or *BIK* (Pearson R). Data from TCGA Ovarian RNAseq cohort (*tcga-data.nci.nih.gov*).

(B) Comparison of upper and lower quartiles of LARP1 expression (dataset normalised RPKM, n=103 in each), by *BCL2* or *BIK* expression (Wilcoxon test). Data as before. Analysis courtesy of Hoanan Lu.

As stated above, BCL2 is an important promoter of chemotherapy resistance and appears to be required for CSC survival [394, 395]. I found LARP1 knockdown reliably led to reduced BCL2 expression using two independent siRNAs in different cell lines (Figure 3-29A). To determine if the changes in BCL2 expression on LARP1 knockdown were sufficient to

explain the observed LARP1 phenotype, I used BCL2-targeting siRNA to reduce expression (Figure 3-29B). As expected, decreased expression of BCL2 resulted in increased apoptosis in response to platinum treatment (Figure 3-29C), and also reductions in $CD133^+$ populations (Figure 3-29D). Having confirmed BCL2 knockdown recapitulated the LARP1 phenotype, I next assessed the ability of BCL2 overexpression to rescue the effects of LARP1 depletion. Indeed, following knockdown of LARP1 and treatment with cisplatin, transfection with a FLAG-tagged BCL2 overexpression construct resulted in a significant decrease in apoptosis when compared to control plasmid-transfected cells (Figure 3-29E). Finally, to confirm that the changes observed in BCL2 transcript levels on LARP1 knockdown were independent of indirect transcriptional effects, I investigated the effect of LARP1 knockdown on BCL2 promoter activity. Following LARP1 knockdown, there was no change in BCL2 promoter activity (Figure 3-29F), confirming that the observed changes in BCL2 transcript abundance and protein expression on LARP1 knockdown (Figure 3-29A, Figure 3-23) are due to alterations in mRNA stability alone.

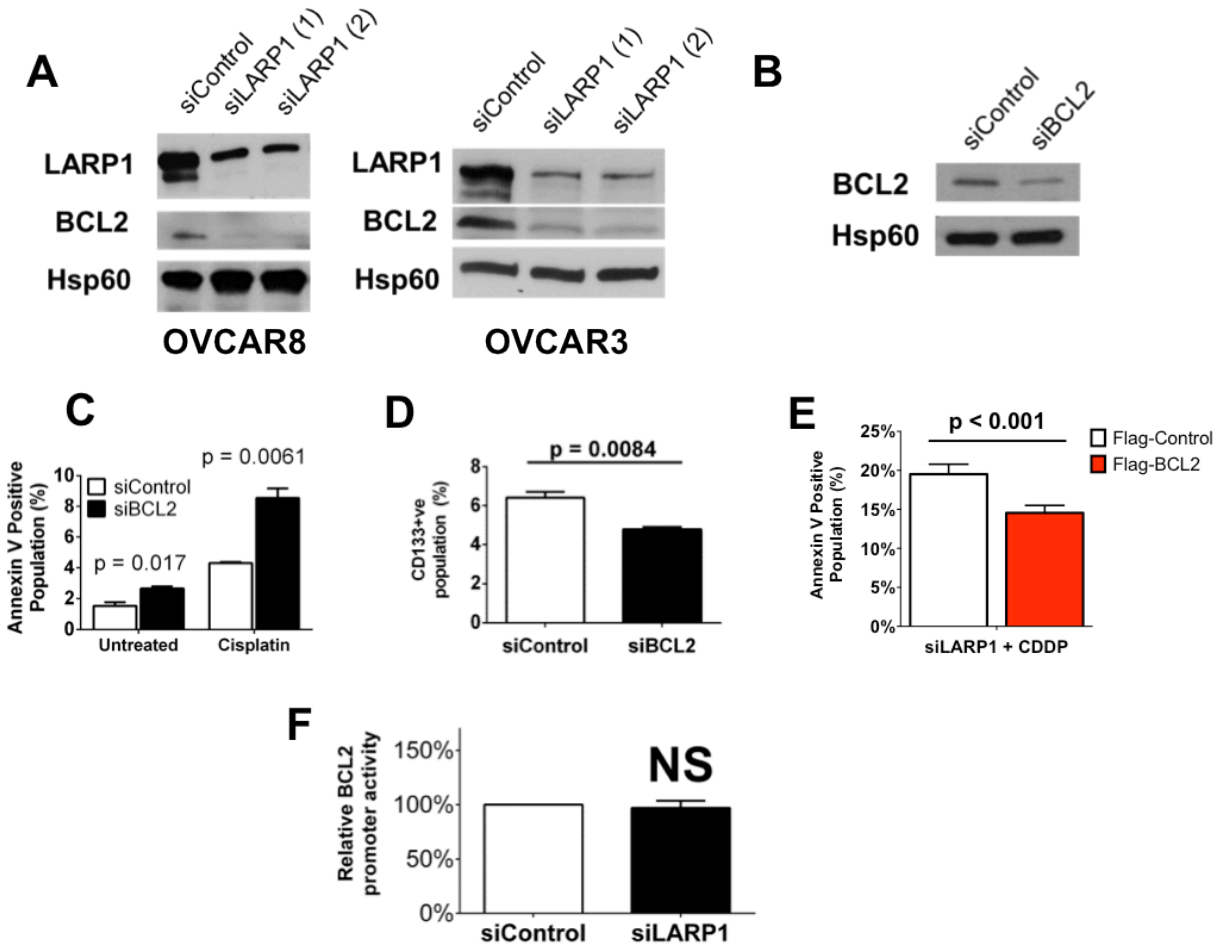

Figure 3-29. LARP1 promotes survival by regulating BCL2 expression.

(A) Western blot analysis of BCL2 protein levels following LARP1 knockdown. Representative image of three repeats.
(B) Western blot analysis of BCL2 protein levels following BCL2 knockdown in OVCAR8 cells. Representative image of three repeats.
(C) Percentage of Annexin V-positive OVCAR8 cells, determined by flow cytometry, following transient BCL2 knockdown, with and without co-treatment with cisplatin (25μM).
(D) Percentage of $CD133^{+}$ OVCAR3 cells, determined by flow cytometry, following transient knockdown of BCL2.
(E) Percentage of Annexin V-positive OVCAR8 cells, determined by flow cytometry, following LARP1 knockdown and treatment with cisplatin (25μM), with co-transfection of a control or BCL2-overexpression construct.
(F) BCL2 promoter activity following LARP1 knockdown (*firefly luciferase* mRNA normalised to *Renilla luciferase* mRNA control). Minimum of three experimental repeats. Student t-test. Error bars indicate SEM.

These data indicate that LARP1 is required for *BCL2* mRNA stability and protein expression, without which cells demonstrate increased apoptosis and decreased chemotherapy resistance. Together with my *in vitro* and *in vivo* data, this suggests a model whereby LARP1

differentially regulates the mRNA stability of pro- and anti-apoptotic transcripts in malignant ovarian tumours to promote survival (Figure 3-30).

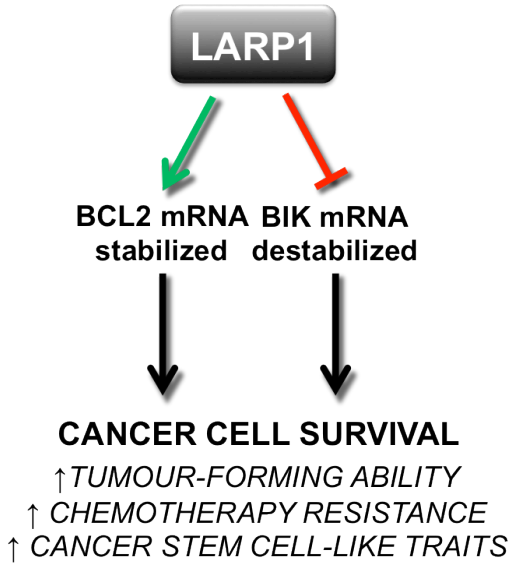

Figure 3-30. A summary of LARP1 action in the ovarian cancer cell.

3.4.5 SILAC MASS SPECTROMETRY IDENTIFIES POTENTIAL LARP1 TARGETS

LARP1 has previously been reported to play a role in regulating the translation of transcripts, as well as stability [335]. Transcripts regulated at a translational, and not stability, level by LARP1 would not be detected using my RNA sequencing-based approach described above (Section 3.4.1). To identify LARP1 translational targets, I performed stable isotope labelling by amino acids in cell culture (SILAC) mass spectrometric analysis [397], following LARP1 knockdown. Cells were cultured in media supplemented with either unlabelled arginine and lysine, or two different combinations of these amino acids containing heavy stable isotopes of carbon (^{13}C) and nitrogen (^{15}N). Protein from siControl-treated cells, and cells treated with two independent LARP1-targeting siRNA, cultured in the three differentially-labelled media,

were combined in equal quantities. When digested, identical peptides from the different conditions were distinguished by their difference in mass, with the ratio between peak intensities reflecting the relative abundance of the peptide in the different experimental conditions (Figure 3-31A,B). Analysis of SILAC data confirmed >70% knockdown of LARP1 protein with both siRNAs. Proteins which showed a fold change between control and LARP1 knockdown in both siRNA of ≥1.5 used were taken as significant.

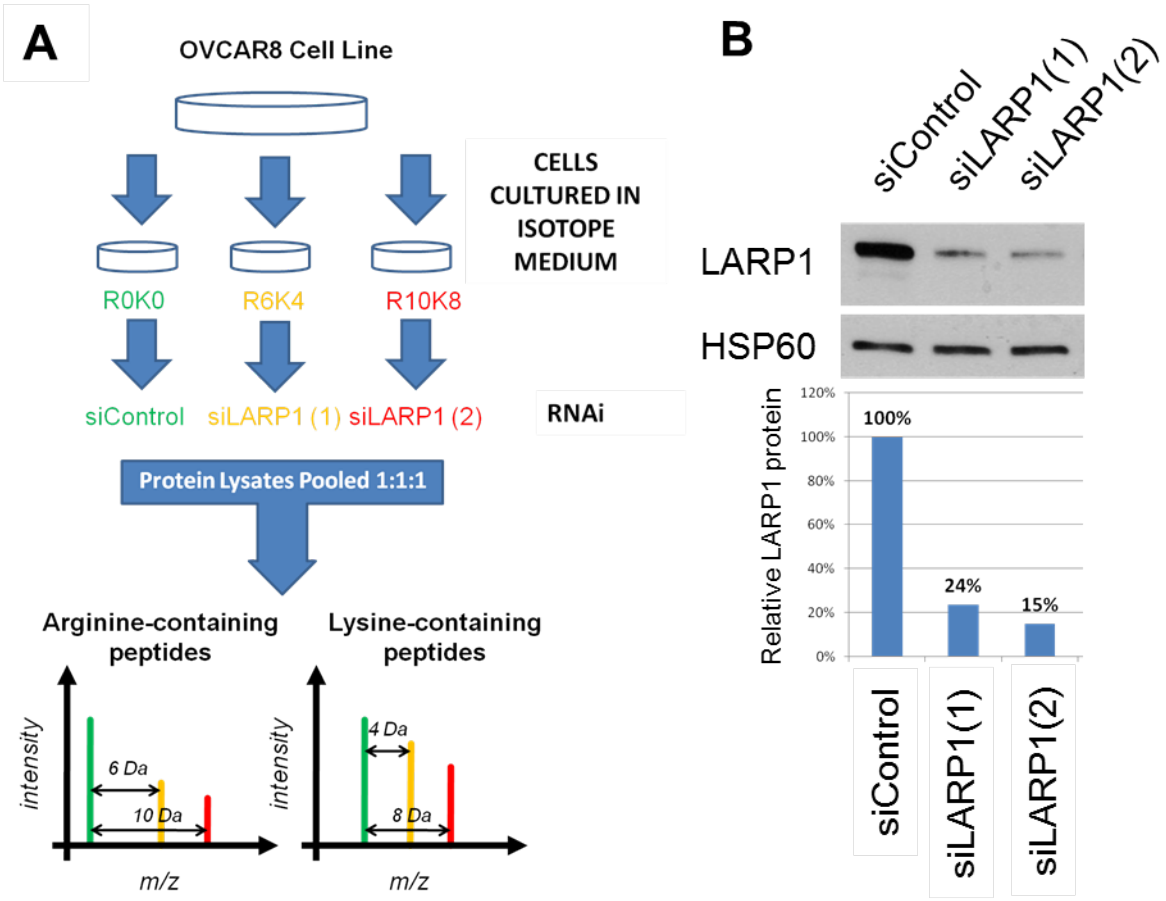

Figure 3-31. SILAC mass spectrometry following LARP1 knockdown.

(A) Schematic of the SILAC labelling process and a representation of the expected peptide traces on mass spectrometry. OVCAR8 cells were cultured in amino acid heavy isotope-labelled media for at least 6 cell divisions. Cells were then replated and LARP1 knockdown was performed. Lysates were collected and protein content quantified using a modified Bradford assay. Equal amounts of protein from each condition were combined, trypsin digested and analysed by mass spectrometry. Unlabelled arginine and lysine (R0K0, light), ^{13}C labelled arginine and ^{2}D labelled lysine amino acids (R6K4, medium) and ^{13}C and ^{15}N labelled lysine (R10K8, heavy).

(B) Western blotting and densitometry for LARP1 of transient transfection samples sent for mass spectrometry analysis.

In total, nine proteins met this criteria, with two decreasing on LARP1 knockdown (DCD, TBRG4) and seven increasing (SDC4, ABCF3,PLEC, SLC38A2, GSR, ZNF217, MLL3; Table 3-3). Neither of the two LARP1-promoted proteins, DCD and TBRG4 were represented in the HeLa LARP-mRNA interactome (Section 3.4.1), derived using a RIP-Chip approach. Surprisingly DCD was not annotated in my RNA-seq dataset, suggesting its expression may have been below the threshold of detection. In support of this hypothesis, an analysis of the TCGA Ovarian RNA-seq data (tcga-data.nci.nih.gov) revealed only 12% of patients had detectable DCD expression. TBRG4 did not vary at an RNA-level on LARP1 knockdown, suggesting it may be regulated at a translational level. Although not identified in the HeLa LARP1-interactome, this may represent an ovarian-specific LARP1-mRNA interaction, and further experiments are necessary to confirm the change at a protein level and determine if the effect is direct.

Table 3-3. SILAC mass spectrometry identifies potential LARP1 targets.

The fold-change in protein levels between siLARP1- and siControl-treated samples was calculated and all genes with ≥1.5 fold change in expression in the same direction in both siRNA were taken as significant. This list was then cross-referenced against the HeLa LARP1 interactome and the RNA-seq dataset following LARP1 knockdown. Mean, siLARP1 (1) and siLARP1 (2) represent percentage change (siLARP1/siControl) in protein abundance as determined by SILAC mass spectrometry. RNA-seq = fold change in mRNA transcript abundance (siLARP1/siControl). RIP=LARP1 RNA immunoprecipitation fold-change (LARP1 vs input) in HeLa cells.

Symbol	Name	SILAC percentage change			RNA-seq		RIP
		Mean	siLARP1 (1)	siLARP1 (2)	Fold Change	P-value (FDR)	
dcd	dermcidin	**14%**	10%	18%	**Not annotated**	**NA**	Not enriched
TBRG4	transforming growth factor beta regulator 4	**27%**	26%	29%	**1.02**	**0.95**	Not enriched

Symbol	Name	SILAC percentage change			RNA-seq		RIP
		Mean	siLARP1 (1)	siLARP1 (2)	Fold Change	P-value (FDR)	
Sdc4	syndecan 4	**258%**	202%	313%	**1.88**	**<0.001**	**2.07**
ABCF3	ATP-binding cassette, sub-family F (GCN20), member 3	**229%**	212%	246%	**1.87**	**<0.001**	Not enriched
LOC652460	Similar to PLEC (Plectin 1)	**179%**	170%	189%	1.06	0.83	**3.12**
slc38a2	solute carrier family 38, member 2	**165%**	172%	159%	**1.56**	**<0.001**	Not enriched
gsr	glutathione reductase	**165%**	158%	172%	**1.97**	**<0.001**	Not enriched
ZNF217	zinc finger protein 217	**163%**	163%	162%	**2.18**	**<0.001**	Not enriched
MLL3	myeloid/lymphoid or mixed-lineage leukemia 3	**158%**	150%	166%	1.25	0.11	**3.06**

Of the genes apparently suppressed by LARP1, only two did not alter at an RNA level, MLL3 and Plectin 1 (PLEC), and both were present in the HeLa LARP1 interactome. LOC652460 is a peptide sequence that has now been withdrawn from RefSeq, but shares 99% identity and 98% coverage with Plectin 1, and likely represents a post-transcriptionally modified variant. Interestingly, high Plectin 1 expression appears protective in ovarian cancer (Figure 3-32). If Plectin 1 is indeed inhibited by LARP1 at a translational level, this suggests the oncogenic effects of LARP1 may be mediated, at least in part, by suppressing Plectin 1 expression. Glutathione reductase (GSR), which increased at a protein and RNA level following LARP1 knockdown, but was not found in the HeLa interactome, also appears to promote survival in ovarian cancer patients (Figure 3-32).

These data represent exciting preliminary work. However, changes in protein and RNA levels need to be confirmed by western blotting and qPCR, respectively. Additionally, ribosome profiling is required to confirm a translational effect and RNA-immunoprecipitations are needed to prove a physical interaction between LARP1 and the putative target transcripts.

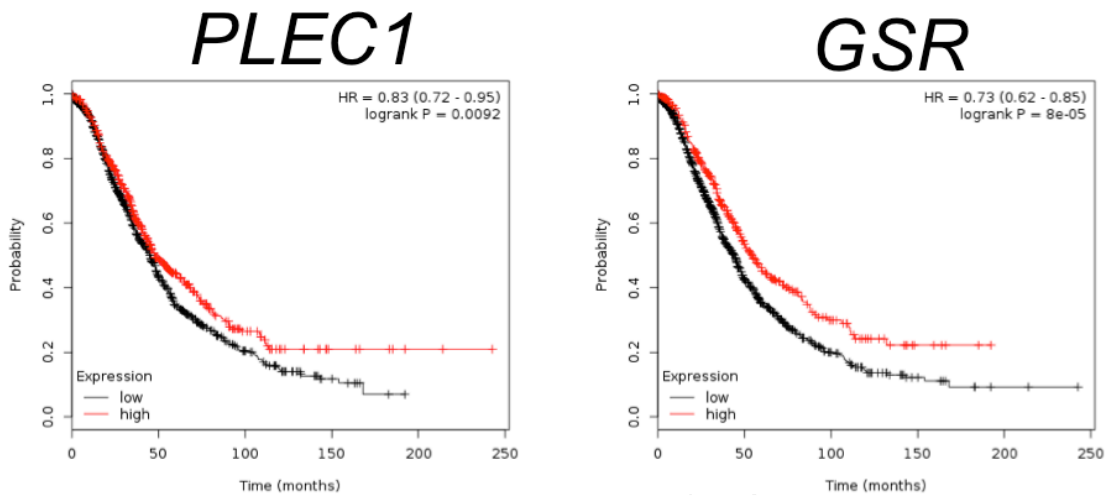

Figure 3-32. Association between potential LARP1 targets and overall survival in ovarian cancer.

Kaplan-Meier analysis of overall survival in ovarian cancer patients, separated by *PLEC* and *GSR* expression (n=1,648). Data from kmplot.com [357].

3.4.6 SUMMARY

In the previous results sections, I demonstrated that high LARP1 expression is a poor prognostic factor in ovarian cancer and that, at the level of cell biology, LARP1 promotes tumourigenicity, cell survival and chemotherapy resistance. In Section 3.4, I used high-throughput strategies to identify potential LARP1-regulated targets that could explain these findings. Transcripts with altered abundance on LARP1 knockdown were identified by mRNA-sequencing (Section 3.4.1). By cross-referencing this data with the published LARP1-mRNA interactome in HeLa cells, I revealed an enrichment for transcripts with functions linked to cell death and survival. Specifically, I showed that LARP1 knockdown results in increased *BIK* expression and decreased *BCL2* expression. LARP1 is present in mRNPs containing these transcripts, and regulates their expression at the level of mRNA stability (Section 3.4.2). I confirmed that this stability-regulating effect was determined at the level of the 3'UTR sequence. In the case of *BCL2*, a previously characterised AU-rich motif-containing region of the 3'UTR was not sufficient by itself to reproduce the LARP1 stability effect, suggesting novel interactions elsewhere in the 3'UTR (Section 3.4.3). BCL2 knockdown is capable of recapitulating the phenotype seen on LARP1 depletion, namely increased basal apoptosis, decreased chemoresistance, and reduction in CSC-like populations. Overexpression of BCL2 partially rescues the pro-apoptotic phenotype of LARP1 knockdown, demonstrating that LARP1 promotes cell survival, at least in part, by post-transcriptionally promoting BCL2 expression (Section 3.4.4). Analysis of over 400 ovarian tumour samples reveals that *LARP1* expression significantly positively correlates with *BCL2* mRNA levels, and is negatively correlated with *BIK* transcript abundance, reinforcing the clinical importance of my findings.

Finally, I have demonstrated that SILAC mass spectrometry is a useful tool to identify potential LARP1 targets regulated at the level of translation (Section 3.4.5), and further work is necessary to explore their significance. The figure below summarises my thesis findings.

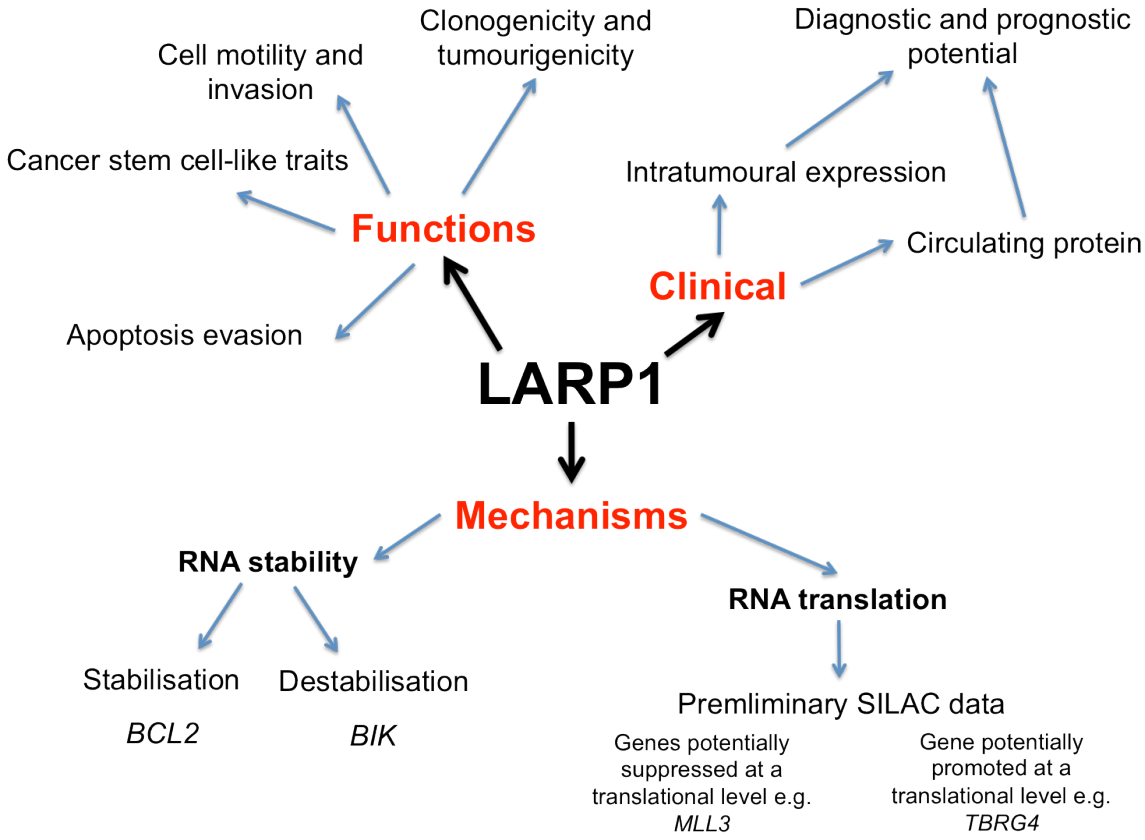

Figure 3-33. Figure summarising the findings of this thesis in relation to LARP1.

4 CHAPTER IV - DISCUSSION

4.1 DISCUSSION

4.1.1 *LARP1 IS A POTENTIAL CANCER BIOMARKER.*

Here, I report for the first time that LARP1 expression is upregulated in ovarian malignancies, with higher intratumoural levels associated with poorer prognosis. In addition, levels of LARP1 protein correlate with malignant progression in cervical cancer and predict prognosis in breast and lung cancers. In a global analysis of publicly available gene expression data, LARP1 expression was elevated across several tumour types, including hepatocellular cancer. LARP1 may therefore be an important driver of malignant progression in several different cancers. The fact that LARP1 has previously been identified as a predictor of poor prognosis in hepatocellular cancer [347], suggests that the results of the global analysis are likely to be clinically meaningful.

Whilst LARP1 intratumoural protein levels may have potential as a cancer biomarker [347], a less invasive disease marker is often clinically preferred. The RBP Argonaute2 has been found in cancer cell-conditioned media and in the human circulation [373, 398], suggesting RBPs may be released into the blood. Circulating autoantibodies to the LARP family member LARP3 are detectable in autoimmune conditions such as Sjogren's syndrome [399]. However, no data currently exists on whether LARP3 itself is present in the circulation, and no circulating RBP has yet been reported to be associated with underlying disease. I established that LARP1 protein was released by ovarian cancer cells in culture. The finding that increased circulating LARP1 protein was detectable in patients with underlying ovarian

malignancy is, to my knowledge, the first example of an RBP acting as a potential circulating disease biomarker. In all ovarian cancer patients, levels of circulating LARP1 protein fell following primary tumour excision, suggesting that plasma LARP1 levels reflect either protein release by the tumour itself, or the wider physiological effects of an underlying malignancy.

4.1.2 LARP1 REGULATES CELL SURVIVAL.

As yet, the role of LARP1 in ovarian cancer cell biology has not been characterised. In this study, transient knockdown of LARP1 in ovarian cancer cell lines increased apoptosis and decreased cell viability, without altering cell cycle distribution. I also observed a dramatic resensitising of platinum-resistant cells to cisplatin chemotherapy. LARP1 was required for tumour initiation and progression in a proliferation-independent manner, with cell stresses such as hypoxia and nutrient deprivation shown to increase apoptosis when combined with LARP1 knockdown. Tcherkezian *et al* also reported that LARP1 knockdown increased apoptosis up to four-fold in lung cancer-derived A549 cells, though the same trend was not seen in endometrial cancer-derived HEC1B or HEK293 embryonic kidney fibroblast cells [335]. These findings suggest there may be cancer-specific differences in the phenotype observed on LARP1 expression modulation. Although the same group reported differences in cell cycle distribution with LARP1 knockdown, no significant differences were previously seen in *Drosophila* embryonic cells [334], supporting my findings.

Mouse models of ovarian malignancy have suggested that transformed stem cells may be the origin of at least some types of EOC [68]. Multiple studies have demonstrated that flow cytometry markers, such as CD133 membrane expression and aldehyde dehydrogenase activity, can identify sub-populations of ovarian cancer cells that demonstrate cancer stem cell-like characteristics; these include enhanced tumour initiating capabilities and increased

chemoresistance [385, 386, 391]. No consensus on the flow cytometry marker profile of such CSC-like cells in EOC has yet been established. However, ovarian cancer cells cultured in stem-enriching conditions to produce spherosomes, display increased CD133 positivity, and these $CD133^+$ populations demonstrate enhanced expression of stem cell-associated genes [381, 382]. In addition, CD133 has been identified as an adverse prognostic factor in EOC [66]. I show here that as well as a role in tumourigenicity, LARP1 is required to maintain $CD133^+$ and $Aldefluor^{bright}$ putative CSC-like populations. I found LARP1 knockdown also leads to reduced expression of stem cell-related transcription factors. Interestingly, in a paper investigating global differences in gene expression between $CD133^+$ and $CD133^-$ daughter populations derived from $CD133^+$ cells from a patient with progressive glioblastoma multiforme, LARP1 was found to be one of the most strongly downregulated genes in non-CSC-like $CD133^-$ daughter populations [400]. LARP1 has also previously been shown to bind mRNA in embryonic stem cells, and expression of LARP1 decreases during cell differentiation [345]. This suggests LARP1 may be an important component in the maintenance of stem cell-like traits.

4.1.3 LARP1 PROMOTES CELL SURVIVAL BY ENHANCING BCL2 EXPRESSION.

I demonstrate that BCL2 expression is dependent on LARP1 protein, with a 50% decrease in *BCL2* mRNA abundance on LARP1 knockdown due to altered mRNA stability alone. BCL2 is a well-characterised anti-apoptotic protein that prevents the activation of BH3-only proteins, such as BIK, which trigger apoptosis via mitochondrial outer membrane permeabilisation [401]. BCL2 is a key promoter of cancer cell survival [402], a negative prognostic factor in ovarian cancer [41, 403] and has been reported to promote platinum resistance [394]. Supporting a key role in the pro-apoptotic effects of LARP1 knockdown, I

show that reduced BCL2 expression induces apoptosis and enhances chemosensitivity. Overexpression of BCL2 partially rescues the pro-apoptotic effects of LARP1 knockdown, demonstrating that LARP1 promotes survival in a BCL2-dependent manner. On LARP1 knockdown, I also observe increased mRNA levels of pro-apoptotic genes, such as *TNF*, *DAPK2* and the direct LARP1 target *BIK,* and reduced expression of anti-apoptotic genes, such as *ERBB3* and *AKT3*. Given these changes, the apoptosis observed following LARP1 knockdown is likely to be due to alterations in expression of multiple LARP1 targets, as well as indirect effects on non-targeted genes.

Expression of BCL2 is elevated in CSC-like populations [404], whilst targeted BCL2 inhibitors selectively kill leukaemic stem cell populations [395]. In addition, overexpression of BCL2 enhances the survival of human embryonic stem cells [393, 395]. In an ovarian cancer context, I show that knockdown of BCL2 is sufficient to reduce CSC-like populations, indicating that LARP1 promotes survival of CSC-like populations, at least in part, by maintaining BCL2 expression.

4.1.4 LARP1 HAS A DUAL EFFECT ON MRNA STABILITY.

LARP1 has been suggested to promote the stability of 5'-terminal oligopyrimidine (5'TOP) mRNAs in human cells [331] and, during heat stress in *Arabidopsis* cells, appears to have a role in the net destabilisation of transcripts [332]. LARP4b [306] and LARP7 [296] have also been identified as RNA stability regulators, supporting a conserved function within the LARP family. I demonstrate here that, under the same conditions, LARP1 can differentially regulate transcript fate, stabilising transcripts of the anti-apoptotic gene *BCL2*, whilst destabilising pro-apoptotic *BIK* mRNAs. Although representing opposing effects on RNA stability, the net consequence is the evasion of apoptosis. Work by Dr Mura has demonstrated that LARP1 is found in both P-bodies and stress granules, sites of RNA degradation and

storage, respectively, supporting a dual role in RNA fate determination. Like LARP1, the RBP HuR has previously been shown to have a dual effect on mRNA stability, stabilising oncogenic transcripts such as VEGF [221] whilst destabilising transcripts encoding the tumour suppressor p16INK4 [222]. Also like LARP1, HuR has also been associated with chemotherapy resistance [405]. This supports a critical role of RBPs in cancer progression.

4.1.5 THE 3'UTR DETERMINES LARP1 ACTION.

Post-transcriptional regulation of expression is co-ordinated by elements within the 5'UTR of transcripts that can affect translation efficiency, and 3'UTR *cis*-acting features that determine message stability [396]. As LARP1 interacts with polyA-binding protein (PABP) [333], it seems likely that LARP1 is localised to the 3'-end of mRNAs. Indeed, LARP1 has been previously been identified as part of a 3'UTR-associated mRNP complex [331]. I show that sequences in the 3'UTR of LARP1 targets are sufficient to recapitulate the stability-regulating function of LARP1. Whether LARP1 interacts directly with 3'UTR sequences, or indirectly via additional co-factors, remains to be determined. One of the best characterised 3'UTR stability-determining features are AU-rich elements (AREs), recognised by RBPs that induce degradation, whilst proteins that compete for this interaction can promote stability [396]. As *BCL2* has a well-characterised ARE-rich region (*BCL2-ARE*) that determines its mRNA stability [178], I hypothesised that LARP1 may require these sequences to induce an effect on stability. However, I found that sequences in both halves of the 3'UTR can regulate *BCL2* mRNA stability: the *BCL2-ARE* alone produces no stability effect. The fact that LARP1 possesses up to three RNA-binding domains (LAM, RRM1, DM15) [223, 330], and in addition may act in conjunction with several other RBPs, may mean that a single mRNA interaction motif is unlikely. However, it is clear that the 3'UTR is highly specific in determining the LARP1 stability effect. We previously identified the proteins

SYNCRIP/HNRNPQ, a factor that can destabilise mRNA [406, 407] and nucleolin (NCL), a protein that can promote transcript stability [178], to be enriched in LARP1-pulldowns in ovarian cancer cells [333]. Significantly, in the same 3'UTR pulldown experiment in which LARP1 was identified, both these proteins were also highly enriched, despite being conducted in a benign cell line [331]. LARP7 also binds both these proteins [295]. This suggests a model in which LARP1 functions as a critical component of a stability-regulating mRNP complex that is associated with the 3'UTR of transcripts. By regulating the components of this complex, LARP1 may be able to differentially regulate stability (Figure 4-1).

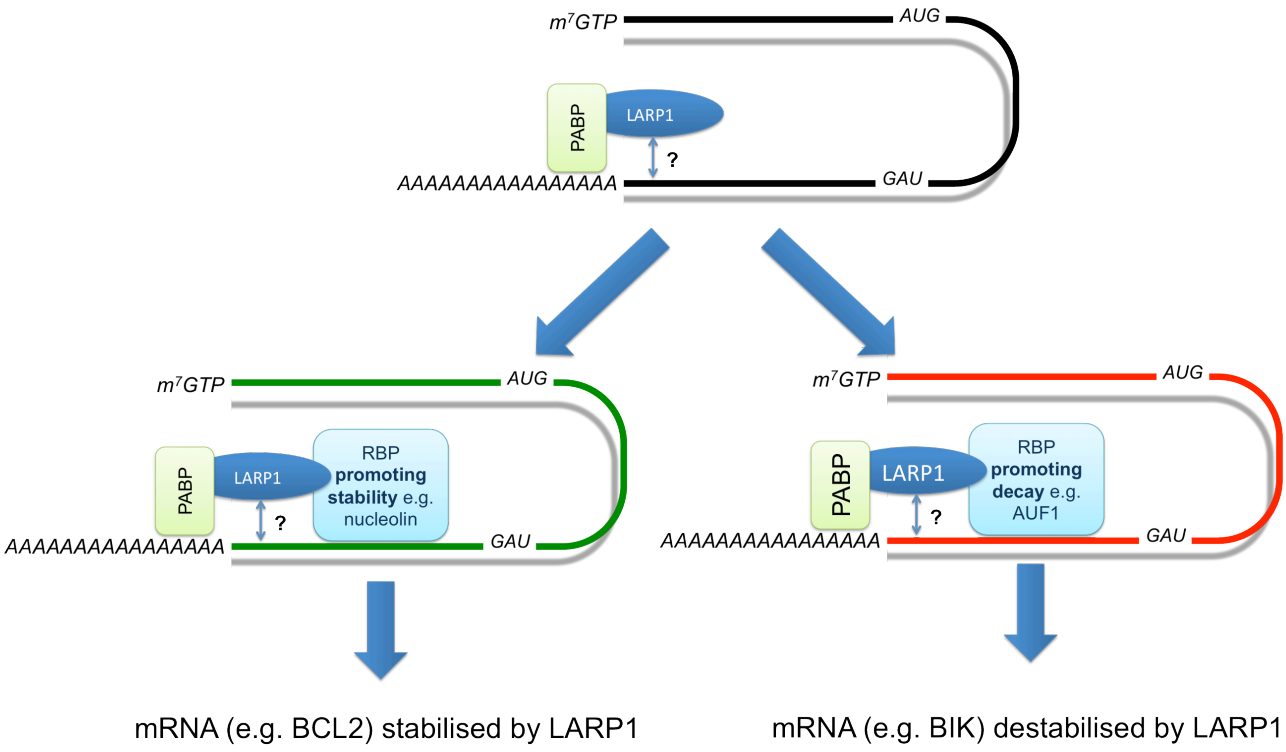

Figure 4-1. A possible model for the role of LARP1 in modulating transcript stability.

LARP1 has previously been shown to bind PABP and 3'UTR-associated RBPs with a role in stability regulation, and has been identified in 3'UTR pulldowns, supporting its localisation at the 3'UTR. In addition, my work has demonstrated that 3'UTR sequences determine whether LARP1 promotes or inhibits mRNA stability. Whether LARP1 binds directly to sequences in the 3'UTR remains to be determined. The differential effect on stability could be due to the recruitment or stabilisation of different RBPs on the 3'UTR. For example, in the case of *BCL2*, LARP1 could act as a scaffold to enhance the binding of nucleolin to the 3'UTR, blocking the recognition of ARE sites by RBPs that

promote destabilisation. In contrast, in the *BIK* 3'UTR, LARP1 could promote the recruitment of destabilising factors.

4.2 FURTHER WORK

4.2.1 DETERMINING DIRECT INTERACTIONS

To arrive at a complete description of the action of LARP1 in the cancer cell, it is necessary to determine if the protein is interacting directly with its mRNA stability targets. The RNA-immunoprecipitations carried out in this study, although conducted in high stringency conditions, do not provide a definitive answer to this question. The short 3'UTR of *BIK* is more amenable to experimental study, and I am currently in the process of investigating the possibility of a direct interaction. To do this, I will perform biotinylated RNA pulldowns with magnetic beads, incubating the beads with either whole cell lysates or recombinant LARP1 protein. If recombinant LARP1 protein is pulled down this will indicate a direct interaction and will be confirmed using electrophoretic mobility shift assays (EMSAs). If LARP1 protein is only isolated following incubation of beads with whole cell lysates, I will perform mass spectrometric analysis of the precipitates, to identify the proteins associated with the *BIK* 3'UTR that could be involved in recruiting LARP1.

The size of the *BCL2* 3'UTR complicates the assessment of a direct LARP1-RNA interaction, and a smaller target sequence is needed for further experiments. I found that the stop codon-proximal half of the 3'UTR (0-2,640bp) cloned into a luciferase reporter construct produced a stronger destabilising effect on LARP1 knockdown, so I have chosen to focus on this region. I have designed a series of 10 overlapping constructs to screen the 3'UTR for a region producing a maximal destabilising effect, using luciferase reporter assays as before (Figure 4-2). The region(s) identified will be cloned into a T7 promoter vector, and investigated for direct interactions as above.

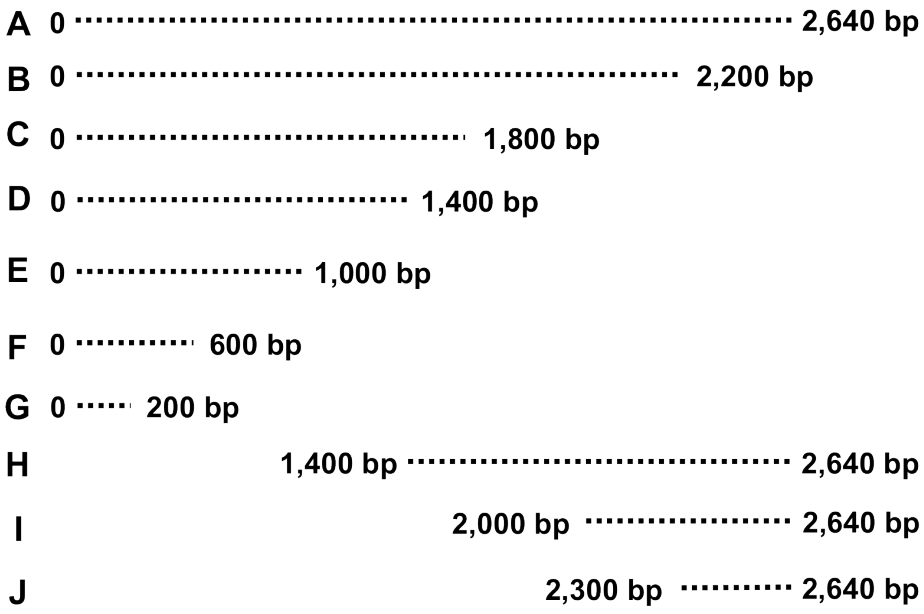

Figure 4-2. Schematic of luciferase reporter constructs covering the first 2,640bp of the BCL2 3'UTR.

4.2.2 ESTABLISHING AN RNA TARGET MOTIF AND GLOBAL REGULOME

As discussed above, key questions remain unanswered about the interaction of LARP1 with mRNA. Although we have identified mRNAs in complex with LARP1 in HeLa cells, we do not know to what extent these interactions are conserved across cell lines and cancer types, nor do we know the sites of interaction with transcripts, or the RNA motifs recognised. In addition, whilst the RIP-Chip experimental design employed to derive the HeLa LARP1 interactome may enrich for more functionally meaningful LARP1-RNA interactions [408], it cannot exclude the possibility that these interactions occur indirectly through an intermediary. All these questions could potentially be answered by performing a LARP1 RNA-crosslinking immunoprecipitation (CLIP) experiment coupled with RNA-sequencing, such as the PAR-CLIP, HITS-CLIP or iCLIP approaches, revealing direct RNA targets, as well as where on the transcript LARP1 binds and the bound sequence [409-411]. In previous studies,

researchers have used CLIP data to attempt to derive a consensus RNA recognition sequence for a given RBP. However, with up to three RNA-binding domains (LAM, RRM DM15) [223, 330], LARP1 may bind more than one recognition motif. CLIP data could be supported by *in vitro* nucleotide affinity studies. Nykamp *et al,* working in *C. elegans*, found LARP1 has a high affinity for PolyG and, to lesser extent, PolyU [330]. In contrast, a different experimental approach by Aoki *et al* suggests that in human HEK293 cells, polyA is the only nucleotide recognised by LARP1 [331]. Incubating recombinant LARP1 with polyA,C,G and U sequences, or putative recognition motifs, and deriving affinities in shift assays, will allow validation of the CLIP-derived motifs.

As CLIP data will provide information on the site of LARP1 binding within target transcripts, it will be interesting to see whether there is a 3'UTR bias, and whether the interaction site can predict the effect on stability. For example, stop codon-proximal binding in the 3'UTR may correlate with stabilisation whilst distal binding may promote destabilisation. Alternatively, the RNA motif bound may produce different effects on stability.

Further inferences can be made from the CLIP data by cross-referencing it with global assessments of RNA stability on LARP1 knockdown, for example using the 5'-bromo-uridine (BrU) immunoprecipitation chase-deep sequencing analysis (BRIC-seq) strategy developed by the Akimitsu lab [412]. In addition, given LARP1 has been shown to play a role in mRNA translation [335], it would be useful to perform a global assessment of shifts in polysomal-associated transcripts following LARP1 knockdown, by sequencing ribosome-protected RNA fragments [413]. Overlaying these three sets of data (information on LARP1-bound mRNAs and RNAs with altered stability or translation following LARP1 depletion), will provide a very powerful step towards understanding the mechanism of LARP1 action.

As discussed in Section 1.3.3.5, microRNAs regulate mRNA stability and translation by binding to the 3'UTR, being part of the RISC. LARP3 has recently been shown to promote miRNA maturation by stabilising precursors [258]. LARP1 could therefore be regulating RNA stability by affecting the ability of miRNAs to target gene UTRs, either by affecting precursor processing, regulating miRNA access to the 3'UTR, or indirectly regulating miRNA transcription. This could be investigated by performing small RNA-sequencing following LARP1 knockdown; a LARP1-RNA CLIP experiment would also identify if LARP1 binds miRNAs directly.

4.2.3 DEVELOPING THE CLINICAL POTENTIAL OF LARP1

Many papers identifying potential intratumoural biomarkers are published every year, but few of these prove suitable for clinical use. Indeed, a systematic review of the literature conducted in 2007 found 1261 candidate protein biomarkers, of which only 9 had reached the stage of FDA approval [414]. Few markers stand up to repeated scrutiny in new patient cohorts. To address this, we have just completed an IHC analysis of a new tissue microarray dataset comprising 283 ovarian cancer patients, that represents a very high quality clinical cohort collected as part of the SCOTROC4 trial. This microarray has been stained, scored by two specialists and analysed completely independently from ourselves, in line with recommendations published by the Biomarker Task Force at the NCI [415]. This has revealed that LARP1 is a highly significant predictor of poor progression-free survival, with elevated intratumoural LARP1 associated with a 50% increased risk of progression at any time point. As one of a panel of prognostic or diagnostic markers, LARP1 may therefore prove useful as a tissue biomarker, and further large patient studies are warranted.

Whilst the patient numbers involved in our intratumoural LARP1 studies are now quite large, the work on LARP1 as a circulating biomarker is at a more preliminary stage. Although our pilot study of LARP1 in the diagnostic setting, using 30 controls and 42 pre-operative patient samples, has proved very promising, there is nonetheless an overlap in plasma LARP1 levels between the two cohorts, creating the potential for false positives or negatives. Autoantibodies to LARP3 are found in several autoimmune conditions, including Sjögren's syndrome [416], although there is no evidence as yet to suggest that LARP3 protein itself is present in the circulation. Whilst LARP1 appears to behave very differently to LARP3 in many respects, it will be important to exclude a link to inflammatory processes, which could be a confounding factor. Considerably larger cohorts will be needed to assess clinical potential, and we have already obtained through collaborations over 900 patient samples for further assessment. These also include post-operative samples collected during chemotherapy treatment, to further assess the potential of LARP1 as a prognostic plasma biomarker. Alongside further work with clinical samples, it will be necessary to clarify the mechanism of LARP1 protein release from cancer cells, and what factors influence this export. In addition, it will be necessary to assess, using filtration and ultracentrifugation strategies, whether the LARP1 protein detected in conditioned media and plasma represents free protein, or is contained within vesicles and/or exosomes. Work with Ago2 and miRNAs in conditioned media and plasma suggest both exist primarily as free RNP complexes [373, 398] and Ago2 appears to also have a role in stabilising these extracellular miRNAs [398, 417]. It will be interesting to determine whether extracellular LARP1 is also bound to RNA, and what effect this binding has on RNA fate.

My work *in vivo* demonstrates that reducing LARP1 expression in ovarian cancer cells can inhibit tumour initiation and development, whilst in the *in vitro* setting it causes cell death and enhances chemotherapy sensitivity. Using conditional knockdown of LARP1 tumours *in*

vivo, the lab is in the process of confirming the clinical significance of this chemosensitisation effect. These traits would be highly desirable in a targeted therapy for cancer. However, the majority of targeted therapies to date involve blocking the activity of protein kinases by competing with ATP for the binding domain [418]. It may be possible to block the interaction of the RNA-binding domain(s) with the target RNA. Indeed, a group in China modelled the LARP3 RNA-binding pocket *in silico* and used this to select small molecule inhibitors with the ability to block LARP3-mediated promotion of Hepatitis B replication [286]. This type of approach requires very detailed knowledge of both LARP1 structure and its RNA targets, which remain to be established. It may be possible to directly decrease LARP1 expression in tumours, through strategies such as therapeutic siRNA *in vivo* delivery [419]. The fact that LARP1 is detectable in the circulation would provide a powerful tool in drug development. It would give a minimally invasive method to predict patients that could potentially respond to this treatment, as well as provide a readout of the success of inhibition after drug administration. Whilst it may be possible to target siRNA delivery to cancer cells [420], it is likely that non-cancer cells will still be affected. At present, we do not know how critical LARP1 is to non-malignant cells. Tcherkezian *et al.* reported that LARP1 knockdown did not cause apoptosis in HEK293 embryonic kidney fibroblast cells [335], though with the same cell line I found a significant increase in apoptosis (*data not shown*), the same trend as that seen in cancer cells. Further *in vitro* work on non-malignant cell lines is required before progressing to testing in model organisms. To establish the importance of LARP1 in normal growth and development, it would be useful to explore the phenotype of LARP1 knockout mice. LARP3 is essential to early embryogenesis [232] and, since LARP1 expression is high in embryonic stem cells and drops during differentiation [345], we may find a critical role for LARP1 in embryogenesis as well; conditional knockouts may therefore be necessary.

4.3 CONCLUSIONS

There is increasing evidence linking the LARP protein family to cancer. La/LARP3 promotes malignant progression by regulating translation [252, 276] whilst the predominantly nuclear LARP7 stabilises 7SK snRNA and acts as a tumour suppressor by inhibiting transcription [301]. Thus, though LARP family members have conserved RNA-binding structural motifs, their roles in post-transcriptional regulation and the cellular consequences of these effects have diverged significantly.

I show here that LARP1, one of the most abundant transcripts in ovarian cancer cells, has a critical role in promoting chemoresistance and tumourigenicity. By differentially regulating the stability of pro- and anti-apoptotic transcripts, LARP1 acts as a post-transcriptional promoter of apoptosis evasion. It is therefore a potential future therapeutic target for the treatment of chemotherapy-resistant ovarian cancer. The fact that it has been shown possible to potentially inhibit the interaction of LARP3 with an RNA target [286] suggests that the LARP1-*BCL2* interaction may also be druggable.

The finding that, like hepatocellular cancer [347], LARP1 expression in ovarian malignancies predicts adverse outcomes suggests it may have potential as an intratumoural biomarker. In addition, given that LARP1 is detectable in human plasma, and levels reflect underlying tumour burden, this presents the possibility of utilising plasma LARP1 protein levels as a non-invasive disease marker. This will also be of considerable utility in the potential development of upstream inhibitors of LARP1 expression.

Although significant progress has been made during this thesis in understanding the role of LARP1 in the ovarian cancer cell, important questions remain unanswered. We have yet to confirm that the interaction of LARP1 with the 3'UTR of target mRNAs is direct. If it is, we

will need to pinpoint the LARP1 mRNA recognition sequence, and to determine whether additional *trans*-acting factors are required to modulate LARP1-dependent mRNA stability regulation. Answering these questions will bring us significantly closer to developing therapeutic inhibitors of LARP1 function.

An increasing number of RBPs have been shown to act as oncogenes across nearly all malignancies through the post-transcriptional regulation of gene expression. This thesis demonstrates that post-transcriptional regulation plays a significant role in ovarian cancer progression and that, as an mRNA stability regulator with oncogenic effects, LARP1 may have potential as a disease biomarker and therapeutic target.

5 REFERENCES

1. Jemal, A., et al., *Global cancer statistics.* CA Cancer J Clin, 2011. **61**(2): p. 69-90.
2. Berrino, F., et al., *Comparative cancer survival information in Europe.* Eur J Cancer, 2009. **45**(6): p. 901-8.
3. *Office of National Statistics. Cancer survival rates, Cancer survival in England, patients diagnosed 2005-2009 and followed up to 2010. 15 November 2011.*
4. Bast, R.C., Jr., B. Hennessy, and G.B. Mills, *The biology of ovarian cancer: new opportunities for translation.* Nat Rev Cancer, 2009. **9**(6): p. 415-28.
5. Vaughan, S., et al., *Rethinking ovarian cancer: recommendations for improving outcomes.* Nat Rev Cancer, 2011. **11**(10): p. 719-25.
6. Colombo, N., et al., *Newly diagnosed and relapsed epithelial ovarian carcinoma: ESMO Clinical Practice Guidelines for diagnosis, treatment and follow-up.* Ann Oncol, 2010. **21 Suppl 5**: p. v23-30.
7. Prat, J., *New insights into ovarian cancer pathology.* Ann Oncol, 2012. **23 Suppl 10**: p. x111-7.
8. Hess, V., et al., *Mucinous epithelial ovarian cancer: a separate entity requiring specific treatment.* J Clin Oncol, 2004. **22**(6): p. 1040-4.
9. Pignata, S., et al., *Activity of chemotherapy in mucinous ovarian cancer with a recurrence free interval of more than 6 months: results from the SOCRATES retrospective study.* BMC Cancer, 2008. **8**: p. 252.
10. Shih Ie, M. and R.J. Kurman, *Ovarian tumorigenesis: a proposed model based on morphological and molecular genetic analysis.* Am J Pathol, 2004. **164**(5): p. 1511-8.
11. Nik, N.N., et al., *Origin and pathogenesis of pelvic (ovarian, tubal, and primary peritoneal) serous carcinoma.* Annu Rev Pathol, 2014. **9**: p. 27-45.
12. Cancer Genome Atlas Research, N., *Integrated genomic analyses of ovarian carcinoma.* Nature, 2011. **474**(7353): p. 609-15.
13. CRUK. November 2014)]; Available from: http://www.cancerresearchuk.org/cancer-info/cancerstats/types/ovary/survival/ovarian-cancer-survival-statistics.
14. Kurman, R.J. and M. Shih Ie, *The origin and pathogenesis of epithelial ovarian cancer: a proposed unifying theory.* Am J Surg Pathol, 2010. **34**(3): p. 433-43.
15. Goff, B.A., et al., *Ovarian carcinoma diagnosis.* Cancer, 2000. **89**(10): p. 2068-75.
16. Gupta, D. and C.G. Lis, *Role of CA125 in predicting ovarian cancer survival - a review of the epidemiological literature.* J Ovarian Res, 2009. **2**: p. 13.
17. Peto, J., et al., *The cervical cancer epidemic that screening has prevented in the UK.* Lancet, 2004. **364**(9430): p. 249-56.
18. Karam, A.K. and B.Y. Karlan, *Ovarian cancer: the duplicity of CA125 measurement.* Nat Rev Clin Oncol, 2010. **7**(6): p. 335-9.
19. Mol, B.W., et al., *The performance of CA-125 measurement in the detection of endometriosis: a meta-analysis.* Fertil Steril, 1998. **70**(6): p. 1101-8.
20. Menon, U., et al., *Sensitivity and specificity of multimodal and ultrasound screening for ovarian cancer, and stage distribution of detected cancers: results of the prevalence screen of the UK Collaborative Trial of Ovarian Cancer Screening (UKCTOCS).* Lancet Oncol, 2009. **10**(4): p. 327-40.

21. Buys, S.S., et al., *Ovarian cancer screening in the Prostate, Lung, Colorectal and Ovarian (PLCO) cancer screening trial: findings from the initial screen of a randomized trial.* Am J Obstet Gynecol, 2005. **193**(5): p. 1630-9.
22. Yurkovetsky, Z., et al., *Development of a multimarker assay for early detection of ovarian cancer.* J Clin Oncol, 2010. **28**(13): p. 2159-66.
23. Moore, R.G., et al., *A novel multiple marker bioassay utilizing HE4 and CA125 for the prediction of ovarian cancer in patients with a pelvic mass.* Gynecol Oncol, 2009. **112**(1): p. 40-6.
24. Agarwal, R. and S.B. Kaye, *Ovarian cancer: strategies for overcoming resistance to chemotherapy.* Nat Rev Cancer, 2003. **3**(7): p. 502-16.
25. Blackledge, G., et al., *Response of patients in phase II studies of chemotherapy in ovarian cancer: implications for patient treatment and the design of phase II trials.* Br J Cancer, 1989. **59**(4): p. 650-3.
26. Ledermann, J.A. and R.S. Kristeleit, *Optimal treatment for relapsing ovarian cancer.* Ann Oncol, 2010. **21 Suppl 7**: p. vii218-22.
27. Gynecologic Oncology, G., et al., *Phase II trial of weekly paclitaxel (80 mg/m2) in platinum and paclitaxel-resistant ovarian and primary peritoneal cancers: a Gynecologic Oncology Group study.* Gynecol Oncol, 2006. **101**(3): p. 436-40.
28. Mutch, D.G., et al., *Randomized phase III trial of gemcitabine compared with pegylated liposomal doxorubicin in patients with platinum-resistant ovarian cancer.* J Clin Oncol, 2007. **25**(19): p. 2811-8.
29. Stordal, B., N. Pavlakis, and R. Davey, *A systematic review of platinum and taxane resistance from bench to clinic: an inverse relationship.* Cancer Treat Rev, 2007. **33**(8): p. 688-703.
30. Jordan, M.A. and L. Wilson, *Microtubules as a target for anticancer drugs.* Nat Rev Cancer, 2004. **4**(4): p. 253-65.
31. Kelland, L.R., *Preclinical perspectives on platinum resistance.* Drugs, 2000. **59 Suppl 4**: p. 1-8; discussion 37-8.
32. Galluzzi, L., et al., *Molecular mechanisms of cisplatin resistance.* Oncogene, 2012. **31**(15): p. 1869-83.
33. Hostetter, A.A., M.F. Osborn, and V.J. DeRose, *RNA-Pt adducts following cisplatin treatment of Saccharomyces cerevisiae.* ACS Chem Biol, 2012. **7**(1): p. 218-25.
34. Rosenberg, J.M. and P.H. Sato, *Cisplatin inhibits in vitro translation by preventing the formation of complete initiation complex.* Mol Pharmacol, 1993. **43**(3): p. 491-7.
35. Mandic, A., et al., *Cisplatin induces endoplasmic reticulum stress and nucleus-independent apoptotic signaling.* J Biol Chem, 2003. **278**(11): p. 9100-6.
36. Orr, G.A., et al., *Mechanisms of Taxol resistance related to microtubules.* Oncogene, 2003. **22**(47): p. 7280-95.
37. Siddik, Z.H., *Cisplatin: mode of cytotoxic action and molecular basis of resistance.* Oncogene, 2003. **22**(47): p. 7265-79.
38. McGrogan, B.T., et al., *Taxanes, microtubules and chemoresistant breast cancer.* Biochim Biophys Acta, 2008. **1785**(2): p. 96-132.
39. Dasari, S. and P.B. Tchounwou, *Cisplatin in cancer therapy: molecular mechanisms of action.* Eur J Pharmacol, 2014. **740**: p. 364-78.
40. Cho, H.J., et al., *Upregulation of Bcl-2 is associated with cisplatin-resistance via inhibition of Bax translocation in human bladder cancer cells.* Cancer Lett, 2006. **237**(1): p. 56-66.
41. Mano, Y., et al., *Bcl-2 as a predictor of chemosensitivity and prognosis in primary epithelial ovarian cancer.* Eur J Cancer, 1999. **35**(8): p. 1214-9.

42. Martin, L.P., T.C. Hamilton, and R.J. Schilder, *Platinum resistance: the role of DNA repair pathways.* Clin Cancer Res, 2008. **14**(5): p. 1291-5.
43. Cummings, M., et al., *XPA versus ERCC1 as chemosensitising agents to cisplatin and mitomycin C in prostate cancer cells: role of ERCC1 in homologous recombination repair.* Biochem Pharmacol, 2006. **72**(2): p. 166-75.
44. Giannakakou, P., et al., *Paclitaxel-resistant human ovarian cancer cells have mutant beta-tubulins that exhibit impaired paclitaxel-driven polymerization.* J Biol Chem, 1997. **272**(27): p. 17118-25.
45. Giannakakou, P., et al., *A common pharmacophore for epothilone and taxanes: molecular basis for drug resistance conferred by tubulin mutations in human cancer cells.* Proc Natl Acad Sci U S A, 2000. **97**(6): p. 2904-9.
46. Kavallaris, M., et al., *Taxol-resistant epithelial ovarian tumors are associated with altered expression of specific beta-tubulin isotypes.* J Clin Invest, 1997. **100**(5): p. 1282-93.
47. Dubeau, L., *The cell of origin of ovarian epithelial tumours.* Lancet Oncol, 2008. **9**(12): p. 1191-7.
48. Piek, J.M., et al., *Dysplastic changes in prophylactically removed Fallopian tubes of women predisposed to developing ovarian cancer.* J Pathol, 2001. **195**(4): p. 451-6.
49. Kindelberger, D.W., et al., *Intraepithelial carcinoma of the fimbria and pelvic serous carcinoma: Evidence for a causal relationship.* Am J Surg Pathol, 2007. **31**(2): p. 161-9.
50. Przybycin, C.G., et al., *Are all pelvic (nonuterine) serous carcinomas of tubal origin?* Am J Surg Pathol, 2010. **34**(10): p. 1407-16.
51. Seidman, J.D., P. Zhao, and A. Yemelyanova, *"Primary peritoneal" high-grade serous carcinoma is very likely metastatic from serous tubal intraepithelial carcinoma: assessing the new paradigm of ovarian and pelvic serous carcinogenesis and its implications for screening for ovarian cancer.* Gynecol Oncol, 2011. **120**(3): p. 470-3.
52. Perets, R., et al., *Transformation of the fallopian tube secretory epithelium leads to high-grade serous ovarian cancer in Brca;Tp53;Pten models.* Cancer Cell, 2013. **24**(6): p. 751-65.
53. Hanahan, D. and R.A. Weinberg, *The hallmarks of cancer.* Cell, 2000. **100**(1): p. 57-70.
54. Hanahan, D. and R.A. Weinberg, *Hallmarks of cancer: the next generation.* Cell, 2011. **144**(5): p. 646-74.
55. Ahmed, N., et al., *Cancerous ovarian stem cells: obscure targets for therapy but relevant to chemoresistance.* J Cell Biochem, 2013. **114**(1): p. 21-34.
56. Pharoah, P.D., et al., *GWAS meta-analysis and replication identifies three new susceptibility loci for ovarian cancer.* Nat Genet, 2013. **45**(4): p. 362-70, 370e1-2.
57. Alsop, K., et al., *BRCA mutation frequency and patterns of treatment response in BRCA mutation-positive women with ovarian cancer: a report from the Australian Ovarian Cancer Study Group.* J Clin Oncol, 2012. **30**(21): p. 2654-63.
58. Bolton, K.L., et al., *Association between BRCA1 and BRCA2 mutations and survival in women with invasive epithelial ovarian cancer.* JAMA, 2012. **307**(4): p. 382-90.
59. Magee, J.A., E. Piskounova, and S.J. Morrison, *Cancer stem cells: impact, heterogeneity, and uncertainty.* Cancer Cell, 2012. **21**(3): p. 283-96.
60. Zhang, S., et al., *Identification and characterization of ovarian cancer-initiating cells from primary human tumors.* Cancer Res, 2008. **68**(11): p. 4311-20.
61. Stewart, J.M., et al., *Phenotypic heterogeneity and instability of human ovarian tumor-initiating cells.* Proc Natl Acad Sci U S A, 2011. **108**(16): p. 6468-73.

62. Curley, M.D., et al., *CD133 expression defines a tumor initiating cell population in primary human ovarian cancer.* Stem Cells, 2009. **27**(12): p. 2875-83.
63. Alvero, A.B., et al., *Molecular phenotyping of human ovarian cancer stem cells unravels the mechanisms for repair and chemoresistance.* Cell Cycle, 2009. **8**(1): p. 158-66.
64. Yasuda, K., et al., *Ovarian cancer stem cells are enriched in side population and aldehyde dehydrogenase bright overlapping population.* PLoS One, 2013. **8**(8): p. e68187.
65. Baba, T., et al., *Epigenetic regulation of CD133 and tumorigenicity of CD133+ ovarian cancer cells.* Oncogene, 2009. **28**(2): p. 209-18.
66. Zhang, J., et al., *CD133 expression associated with poor prognosis in ovarian cancer.* Mod Pathol, 2012. **25**(3): p. 456-64.
67. Liu, S., et al., *Prognostic value of cancer stem cell marker aldehyde dehydrogenase in ovarian cancer: a meta-analysis.* PLoS One, 2013. **8**(11): p. e81050.
68. Flesken-Nikitin, A., et al., *Ovarian surface epithelium at the junction area contains a cancer-prone stem cell niche.* Nature, 2013. **495**(7440): p. 241-5.
69. Cooke, S.L., et al., *Genomic analysis of genetic heterogeneity and evolution in high-grade serous ovarian carcinoma.* Oncogene, 2010. **29**(35): p. 4905-13.
70. Konstantinopoulos, P.A., D. Spentzos, and S.A. Cannistra, *Gene-expression profiling in epithelial ovarian cancer.* Nat Clin Pract Oncol, 2008. **5**(10): p. 577-87.
71. Schwanhausser, B., et al., *Corrigendum: Global quantification of mammalian gene expression control.* Nature, 2013. **495**(7439): p. 126-7.
72. Lee, R.C., R.L. Feinbaum, and V. Ambros, *The C. elegans heterochronic gene lin-4 encodes small RNAs with antisense complementarity to lin-14.* Cell, 1993. **75**(5): p. 843-54.
73. Wightman, B., I. Ha, and G. Ruvkun, *Posttranscriptional regulation of the heterochronic gene lin-14 by lin-4 mediates temporal pattern formation in C. elegans.* Cell, 1993. **75**(5): p. 855-62.
74. Wurth, L., *Versatility of RNA-Binding Proteins in Cancer.* Comp Funct Genomics, 2012. **2012**: p. 178525.
75. Kechavarzi, B. and S.C. Janga, *Dissecting the expression landscape of RNA-binding proteins in human cancers.* Genome Biol, 2014. **15**(1): p. R14.
76. Ehlen, A., et al., *Expression of the RNA-binding protein RBM3 is associated with a favourable prognosis and cisplatin sensitivity in epithelial ovarian cancer.* J Transl Med, 2010. **8**: p. 78.
77. Guo, Y., et al., *Silencing the Double-Stranded RNA Binding Protein DGCR8 Inhibits Ovarian Cancer Cell Proliferation, Migration, and Invasion.* Pharm Res, 2013.
78. Crick, F., *Central dogma of molecular biology.* Nature, 1970. **227**(5258): p. 561-3.
79. Keene, J.D., *Minireview: global regulation and dynamics of ribonucleic Acid.* Endocrinology, 2010. **151**(4): p. 1391-7.
80. Robertson, M.P. and G.F. Joyce, *The origins of the RNA world.* Cold Spring Harb Perspect Biol, 2012. **4**(5).
81. Harel-Sharvit, L., et al., *RNA polymerase II subunits link transcription and mRNA decay to translation.* Cell, 2010. **143**(4): p. 552-63.
82. Baek, D., et al., *The impact of microRNAs on protein output.* Nature, 2008. **455**(7209): p. 64-71.
83. Tenenbaum, S.A., et al., *Identifying mRNA subsets in messenger ribonucleoprotein complexes by using cDNA arrays.* Proc Natl Acad Sci U S A, 2000. **97**(26): p. 14085-90.

84. Muller-McNicoll, M. and K.M. Neugebauer, *How cells get the message: dynamic assembly and function of mRNA-protein complexes.* Nat Rev Genet, 2013. **14**(4): p. 275-87.
85. Anderson, P., et al., *Post-transcriptional regulation of proinflammatory proteins.* J Leukoc Biol, 2004. **76**(1): p. 42-7.
86. Cook, K.B., et al., *RBPDB: a database of RNA-binding specificities.* Nucleic Acids Res, 2011. **39**(Database issue): p. D301-8.
87. Castello, A., et al., *Insights into RNA biology from an atlas of mammalian mRNA-binding proteins.* Cell, 2012. **149**(6): p. 1393-406.
88. Flicek, P., et al., *Ensembl 2012.* Nucleic Acids Res, 2012. **40**(Database issue): p. D84-90.
89. Halbeisen, R.E., et al., *Post-transcriptional gene regulation: from genome-wide studies to principles.* Cell Mol Life Sci, 2008. **65**(5): p. 798-813.
90. Hogan, D.J., et al., *Diverse RNA-binding proteins interact with functionally related sets of RNAs, suggesting an extensive regulatory system.* PLoS Biol, 2008. **6**(10): p. e255.
91. Lunde, B.M., C. Moore, and G. Varani, *RNA-binding proteins: modular design for efficient function.* Nat Rev Mol Cell Biol, 2007. **8**(6): p. 479-90.
92. Voss, T.C. and G.L. Hager, *Dynamic regulation of transcriptional states by chromatin and transcription factors.* Nat Rev Genet, 2014. **15**(2): p. 69-81.
93. Smolle, M. and J.L. Workman, *Transcription-associated histone modifications and cryptic transcription.* Biochim Biophys Acta, 2013. **1829**(1): p. 84-97.
94. Coulon, A., et al., *Eukaryotic transcriptional dynamics: from single molecules to cell populations.* Nat Rev Genet, 2013. **14**(8): p. 572-84.
95. Thomas, M.C. and C.M. Chiang, *The general transcription machinery and general cofactors.* Crit Rev Biochem Mol Biol, 2006. **41**(3): p. 105-78.
96. Shandilya, J. and S.G. Roberts, *The transcription cycle in eukaryotes: from productive initiation to RNA polymerase II recycling.* Biochim Biophys Acta, 2012. **1819**(5): p. 391-400.
97. Bentley, D.L., *Coupling mRNA processing with transcription in time and space.* Nat Rev Genet, 2014. **15**(3): p. 163-75.
98. Hsin, J.P. and J.L. Manley, *The RNA polymerase II CTD coordinates transcription and RNA processing.* Genes Dev, 2012. **26**(19): p. 2119-37.
99. Cowling, V.H., *Regulation of mRNA cap methylation.* Biochem J, 2010. **425**(2): p. 295-302.
100. Rasmussen, E.B. and J.T. Lis, *In vivo transcriptional pausing and cap formation on three Drosophila heat shock genes.* Proc Natl Acad Sci U S A, 1993. **90**(17): p. 7923-7.
101. Inoue, K., et al., *Effect of the cap structure on pre-mRNA splicing in Xenopus oocyte nuclei.* Genes Dev, 1989. **3**(9): p. 1472-9.
102. Izaurralde, E., et al., *A cap-binding protein complex mediating U snRNA export.* Nature, 1995. **376**(6542): p. 709-12.
103. Sakharkar, M.K., V.T. Chow, and P. Kangueane, *Distributions of exons and introns in the human genome.* In Silico Biol, 2004. **4**(4): p. 387-93.
104. Deutsch, M. and M. Long, *Intron-exon structures of eukaryotic model organisms.* Nucleic Acids Res, 1999. **27**(15): p. 3219-28.
105. Wang, E.T., et al., *Alternative isoform regulation in human tissue transcriptomes.* Nature, 2008. **456**(7221): p. 470-6.
106. Beyer, A.L. and Y.N. Osheim, *Splice site selection, rate of splicing, and alternative splicing on nascent transcripts.* Genes Dev, 1988. **2**(6): p. 754-65.

107. Lee, K.M. and W.Y. Tarn, *Coupling pre-mRNA processing to transcription on the RNA factory assembly line.* RNA Biol, 2013. **10**(3): p. 380-90.
108. Singh, J. and R.A. Padgett, *Rates of in situ transcription and splicing in large human genes.* Nat Struct Mol Biol, 2009. **16**(11): p. 1128-33.
109. Jurica, M.S. and M.J. Moore, *Pre-mRNA splicing: awash in a sea of proteins.* Mol Cell, 2003. **12**(1): p. 5-14.
110. Wahl, M.C., C.L. Will, and R. Luhrmann, *The spliceosome: design principles of a dynamic RNP machine.* Cell, 2009. **136**(4): p. 701-18.
111. Will, C.L. and R. Luhrmann, *Spliceosome structure and function.* Cold Spring Harb Perspect Biol, 2011. **3**(7).
112. Ruskin, B., P.D. Zamore, and M.R. Green, *A factor, U2AF, is required for U2 snRNP binding and splicing complex assembly.* Cell, 1988. **52**(2): p. 207-19.
113. Laurencikiene, J., et al., *RNA editing and alternative splicing: the importance of co-transcriptional coordination.* EMBO Rep, 2006. **7**(3): p. 303-7.
114. Wang, Q., et al., *Stress-induced apoptosis associated with null mutation of ADAR1 RNA editing deaminase gene.* J Biol Chem, 2004. **279**(6): p. 4952-61.
115. Park, E., et al., *RNA editing in the human ENCODE RNA-seq data.* Genome Res, 2012. **22**(9): p. 1626-33.
116. Peng, Z., et al., *Comprehensive analysis of RNA-Seq data reveals extensive RNA editing in a human transcriptome.* Nat Biotechnol, 2012. **30**(3): p. 253-60.
117. Nishikura, K., *Functions and regulation of RNA editing by ADAR deaminases.* Annu Rev Biochem, 2010. **79**: p. 321-49.
118. Blow, M.J., et al., *RNA editing of human microRNAs.* Genome Biol, 2006. **7**(4): p. R27.
119. Ahn, S.H., M. Kim, and S. Buratowski, *Phosphorylation of serine 2 within the RNA polymerase II C-terminal domain couples transcription and 3' end processing.* Mol Cell, 2004. **13**(1): p. 67-76.
120. Licatalosi, D.D. and R.B. Darnell, *RNA processing and its regulation: global insights into biological networks.* Nat Rev Genet, 2010. **11**(1): p. 75-87.
121. Kuehner, J.N., E.L. Pearson, and C. Moore, *Unravelling the means to an end: RNA polymerase II transcription termination.* Nat Rev Mol Cell Biol, 2011. **12**(5): p. 283-94.
122. Shi, Y., et al., *Molecular architecture of the human pre-mRNA 3' processing complex.* Mol Cell, 2009. **33**(3): p. 365-76.
123. Brune, C., et al., *Yeast poly(A)-binding protein Pab1 shuttles between the nucleus and the cytoplasm and functions in mRNA export.* RNA, 2005. **11**(4): p. 517-31.
124. Herold, A., L. Teixeira, and E. Izaurralde, *Genome-wide analysis of nuclear mRNA export pathways in Drosophila.* EMBO J, 2003. **22**(10): p. 2472-83.
125. Erkmann, J.A. and U. Kutay, *Nuclear export of mRNA: from the site of transcription to the cytoplasm.* Exp Cell Res, 2004. **296**(1): p. 12-20.
126. Stutz, F., et al., *REF, an evolutionary conserved family of hnRNP-like proteins, interacts with TAP/Mex67p and participates in mRNA nuclear export.* RNA, 2000. **6**(4): p. 638-50.
127. Kohler, A. and E. Hurt, *Exporting RNA from the nucleus to the cytoplasm.* Nat Rev Mol Cell Biol, 2007. **8**(10): p. 761-73.
128. Tieg, B. and H. Krebber, *Dbp5 - from nuclear export to translation.* Biochim Biophys Acta, 2013. **1829**(8): p. 791-8.
129. Macdonald, P.M. and G. Struhl, *cis-acting sequences responsible for anterior localization of bicoid mRNA in Drosophila embryos.* Nature, 1988. **336**(6199): p. 595-8.

130. Johnstone, O. and P. Lasko, *Translational regulation and RNA localization in Drosophila oocytes and embryos.* Annu Rev Genet, 2001. **35**: p. 365-406.
131. Kislauskis, E.H., X. Zhu, and R.H. Singer, *beta-Actin messenger RNA localization and protein synthesis augment cell motility.* J Cell Biol, 1997. **136**(6): p. 1263-70.
132. Lecuyer, E., et al., *Global analysis of mRNA localization reveals a prominent role in organizing cellular architecture and function.* Cell, 2007. **131**(1): p. 174-87.
133. Cajigas, I.J., et al., *The local transcriptome in the synaptic neuropil revealed by deep sequencing and high-resolution imaging.* Neuron, 2012. **74**(3): p. 453-66.
134. Martin, K.C. and A. Ephrussi, *mRNA localization: gene expression in the spatial dimension.* Cell, 2009. **136**(4): p. 719-30.
135. Knowles, R.B., et al., *Translocation of RNA granules in living neurons.* J Neurosci, 1996. **16**(24): p. 7812-20.
136. Medioni, C., K. Mowry, and F. Besse, *Principles and roles of mRNA localization in animal development.* Development, 2012. **139**(18): p. 3263-76.
137. Ferrandon, D., et al., *Staufen protein associates with the 3'UTR of bicoid mRNA to form particles that move in a microtubule-dependent manner.* Cell, 1994. **79**(7): p. 1221-32.
138. Ross, A.F., et al., *Characterization of a beta-actin mRNA zipcode-binding protein.* Mol Cell Biol, 1997. **17**(4): p. 2158-65.
139. Sonenberg, N. and A.G. Hinnebusch, *Regulation of translation initiation in eukaryotes: mechanisms and biological targets.* Cell, 2009. **136**(4): p. 731-45.
140. Yanagiya, A., et al., *Requirement of RNA binding of mammalian eukaryotic translation initiation factor 4GI (eIF4GI) for efficient interaction of eIF4E with the mRNA cap.* Mol Cell Biol, 2009. **29**(6): p. 1661-9.
141. Safaee, N., et al., *Interdomain allostery promotes assembly of the poly(A) mRNA complex with PABP and eIF4G.* Mol Cell, 2012. **48**(3): p. 375-86.
142. Wells, S.E., et al., *Circularization of mRNA by eukaryotic translation initiation factors.* Mol Cell, 1998. **2**(1): p. 135-40.
143. Kozak, M., *An analysis of 5'-noncoding sequences from 699 vertebrate messenger RNAs.* Nucleic Acids Res, 1987. **15**(20): p. 8125-48.
144. Hinnebusch, A.G. and J.R. Lorsch, *The mechanism of eukaryotic translation initiation: new insights and challenges.* Cold Spring Harb Perspect Biol, 2012. **4**(10).
145. Pelletier, J. and N. Sonenberg, *Internal initiation of translation of eukaryotic mRNA directed by a sequence derived from poliovirus RNA.* Nature, 1988. **334**(6180): p. 320-5.
146. Mokrejs, M., et al., *IRESite--a tool for the examination of viral and cellular internal ribosome entry sites.* Nucleic Acids Res, 2010. **38**(Database issue): p. D131-6.
147. Pinkstaff, J.K., et al., *Internal initiation of translation of five dendritically localized neuronal mRNAs.* Proc Natl Acad Sci U S A, 2001. **98**(5): p. 2770-5.
148. Koritzinsky, M., et al., *Gene expression during acute and prolonged hypoxia is regulated by distinct mechanisms of translational control.* EMBO J, 2006. **25**(5): p. 1114-25.
149. Xia, X. and M. Holcik, *Strong eukaryotic IRESs have weak secondary structure.* PLoS One, 2009. **4**(1): p. e4136.
150. Komar, A.A. and M. Hatzoglou, *Cellular IRES-mediated translation: the war of ITAFs in pathophysiological states.* Cell Cycle, 2011. **10**(2): p. 229-40.
151. Braunstein, S., et al., *A hypoxia-controlled cap-dependent to cap-independent translation switch in breast cancer.* Mol Cell, 2007. **28**(3): p. 501-12.
152. Hsieh, A.C., et al., *The translational landscape of mTOR signalling steers cancer initiation and metastasis.* Nature, 2012. **485**(7396): p. 55-61.

153. Wilker, E.W., et al., *14-3-3sigma controls mitotic translation to facilitate cytokinesis.* Nature, 2007. **446**(7133): p. 329-32.
154. Babendure, J.R., et al., *Control of mammalian translation by mRNA structure near caps.* RNA, 2006. **12**(5): p. 851-61.
155. Muckenthaler, M., N.K. Gray, and M.W. Hentze, *IRP-1 binding to ferritin mRNA prevents the recruitment of the small ribosomal subunit by the cap-binding complex eIF4F.* Mol Cell, 1998. **2**(3): p. 383-8.
156. Jackson, R.J., C.U. Hellen, and T.V. Pestova, *The mechanism of eukaryotic translation initiation and principles of its regulation.* Nat Rev Mol Cell Biol, 2010. **11**(2): p. 113-27.
157. Hamilton, T.L., et al., *TOPs and their regulation.* Biochem Soc Trans, 2006. **34**(Pt 1): p. 12-6.
158. Jefferies, H.B., et al., *Rapamycin selectively represses translation of the "polypyrimidine tract" mRNA family.* Proc Natl Acad Sci U S A, 1994. **91**(10): p. 4441-5.
159. Patursky-Polischuk, I., et al., *The TSC-mTOR pathway mediates translational activation of TOP mRNAs by insulin largely in a raptor- or rictor-independent manner.* Mol Cell Biol, 2009. **29**(3): p. 640-9.
160. Thoreen, C.C., et al., *A unifying model for mTORC1-mediated regulation of mRNA translation.* Nature, 2012. **485**(7396): p. 109-13.
161. Meyuhas, O. and T. Kahan, *The race to decipher the top secrets of TOP mRNAs.* Biochim Biophys Acta, 2014.
162. Barbosa, C., I. Peixeiro, and L. Romao, *Gene expression regulation by upstream open reading frames and human disease.* PLoS Genet, 2013. **9**(8): p. e1003529.
163. Calvo, S.E., D.J. Pagliarini, and V.K. Mootha, *Upstream open reading frames cause widespread reduction of protein expression and are polymorphic among humans.* Proc Natl Acad Sci U S A, 2009. **106**(18): p. 7507-12.
164. Yepiskoposyan, H., et al., *Autoregulation of the nonsense-mediated mRNA decay pathway in human cells.* RNA, 2011. **17**(12): p. 2108-18.
165. Spriggs, K.A., M. Bushell, and A.E. Willis, *Translational regulation of gene expression during conditions of cell stress.* Mol Cell, 2010. **40**(2): p. 228-37.
166. Vattem, K.M. and R.C. Wek, *Reinitiation involving upstream ORFs regulates ATF4 mRNA translation in mammalian cells.* Proc Natl Acad Sci U S A, 2004. **101**(31): p. 11269-74.
167. Garneau, N.L., J. Wilusz, and C.J. Wilusz, *The highways and byways of mRNA decay.* Nat Rev Mol Cell Biol, 2007. **8**(2): p. 113-26.
168. Wu, X. and G. Brewer, *The regulation of mRNA stability in mammalian cells: 2.0.* Gene, 2012. **500**(1): p. 10-21.
169. Liu, H., et al., *The scavenger mRNA decapping enzyme DcpS is a member of the HIT family of pyrophosphatases.* EMBO J, 2002. **21**(17): p. 4699-708.
170. Decker, C.J. and R. Parker, *P-bodies and stress granules: possible roles in the control of translation and mRNA degradation.* Cold Spring Harb Perspect Biol, 2012. **4**(9): p. a012286.
171. Morey, J.S. and F.M. Van Dolah, *Global analysis of mRNA half-lives and de novo transcription in a dinoflagellate, Karenia brevis.* PLoS One, 2013. **8**(6): p. e66347.
172. Sharova, L.V., et al., *Database for mRNA half-life of 19 977 genes obtained by DNA microarray analysis of pluripotent and differentiating mouse embryonic stem cells.* DNA Res, 2009. **16**(1): p. 45-58.
173. Goodarzi, H., et al., *Systematic discovery of structural elements governing stability of mammalian messenger RNAs.* Nature, 2012. **485**(7397): p. 264-8.

174. Mayr, C. and D.P. Bartel, *Widespread shortening of 3'UTRs by alternative cleavage and polyadenylation activates oncogenes in cancer cells.* Cell, 2009. **138**(4): p. 673-84.
175. Bakheet, T., B.R. Williams, and K.S. Khabar, *ARED 3.0: the large and diverse AU-rich transcriptome.* Nucleic Acids Res, 2006. **34**(Database issue): p. D111-4.
176. Caput, D., et al., *Identification of a common nucleotide sequence in the 3'-untranslated region of mRNA molecules specifying inflammatory mediators.* Proc Natl Acad Sci U S A, 1986. **83**(6): p. 1670-4.
177. Ishimaru, D., et al., *Regulation of Bcl-2 expression by HuR in HL60 leukemia cells and A431 carcinoma cells.* Mol Cancer Res, 2009. **7**(8): p. 1354-66.
178. Ishimaru, D., et al., *Mechanism of regulation of bcl-2 mRNA by nucleolin and A+U-rich element-binding factor 1 (AUF1).* J Biol Chem, 2010. **285**(35): p. 27182-91.
179. Balmer, L.A., et al., *Identification of a novel AU-Rich element in the 3' untranslated region of epidermal growth factor receptor mRNA that is the target for regulated RNA-binding proteins.* Mol Cell Biol, 2001. **21**(6): p. 2070-84.
180. Kontoyiannis, D., et al., *Impaired on/off regulation of TNF biosynthesis in mice lacking TNF AU-rich elements: implications for joint and gut-associated immunopathologies.* Immunity, 1999. **10**(3): p. 387-98.
181. Mukherjee, N., et al., *Global target mRNA specification and regulation by the RNA-binding protein ZFP36.* Genome Biol, 2014. **15**(1): p. R12.
182. Chen, C.Y., et al., *AU binding proteins recruit the exosome to degrade ARE-containing mRNAs.* Cell, 2001. **107**(4): p. 451-64.
183. Tiedje, C., et al., *The p38/MK2-driven exchange between tristetraprolin and HuR regulates AU-rich element-dependent translation.* PLoS Genet, 2012. **8**(9): p. e1002977.
184. Yang, E., et al., *Decay rates of human mRNAs: correlation with functional characteristics and sequence attributes.* Genome Res, 2003. **13**(8): p. 1863-72.
185. Meka, H., et al., *Crystal structure and RNA binding of the Rpb4/Rpb7 subunits of human RNA polymerase II.* Nucleic Acids Res, 2005. **33**(19): p. 6435-44.
186. Choder, M., *Rpb4 and Rpb7: subunits of RNA polymerase II and beyond.* Trends Biochem Sci, 2004. **29**(12): p. 674-81.
187. Farago, M., et al., *Rpb4p, a subunit of RNA polymerase II, mediates mRNA export during stress.* Mol Biol Cell, 2003. **14**(7): p. 2744-55.
188. Lotan, R., et al., *The RNA polymerase II subunit Rpb4p mediates decay of a specific class of mRNAs.* Genes Dev, 2005. **19**(24): p. 3004-16.
189. Lotan, R., et al., *The Rpb7p subunit of yeast RNA polymerase II plays roles in the two major cytoplasmic mRNA decay mechanisms.* J Cell Biol, 2007. **178**(7): p. 1133-43.
190. Goler-Baron, V., et al., *Transcription in the nucleus and mRNA decay in the cytoplasm are coupled processes.* Genes Dev, 2008. **22**(15): p. 2022-7.
191. Trcek, T., et al., *Single-molecule mRNA decay measurements reveal promoter-regulated mRNA stability in yeast.* Cell, 2011. **147**(7): p. 1484-97.
192. Bregman, A., et al., *Promoter elements regulate cytoplasmic mRNA decay.* Cell, 2011. **147**(7): p. 1473-83.
193. Friedlander, M.R., et al., *Evidence for the biogenesis of more than 1,000 novel human microRNAs.* Genome Biol, 2014. **15**(4): p. R57.
194. Kozomara, A. and S. Griffiths-Jones, *miRBase: annotating high confidence microRNAs using deep sequencing data.* Nucleic Acids Res, 2014. **42**(Database issue): p. D68-73.
195. Bartel, D.P., *MicroRNAs: target recognition and regulatory functions.* Cell, 2009. **136**(2): p. 215-33.

196. Wilczynska, A. and M. Bushell, *The complexity of miRNA-mediated repression.* Cell Death Differ, 2014.
197. Cai, X., C.H. Hagedorn, and B.R. Cullen, *Human microRNAs are processed from capped, polyadenylated transcripts that can also function as mRNAs.* RNA, 2004. **10**(12): p. 1957-66.
198. Filipowicz, W., S.N. Bhattacharyya, and N. Sonenberg, *Mechanisms of post-transcriptional regulation by microRNAs: are the answers in sight?* Nat Rev Genet, 2008. **9**(2): p. 102-14.
199. Ha, M. and V.N. Kim, *Regulation of microRNA biogenesis.* Nat Rev Mol Cell Biol, 2014. **15**(8): p. 509-24.
200. Ameres, S.L. and P.D. Zamore, *Diversifying microRNA sequence and function.* Nat Rev Mol Cell Biol, 2013. **14**(8): p. 475-88.
201. Wilczynska, A. and M. Bushell, *The complexity of miRNA-mediated repression.* Cell Death Differ, 2015. **22**(1): p. 22-33.
202. Meijer, H.A., et al., *Translational repression and eIF4A2 activity are critical for microRNA-mediated gene regulation.* Science, 2013. **340**(6128): p. 82-5.
203. Chen, Y., et al., *A DDX6-CNOT1 complex and W-binding pockets in CNOT9 reveal direct links between miRNA target recognition and silencing.* Mol Cell, 2014. **54**(5): p. 737-50.
204. Mathys, H., et al., *Structural and biochemical insights to the role of the CCR4-NOT complex and DDX6 ATPase in microRNA repression.* Mol Cell, 2014. **54**(5): p. 751-65.
205. Friedman, R.C., et al., *Most mammalian mRNAs are conserved targets of microRNAs.* Genome Res, 2009. **19**(1): p. 92-105.
206. Croce, C.M., *Causes and consequences of microRNA dysregulation in cancer.* Nat Rev Genet, 2009. **10**(10): p. 704-14.
207. Chang, J.S., et al., *High levels of the BCR/ABL oncoprotein are required for the MAPK-hnRNP-E2 dependent suppression of C/EBPalpha-driven myeloid differentiation.* Blood, 2007. **110**(3): p. 994-1003.
208. Perrotti, D. and P. Neviani, *From mRNA metabolism to cancer therapy: chronic myelogenous leukemia shows the way.* Clin Cancer Res, 2007. **13**(6): p. 1638-42.
209. Trotta, R., et al., *BCR/ABL activates mdm2 mRNA translation via the La antigen.* Cancer Cell, 2003. **3**(2): p. 145-60.
210. Blagden, S.P. and A.E. Willis, *The biological and therapeutic relevance of mRNA translation in cancer.* Nat Rev Clin Oncol, 2011. **8**(5): p. 280-91.
211. Frederickson, R.M., K.S. Montine, and N. Sonenberg, *Phosphorylation of eukaryotic translation initiation factor 4E is increased in Src-transformed cell lines.* Mol Cell Biol, 1991. **11**(5): p. 2896-900.
212. Smith, M.R., et al., *Translation initiation factors induce DNA synthesis and transform NIH 3T3 cells.* New Biol, 1990. **2**(7): p. 648-54.
213. Lazaris-Karatzas, A. and N. Sonenberg, *The mRNA 5' cap-binding protein, eIF-4E, cooperates with v-myc or E1A in the transformation of primary rodent fibroblasts.* Mol Cell Biol, 1992. **12**(3): p. 1234-8.
214. Hsieh, A.C. and D. Ruggero, *Targeting eukaryotic translation initiation factor 4E (eIF4E) in cancer.* Clin Cancer Res, 2010. **16**(20): p. 4914-20.
215. Ruggero, D., et al., *The translation factor eIF-4E promotes tumor formation and cooperates with c-Myc in lymphomagenesis.* Nat Med, 2004. **10**(5): p. 484-6.
216. Zhang, J. and J.L. Manley, *Misregulation of pre-mRNA alternative splicing in cancer.* Cancer Discov, 2013. **3**(11): p. 1228-37.

217. Gao, A.C., et al., *Metastasis suppression by the standard CD44 isoform does not require the binding of prostate cancer cells to hyaluronate.* Cancer Res, 1998. **58**(11): p. 2350-2.
218. Matter, N., P. Herrlich, and H. Konig, *Signal-dependent regulation of splicing via phosphorylation of Sam68.* Nature, 2002. **420**(6916): p. 691-5.
219. Busa, R., et al., *The RNA-binding protein Sam68 contributes to proliferation and survival of human prostate cancer cells.* Oncogene, 2007. **26**(30): p. 4372-82.
220. Paronetto, M.P., et al., *Alternative splicing of the cyclin D1 proto-oncogene is regulated by the RNA-binding protein Sam68.* Cancer Res, 2010. **70**(1): p. 229-39.
221. Levy, N.S., et al., *Hypoxic stabilization of vascular endothelial growth factor mRNA by the RNA-binding protein HuR.* J Biol Chem, 1998. **273**(11): p. 6417-23.
222. Chang, N., et al., *HuR uses AUF1 as a cofactor to promote p16INK4 mRNA decay.* Mol Cell Biol, 2010. **30**(15): p. 3875-86.
223. Bousquet-Antonelli, C. and J.M. Deragon, *A comprehensive analysis of the La-motif protein superfamily.* RNA, 2009. **15**(5): p. 750-64.
224. Merret, R., et al., *The association of a La module with the PABP-interacting motif PAM2 is a recurrent evolutionary process that led to the neofunctionalization of La-related proteins.* RNA, 2013. **19**(1): p. 36-50.
225. Alfano, C., et al., *Structural analysis of cooperative RNA binding by the La motif and central RRM domain of human La protein.* Nat Struct Mol Biol, 2004. **11**(4): p. 323-9.
226. Bayfield, M.A., R. Yang, and R.J. Maraia, *Conserved and divergent features of the structure and function of La and La-related proteins (LARPs).* Biochim Biophys Acta, 2010. **1799**(5-6): p. 365-78.
227. Berney, C. and J. Pawlowski, *A molecular time-scale for eukaryote evolution recalibrated with the continuous microfossil record.* Proc Biol Sci, 2006. **273**(1596): p. 1867-72.
228. Baltz, A.G., et al., *The mRNA-bound proteome and its global occupancy profile on protein-coding transcripts.* Mol Cell, 2012. **46**(5): p. 674-90.
229. Mattioli, M. and M. Reichlin, *Heterogeneity of RNA protein antigens reactive with sera of patients with systemic lupus erythematosus. Description of a cytoplasmic nonribosomal antigen.* Arthritis Rheum, 1974. **17**(4): p. 421-9.
230. Reichlin, M., *Current perspectives on serological reactions in SLE patients.* Clin Exp Immunol, 1981. **44**(1): p. 1-10.
231. Gottlieb, E. and J.A. Steitz, *The RNA binding protein La influences both the accuracy and the efficiency of RNA polymerase III transcription in vitro.* EMBO J, 1989. **8**(3): p. 841-50.
232. Park, J.M., et al., *The multifunctional RNA-binding protein La is required for mouse development and for the establishment of embryonic stem cells.* Mol Cell Biol, 2006. **26**(4): p. 1445-51.
233. Bai, C. and P.P. Tolias, *Genetic analysis of a La homolog in Drosophila melanogaster.* Nucleic Acids Res, 2000. **28**(5): p. 1078-84.
234. Chakshusmathi, G., et al., *A La protein requirement for efficient pre-tRNA folding.* EMBO J, 2003. **22**(24): p. 6562-72.
235. Gaidamakov, S., et al., *Targeted deletion of the gene encoding the La autoantigen (Sjogren's syndrome antigen B) in B cells or the frontal brain causes extensive tissue loss.* Mol Cell Biol, 2014. **34**(1): p. 123-31.
236. Stefano, J.E., *Purified lupus antigen La recognizes an oligouridylate stretch common to the 3′ termini of RNA polymerase III transcripts.* Cell, 1984. **36**(1): p. 145-54.
237. Reddy, R., et al., *Identification of a La protein binding site in a RNA polymerase III transcript (4.5 I RNA).* J Biol Chem, 1983. **258**(13): p. 8352-6.

238. Wolin, S.L. and T. Cedervall, *The La protein.* Annu Rev Biochem, 2002. **71**: p. 375-403.
239. Huang, Y., et al., *Separate RNA-binding surfaces on the multifunctional La protein mediate distinguishable activities in tRNA maturation.* Nat Struct Mol Biol, 2006. **13**(7): p. 611-8.
240. Bayfield, M.A. and R.J. Maraia, *Precursor-product discrimination by La protein during tRNA metabolism.* Nat Struct Mol Biol, 2009. **16**(4): p. 430-7.
241. Hussain, R.H., M. Zawawi, and M.A. Bayfield, *Conservation of RNA chaperone activity of the human La-related proteins 4, 6 and 7.* Nucleic Acids Res, 2013. **41**(18): p. 8715-25.
242. Rinke, J. and J.A. Steitz, *Precursor molecules of both human 5S ribosomal RNA and transfer RNAs are bound by a cellular protein reactive with anti-La lupus antibodies.* Cell, 1982. **29**(1): p. 149-59.
243. Kufel, J., et al., *Precursors to the U3 small nucleolar RNA lack small nucleolar RNP proteins but are stabilized by La binding.* Mol Cell Biol, 2000. **20**(15): p. 5415-24.
244. Meerovitch, K., et al., *La autoantigen enhances and corrects aberrant translation of poliovirus RNA in reticulocyte lysate.* J Virol, 1993. **67**(7): p. 3798-807.
245. Svitkin, Y.V., et al., *Internal translation initiation on poliovirus RNA: further characterization of La function in poliovirus translation in vitro.* J Virol, 1994. **68**(3): p. 1544-50.
246. Shiroki, K., et al., *Intracellular redistribution of truncated La protein produced by poliovirus 3Cpro-mediated cleavage.* J Virol, 1999. **73**(3): p. 2193-200.
247. Ali, N. and A. Siddiqui, *The La antigen binds 5′ noncoding region of the hepatitis C virus RNA in the context of the initiator AUG codon and stimulates internal ribosome entry site-mediated translation.* Proc Natl Acad Sci U S A, 1997. **94**(6): p. 2249-54.
248. Ali, N., et al., *Human La antigen is required for the hepatitis C virus internal ribosome entry site-mediated translation.* J Biol Chem, 2000. **275**(36): p. 27531-40.
249. Ray, P.S. and S. Das, *La autoantigen is required for the internal ribosome entry site-mediated translation of Coxsackievirus B3 RNA.* Nucleic Acids Res, 2002. **30**(20): p. 4500-8.
250. Holcik, M., et al., *Translational upregulation of X-linked inhibitor of apoptosis (XIAP) increases resistance to radiation induced cell death.* Oncogene, 2000. **19**(36): p. 4174-7.
251. Kim, Y.K., et al., *La autoantigen enhances translation of BiP mRNA.* Nucleic Acids Res, 2001. **29**(24): p. 5009-16.
252. Sommer, G., et al., *The RNA-binding protein La contributes to cell proliferation and CCND1 expression.* Oncogene, 2011. **30**(4): p. 434-44.
253. Pellizzoni, L., et al., *A Xenopus laevis homologue of the La autoantigen binds the pyrimidine tract of the 5′ UTR of ribosomal protein mRNAs in vitro: implication of a protein factor in complex formation.* J Mol Biol, 1996. **259**(5): p. 904-15.
254. Crosio, C., et al., *La protein has a positive effect on the translation of TOP mRNAs in vivo.* Nucleic Acids Res, 2000. **28**(15): p. 2927-34.
255. Intine, R.V., et al., *Differential phosphorylation and subcellular localization of La RNPs associated with precursor tRNAs and translation-related mRNAs.* Mol Cell, 2003. **12**(5): p. 1301-7.
256. Zhu, J., et al., *Binding of the La autoantigen to the 5′ untranslated region of a chimeric human translation elongation factor 1A reporter mRNA inhibits translation in vitro.* Biochim Biophys Acta, 2001. **1521**(1-3): p. 19-29.

257. Ford, L.P., J.W. Shay, and W.E. Wright, *The La antigen associates with the human telomerase ribonucleoprotein and influences telomere length in vivo.* RNA, 2001. **7**(8): p. 1068-75.
258. Liang, C., et al., *Sjogren syndrome antigen B (SSB)/La promotes global microRNA expression by binding microRNA precursors through stem-loop recognition.* J Biol Chem, 2013. **288**(1): p. 723-36.
259. Brenet, F., et al., *Mammalian peptidylglycine alpha-amidating monooxygenase mRNA expression can be modulated by the La autoantigen.* Mol Cell Biol, 2005. **25**(17): p. 7505-21.
260. Huang, M., et al., *La autoantigen translocates to cytoplasm after cleavage during granzyme B-mediated cytotoxicity.* Life Sci, 2007. **81**(19-20): p. 1461-6.
261. Ayukawa, K., et al., *La autoantigen is cleaved in the COOH terminus and loses the nuclear localization signal during apoptosis.* J Biol Chem, 2000. **275**(44): p. 34465-70.
262. Casciola-Rosen, L.A., G. Anhalt, and A. Rosen, *Autoantigens targeted in systemic lupus erythematosus are clustered in two populations of surface structures on apoptotic keratinocytes.* J Exp Med, 1994. **179**(4): p. 1317-30.
263. Dong, G., et al., *Structure of the La motif: a winged helix domain mediates RNA binding via a conserved aromatic patch.* EMBO J, 2004. **23**(5): p. 1000-7.
264. Teplova, M., et al., *Structural basis for recognition and sequestration of UUU(OH) 3′ temini of nascent RNA polymerase III transcripts by La, a rheumatic disease autoantigen.* Mol Cell, 2006. **21**(1): p. 75-85.
265. Kotik-Kogan, O., et al., *Structural analysis reveals conformational plasticity in the recognition of RNA 3′ ends by the human La protein.* Structure, 2008. **16**(6): p. 852-62.
266. Simons, F.H., et al., *Characterization of cis-acting signals for nuclear import and retention of the La (SS-B) autoantigen.* Exp Cell Res, 1996. **224**(2): p. 224-36.
267. Jacks, A., et al., *Structure of the C-terminal domain of human La protein reveals a novel RNA recognition motif coupled to a helical nuclear retention element.* Structure, 2003. **11**(7): p. 833-43.
268. Horke, S., et al., *Molecular characterization of the human La protein.hepatitis B virus RNA.B interaction in vitro.* J Biol Chem, 2002. **277**(38): p. 34949-58.
269. Craig, A.W., et al., *The La autoantigen contains a dimerization domain that is essential for enhancing translation.* Mol Cell Biol, 1997. **17**(1): p. 163-9.
270. Intine, R.V., et al., *Aberrant nuclear trafficking of La protein leads to disordered processing of associated precursor tRNAs.* Mol Cell, 2002. **9**(5): p. 1113-23.
271. Bayfield, M.A., et al., *Conservation of a masked nuclear export activity of La proteins and its effects on tRNA maturation.* Mol Cell Biol, 2007. **27**(9): p. 3303-12.
272. Goodier, J.L., H. Fan, and R.J. Maraia, *A carboxy-terminal basic region controls RNA polymerase III transcription factor activity of human La protein.* Mol Cell Biol, 1997. **17**(10): p. 5823-32.
273. Intine, R.V., et al., *Nonphosphorylated human La antigen interacts with nucleolin at nucleolar sites involved in rRNA biogenesis.* Mol Cell Biol, 2004. **24**(24): p. 10894-904.
274. Fan, H., et al., *Phosphorylation of the human La antigen on serine 366 can regulate recycling of RNA polymerase III transcription complexes.* Cell, 1997. **88**(5): p. 707-15.
275. Schwartz, E.I., R.V. Intine, and R.J. Maraia, *CK2 is responsible for phosphorylation of human La protein serine-366 and can modulate rpL37 5′-terminal oligopyrimidine mRNA metabolism.* Mol Cell Biol, 2004. **24**(21): p. 9580-91.

276. Sommer, G., et al., *Implication of RNA-binding protein La in proliferation, migration and invasion of lymph node-metastasized hypopharyngeal SCC cells.* PLoS One, 2011. **6**(10): p. e25402.
277. Al-Ejeh, F., J.M. Darby, and M.P. Brown, *The La autoantigen is a malignancy-associated cell death target that is induced by DNA-damaging drugs.* Clin Cancer Res, 2007. **13**(18 Pt 2): p. 5509s-5518s.
278. Petz, M., et al., *La enhances IRES-mediated translation of laminin B1 during malignant epithelial to mesenchymal transition.* Nucleic Acids Res, 2012. **40**(1): p. 290-302.
279. Martini, M., et al., *PI3K/AKT signaling pathway and cancer: an updated review.* Ann Med, 2014. **46**(6): p. 372-83.
280. Brenet, F., et al., *Akt phosphorylation of La regulates specific mRNA translation in glial progenitors.* Oncogene, 2009. **28**(1): p. 128-39.
281. Zhang, J., et al., *La autoantigen mediates oxidant induced de novo Nrf2 protein translation.* Mol Cell Proteomics, 2011.
282. Niture, S.K. and A.K. Jaiswal, *Nrf2 protein up-regulates antiapoptotic protein Bcl-2 and prevents cellular apoptosis.* J Biol Chem, 2012. **287**(13): p. 9873-86.
283. Al-Ejeh, F., et al., *In vivo targeting of dead tumor cells in a murine tumor model using a monoclonal antibody specific for the La autoantigen.* Clin Cancer Res, 2007. **13**(18 Pt 2): p. 5519s-5527s.
284. Ren, R., *Mechanisms of BCR-ABL in the pathogenesis of chronic myelogenous leukaemia.* Nat Rev Cancer, 2005. **5**(3): p. 172-83.
285. Nakatake, M., et al., *JAK2(V617F) negatively regulates p53 stabilization by enhancing MDM2 via La expression in myeloproliferative neoplasms.* Oncogene, 2012. **31**(10): p. 1323-33.
286. Tang, J., et al., *A Novel Inhibitor of Human La Protein with Anti-HBV Activity Discovered by Structure-Based Virtual Screening and In Vitro Evaluation.* PLoS One, 2012. **7**(4): p. e36363.
287. Aigner, S. and T.R. Cech, *The Euplotes telomerase subunit p43 stimulates enzymatic activity and processivity in vitro.* RNA, 2004. **10**(7): p. 1108-18.
288. Aigner, S., et al., *Euplotes telomerase contains an La motif protein produced by apparent translational frameshifting.* EMBO J, 2000. **19**(22): p. 6230-9.
289. Aigner, S., et al., *The Euplotes La motif protein p43 has properties of a telomerase-specific subunit.* Biochemistry, 2003. **42**(19): p. 5736-47.
290. Witkin, K.L. and K. Collins, *Holoenzyme proteins required for the physiological assembly and activity of telomerase.* Genes Dev, 2004. **18**(10): p. 1107-18.
291. Peterlin, B.M., J.E. Brogie, and D.H. Price, *7SK snRNA: a noncoding RNA that plays a major role in regulating eukaryotic transcription.* Wiley Interdiscip Rev RNA, 2012. **3**(1): p. 92-103.
292. Wassarman, D.A. and J.A. Steitz, *Structural analyses of the 7SK ribonucleoprotein (RNP), the most abundant human small RNP of unknown function.* Mol Cell Biol, 1991. **11**(7): p. 3432-45.
293. Xue, Y., et al., *A capping-independent function of MePCE in stabilizing 7SK snRNA and facilitating the assembly of 7SK snRNP.* Nucleic Acids Res, 2010. **38**(2): p. 360-9.
294. Barboric, M., et al., *7SK snRNP/P-TEFb couples transcription elongation with alternative splicing and is essential for vertebrate development.* Proc Natl Acad Sci U S A, 2009. **106**(19): p. 7798-803.

295. Krueger, B.J., et al., *LARP7 is a stable component of the 7SK snRNP while P-TEFb, HEXIM1 and hnRNP A1 are reversibly associated.* Nucleic Acids Res, 2008. **36**(7): p. 2219-29.
296. He, N., et al., *A La-related protein modulates 7SK snRNP integrity to suppress P-TEFb-dependent transcriptional elongation and tumorigenesis.* Mol Cell, 2008. **29**(5): p. 588-99.
297. Markert, A., et al., *The La-related protein LARP7 is a component of the 7SK ribonucleoprotein and affects transcription of cellular and viral polymerase II genes.* EMBO Rep, 2008. **9**(6): p. 569-75.
298. Dai, Q., et al., *Primordial dwarfism gene maintains Lin28 expression to safeguard embryonic stem cells from premature differentiation.* Cell Rep, 2014. **7**(3): p. 735-46.
299. Alazami, A.M., et al., *Loss of function mutation in LARP7, chaperone of 7SK ncRNA, causes a syndrome of facial dysmorphism, intellectual disability, and primordial dwarfism.* Hum Mutat, 2012. **33**(10): p. 1429-34.
300. Najmabadi, H., et al., *Deep sequencing reveals 50 novel genes for recessive cognitive disorders.* Nature, 2011. **478**(7367): p. 57-63.
301. Ji, X., et al., *LARP7 suppresses P-TEFb activity to inhibit breast cancer progression and metastasis.* Elife, 2014. **3**: p. e02907.
302. Mori, Y., et al., *Instabilotyping reveals unique mutational spectra in microsatellite-unstable gastric cancers.* Cancer Res, 2002. **62**(13): p. 3641-5.
303. Cheng, Y., et al., *LARP7 is a potential tumor suppressor gene in gastric cancer.* Lab Invest, 2012. **92**(7): p. 1013-9.
304. Biewenga, P., et al., *Gene expression in early stage cervical cancer.* Gynecol Oncol, 2008. **108**(3): p. 520-6.
305. Schaffler, K., et al., *A stimulatory role for the La-related protein 4B in translation.* RNA, 2010. **16**(8): p. 1488-99.
306. Yang, R., et al., *La-related protein 4 binds poly(A), interacts with the poly(A)-binding protein MLLE domain via a variant PAM2w motif, and can promote mRNA stability.* Mol Cell Biol, 2011. **31**(3): p. 542-56.
307. Albrecht, M. and T. Lengauer, *Survey on the PABC recognition motif PAM2.* Biochem Biophys Res Commun, 2004. **316**(1): p. 129-38.
308. Amrani, N., et al., *Translation factors promote the formation of two states of the closed-loop mRNP.* Nature, 2008. **453**(7199): p. 1276-80.
309. Goss, D.J. and F.E. Kleiman, *Poly(A) binding proteins: are they all created equal?* Wiley Interdiscip Rev RNA, 2013. **4**(2): p. 167-79.
310. Hosoda, N., F. Lejeune, and L.E. Maquat, *Evidence that poly(A) binding protein C1 binds nuclear pre-mRNA poly(A) tails.* Mol Cell Biol, 2006. **26**(8): p. 3085-97.
311. Jenal, M., et al., *The poly(A)-binding protein nuclear 1 suppresses alternative cleavage and polyadenylation sites.* Cell, 2012. **149**(3): p. 538-53.
312. Adams, D.R., D. Ron, and P.A. Kiely, *RACK1, A multifaceted scaffolding protein: Structure and function.* Cell Commun Signal, 2011. **9**: p. 22.
313. Bai, S.W., et al., *Identification and characterization of a set of conserved and new regulators of cytoskeletal organization, cell morphology and migration.* BMC Biol, 2011. **9**: p. 54.
314. Valavanis, C., et al., *Acheron, a novel member of the Lupus Antigen family, is induced during the programmed cell death of skeletal muscles in the moth Manduca sexta.* Gene, 2007. **393**(1-2): p. 101-9.
315. Shao, R., et al., *The novel lupus antigen related protein acheron enhances the development of human breast cancer.* Int J Cancer, 2012. **130**(3): p. 544-54.

316. Cai, L., et al., *Binding of LARP6 to the conserved 5′ stem-loop regulates translation of mRNAs encoding type I collagen.* J Mol Biol, 2010. **395**(2): p. 309-26.
317. Wang, Z., et al., *Regulation of muscle differentiation and survival by Acheron.* Mech Dev, 2009. **126**(8-9): p. 700-9.
318. Glenn, H.L., Z. Wang, and L.M. Schwartz, *Acheron, a Lupus antigen family member, regulates integrin expression, adhesion, and motility in differentiating myoblasts.* Am J Physiol Cell Physiol, 2010. **298**(1): p. C46-55.
319. Stefanovic, B. and D.A. Brenner, *5′ stem-loop of collagen alpha 1(I) mRNA inhibits translation in vitro but is required for triple helical collagen synthesis in vivo.* J Biol Chem, 2003. **278**(2): p. 927-33.
320. Manojlovic, Z. and B. Stefanovic, *A novel role of RNA helicase A in regulation of translation of type I collagen mRNAs.* RNA, 2012. **18**(2): p. 321-34.
321. Challa, A.A. and B. Stefanovic, *A novel role of vimentin filaments: binding and stabilization of collagen mRNAs.* Mol Cell Biol, 2011. **31**(18): p. 3773-89.
322. Weng, H., et al., *Acheron, an novel LA antigen family member, binds to CASK and forms a complex with Id transcription factors.* Cell Mol Biol Lett, 2009. **14**(2): p. 273-87.
323. Zhou, X., et al., *Down-regulation of miR-203 induced by Helicobacter pylori infection promotes the proliferation and invasion of gastric cancer by targeting CASK.* Oncotarget, 2014.
324. Wang, Q., et al., *CASK and its target gene Reelin were co-upregulated in human esophageal carcinoma.* Cancer Lett, 2002. **179**(1): p. 71-7.
325. Wei, J.L., et al., *High expression of CASK correlates with progression and poor prognosis of colorectal cancer.* Tumour Biol, 2014. **35**(9): p. 9185-94.
326. Hsueh, Y.P., et al., *Nuclear translocation and transcription regulation by the membrane-associated guanylate kinase CASK/LIN-2.* Nature, 2000. **404**(6775): p. 298-302.
327. Sun, R.J., et al., *[Regulation of proliferation and apoptosis of human vascular endothelial cell by Acheron].* Zhonghua Shao Shang Za Zhi, 2011. **27**(2): p. 156-60.
328. Sun, R., et al., *Acheron regulates vascular endothelial proliferation and angiogenesis together with Id1 during wound healing.* Cell Biochem Funct, 2011. **29**(8): p. 636-40.
329. Weigand, J.E., et al., *Hypoxia-induced alternative splicing in endothelial cells.* PLoS One, 2012. **7**(8): p. e42697.
330. Nykamp, K., M.H. Lee, and J. Kimble, *C. elegans La-related protein, LARP-1, localizes to germline P bodies and attenuates Ras-MAPK signaling during oogenesis.* RNA, 2008. **14**(7): p. 1378-89.
331. Aoki, K., et al., *LARP1 specifically recognizes the 3′ terminus of poly(A) mRNA.* FEBS Lett, 2013. **587**(14): p. 2173-8.
332. Merret, R., et al., *XRN4 and LARP1 are required for a heat-triggered mRNA decay pathway involved in plant acclimation and survival during thermal stress.* Cell Rep, 2013. **5**(5): p. 1279-93.
333. Burrows, C., et al., *The RNA binding protein Larp1 regulates cell division, apoptosis and cell migration.* Nucleic Acids Res, 2010. **38**(16): p. 5542-53.
334. Blagden, S.P., et al., *Drosophila Larp associates with poly(A)-binding protein and is required for male fertility and syncytial embryo development.* Dev Biol, 2009. **334**(1): p. 186-97.
335. Tcherkezian, J., et al., *Proteomic analysis of cap-dependent translation identifies LARP1 as a key regulator of 5′TOP mRNA translation.* Genes Dev, 2014. **28**(4): p. 357-71.

336. Vazquez-Pianzola, P., H. Urlaub, and B. Suter, *Pabp binds to the osk 3'UTR and specifically contributes to osk mRNA stability and oocyte accumulation.* Dev Biol, 2011. **357**(2): p. 404-18.
337. Coller, J.M., N.K. Gray, and M.P. Wickens, *mRNA stabilization by poly(A) binding protein is independent of poly(A) and requires translation.* Genes Dev, 1998. **12**(20): p. 3226-35.
338. Zanin, E., et al., *LARP-1 promotes oogenesis by repressing fem-3 in the C. elegans germline.* J Cell Sci, 2010. **123**(Pt 16): p. 2717-24.
339. Hsu, P.P., et al., *The mTOR-regulated phosphoproteome reveals a mechanism of mTORC1-mediated inhibition of growth factor signaling.* Science, 2011. **332**(6035): p. 1317-22.
340. Yu, Y., et al., *Phosphoproteomic analysis identifies Grb10 as an mTORC1 substrate that negatively regulates insulin signaling.* Science, 2011. **332**(6035): p. 1322-6.
341. Deak, P., et al., *P-element insertion alleles of essential genes on the third chromosome of Drosophila melanogaster: correlation of physical and cytogenetic maps in chromosomal region 86E-87F.* Genetics, 1997. **147**(4): p. 1697-722.
342. Ichihara, K., et al., *A Drosophila orthologue of larp protein family is required for multiple processes in male meiosis.* Cell Struct Funct, 2007. **32**(2): p. 89-100.
343. Chauvet, S., et al., *dlarp, a new candidate Hox target in Drosophila whose orthologue in mouse is expressed at sites of epithelium/mesenchymal interactions.* Dev Dyn, 2000. **218**(3): p. 401-13.
344. Doss, M.X., et al., *Global transcriptomic analysis of murine embryonic stem cell-derived brachyury (T) cells.* Genes Cells, 2010. **15**(3): p. 209-228.
345. Kwon, S.C., et al., *The RNA-binding protein repertoire of embryonic stem cells.* Nat Struct Mol Biol, 2013. **20**(9): p. 1122-30.
346. Eswaran, J., et al., *RNA sequencing of cancer reveals novel splicing alterations.* Sci Rep, 2013. **3**: p. 1689.
347. Xie, C., et al., *LARP1 predict the prognosis for early-stage and AFP-normal hepatocellular carcinoma.* J Transl Med, 2013. **11**: p. 272.
348. Andersen, J.N., et al., *Pathway-based identification of biomarkers for targeted therapeutics: personalized oncology with PI3K pathway inhibitors.* Sci Transl Med, 2010. **2**(43): p. 43ra55.
349. Matsuoka, S., et al., *ATM and ATR substrate analysis reveals extensive protein networks responsive to DNA damage.* Science, 2007. **316**(5828): p. 1160-6.
350. Crawford, N.P., et al., *The metastasis efficiency modifier ribosomal RNA processing 1 homolog B (RRP1B) is a chromatin-associated factor.* J Biol Chem, 2009. **284**(42): p. 28660-73.
351. Chatel-Chaix, L., et al., *A Host Yb-1 Ribonucleoprotein Complex Is Hijacked by Hepatitis C Virus for the Control of Ns3-Dependent Particle Production.* J Virol, 2013.
352. Binder, J.X., et al., *COMPARTMENTS: unification and visualization of protein subcellular localization evidence.* Database (Oxford), 2014. **2014**: p. bau012.
353. Yap, T.A., C.P. Carden, and S.B. Kaye, *Beyond chemotherapy: targeted therapies in ovarian cancer.* Nat Rev Cancer, 2009. **9**(3): p. 167-81.
354. Hendrix, N.D., et al., *Fibroblast growth factor 9 has oncogenic activity and is a downstream target of Wnt signaling in ovarian endometrioid adenocarcinomas.* Cancer Res, 2006. **66**(3): p. 1354-62.
355. Bonome, T., et al., *A gene signature predicting for survival in suboptimally debulked patients with ovarian cancer.* Cancer Res, 2008. **68**(13): p. 5478-86.

356. Gyorffy, B., et al., *An online survival analysis tool to rapidly assess the effect of 22,277 genes on breast cancer prognosis using microarray data of 1,809 patients.* Breast Cancer Res Treat, 2010. **123**(3): p. 725-31.
357. Gyorffy, B., A. Lanczky, and Z. Szallasi, *Implementing an online tool for genome-wide validation of survival-associated biomarkers in ovarian-cancer using microarray data from 1287 patients.* Endocr Relat Cancer, 2012. **19**(2): p. 197-208.
358. Gyorffy, B., et al., *Online survival analysis software to assess the prognostic value of biomarkers using transcriptomic data in non-small-cell lung cancer.* PLoS One, 2013. **8**(12): p. e82241.
359. Reinhold, W.C., et al., *CellMiner: a web-based suite of genomic and pharmacologic tools to explore transcript and drug patterns in the NCI-60 cell line set.* Cancer Res, 2012. **72**(14): p. 3499-511.
360. Workman, P., et al., *Guidelines for the welfare and use of animals in cancer research.* Br J Cancer, 2010. **102**(11): p. 1555-77.
361. Li, R., et al., *SOAP2: an improved ultrafast tool for short read alignment.* Bioinformatics, 2009. **25**(15): p. 1966-7.
362. Mortazavi, A., et al., *Mapping and quantifying mammalian transcriptomes by RNA-Seq.* Nat Methods, 2008. **5**(7): p. 621-8.
363. Keene, J.D., J.M. Komisarow, and M.B. Friedersdorf, *RIP-Chip: the isolation and identification of mRNAs, microRNAs and protein components of ribonucleoprotein complexes from cell extracts.* Nat Protoc, 2006. **1**(1): p. 302-7.
364. Kent, W.J., et al., *The human genome browser at UCSC.* Genome Res, 2002. **12**(6): p. 996-1006.
365. Heckman, C.A., et al., *A-Myb up-regulates Bcl-2 through a Cdx binding site in t(14;18) lymphoma cells.* J Biol Chem, 2000. **275**(9): p. 6499-508.
366. Cox, J. and M. Mann, *MaxQuant enables high peptide identification rates, individualized p.p.b.-range mass accuracies and proteome-wide protein quantification.* Nat Biotechnol, 2008. **26**(12): p. 1367-72.
367. Cox, J., et al., *Andromeda: a peptide search engine integrated into the MaxQuant environment.* J Proteome Res, 2011. **10**(4): p. 1794-805.
368. Bowen, N.J., et al., *Gene expression profiling supports the hypothesis that human ovarian surface epithelia are multipotent and capable of serving as ovarian cancer initiating cells.* BMC Med Genomics, 2009. **2**: p. 71.
369. Tone, A.A., et al., *Gene expression profiles of luteal phase fallopian tube epithelium from BRCA mutation carriers resemble high-grade serous carcinoma.* Clin Cancer Res, 2008. **14**(13): p. 4067-78.
370. Kim, J., et al., *High-grade serous ovarian cancer arises from fallopian tube in a mouse model.* Proc Natl Acad Sci U S A, 2012. **109**(10): p. 3921-6.
371. Cerami, E., et al., *The cBio cancer genomics portal: an open platform for exploring multidimensional cancer genomics data.* Cancer Discov, 2012. **2**(5): p. 401-4.
372. Iwakawa, M., et al., *The radiation-induced cell-death signaling pathway is activated by concurrent use of cisplatin in sequential biopsy specimens from patients with cervical cancer.* Cancer Biol Ther, 2007. **6**(6): p. 905-11.
373. Arroyo, J.D., et al., *Argonaute2 complexes carry a population of circulating microRNAs independent of vesicles in human plasma.* Proc Natl Acad Sci U S A, 2011. **108**(12): p. 5003-8.
374. Markmann, S., B. Gerber, and V. Briese, *Prognostic value of Ca 125 levels during primary therapy.* Anticancer Res, 2007. **27**(4A): p. 1837-9.

375. Hou, J.Y., et al., *Exploiting MEK inhibitor-mediated activation of ERalpha for therapeutic intervention in ER-positive ovarian carcinoma.* PLoS One, 2013. **8**(2): p. e54103.
376. Stronach, E.A., et al., *HDAC4-regulated STAT1 activation mediates platinum resistance in ovarian cancer.* Cancer Res, 2011. **71**(13): p. 4412-22.
377. Nguyen, L.V., et al., *Cancer stem cells: an evolving concept.* Nat Rev Cancer, 2012. **12**(2): p. 133-43.
378. Yin, A.H., et al., *AC133, a novel marker for human hematopoietic stem and progenitor cells.* Blood, 1997. **90**(12): p. 5002-12.
379. Singh, S.K., et al., *Identification of human brain tumour initiating cells.* Nature, 2004. **432**(7015): p. 396-401.
380. Grosse-Gehling, P., et al., *CD133 as a biomarker for putative cancer stem cells in solid tumours: limitations, problems and challenges.* J Pathol, 2013. **229**(3): p. 355-78.
381. Guo, R., et al., *Description of the CD133+ subpopulation of the human ovarian cancer cell line OVCAR3.* Oncol Rep, 2011. **25**(1): p. 141-6.
382. Nam, E.J., et al., *MicroRNA profiling of a CD133(+) spheroid-forming subpopulation of the OVCAR3 human ovarian cancer cell line.* BMC Med Genomics, 2012. **5**: p. 18.
383. Shankavaram, U.T., et al., *Transcript and protein expression profiles of the NCI-60 cancer cell panel: an integromic microarray study.* Mol Cancer Ther, 2007. **6**(3): p. 820-32.
384. Kuroda, T., et al., *ALDH1-high ovarian cancer stem-like cells can be isolated from serous and clear cell adenocarcinoma cells, and ALDH1 high expression is associated with poor prognosis.* PLoS One, 2013. **8**(6): p. e65158.
385. Silva, I.A., et al., *Aldehyde dehydrogenase in combination with CD133 defines angiogenic ovarian cancer stem cells that portend poor patient survival.* Cancer Res, 2011. **71**(11): p. 3991-4001.
386. Kryczek, I., et al., *Expression of aldehyde dehydrogenase and CD133 defines ovarian cancer stem cells.* Int J Cancer, 2012. **130**(1): p. 29-39.
387. Gupta, P.B., et al., *Identification of selective inhibitors of cancer stem cells by high-throughput screening.* Cell, 2009. **138**(4): p. 645-59.
388. Tang, Q.L., et al., *Salinomycin inhibits osteosarcoma by targeting its tumor stem cells.* Cancer Lett, 2011. **311**(1): p. 113-21.
389. Fuchs, D., et al., *Salinomycin overcomes ABC transporter-mediated multidrug and apoptosis resistance in human leukemia stem cell-like KG-1a cells.* Biochem Biophys Res Commun, 2010. **394**(4): p. 1098-104.
390. Noh, K.H., et al., *Nanog signaling in cancer promotes stem-like phenotype and immune evasion.* J Clin Invest, 2012. **122**(11): p. 4077-93.
391. Bareiss, P.M., et al., *SOX2 expression associates with stem cell state in human ovarian carcinoma.* Cancer Res, 2013. **73**(17): p. 5544-55.
392. Seko, Y., et al., *Selective cytoplasmic translocation of HuR and site-specific binding to the interleukin-2 mRNA are not sufficient for CD28-mediated stabilization of the mRNA.* J Biol Chem, 2004. **279**(32): p. 33359-67.
393. Ardehali, R., et al., *Overexpression of BCL2 enhances survival of human embryonic stem cells during stress and obviates the requirement for serum factors.* Proc Natl Acad Sci U S A, 2011. **108**(8): p. 3282-7.
394. Wang, J., et al., *Involvement of MKP-1 and Bcl-2 in acquired cisplatin resistance in ovarian cancer cells.* Cell Cycle, 2009. **8**(19): p. 3191-8.

395. Lagadinou, E.D., et al., *BCL-2 inhibition targets oxidative phosphorylation and selectively eradicates quiescent human leukemia stem cells.* Cell Stem Cell, 2013. **12**(3): p. 329-41.
396. Mignone, F., et al., *Untranslated regions of mRNAs.* Genome Biol, 2002. **3**(3): p. REVIEWS0004.
397. Ong, S.E., *The expanding field of SILAC.* Anal Bioanal Chem, 2012. **404**(4): p. 967-76.
398. Turchinovich, A., et al., *Characterization of extracellular circulating microRNA.* Nucleic Acids Res, 2011. **39**(16): p. 7223-33.
399. Hernandez-Molina, G., G. Leal-Alegre, and M. Michel-Peregrina, *The meaning of anti-Ro and anti-La antibodies in primary Sjogren's syndrome.* Autoimmun Rev, 2011. **10**(3): p. 123-5.
400. Liu, Q., et al., *Molecular properties of CD133+ glioblastoma stem cells derived from treatment-refractory recurrent brain tumors.* J Neurooncol, 2009. **94**(1): p. 1-19.
401. Juin, P., et al., *Decoding and unlocking the BCL-2 dependency of cancer cells.* Nat Rev Cancer, 2013. **13**(7): p. 455-65.
402. Jiang, M. and J. Milner, *Bcl-2 constitutively suppresses p53-dependent apoptosis in colorectal cancer cells.* Genes Dev, 2003. **17**(7): p. 832-7.
403. Kupryjanczyk, J., et al., *Evaluation of clinical significance of TP53, BCL-2, BAX and MEK1 expression in 229 ovarian carcinomas treated with platinum-based regimen.* Br J Cancer, 2003. **88**(6): p. 848-54.
404. Chiou, S.H., et al., *Identification of CD133-positive radioresistant cells in atypical teratoid/rhabdoid tumor.* PLoS One, 2008. **3**(5): p. e2090.
405. Latorre, E., et al., *Downregulation of HuR as a new mechanism of doxorubicin resistance in breast cancer cells.* Molecular Cancer, 2012. **11**.
406. Kuchler, L., et al., *SYNCRIP-Dependent Nox2 mRNA Destabilization Impairs ROS Formation in M2-Polarized Macrophages.* Antioxid Redox Signal, 2014.
407. Kim, D.Y., et al., *hnRNP Q mediates a phase-dependent translation-coupled mRNA decay of mouse Period3.* Nucleic Acids Res, 2011. **39**(20): p. 8901-14.
408. Mukherjee, N., et al., *Integrative regulatory mapping indicates that the RNA-binding protein HuR couples pre-mRNA processing and mRNA stability.* Mol Cell, 2011. **43**(3): p. 327-39.
409. Huppertz, I., et al., *iCLIP: protein-RNA interactions at nucleotide resolution.* Methods, 2014. **65**(3): p. 274-87.
410. Licatalosi, D.D., et al., *HITS-CLIP yields genome-wide insights into brain alternative RNA processing.* Nature, 2008. **456**(7221): p. 464-9.
411. Hafner, M., et al., *Transcriptome-wide identification of RNA-binding protein and microRNA target sites by PAR-CLIP.* Cell, 2010. **141**(1): p. 129-41.
412. Tani, H., et al., *Genome-wide determination of RNA stability reveals hundreds of short-lived noncoding transcripts in mammals.* Genome Res, 2012. **22**(5): p. 947-56.
413. Ingolia, N.T., et al., *The ribosome profiling strategy for monitoring translation in vivo by deep sequencing of ribosome-protected mRNA fragments.* Nat Protoc, 2012. **7**(8): p. 1534-50.
414. Polanski, M. and N.L. Anderson, *A list of candidate cancer biomarkers for targeted proteomics.* Biomark Insights, 2007. **1**: p. 1-48.
415. Dancey, J.E., et al., *Guidelines for the development and incorporation of biomarker studies in early clinical trials of novel agents.* Clin Cancer Res, 2010. **16**(6): p. 1745-55.
416. Franceschini, F. and I. Cavazzana, *Anti-Ro/SSA and La/SSB antibodies.* Autoimmunity, 2005. **38**(1): p. 55-63.

417. Wang, K., et al., *Export of microRNAs and microRNA-protective protein by mammalian cells.* Nucleic Acids Res, 2010. **38**(20): p. 7248-59.
418. Traxler, P., *Tyrosine kinases as targets in cancer therapy - successes and failures.* Expert Opin Ther Targets, 2003. **7**(2): p. 215-34.
419. Resnier, P., et al., *A review of the current status of siRNA nanomedicines in the treatment of cancer.* Biomaterials, 2013. **34**(27): p. 6429-43.
420. Huang, X., et al., *Modular plasmonic nanocarriers for efficient and targeted delivery of cancer-therapeutic siRNA.* Nano Lett, 2014. **14**(4): p. 2046-51.

1 APPENDICES

1.1 APPENDIX I – SYSTEMATIC REVIEW OF LARP1 EXPRESSION IN CANCER

Using the search criteria specified below, Oncomine (www.oncomine.org) was searched for studies comparing LARP1 expression in cancer and non-cancer tissue.

ONCOMINE SEARCH CRITERIA/THRESHOLDS

Cancer	Adult Carcinomas
Dataset Size	151+ (minimum 40 per cancer subtype)
Analysis	Cancer vs Normal
Data Type	mRNA
Platform	Affymetrix U133 (where possible)
Fold change	>1.1 or <0.9
P value	less that 0.01

	Oncomine Database Name (Data Source)	Platform	Cancer Type Investigated	Controls	Cases	Probe	Fold Change	P-Value
1	Bonome Ovarian (Cancer Res 2008/07/01)	Affymetrix U133	Ovarian Carcinoma	10	185	212193_s_at	**1.98**	***< 0.0001***
2	Haferlach Leukaemia (J Clin Oncol 2010/05/20)	Affymetrix U133 plus 2.0	EXCLUDED					
3	Roessler Liver 2 (Cancer Res 2010/12/15)	Affymetrix U133	Hepatocellular Carcinoma	220	225	212193_s_at	**1.84**	***< 0.0001***
4	Hou Lung (PLoS One 2010/04/22)	Affymetrix U133 plus 2.0	Lung Adenocarcinoma	65	45	212193_s_at	**1.40**	***0.0002***
5	TCGA Ovarian (TCGA 2011/03/24)	Affymetrix U133	Ovarian Serous Carcinoma	8	509	212193_s_at	**1.70**	***0.0017***
6	Agnelli Myeloma (Genes Chrom Cancer 2009/07/01)	Affymetrix U133	EXCLUDED					
7	Sun Brain (Cancer Cell 2006/04/01)	Affymetrix U133 plus 2.0	Glioblastoma	23	81	212193_s_at	**0.56**	***< 0.0001***
8	TCGA Brain (TCGA 2012/03/01)	Affymetrix U133	Glioblastoma	10	515	212193_s_at	**0.83**	***0.0037***
9	Coustan-Smith Leukaemia (Lancet Oncol 2009/10/02)	Affymetrix U133	EXCLUDED					
10	Valk Leukaemia (N Engl J Med 2004/04/15)	Affymetrix U133	EXCLUDED					
11	Sanchez-Carbayo Bladder 2 (J Clin Oncol 2006/02/10)	Affymetrix U133	Infiltrating Bladder Uroepithelial Cancer	48	81	212193_s_at	**1.50**	***< 0.0001***
12	Barretina Sarcoma (Nat Genet 2010/07/04)	Affymetrix U133	EXCLUDED					

NON-AFFYMETRIX STUDIES (largest studies added to include common cancers otherwise not represented)

13	TCGA Colorectal (TCGA 2011/09/08)	Agilent 244K Microarray (AMDID019760)	Colon/Caecal Adenocarcinoma	22	123	A_24_P7212	**1.82**	***< 0.0001***
14	Curtis Breast (Nature 2012/06/21)	IlluminaHT	Invasive Ductal Breast Cancer	144	1556	ILMN_1681590	**1.18**	***< 0.0001***

1.2 APPENDIX II – CHANGES IN MRNA ABUNDANCE FOLLOWING LARP1 KNOCKDOWN.

Following LARP1 knockdown, mRNA sequencing was performed to a 35Gbp depth. The ratio change in mRNA abundance between siLARP1-treated cells and control cells was calculated using the RPKM method. The top 50 most upregulated and downregulated genes are presented below.

Top 50 most upregulated genes following LARP1 knockdown

Rank	Symbol	RATIO (siLARP1/siControl)	FDR (False-discovery rate corrected p-value)
1	FAM167B	**10.76321664**	5.14E-03
2	COL5A3	**9.083512367**	1.81E-02
3	NPY2R	**8.208613432**	9.05E-03
4	LGI4	**7.715238872**	2.08E-02
5	COL15A1	**7.283694409**	3.50E-04
6	ATOH8	**5.744118793**	1.18E-04
7	LOC100270804	**5.309321106**	2.65E-02
8	TNNT2	**4.926271115**	3.66E-02
9	TESC	**4.910900426**	1.09E-02
10	BTC	**4.564401237**	3.27E-02
11	HHLA2	**4.50159881**	1.35E-07
12	PPPDE1	**4.439301175**	3.14E-56
13	THBS4	**4.358276542**	3.53E-07
14	SUSD2	**4.348501937**	3.53E-02
15	NXPH3	**4.256337412**	1.46E-09
16	FGF13	**4.060830153**	4.24E-05
17	YPEL1	**4.007838119**	3.54E-13
18	ISM1	**3.713630659**	6.76E-09
19	F2RL1	**3.688509443**	1.59E-04
20	IRS4	**3.667739602**	1.00E-02
21	TMEFF2	**3.579925731**	5.80E-03
22	DAPK2	**3.573588719**	2.25E-03

23	TMEM64	**3.532437095**	5.06E-06
24	CALHM2	**3.528483036**	4.35E-07
25	WIF1	**3.516303256**	9.76E-03
26	STC1	**3.480241305**	6.78E-06
27	KLHL4	**3.473040184**	3.59E-03
28	KCNT1	**3.44573744**	3.94E-02
29	CRISPLD2	**3.425299673**	7.98E-05
30	DENND1C	**3.256160782**	1.21E-03
31	C1orf38	**3.245543804**	5.63E-06
32	FOXF2	**3.235893741**	2.69E-06
33	STAC2	**3.221803261**	1.36E-05
34	RCOR2	**3.165673593**	1.68E-10
35	C9orf170	**3.131846575**	4.59E-02
36	TMEM150C	**3.103489976**	1.75E-06
37	ZMYM6NB	**3.094376226**	1.69E-09
38	CLIP3	**3.037756279**	3.03E-08
39	IL2RB	**2.904075488**	6.75E-05
40	CORO1A	**2.871391551**	3.37E-02
41	RUNX2	**2.822265376**	2.48E-02
42	LRRC2	**2.818792673**	5.88E-04
43	PANX2	**2.739400173**	1.39E-04
44	KIF5C	**2.673154375**	2.47E-23
45	SIGIRR	**2.663312736**	4.20E-02
46	FBXO2	**2.633999887**	1.89E-02
47	TMEM45A	**2.609776229**	5.51E-07
48	ALPK3	**2.589775632**	5.74E-03
49	PTPRA	**2.555785399**	2.39E-04
50	LRRC7	**2.552562068**	3.58E-02

Top 50 most downregulated genes following LARP1 knockdown

Rank	Symbol	RATIO (siLARP1/siControl)	FDR (False-discovery rate corrected p-value)
1	FLJ42393	**0.042542733**	3.84E-02
2	C3AR1	**0.106867308**	4.86E-02
3	SCARNA9L	**0.135332271**	1.11E-05
4	PDCD1LG2	**0.136407086**	1.05E-02
5	S1PR1	**0.157007047**	9.35E-136
6	KRTAP2-1	**0.184470415**	1.29E-19
7	HEBP2	**0.188532256**	8.05E-66
8	PKI55	**0.196298783**	1.19E-51
9	LOC730755	**0.198886458**	6.09E-55
10	LARP1	**0.210771962**	1.78E-112
11	IGFBP3	**0.221314705**	1.12E-17

12	OXNAD1	**0.232277516**	5.82E-49
13	B3GNT5	**0.2329099**	8.92E-09
14	GNMT	**0.238011796**	2.66E-02
15	LUM	**0.238510402**	1.40E-07
16	LOC644242	**0.247863952**	3.36E-02
17	SLC26A2	**0.253267538**	1.32E-58
18	LRFN5	**0.255301564**	5.12E-04
19	MDGA2	**0.258154169**	2.21E-02
20	NCRNA00324	**0.268021972**	1.89E-02
21	ETV4	**0.268185058**	2.56E-08
22	AK4	**0.276307614**	2.44E-04
23	SLC35B1	**0.283881398**	7.04E-54
24	ULBP2	**0.291455886**	4.90E-21
25	IFI44L	**0.292113415**	7.31E-03
26	ITPK1	**0.292171416**	4.74E-03
27	ZNF542	**0.292350633**	3.89E-09
28	GBP1	**0.292583124**	1.02E-28
29	CCDC3	**0.292856281**	1.65E-09
30	VCL	**0.29325466**	3.97E-34
31	VMA21	**0.300852251**	2.56E-50
32	PAK3	**0.30578632**	1.68E-10
33	TTLL11	**0.311776341**	4.07E-08
34	PTCHD1	**0.313498802**	3.83E-04
35	ZNHIT3	**0.313566042**	1.76E-30
36	EPCAM	**0.315879903**	1.40E-22
37	SCD5	**0.316781535**	7.45E-34
38	IL17RD	**0.319062818**	1.96E-18
39	LOX	**0.319915695**	3.12E-10
40	LYRM1	**0.322561521**	1.07E-04
41	GXYLT1	**0.326735525**	4.59E-02
42	LOXL2	**0.327276132**	2.69E-56
43	RNF43	**0.327974721**	2.08E-03
44	FNIP2	**0.329307381**	1.35E-14
45	BIRC3	**0.331363902**	4.74E-04
46	ACER2	**0.333643407**	2.02E-06
47	DDA1	**0.335336684**	9.34E-46
48	EIF4EBP2	**0.335545949**	3.17E-47
49	CCNG1	**0.336000105**	1.36E-08
50	DDX11L2	**0.340558606**	4.34E-02

1.3 APPENDIX III – 3'UTR LUCIFERASE REPORTER ASSAY DATA PROCESSING.

Overleaf is an example of the data processing steps (1 to 5) for the 3'UTR luciferase reporter assay experiments. The example chosen is one experimental repeat in SKOV3 cells, transfected with *renilla* luciferase 3'UTR reporter constructs, or a control vector without additional 3'UTR sequences, and co-transfected with a *firefly* luciferase reporter vector for data normalisation. Data in steps 1 and 2 represent the raw luciferase values from the same wells of each condition, analysed twice, once for *renilla* and once for *firefly* luciferase activity.

1 *Renilla* luciferase values (experimental vectors with additional 3'UTR sequences)

3'UTR vector construct	siControl	siLARP1
Control	547186	403306
ARE	327670	274640
BCL2 0-2.7kbp	26458	6269
BCL2 2.6kbp-5.2kbp	101982	73100

2 Matched *firefly* luciferase values from the same wells (co-transfected control vector for data normalisation)

3'UTR vector construct	siControl	siLARP1
Control	24505	16205
ARE	21464	16575
BCL2 0-2.7kbp	27811	17008
BCL2 2.6kbp-5.2kbp	29466	27162

3 Normalised *renilla* luciferase values (*renilla/firefly)*

3'UTR vector construct	siControl	siLARP1
Control	22.3	24.9
ARE	15.3	16.6
BCL2 0-2.7kbp	1.0	0.4
BCL2 2.6kbp-5.2kbp	3.5	2.7

4 siLARP1/siControl

3'UTR vector construct	siLARP1/siControl
Control	111%
ARE	109%
BCL2 0-2.7kbp	39%
BCL2 2.6kbp-5.2kbp	78%

5 Data normalised to control vector (with no additioal UTR sequence)

3'UTR vector construct	siLARP1/siControl
Control	100%
ARE	97%
BCL2 0-2.7kbp	35%
BCL2 2.6kbp-5.2kbp	70%